A comparison of Reduced Beam Section moment connection and Kaiser Bolted Bracket® moment connections in steel Special Moment Frames

by

Curtis Mathias Johnson

B.S., Kansas State University, 2013

A THESIS

submitted in partial fulfillment of the requirements for the degree

MASTER OF SCIENCE

Department of Architectural Engineering
College of Engineering

KANSAS STATE UNIVERSITY
Manhattan, Kansas

2017

Approved by:

Major Professor
Kimberly Kramer

Copyright

Abstract

Of seismic steel lateral force resisting systems in practice today, the Moment Frame has most diverse connection types. Special Moment frames resist lateral loads through energy dissipation of the inelastic deformation of the beam members. The 1994 Northridge earthquake proved that the standard for welded beam-column connections were not sufficient to prevent damage to the connection or failure of the connection. Through numerous studies, new methods and standards for Special Moment Frame connections are presented in the Seismic Design Manual 2nd Edition to promote energy dissipation away from the beam-column connection.

A common type of SMF is the Reduce Beams Section (RBS). To encourage inelastic deformation away from the beam-column connection, the beam flange's dimensions are reduced a distance away from the beam-column connection; making the member "weaker" at that specific location dictating where the plastic hinging will occur during a seismic event. The reduction is usually taken in a semi-circular pattern. Another type of SMF connection is the Kaiser Bolted Bracket® (KBB) which consists of brackets that stiffen the beam-column connection. KBB connections are similar to RBS connections as the stiffness is higher near the connection and lower away from the connection. Instead of reducing the beam's sectional properties, KBB uses a bracket to stiffen the connection.

The building used in this parametric study is a 4-story office building. This thesis reports the results of the parametric study by comparing two SMF connections: Reduced Beam Section and Kaiser Bolted Brackets. This parametric study includes results from three Seismic Design Categories; B, C, and D, and the use of two different foundation connections; fixed and pinned. The purpose of this parametric study is to compare member sizes, member forces, and story drift.

The results of Seismic Design Category D are discussed in depth in this thesis, while the results of Seismic Design Category B and C are provided in the Appendices.

Table of Contents

List of Figures

List of Tables

List of Notations

AISC – American Institute of Steel Construction
ASCE – American Society of Civil Engineers
b_{bf} – Beam flange width
C_d – Deflection amplification factor
CJP – Complete joint penetration
C_s – Seismic Response Coefficient
D – Dead Load
ELFP – Equivalent Lateral Force Procedure
F_{yb} – Beam yield stress
F_{yc} – Column yield stress
F_{yf} – Yield stress of the flange
H – Hydrostatic Load
IMF – Intermediate Moment Frame
J – Torsional Constant
KBB – Kaiser Bolted Brackets
L – Live Load
lb./ft. – pounds per foot
LFRS – Lateral Force Resisting System
L_h – distance between plastic hinge locations
L_r – Roof Live Load
LRFD – Load Resistance Factor Design
M^*_{pb} – Moment at the intersection of the beam and column centerlines
M_f – Probable maximum moment at the face of the column
M_{pr} – Probable maximum moment
M_{uv} – Additional moment due to shear amplification from the center of RBS to the centerline of the column
psf – pounds per square foot
R – Rain Load
R – Response modification factor
RBS – Reduced Beam Sections
R_{yb} – Beam material overstrength factor
R_{yc} – Column material overstrength factor
S – Snow Load
S_{D1} - Design spectral response acceleration parameter for periods of 1 second
SDC – Seismic Design Category (ies)
S_{DS} – Design spectral response acceleration parameter for short periods
SMF – Special Moment Frame(s)
t_{cf} – Column flange thickness
V – Design Seismic Shear
V_E – 2% seismic shear
$V_{gravity}$ – beam shear force resulting from $1.2D + f_1L + 0.2S$
V_{RBS} – Shear at the reduced beam section
V_u – Required Shear Strength
V_y – Yield Shear

W – Wind Load
W_E – Effective Seismic Weight
Y_m – Simplified column flange yield-line mechanism parameter
Z_x – Section Modulus
a – Horizontal distance from the face of the column flange to the start of the RBS cut
b – Length of the RBS cut
d – depth in beam
d_c – Depth of column
d_{eff} – Effective beam depth, calculated as the centroidal distance between bolt groups in the upper and lower brackers
Δ – Design Drift
Δ_y – Yield Drift
Δ_{max} – Max Inelastic Drift
ρ – Redundancy factor
ϕ_d – Resistance factor for ductile limit states
Ω_0 – System overstrength factor

Acknowledgements

Thank you to all my friends and family who have supported me through my academic career. Thank you to my committee members, James Goddard, Fred Hasler, and Bill Zhang for providing feedback and guidance on this parametric study. A special thank you to Kimberly Kramer, my major professor, for the significant investment made in my personal and professional development.

Chapter 1 - Description of Parametric Study

Structural steel special moment frames are commonly used as part of the seismic force-resisting systems in buildings designed to resist severe ground shaking and are permitted by ASCE 7 *Minimum Design Loads for Buildings and Other Structures* (ASCE, 2010). The design responsibility of steel connections has been debated for many decades: (A) the engineer-of-record should be responsible for the complete design of framing connections on their design drawings or (B) the framing connections should be delegated to a licensed engineer working on behalf of the fabricator. Following the 1994 Northridge earthquake, a number of proprietary connection technologies, with design furnished by the licensor, began to emerge on the market and to gain acceptance by engineers around the country, including those in the western United States of America who prior to this time typically debated on the side of (A).

A number of public domain connection designs are available for both moment-resisting and braced frames. For special moment frames (SMF) intended for seismic applications, an engineer can go to ANSI/AISC 358, *Prequalified Connections for Special and Intermediate Steel Moment Frames for Seismic Applications*, select and design any of several connection types in accordance with the criteria in that standard, obtain permit approval and have confidence that the building is designed to an appropriate standard of care. Prequalified connections have been thoroughly tested and evaluated by an American Institute of Steel Construction (AISC) - sponsored standards body, which lends confidence in their expected performance in the next big earthquake (CorDova 2011).

Public domain connections with prequalification include the reduced beam section (RBS), bolted flange plate (BFP), and welded unreinforced flange (WUF_W). Proprietary connections listed in the standard include: the Kaiser Bolted Bracket® (KBB) and ConXtech connections. A parametric study comparing a SMF-RBS to SMF-KBB is presented.

The purpose of this parametric study is to compare two different SMF systems and their beam-to-column connections. A comparison of SMF-RBS and SMF-KBB frames and connections is presented. The comparison focuses on the similarities and differences of the story drift, axial force, shear force, moment, and the member sizes (wide flange) used as the result from using these two systems. These SMFs are compared at different Seismic Design Categories (SDC): B, C, and D. The design of the SMFs located in the longitudinal direction of the building described in the next section is the focus of this study. The last element of the study is comparing the fixity of the SMF columns to the foundation (connections) assumed in the design process, which can be idealized as either fixed or pinned.

The RBS connection involves a single angle that is connected to the column with welds and is bolted to the beam. The connection of column-angle-beam is designed to as a temporary support until the full welded connection between beam and column is developed. RBS moment connection, as the name implies, reduces the beam section is to allow inelastic deformations to form where the section has been reduced. The KBB moment connection applies a stiffener to the top and bottom the beam. These stiffeners are broken in to two groups: the W series (bolted to the column and welded to the beam) and the B series (bolted to both beam and column). In the design of the connection, a single angle shear connection is prescribed. The brackets attached to the top and bottom of the beam stiffen the beam near the beam-column connection. Similar to the RBS moment connection, this allows for inelastic deformations to occur in a desired location away from the beam-column connection. The reason for RBS moment connection is used in this study is out of familiarity or for a control in the study. The use of RBS moment connection is a topic in Building Seismic Design; therefore a background had been developed. As for KBB moment connection, as it proved to be an interesting connection to pursue and has a step-by-step design procedure in Chapter 9 of the Seismic Design Manual 2nd Edition.

1.1 Building Description

A similar building to the example building in the AISC Seismic Design Manuel 2nd Edition is used. The four-story office building in plan consists of four bays of 30 feet in the longitudinal direction and 3 bays of 25 feet in the transverse direction. Refer to Figures 1.1 and 1.2 which are reproductions of Figures 4-7 and 4-8 in the Seismic Design Manuel. The LFRS in the longitudinal direction is located along grids A and D between columns A-1 through A-4 and D-1 through D-4 and is the focus of this study. In the transverse direction, the lateral force resisting system is located in along grids 1 and 5, between B-1 and C-1; and B-5 and C-5. In the Seismic Design Manuel example, one opening is assumed to be reserved for stairs and in the south east bay and three other openings in the center of the floor are for elevators and stairs.

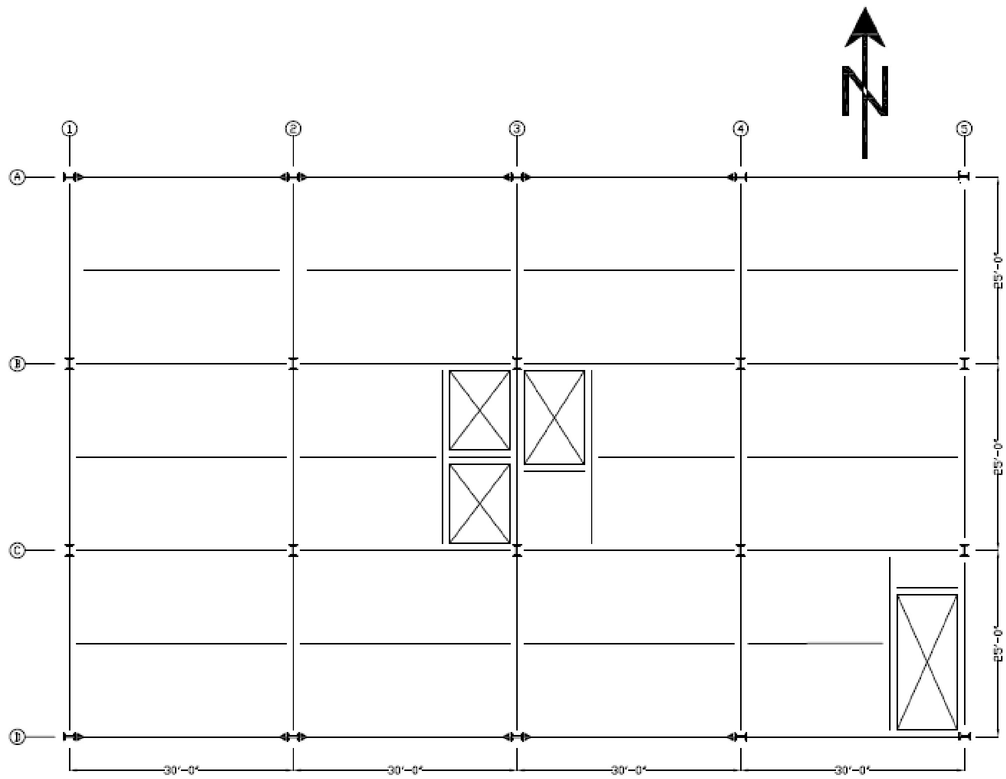

Figure 1-1 Example Framing Plan

The SMF elevation in Figure 1-2 depicts the dimensions of the bays used for the example in the Seismic Design Manuel 2nd Edition. The base to the second floor is 14 feet, and the change in elevation between the second, third, fourth, and roof is 12 feet 6 inches. The figure also depicts the location of column splices at 4 feet above the third floor, and the column has a fixed connection at the base. As stated earlier, this study also includes analysis of SMF pinned connection at the base.

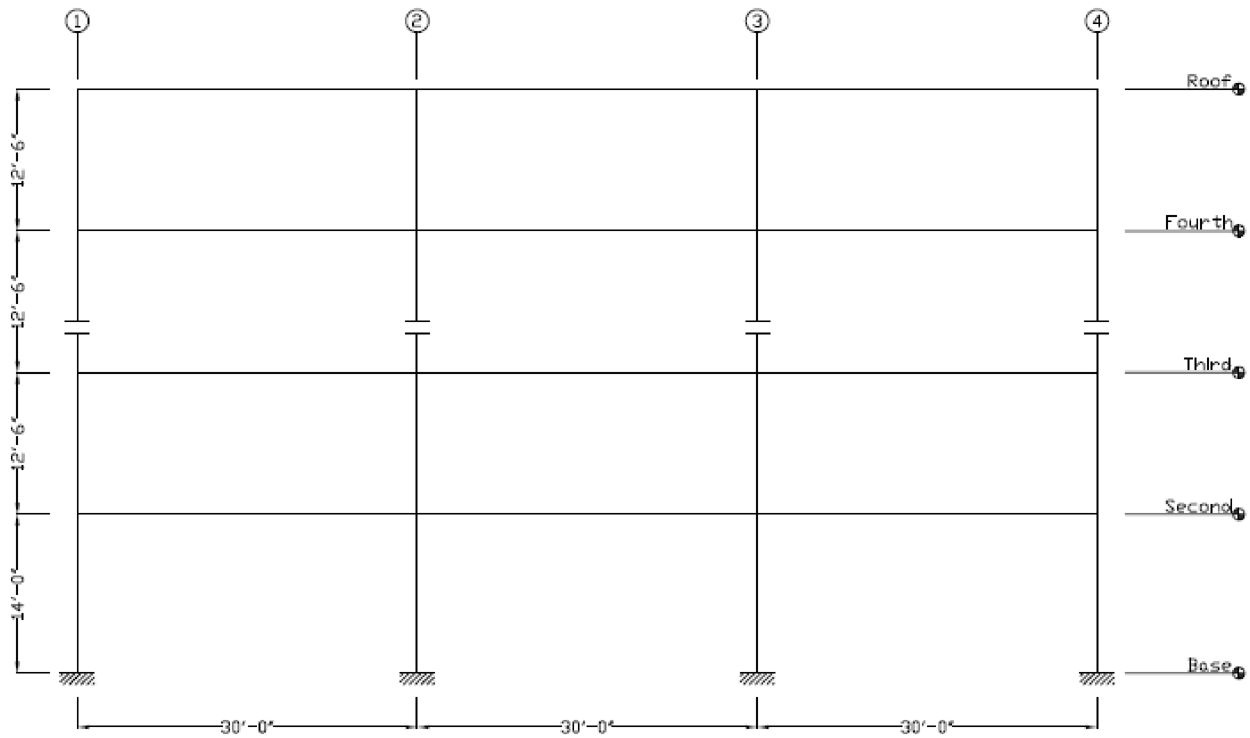

Figure 1-2 Example SMF Elevation

Although the design process for the RBS will be the same, with exception to the beam-to-column connection for the KBB, it is not the purpose of this study to confirm the Seismic Design Manual's examples. Therefore, changes to the floor plan have been made for this parametric study. An additional bay in the longitudinal direction has been added, and another opening has been allocated for stairs in the north-west corner of the building. The spaces for elevators and stairs have been rearranged in the center bay to maintain the center of mass near the actual plan center of the building to reduce torsional shear. Accidental torsional shear is considered in the design of the LFRS. Dimensions have been given to these openings such that the stairs are 10 feet by 30 feet, and the other openings are 10 feet by 12.5 feet. The total longitudinal distance upon adding the new bays is 150 feet with five bays being 30 feet in length and the transverse direction consists of 3 bays of 25 feet which in total equals 75 feet as shown in Figure 1-3. Although the design of the foundation is beyond the scope of this study, selection of the SMF column-to-foundation connection (pinned or fixed) is required for the design of the SMF, since this effects the forces and drift the system is designed to resist. Therefore, the column-foundation connection is analyzed to be both pinned and fixed (not simultaneously, but individual case studies are performed) and the resulting member sizes, member forces, and floor drift are compared. Figure 1.3 provides a visual representation of the framing plan for the parametric study.

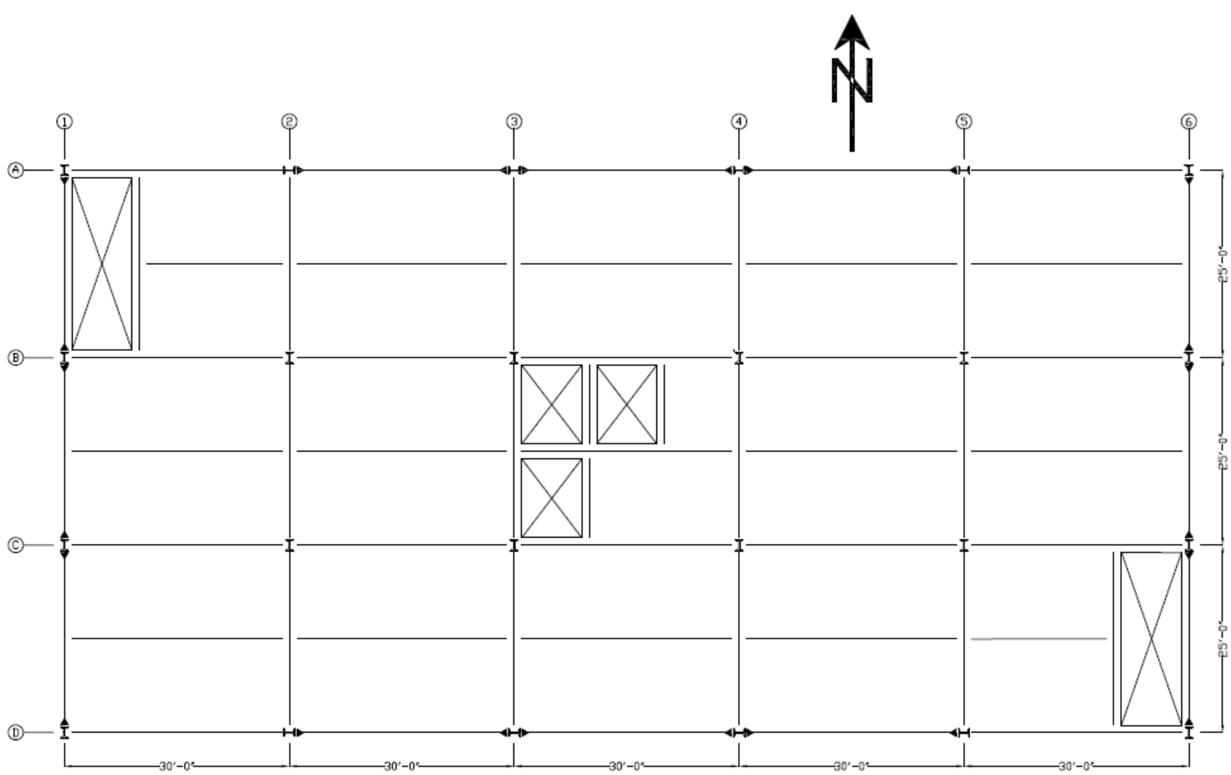

Figure 1-3 Parametric Study Framing Plan

1.2 Design Considerations

Now that the building structural frame has been established, the next step is to determine the loads applied to the structural system. In conjunction with determining the applied loads, a design procedure must be chosen. Load and Resistance Factor Design (LRFD) method and the Equivalent Lateral Force Procedure (ELFP) are used. The idea of the ELFP is to distribute part of the seismic force (base shear) to every floor which are able to transfer lateral forces. Loads applied to the structural system can be categorized into two types: lateral and gravity. The typical gravity loads considered are dead, live, and snow. Not every type of load that can be applied to a structural system are applicable to the building being designed. Load designations are important since each type of load has uncertainties associated with it and the probability that the loads will occur at the same time need to be taken into account. A safety factor is applied to ensure that the structural system will be able to support the service design loads. Many structures will see most, if not all, loads sometime in the life of the structure. The challenge is how to combine these loads reasonably and which load combination is going to apply to the specific member being analyzed. A direct combination of all loads at their maximum is not considered due to the low probably of these loads occurring at the exact same time over every square foot of the structure. The list of load combinations found in the ASCE 7-10 Section 2.3.3 and Section 12.4.2.3.

1. $1.4D$ Eqn. 1.3-1
2. $1.2D + 1.6L + 0.5(L_r \text{ or } S \text{ or } R)$ Eqn. 1.3-2
3. $1.2D + 1.6(L_r \text{ or } S \text{ or } R)$ Eqn. 1.3-3
4. $1.2D + 1.0W + L + 0.5(Lr \text{ or } S \text{ or } R)$ Eqn. 1.3-4

5. $(1.2 + 0.2S_{DS})D + \rho E + L\ 0.2S$ Eqn. 1.3-5a

6. $(1.2 + 0.2S_{DS})D + \Omega_0 E + L + 0.2S$ Eqn. 1.3-5b

7. $0.9D + 1.0W$ Eqn. 1.3-6

8. $(0.9 – 0.2S_{DS})D + \rho E$ Eqn. 1.3-7a

9. $(0.9 – 0.2S_{DS})D + \Omega_0 E + 1.6H$ Eqn. 1.3-7b

For this parametric study, the loads applied to the roof are a dead load of 70 pounds per square foot (psf) and a roof live load of 20 psf. For the fourth, third, and second floors, the dead load is 85 psf, and the live load is 80 psf. These live and dead loads are typical for an office building constructed from steel beams with metal deck and concrete topping and are similar to the example in the Seismic Design Manual Second Edition. The curtain wall load is 15 psf or for 12'-6" of curtain wall is 187.5 plf. The 15 pounds per square foot is determined by combining the weights of a rough wall construction through ASCE 7-10 Table C3-1. The floor live load was not reduced, since the main focus is the LFRS, and a unreduced 20 psf roof live load is used which will also account for a flat roof snow load up to 20 psf. This snow load assumes the regions that the building could be located does not accumulate a significant amount of snow.

Before determining the seismic loads through the ELFP, additional information is needed. A summary on how to determine the seismic loads is discussed in Chapter 2.2. The Risk Category is the first piece of information determined. The study conducted assumes a Risk Category of II giving a seismic importance factor of 1.

Instead of specifically choosing a site and determining the SDC, a predetermined short period design spectral response acceleration parameter, S_{DS}, value in the desired SDC is chosen for this study. The value used for the study, listed in the Table 1.1, gives an upper range of the desired SDC. Choosing S_{DS} allows a range of locations for the study building. The range of values that determine the SDC is present in ASCE 7-10 Table 11.6-1 along with the used S_{DS} values for this study. S_{DS} significance will be expanded on later and can be found in load combinations 5, 6, 8, and 9.

Table 1-1 Table 11.6-1 Seismic Design Category Based on Short Period Response Acceleration Parameter

		Risk Category	**Study Values Used**
Value of S_{DS}	**I or II or III**	**IV**	
$S_{DS} \leq 0.167$	A	A	NA
$0.167 \leq S_{DS} \leq 0.33$	B	C	0.32
$0.33 \leq S_{DS} \leq 0.50$	C	D	0.49
$0.50 \leq S_{DS}$	D	D	1.0

The S_{DS} value both increases the factor in load combination 5 and 6 and decreases the factor in load combination 8 and 9 multiplied to the dead load. The S_{DS} also factors in determining the seismic shear, in which a higher value will increase the seismic base shear. The next factor in the load combinations to determine is the reliability/redundancy factor, ρ, found in load combinations 5 and 8. In the "Blue Book," published by the Structural Engineers Association of California (SEAOC, 1999), *Recommended Lateral Force Requirements and Commentary*, redundancy is defined as a "characteristic of structures in which multiple paths of resistance to loads are provided." The importance of structural redundancy have been long recognized but became the focus of research after 1994 Northridge and 1995 Kobe earthquakes. The reliability/redundancy factor was introduced in NEHRP 97, UBC 1997, and IBC 2000. The modified factor is primary a function of plan configuration of the structures, i.e. the number of moment frames in the direction of earthquake excitations and maximum element-story shear ratio. Structural systems are classified into redundancy or non-redundancy structures. If the structures are judged as non-redundancy buildings, the penalty factor for lateral design force is 1.3 (Kuo-Wei, 2004).

When using the ELFP, determining the redundancy factor is found in ASCE 7-10 Section 12.3.4. Section 12.3.4.1 gives a list of conditions in which ρ is permitted to equal 1.0. The first condition described in the section states that "Structures assigned to Seismic Design Category B or C is permitted to have a redundancy factor of 1.0. Therefore for the study conducted, ρ is equal to 1.0 for SDC B and C. Determining ρ for SDC D is found in ASCE 7 Section 12.3.4.2 which states that ρ equals 1.3 unless one of the two following conditions are met: 1) When a story resists more than 35% of the base shear, the loss of moment resistance at the beam-to-column connections at both ends of a single beam does not result in more than a 33% reduction in story strength, nor does the resulting system have an extreme torsional irregularity; or 2) At all levels, structures are regular in plan and at least two bays of seismic force-resisting perimeter framing is provided on each side of the structure in each orthogonal direction at each story. After determining the seismic shear for each story, considering the floor, and the SMF layout, it has been determined that for SDC D ρ equals 1.0 as it meets the requirements of condition 2 for this parametric study.

The last values to be determined is the response modification coefficient, R, the deflection amplification factor, C_d and the overstrength factor, Ω_0. In the development of seismic design provisions for building structures, the most controversial part has been the development of the force reduction factors and the displacement amplification factors. The force reduction factor, expressed as a response modification factor, R, is used to reduce the linear elastic design response spectra. A displacement amplification factor C_d is used to compute the expected maximum inelastic displacement from the elastic displacement induced by the design seismic forces. Consider a typical global structural response, Figure 1-4 shows the required elastic strength, expressed in terms of base shear, V_E, equals the maximum base shear that develops in the structure if it were to remain in the elastic range during the maximum considered earthquake. Since a properly designed structure usually can provide a certain amount of ductility, a structure can be designed economically to develop an actual maximum strength of V_y. The corresponding maximum deformation demand, expressed in terms of story drift, Δ, is Δ_{max}. Since the calculation of V_y which corresponds to the structural mechanism or yield strength and Δ_{max} involves nonlinear analysis, these quantities are generally not quantified in an explicit manner. For design purposes, ASCE 7 reduces the V_y level to the V level, which corresponds to the formation of the first plastic hinge, allowing some inelastic deformations to occur in specific locations to dissipate the seismic forces. This level is commonly called the "first significant yield" level—a level beyond which the global structural response starts to deviate significantly from the elastic response. The ASCE 7 uses the displacement amplification factor C_d to predict the maximum inelastic displacement from the elastic displacement produced by the seismic design forces. Figure 1.4 illustrates the relationship that the factors R, C_d, and Ω_0 affects the seismic base shear and the drift of the system.

Previous investigations on performance of buildings during severe earthquakes indicate that structural overstrength plays an important role in protecting buildings from collapse (Osteraas and Krawinkler, 1989). Quantification of actual overstrength can be used to reduce the forces used in the design, leading to more economical structures. The overstrength factor is an amplification factor applied to the elastic design forces to estimate the maximum expected force that will develop; i.e., the reserve strength that exists between the actual structural yield level and the prescribed first significant yield level. The overstrength factor accounts for the material used in the design of LFRS is stronger than the minimum strength considered in design; members are larger than required for strength (designed for drift and deflection limits); non-structural elements adding stiffness; conservatism of the design procedure and ductility requirements; load factors and multiple load cases; accidental torsion consideration; serviceability limit state provisions; redundancy; strain hardening; and utilizing the elastic period to obtain the design forces. Using the ELFP, the seismic base shear is the elastic force that the LFRS system is designed to resist. However, the material being used for the LFRS can endure more as it enters in the inelastic range. Once the system enters the inelastic range, the system cannot return to its original state. The amount the system can endure is determined by Ω_0, which can be two to four times the design shear. The overstrength, response modification, and deflection amplification factor are given in ASCE 7-10 Table 12.2-1. For a steel SMF, Ω_0 is 3, R is 8, and C_d is 5.5.

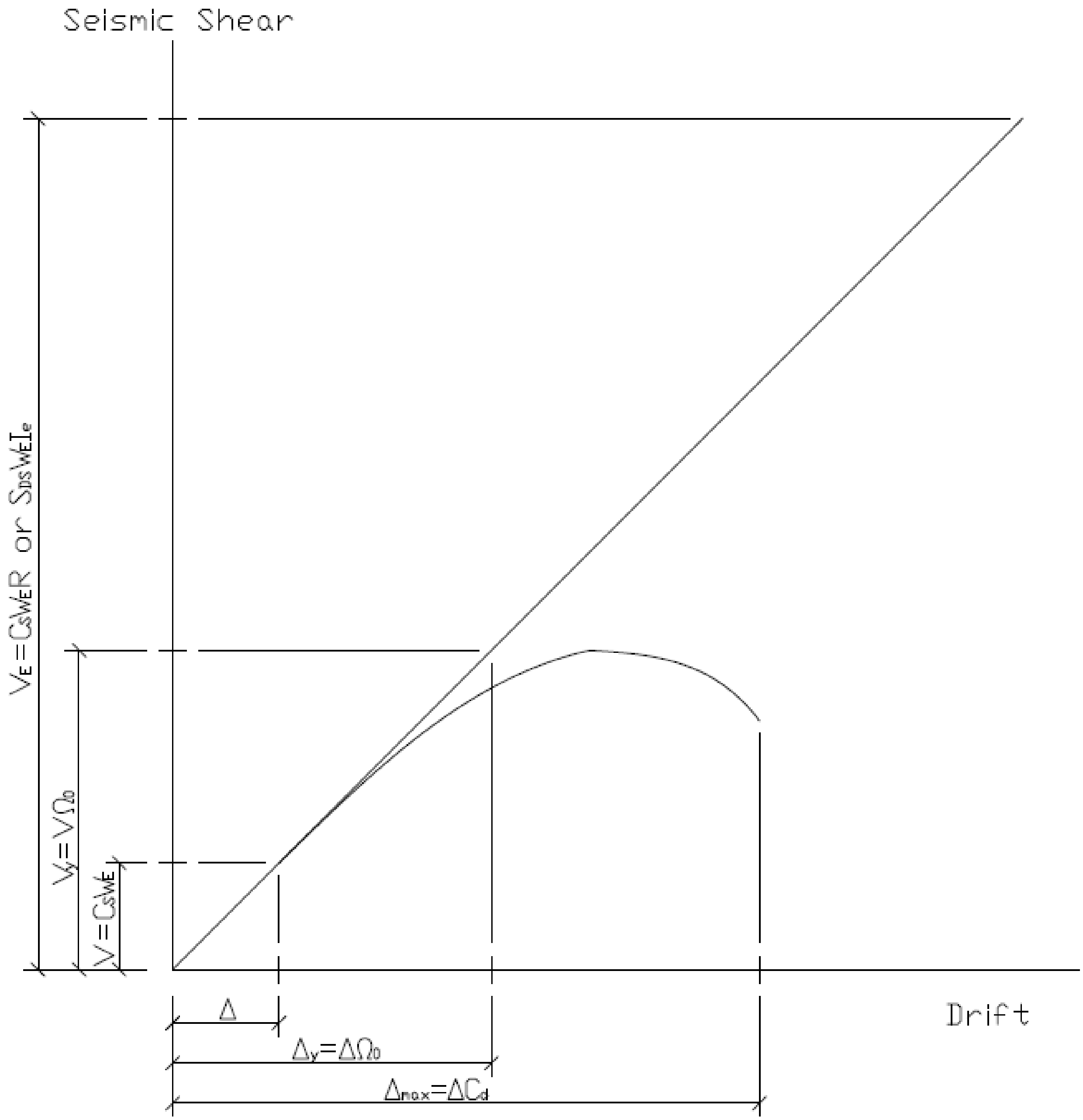

Figure 1-4 Seismic Base Shear vs. Drift

Chapter 2 - System Design

In this chapter, the elastic portion of the design process is discussed. Elastic performance signifies that it is able to return to its original state after being unloaded. The gravity system (takes only vertical loads) consists of the floor framing, such as, beams, girders, and columns not part of the LFRS. The floor framing is sized to resist gravity loads first and then is designed to resist lateral loads, seismic for this study. The seismic forces are based on the ELFP of the ASCE 7.

2.1 Gravity System

For this parametric study, the structure, a composite beam-girder system, will transfer the dead and live loads to a non-composite column system. It is beyond the scope of this study to discuss in depth the design procedure for a composite floor system. However, some key concepts in the design of a composite floor system are discussed. A composite system is used for the economy of the design. The concrete endures the compression and the steel beam/girder endures the tension. The materials work together, compositely; this reduces the steel member sizes needed to carry the gravity loads and reduces the deflection due to the increased stiffness. For this study, the composite floor system, at the time of construction, is shored. This means that as the concrete is being placed on the 2-inch metal deck with 3-inch of normal weight concrete topping for a total thickness of 5 inches, the beams and girders are not supporting the weight of the wet concrete – shoring is supporting the metal deck and wet concrete. Once the concrete has cured, the steel beams, shear studs, and concrete slab work together to support its self-weight, the remaining dead load, and the live load. Without shored construction, the first considerations are can the metal deck support the wet concrete and can the beam/girder handling the weight of the concrete until it cures when composite action can be obtained. Then the remaining weight of the dead load and the full live load can be applied to the composite system. Using shored construction is typically not economical, but is used for its simplicity in the design process and to match the spans of the example building in the Seismic Design Manual 2nd Edition. The load combinations used for gravity systems are 1 through 3, with load combinations 2 or 3 governing the design depending on the live loads applied. The steel columns are not composite and the design is based on axial compression of the steel member and any bending due to unbalanced loading at the beam supports. The axial compression force that the column experiences is the result of dead and live loads applied to the composite floor system being transfer to the column.

A typical Roof, 4th, 3rd, and 2nd Floor Beam for an interior bay is a W18x35. A typical Roof Girder is a W24x62, and a typical 4th, 3rd, and 2nd Floor Girder is a W30x99. A typical interior column is a W14x68.

2.2 Lateral System

In a moment frame system, the same members that resist the gravity loads also resists the lateral loads applied to the structure. These steel members, beams and columns, are connected rigidly, moment connections, to transfer the lateral loads. These special moment frames (SMF) often are used as part of the seismic force-resisting systems in buildings designed to resist earthquakes with substantial inelastic energy dissipation. Beams, columns, and beam-column connections in steel SMF are proportioned and detailed to resist flexural, axial, and shearing actions that result as a building sways through multiple inelastic displacement cycles during strong earthquake ground shaking. Special proportioning and detailing requirements are therefore essential in resisting strong earthquake shaking with substantial inelastic behavior.

These moment-resisting frames are called SMF because of these additional requirements, which improve the inelastic response characteristics of these frames in comparison with less stringently detailed Intermediate and Ordinary Moment Frames. In order to design these frames, the seismic forces are needed.

2.2.1 Seismic Forces

When an earthquake occurs, a building is subjected to dynamic motion, inertia forces which act in opposite direction to the acceleration of earthquake excitations. These inertia forces, seismic loads, are typically assumed as forces external to the building for design purposes. The concept employed in ELFP is to place static loads on a structure with magnitudes and direction that closely approximate the effects of dynamic loading caused by earthquakes. Concentrated lateral forces due to dynamic loading tend to occur at floor and ceiling/roof levels in buildings, where concentration of mass is the highest. Furthermore, concentrated lateral forces tend to be larger at higher elevations in a structure. Thus, the greatest lateral displacements and the largest lateral forces often occur at the top level of a structure. These effects are modeled in ELPF of the IBC by placing a force at each story level in a structure.

In designing buildings, the maximum story shear force is considered to be the most influential. The seismic force the LFRS is likely to experience is determined by shear caused by the weight of the building and accidental torsional shear. The majority of what influences the seismic action due to itself weight has been discussed in the previous chapter. However, a few more variables need to be discuss: seismic response coefficient, C_s; the design spectral response for short-terms, S_{DS}; the design spectral response for long-terms, S_{D1}; the Response Modification Coefficient, R; and the approximate fundamental period of the building, T. S_{DS} represents the maximum considered ground motion with five percent damping for 0.2 second ground accelerations for a specific site that has been adjusted for site specific soil conditions and reduced for design. S_{D1} represents the maximum considered ground motion with five percent damping for 1 second ground accelerations for a specific site that has been adjusted for site specific soil conditions. S_{DS} and S_{D1} are used to determine the Seismic Design Category (SDC) and seismic analysis method, ELFP or Model Analysis (dynamic analysis), allowed by code. The response modification coefficient represents the overstrength capacity beyond the point at which the elastic response of the structure is exceeded. The value of the response modification factor always exceeds unity indicating the structures are design for forces less than would be produced in a completely elastic structure. This reduced force level is made possible by the energy absorption and displacement capacity of the structure at displacements in excess of initial yield. If a structure is capable of high energy absorption and remains stable, it is considered ductility and has a higher *R*-value. For example, a steel SMF *R*-value is 8 while a steel ordinary moment frame *R*-value is 3.5 (ASCE 7, 2010). The response modification factor is used to determine the seismic response coefficient. The seismic response coefficient is used to represent the design elastic acceleration response of a structure to the input ground motion. Three equations are used to determine C_s, each with a governing situation. Ultimately, the smallest C_s value produced will be used to determine the seismic shear; C_s is then multiplied by the effective seismic weight, the weight of the building including the weight of the gravity system. Then, the base shear is proportionally distributed, based on story mass and height above the ground level among the number of floors, giving the individual story shear. The sum of the story shears is to equal the seismic shear previously calculated.

Torsional shear that a building experiences in a seismic event is a phenomenon resulting from eccentricities caused by irregularities in the building and/or imperfect construction of the building, in addition to distribution of mass at each level. Even if the building is designed to have no irregularities, actual stiffness of the structure may be different than the theoretical which can affect the performance of building during a seismic event - accidental torsion shear is used to account for this. In order to accommodate for accidental torsional shear, a ±5% eccentricity is assumed in the building's center of gravity. Coupled with any design irregularities, the build will experience additional shear for each story during a seismic event. The first step to determining torsional shear is to determine the rigidity of the building and the eccentricity caused by the floor plan irregularities. This will result in obtaining the torsion constant, polar moment of inertia of the LFRS, J, for each floor. Next is to calculate the direct shear which is a product of the story shear, from the ASCE 7-10 seismic load calculations, and the ratio of the rigidities of the LFRS. Then use the information determined above to find the effects of accidental torsion shear. Next, determine which situation will result in the largest shear and checking the displacement as a result of the torsional shear. The total shear that the building is design to experience if the summation of the seismic forces calculated by the use of ASCE 7-10 Chapters 11 and 12 and the shear caused by torsion.

2.2.2 Preliminary RISA Design

The software used to expedite the design process is RISA 3D 12.0. It is a software that uses matrices to determine forces and deflections. When using this software, it will prompt the user to determine which codes and specifications so to know what information to pull from its data bases while performing the calculations. Before creating the model, it is a good practice to determine the units for forces, measurements and properties. The next step is to create the structural model that is to be analyzed. The model for this study is a 3 bay, 4 story SMF.

Another practice that proves advantageous, is the creation of section sets. Sections allows you to assign a member type/size to group of members draw in the model. This will save time as the need for changing individual members is eliminated. Next is to establish the nodes in the structural system. The nodes define connections between members or points of interest. Doing so, will make it easier to draw the model. Using the drawing tools provided and selecting the section set to be drawn, place the members as designated. For this study, the boundary conditions that need to be inputted into RISA is the interaction at the foundation (pinned or fixed), the end releases (for a SMF it is fully fixed at both ends), and joint reactions (for SMF set a reaction in the Z direction to prevent translation in that direction). Loads are to be placed on the members. For this study, two type of loads are placed on the SMF; joint loads and distributed loads. Seismic, roof live, live and dead loads will use both types. Seismic will be model with a joint load on each side of the 3 bay system with a horizontally distributed load along each member to the other side. The seismic force was applied to the SMFs in RISA as an unit load along the length of the moment frame beams and applied as a point load from the drag struts/collectors to the exterior SMF columns at each level. Table 2.1 indicates the seismic unit shear forces from the diaphram for the different SCDs. In a similar way, the dead, roof, and live load are placed onto the model, except they are vertical forces instead of horizontal forces. Using members designed to resist the gravity loads and placing them in the appropriate section set. The last step before running the analysis portion of the program is to input the load combinations. Since drift is determined by unfactored loads (service), the load combinations listed in Chapter 1 need to inputted twice with ultimate strength design combinations and allow stress combinations. Last, run the analysis and choose the applicable load combinations to run the program.

Table 2-1 Seismic Unit Force Summary						
Story	SDC B		SDC C		SDC D	
Roof	0.210	lb/ft	0.473	lb/ft	0.789	lb/ft
4th	0.156	lb/ft	0.351	lb/ft	0.585	lb/ft
3rd	0.103	lb/ft	0.231	lb/ft	0.382	lb/ft
2nd	0.052	lb/ft	0.116	lb/ft	0.194	lb/ft

Table 2-1 Seismic Force Summary

Chapter 3 - Inelastic Behavior - Seismic Design Checks

Severe earthquakes are rare events at average intervals of hundreds of years. Therefore, it is economically impractical to design structures to resist such severe but rare earthquakes without damage. The building codes have adopted a design philosophy intended to provide safety by avoiding earthquake-induced collapse in severe events, while permitting extensive structural and nonstructural damage. Inelastic behavior in steel SMF structures is intended to be accommodated through the formation of plastic hinges at beam-column joints and column bases. Plastic hinges form through flexural yielding of beams and columns and shear yielding of panel zones (Hamburger et al, 2009).

Structural steel SMF are designed to resist earthquakes with substantial inelastic energy dissipation. Beams, columns, and beam-column connections in steel SMF are proportioned and detailed to resist flexural, axial, and shearing actions resulting from the multiple inelastic displacement cycles during strong earthquake ground shaking. Special proportioning and detailing requirements are essential in resisting strong earthquake shaking with substantial inelastic behavior.

The results obtained in the process describe in the previous chapter verify the structural element capacities in the elastic range, but not entirely complete – the inelastic behavior needs to be checked. RISA will check, depending on the code chosen for the material used, (this study uses AISC 14th Edition) elastic compatibility. Running RISA the first time may not yield results that are acceptable for elastic performance. A few iterations may be necessary to achieve a design that meets elastic performance requirements. Once a design proves acceptable for elastic performance, design checks for desired inelastic performance begins.

The inelastic performance checks are story drift and stability, beam performance, column performance, and beam-to-column connection performance. Beam-to-column performance checks are discussed in the next chapter. Failing to meet the inelastic requirements means determining the reason for why the requirement(s) are not met, finding a member that is acceptable, and double checking that the new change does not adversely affect the elastic and inelastic performance of other members. This is an iterative process that can be very time consuming to find the most economical design. However, with enough practice, insight is gained to lessen the time consumption of the process (i.e. the designer's intuition improves). Sample calculations of this study undergoing these design checks are located in Appendix A. Specifics for elastic design checks for the RBS SMF and the KBB SMF are given in Chapters 4 and 5, respectively.

3.1 Story Drift and Stability

The RISA model checks the global stability of the structure in the elastic range. The global stability of the structure in the inelastic range is vital to prevent collapse during an extreme earthquake. Story drift when high enough can cause sidesway collapse which can occur when the effective story shear due to inertial forces and P-delta effects exceeds the story shear resistance. Inelastic structural P-delta effects is the amplification of internal forces and lateral displacements caused by the inelastic deformations, plastic hinges, which occur when a structure is simultaneously subjected to gravity loads and lateral sidesway. This effect reduces frame lateral resistance and stiffness, might cause a negative effective lateral tangent stiffness once a mechanism, plastic hinge, has formed, and can lead to collapse. Stability of the structure is imperative.

AISC Seismic Design Manual Example 4.3.1 highlights the process to check the story drift and stability of the structure. The example references ASCE 7-10 Section 12.8.6, Table 12.12-1, Equations 12.8-16 and 17. This check is in place to limit the amount each story is allow to drift and to prevent overturning of the structure. Drift is checked at service, actual, load levels. Therefore, a second set of load combinations with factors set to 1.0 (ASD load combinations) are used in the RISA model. This gives the elastic drift of the structure at the reduced seismic force level, the ELFP base shear that is distributed to each story. To take into account the actual maximum considered earthquake and inelastic behavior of the SMF, these story drifts from the RISA model are increased by the deflection amplification factor to obtain the actual story drift of the structure. Depending on the type of the SMF, additional factors may increase the story drift; these are discussed in later sections with the specific type of SMF being discussed. Using the calculated drift obtained from RISA, a comparison and an analysis can be made on whether or not the structure has drifted beyond acceptable limits. Then, incorporating the building weight and the section modulus, Z_x, of the beams on the SMF are used to find the building self-weight and the plastic moment. The plastic moment is used to toe determine the story shear. The story shear and the weight of the building are used to determine the angle of rotation at each floor. An example of drift and stability calculations is provided in Appendix A. If the members pass story drift and stability checks, then proceed to beam and column checks.

Changing one aspect of the SMF will change the performance of the entire system. Increasing one beam might mean the reduction in size of the columns. Decreasing a column size may require that all the beams will see an increase in size. A fixed connection does not rotate as a pinned connection does; meaning a pinned connection will have more deflection than a fixed connection. However, similar drift and rotations can be obtained from between the two types of foundation connections by changing beam and column sizes. Selection of beam and column sizes were first selected based on strength requirements and then selected based on stiffness requirements. This process is iterative – column sizes were selected to meet overall frame drift. Then allowable story drift is checked. The allowable story drift is affected by the building weight, the building height, the beam section modulus, and the calculated story drift. Though the calculated story drift is affected by the forces the LFRS acquires, the limitations set by ASCE 7-10 Table 12.12-1 and Section 12.8.6 prevent large story drift from occurring, and thus the designer must choose the system's members to meet these requirements. It is common for SMF beam and column sizes to increase to meet the requirements for drift and stability.

According to ASCE 7-10 Eqn. 12.8-17, for a beam member to be considered stable the member rotation for this SMF is not allowed to exceed 0.091 radians (AISC 358, 2010). The stability limitations are provided by ASCE 7-10 Eqn. 12.8-16 and Eqn. 12.8-17. For RBS connections, peak strength can be observed at rotations between 0.02 to 0.03 radians with failure occurring around 0.05 to 0.07 radians (AISC 358, 2010). For KBB, peak strength can be observed at rotations between 0.025 to 0.045 radians with failure occurring after 0.055 radians. The reason for the difference in the rotation is the rigidity of the connection. RBS is more flexible connection than the KBB. Peak strength in the RBS connection my obtained earlier than the KB, but can endure more rotation of the member. Stability requirements does not take beam-column connection type, foundation connection type, and SDC into consideration. Stability is affected by the seismic shear generated by the weight of the building, story height, weight of the building, and LFRS.

Just considering drift and stability as the only limitations for the LFRS, the designer need not be concerned with anything more than economy of the system. Finding the beam members that meet drift and stability requirements while being able to resist the applied loads. Frequently, the most economical member to resist the applied loads is not able to meet drift and stability limitations. Experience from the designer will help in determining the next most economical system that is capable of meeting drift and stability limitations and the applied loads. However, other limitations dictate which members can be used in a SMF. Inelastic behavior in steel SMF structures is intended to be accommodated through the formation of plastic hinges at beam-column joints and column bases. Plastic hinges form through flexural yielding of beams and columns and shear yielding of panel zones. Since this parametric study acknowledges beam-column connection types, foundation connection types, drift for the LFRS system will vary.

3.2 Beam, Column, and Beam-Column Connections

In steel SMFs, it is expected that beams will undergo large inelastic rotations at targeted plastic hinge locations which can have excessive local buckling or lateral torsional buckling failure modes. Each mode by itself, or the combination of both, leads to a continuous decrease in strength and stiffness. The beam-to-column connections must be capable of transferring the moment and shear forces including material overstrength and strain hardening effects that can be developed in the beam to the column; if the beam sizes have been increased to satisfy stability requirements, these forces can be very high which can cause local failure in the columns causing column sizes to be increase or the addition of plates to the column flanges and/or web. Depending on the type of beam-to-column connection used, the following failure modes can develop: fracture in or around welds, fracture in highly strained base material, fractures at weld access holes, net section fracture at bolt holes, shearing and tensile failure of bolts, bolt bearing and block shear failures. The panel zone, the part of the column where the beam frames into it, resists significant shear forces from the beams framing into a column. Acting as part of the column, it can also be subjected to significant compressive stresses. Potential failure modes of the panel zone include shear buckling and, if doubler plates are used to reinforce the panel zone, fracture at welds. Additional panel zone failure modes can include column flange bending, web crippling, and web buckling; these are associated with the direct transfer of forces from the beam flange to the column. Beyond the panel zone locations, the code intends to keep inelastic deformations out of most columns to minimize detrimental effects of high axial loads on bending behavior and potential formation of single-story mechanisms. Regardless, many columns designed in accordance with the strong-column/weak beam requirements in AISC 341might experience significant inelastic rotations in a major seismic event. Therefore, excessive local buckling and lateral-torsional buckling are potential failure modes, in addition to basic flexural buckling of columns.

Individually, for beams and columns, the section modulus proves to be most influential property of the member. The section modulus is used calculate the plastic moment or the flexural strength of the member, and moments in moment frames are high. About half of the process for checking beams and columns adequacy involve its flexural strength. For story drift and stability, the only section property that is required is the section modulus of each floor's beam. Equal to the section modulus is the slenderness of the member. Slenderness is important due to the fact that moment frames dissipate energy through the deformation of the members at locations specified by the designer. A non-slender member will not deform in order to dissipate energy, or at least not in the manner that is desire. A brittle failure may occur and the member unable to perform after a seismic event. Examples 4.3.2 and 4.3.3 in the *AISC Seismic Design Manual* 2nd Edition highlight the process for checking the adequacy of columns and beams. This process heavily references the AISC *Steel Construction Manual* 14th Edition, AISC *341Seismic Provisions for Structural Steel Buildings*, and AISC 358 *Prequalified Connections for Special and Intermediate Steel Moment Frames for Seismic Applications*.

The philosophy when designing moment frames is to have a strong column-weak beam relationship. A beam failing, having inelastic behavior (that what it is designed to do in a high seismic event), does not mean that the floor is going to fail and progressive collapse is going to occur. It means that the building can no longer be used for its original intent, but the occupants can safely exit the building after the maximum consider earthquake occurs. A column failing, on the other hand, will cause a redistribution of loads to other members. This redistribution of loads may cause over loading of members that are depending on the failed column for support, which may cause them to fail catastrophically. Thus, causing a chain reaction which could cause the building to collapse on the occupants before they have a chance to escape the building.

Chapter 4 - RBS SMF Limitations

A discussion of the limitations of the prequalified steel SMF for seismic applications using RBS is provided. Section 4.1 presents beam-to-column connection limitations. Sections 4.2 and 4.3 discuss beam and column limitations, specifically what types of members can be used in SMF while using RBS connections. These two sections deal with the selection process for acceptable members used in the RBS SMF; meaning through testing these members have performed in an acceptable manner for the use in this type of connection. Section 4.4 discusses the relationship between the beam and the column at the connection to be developed. The last two sections, 4.5 and 4.6, discuss the limitations for where the column flange is connected to the beam web and flange. The last three sections limitations are present in the design calculations of the RBS SMF connection, as they specify the specifics of the connection. The general format of this chapter is list the limitation and to provide commentary below the listed item.

4.1 Beam-to-Column Connection Limitations

The AISC 358 *Prequalified Connections for Special and Intermediate Steel Moment Frames for Seismic Applications* provide references for the use of RBS connections, which are summarized in the Chapter 5 and the Commentary. The reduction of the beam section forces encourages yielding to occur within the reduced section of the beam, an area that can sustain large inelastic strains. At the same time, the reduced section acts as a fuse, limiting stress at the less ductile region near the face of the column. These references provide insight into the performance of the RBS connection through studies that have been conducted. "Review of available test data indicates that RBS specimens presented herein, have developed interstory drift angles of at least 0.04 radians under cyclic loading on a consistent basis" and that tests show "yielding is generally concentrated within the reduced section of the beam and may extend, to a limited extent, to the face of the column. Peak strength interstory drift angles occurs around 0.02 to 0.03 radians while ultimate yielding at interstory drift angles of 0.05 to 0.07 radians. "RBS connections have been tested using single-cantilevered type specimens and double-side specimens." Tests with composite slabs have shown that the presence of the slab provides a beneficial effect by helping to maintain the stability of the beam at larger interstory drift angles."

In Figures 4-1 and 4-2, illustrates a RBS connection. Figure 4-1 is a top view of the connection. The top view exemplifies the location of the RBS in the beam. The range/limitation of the amount of reduction of the beam flange and the location of the RBS have been determined through numerous tests (Englehardt et al., 1996). The *Seismic Design Manual* 2nd Edition allows three methods of reducing the beam section: a straight reduced segment, and angularly tapered, and a circular reduced section. It is typical that the RBS be manufactured with a circular reduced segment and that higher ductility has been noted in its use (Engelhardt et al., 1997). As shown in Figure 4-1, the distance from the column flange to the start of the beam flange reduction, a, can vary from $0.5b_{bf}$ to $0.75b_{bf}$ where b_{bf} is the width of the beam flange; the length of flange cut, b, can vary from $0.65d$ to $0.85d$ where d is the depth of the beam; and the depth of the beam flange reduction on both sides, c, can vary from $0.1b_{bf}$ to $0.25b_{bf}$. Englehardt, Winneberger, Zekany & Potyraj (1998) found that these ranges had ductile performance during testing. If the columns are deep wide flange sections with lighter weights or the reduced beam is capable of directly transferring high forces from the beam flange to the column, local column flange bending, local column web yielding, and local column web crippling, panel zone failures, can occur prior to the reduce beam section fusing. Continuity plates can be added to the column to prevent these types of failures. The continuity plates in between the column flanges are at least the thickness of the beam flange. Determining the need for continuity plates requires satisfying two equations (FEMA, 2000):

$t_{cf} \geq 0.4\sqrt{1.8 b_{bf} t_{bf} R_{yb} F_{yb} / (R_{yc} F_{yc})}$ AISC 341 Eqn. E3-8

$t_{cf} \geq b_{bf}/6$ AISC 341 Eqn. E3-9

It is highly probable that continuity plates are may be need in the connection. Transverse stiffeners, continuity plates, are extremely labor-intensive detail materials due primarily to the fit-up and welding that is associated with their use. Additionally, issues such as restraint, lamellar tearing and welding sequence must be addressed when continuity plates are used. As such, they add considerable cost in spite of their disproportionately low material cost. If continuity plates can be eliminated by increasing the column size, cost savings can often be realized. Based on ASIC *Design Guide 13 Stiffening of Wide-Flange Columns at Moment Connections: Wind and Seismic Applications* (1999), full-depth, 3/4"-inch thickness, transverse stiffeners with corner clips each (two pairs) made of ASTM A36 steel is equivalent to 55 pounds per lineal feet (plf) of column. In other words, increasing the column size less than 55 plf and eliminating continuity plates is more economical than the addition of continuity plates on the original column. In this study, continuity plates were required. When the column web thickness is inadequate to resist the required panel-zone shear strength including the effect of inelastic panel-zone deformation on frame stability, a web doubler plate is required, but typically avoided for economy. Doubler plates are needed to increase the column panel zone shear strength. Increasing the column size between 70 plf to 120 plf may avoid the need for doubler plates.

Beyond this, the cost of the added material in the column will exceed the cost of the welding requirements (Carter, 1999).

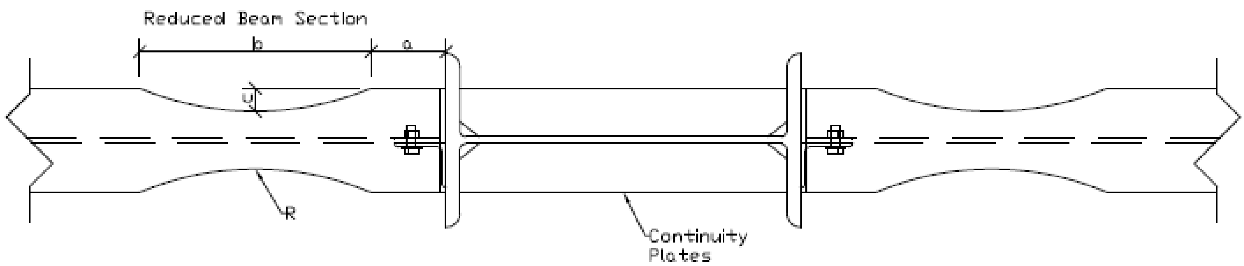

Figure 4-1 RBS Connection Top View

The single shear plate connects the beam and column together. Lee and Kim (2004) research on RBS steel moment connections showed that specimens with a bolted web connection performed poorly due to premature brittle fracture of the beam flange at the weld access hole. "The measured strain data appeared to imply that a higher incidence of base metal fracture in specimens with bolted web connections is related to, at least in part, the increased demand on the beam flanges due to the web bolt slippage and the actual load transfer mechanism which is completely different from that usually assumed in connection design." They confirmed that the load transfer mechanism in the connection is completely different from that universally assumed in the simple shear connection design. The single-plate connection adds stiffness to the beam web connection, drawing stress toward the web connection and away from the beam flange to column connections. The results of their study gives the practice of providing full-beam-depth shear plate with CJP groove welds to the column and slip-critical web bolts uniformly spaced along the beam depth based on the beam shear. The single plate also serves as backing for the CJP groove weld connecting the beam web to the column flange. The slip-critical design of the web bolt group is based on the eccentric horizontal and vertical force components at the interface between the shear tap and the column flange which is much higher than that from the conventional design method (Kim and Lee, 2004).

Sections cut from the beam web, as depicted in Figure 4-2, are weld access holes. Instead of using a conventional weld access hole detail as specified in Section J1.6 of ANSI/AISC 360 AISC Specification, the moment connection employs a special seismic weld access hole with requirements on size, shape, and finish that reduce stress concentrations in the region around the access hole. Figure 4-2 also shows the beam flanges welded to the column flange using CJP groove welds that meet the requirements of demand critical welds in the *AISC Seismic Provisions*, along with specific requirements for treatment of backing and weld tabs and welding quality control and quality assurance requirements.

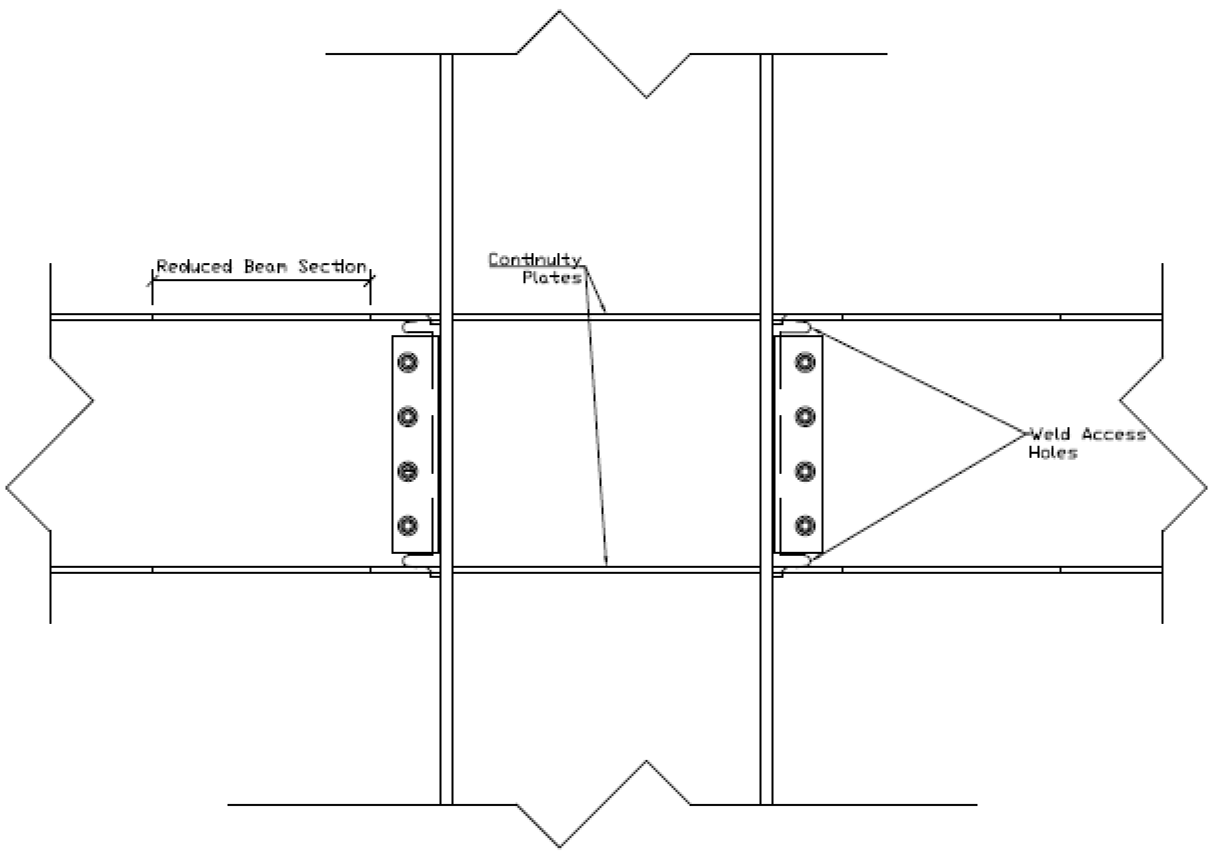

Figure 4-2 RBS Connection Side View

4.2 Beam Limitations

Since these are prequalified SMF with RBS frames, the beams must meet the AISC 358 *Prequalified Connections for Special and Intermediate Steel Moment Frames for Seismic Applications* Section 5.3.1 and Comm. 5.3.1:

1. Beams must be rolled wide-flange or built-up I-shaped members conforming to Section 2.3.
2. Beam depth is limited to W36 for rolled shapes.
3. Beam weight is limited to 300 plf.
4. Beam flange thickness is limited to 1-¾ inches.

The above four limitations are to limit the maximum size of the member that is used in the design of a RBS connection. It is through testing that found that the "adherence" to the use of members at or lower than a W36x300 will produce an "appropriately conservative" design.

5. For SMF systems, the clear span-to-depth ratio of the beam is limited to 7 or greater. In the inelastic behavior of beam-to-column connections, beam depth and beam span-to-depth ratio play a significant role. Deep beams experience greater strains than shallower beams for the same induced curvature. Beams with shorter span-to-depth ratio have a sharper moment gradient across their span, resulting in reduced length of the beam participating in plastic hinging and increased strains under inelastic rotation demands.
6. Width-to-thickness ratios for the flanges and web of the beam shall conform to…"When determining the width-to-thickness ratio of the flange, the value of b_f shall not be taken as less than the flange width at the ends center two-thirds of the reduced section provided that gravity loads do not shift the location of the plastic hinge a significant distance from the center of the reduced beam section." This is intended to allow some plastic rotation

of the beam to occur before the onset of local buckling of the flanges. Buckling of most of the beam flanges in a moment resisting frame results in development of frame strength degradation increasing both story drifts and the severity of P-delta effects and should be avoided. Local flange buckling results in large local straining of the flanges and the early on-set of low-cycle fatigue induced tearing of the beam flanges, which ultimately limits the ability of the assembly to withstand cyclic inelastic rotation demands.

7. "Lateral bracing of beams shall be provided in conformance with the AISC Seismic Provisions. Supplemental lateral bracing shall be provided near the reduced section in conformance with the AISC Seismic Provisions for lateral bracing provided adjacent to the plastic hinges." Engelhardt et al. (1998) research indicated each of the specimens had a gradual deterioration of strength occurring due to local flange and web buckling combined with lateral torsional buckling of the beam. For predictable performance of SMF with RBS, lateral bracing is required. Based on Jones, Fry and Engelhardt (2002) when this lateral bracing of the beam should be within the half the beam depth beyond the end of the reduced beam section farthest from the face of the column. Attachments of lateral bracing cannot be within the protected zone, the region extending from the flange (face) of the column to the end of the reduced beam section farthest from the face of the column. Lateral bracing is used to combat lateral-torsional buckling at the narrower beam section.

8. The protected zone consists of the portion of beam between the face of the column and the end of the reduced beam section cut farthest from the face of the column. Nonlinear deformation of frame structures is accommodated through the development of inelastic flexural or shear strains within discrete regions of the structure, fuses. At large inelastic

strains these regions, fuse locations, can develop into plastic hinges that can accommodate significant concentrated rotations at nearly constant load through yielding at tensile fibers and yielding and buckling at compressive fibers. If other members are connected within the protected zone, the plastic hinge may not develop preventing seismic energy dissipation.

4.3 Column Limitations

The approach to seismic design of steel columns in SMF is to keep inelastic deformations out of most columns to minimize detrimental effects of high axial loads on bending behavior and potential formation of single-story mechanisms. Nevertheless, many columns designed in accordance with the strong-column/weak-beam requirements in AISC 341 *Seismic Provisions for Structural Steel Buildings* may experience significant inelastic rotations in a major seismic event. Producing excessive local buckling and lateral-torsional buckling as potential failure modes, in addition to basic flexural buckling of columns. AISC 358 *Prequalified Connections for Special and Intermediate Steel Moment Frames for Seismic Applications* Section 5.3.2 and Comm. 5.3.2 states:

1. Columns can be any of the rolled shapes or built-up sections meeting the requirements of Section 2.3.
2. Beams are to connect into the flange of the column. Very little testing has occurred on weak-axis bending since this type of system is uneconomical when considering story drift and stability requirements of a structure. In the absence of more tests, it is recommended limiting prequalification to strong-axis connections only.
3. Rolled shapes column depth are limited to W36 maximum. The majority of RBS specimens were constructed with W14 columns. Testing of deep-column RBS under the

Federal Emergency Management Agency/Special Agency in Charge (FEMA/SAC) program indicated that stability problems may occur when RBS connections are used with deep beams without composite slab or in the absence of adequate bracing.

4. Width-to-thickness ratios for the flanges and webs of columns shall conform to the requirements of the AISC 341 *Seismic Provisions for Structural Steel Buildings*. Reliable inelastic deformation requires that width-thickness ratios of compression elements be limited to a range that provides a cross section resistant to local buckling into the inelastic range.
5. Lateral bracing of columns shall conform to the requirements of the AISC 341 *Seismic Provisions for Structural Steel Buildings.*

4.4 Column-Beam Relationship Limitations

AISC 358 *Prequalified Connections for Special and Intermediate Steel Moment Frames for Seismic Applications* Section 5.3.3 and Comm. 5.3.3 require:

1. Panel zones are required to conform to AISC 341 Seismic Provisions *Seismic Provisions for Structural Steel Buildings*. The joint panel zone resists significant shear forces from the beams framing into a column. Since it is part of the column, it can also be subjected to significant compressive stresses. As these shear forces increase, a panel zone starts to yield at its center. Consequently, yielding propagates towards the panel zone corners. Very weak panel zones may promote fracture in the vicinity of the beam-flange groove welds due to "kinking" of the column flanges at the boundaries of the panel zone. Therefore, a minimum panel zone strength is specified in Section E3.6e of the Seismic Provisions.

2. Column-beam moment ratios for SMF systems are limited to having the column-beam moment ratio conforming to the requirements of the AISC 341 *Seismic Provisions for Structural Steel Buildings*. As shown in Figure 4-3, the value of ΣM^*_{pb} shall be taken equal to $\Sigma(M_{pr} + M_{uv})$, where M_{pr} is the computed according to Equation 5.8-5, and where M_{uv} is the additional moment due to shear amplification from the center of the reduced beam section to the centerline of the column. M_{uv} can be computed as $V_{RBS}\,(a + b/2 + d_c/2)$, where V_{RBS} is the shear at the center of the reduced beam section computed per Step 4 of Section 5.8, a and b are the dimensions show in Figure 5.1, and d_c is the depth of the column. Figure 4-3 is a free body diagram of the forces.

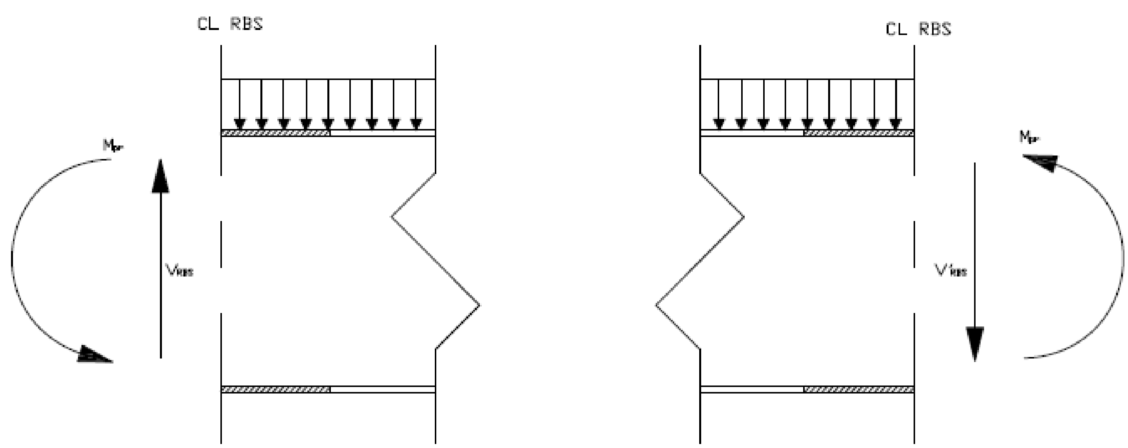

Figure 4-3 RBS Free Body Diagram

These requirements are to achieve strong-column/weak-beam system. It is desirable to dissipate earthquake induced energy by yielding of the beams rather than the columns which are responsible of the overall strength and stability of the structure. Therefore, it is preferable to control inelasticity in columns while dissipating most of the energy through yielding of the beams. The larger the ratio $\Sigma M_{pc}^*/\ \Sigma M_{pb}^*$, it is the less likely plastic hinges will form in columns.

4.5 Beam Flange-to-Column Flange Weld Limitations

AISC 358 *Prequalified Connections for Special and Intermediate Steel Moment Frames for Seismic Applications* Section 5.3.4 and Comm. 5.3.4:

1. Column flanges-to-beam flanges are connected using complete-joint-penetration (CJP) groove welds. Beam flange welds shall conform to the requirements for demand critical welds in the AISC 341 Seismic Provisions. Demand-critical welds require increased quality and toughness requirements based upon inelastic strain demand and the consequence of failure.
2. Weld access hole geometry must meet the requirements of the AISC Seismic Provisions. Instead of using a conventional weld access hole, the SMF with RBS connection employs a special seismic weld access hole with requirements on size, shape, and finish that reduce stress concentrations in the region around the access hole, although test specimens have employed a range of weld access-hole geometries, and results suggest that connection performance is not highly sensitive to weld access-hole geometry.

4.6 Beam Web-to-Column Flange Connection Limitations

AISC 358 *Prequalified Connections for Special and Intermediate Steel Moment Frames for Seismic Applications* Section 5.3.5 and Comm. 5.3.5:

1. "The required shear strength of the beam web connection shall be determined according to Equation 5.8-9." The equation is $V_u = (2M_{pr}/L_h) + V_{gravity}$, and it is used to check the design shear strength of the beam.
2. Web connection details for SMF systems are limited to the beam web connected to the column flange using a CJP groove weld that extends the full-depth of the web (that is, from weld access hole to weld access hole). The single plate shear connection can be used as backing for the CJP groove weld. A minimum of 3/8-inch plate is required. Weld tabs are not required at the ends of the CJP groove weld at the beam web. Bolt holes in the beam web for the purpose of erection are permitted. The single-plate connection adds stiffness to the beam web connection, drawing stress toward the web connection and away from the beam flange to column connections to minimize the potential for crack-initiation at the end of the welds. Until further data is available, a welded web connection is required for RBS connections prequalified for use in SMF.

Chapter 5 - KBB Connection Limitations

The Kaiser Bolted Bracket® (KBB) is a beam-to-column moment connection that consists of proprietary cast high-strength steel brackets fastened to the flanges of a beam and bolted to a column. This moment connection is designed to eliminate field welding in steel MF construction. The cast Kaiser brackets are manufactured in a variety of sizes. These brackets are proportioned to develop the probable maximum moment capacity of the connecting beam. When subjected to cyclic inelastic loading, yielding and plastic hinge formation occur primarily in the beam near the end of the bracket, thereby eliminating inelastic deformation demands at the face of the column.

KBB increased in popularity after the 1994 Northridge earthquake. According to the article in the KBB Engineering Journal, Experimental Evaluation of Kaiser Bolted Bracket Steel Moment Resisting Connections by Scott M. Adan and William Gibb and FEMA 350 2000, its use was investigated as an alternate means of repairing weak or damage moment frame connections in lieu of repairing the damage welds with more welding. The fractures in the CPJ welds were caused by "poor welding procedures, including the use of filler metals with inherent low toughness, uncontrolled deposition rates and inadequate quality control; connection design and detailing that led to larger moment-frame members, less system redundancy and higher strain demands on the connections: the use of higher strength girders, leading to unintentional undermatching of the welds; and a number of other connection detailing and construction practices that were typical prior to the earthquake." Using KBB proved to be an economical alternative as it reduced the demand for weld repairs in confined locations and in difficult welding positions (welding labor and inspections), reduced/eliminated the need for ventilation due the build-up gases during the welding process for retrofit work, and the bracket serves as a template for drilling bolt holes into the flanges of the beams and columns.

A discussion of the limitations of the prequalified steel SMF for seismic applications using KBB is provided in this chapter. Section 5.1 presents beam-to-column connection limitations. Sections 5.2 and 5.3 discuss beam and column limitations, respectively. These two sections deal with the selection process for acceptable members used in the KKB SMF. Section 5.4 discusses the relationship between the beam and the column at the connection to be developed. The last two sections, 5.5 and 5.6, discuss the limitations for where the column flange is connected to the beam web and flange. The last three sections limitations are present in the design calculations of the KBB SMF connection, as they specify the specifics of the connection. The general format of this chapter is list the limitation and to provide commentary below the listed item.

5.1 Connection Limitations

Brackets are classified into two types: the W-series and B-series. The W-series is a bolt-weld combination bracket - bolted to the column flange and welded to the beam flange. The B-series is bolt-bolt combination bracket - bolted to both the column flange and the beam flange. The W-series is typically used in new construction while the B-series is typically used in retrofit construction. KBB connections are similar to RBS connections in that they encourage inelastic deformation of the beam to occur a distance, *d*, from the beam-column connection. Unlike RBS connection, reducing the section properties of the beam a distance away from the connection, KBB increases the stiffness of the beam near the beam-column connection, and the inelastic deformation occurs at the end of the bracket. Energy dissipation is through the formation of the plastic hinges in the beams. The addition of a composite concrete floor system increases the stability of the beam and decreases the degradation of strength. In the AISC 358 *Prequalified Connections for Special and Intermediate Steel Moment Frames for Seismic Applications* Chapter 9, peak strength of the system was achieved between an interstory drift of 0.025 to 0.045 radians.

Figures 5-1 and 5-2 are the top and side views of a typical KBB connection. The brackets are placed on top and bottom of the beam. For the connection displayed, the bracket is from the W-series as it is welded to the beam flange. If it were a B-series bracket, it would be bolted to the beam flange. The series available for use is determined by the beam flange width. The minimum beam flange width for the W-series is 6 inches, and the minimum for the B-series is 10 inches. An additional benefit of KBB is that the bracket serves as a template for drilling bolt holes which are not permitted to be made by any other method. The need for continuity plates are determined differently for KBB. To eliminate the need for continuity plates, this equation AISC 358 Eqn 9.9-7 must be satisfied otherwise continuity plates are necessary.

$$t_{cf} \geq \sqrt{M_f/(\theta_f F_{yf} d_{eff} Y_m)} \qquad \text{AISC 358 Eqn. 9.9-7}$$

Meeting this condition only applies to column sizes of W14 or smaller. Otherwise, continuity plates are required regardless if this condition is met. The simplified column flange yield line mechanism parameter is determined by the bracket used in the connection. The larger Y_m/bracket size the thinner required column flange.

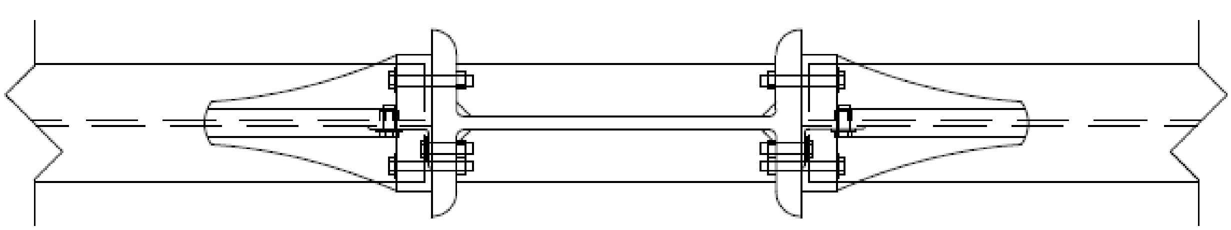

Figure 5-1 KBB Connection Top View

Part of the connection is a single shear plate connection. In Figure 5-2, it is connected to the beam using bolts and connected to the column using welds. This is one of the limitations that is discussed later in this chapter in the *Beam Web-to-Column Connection Section*.

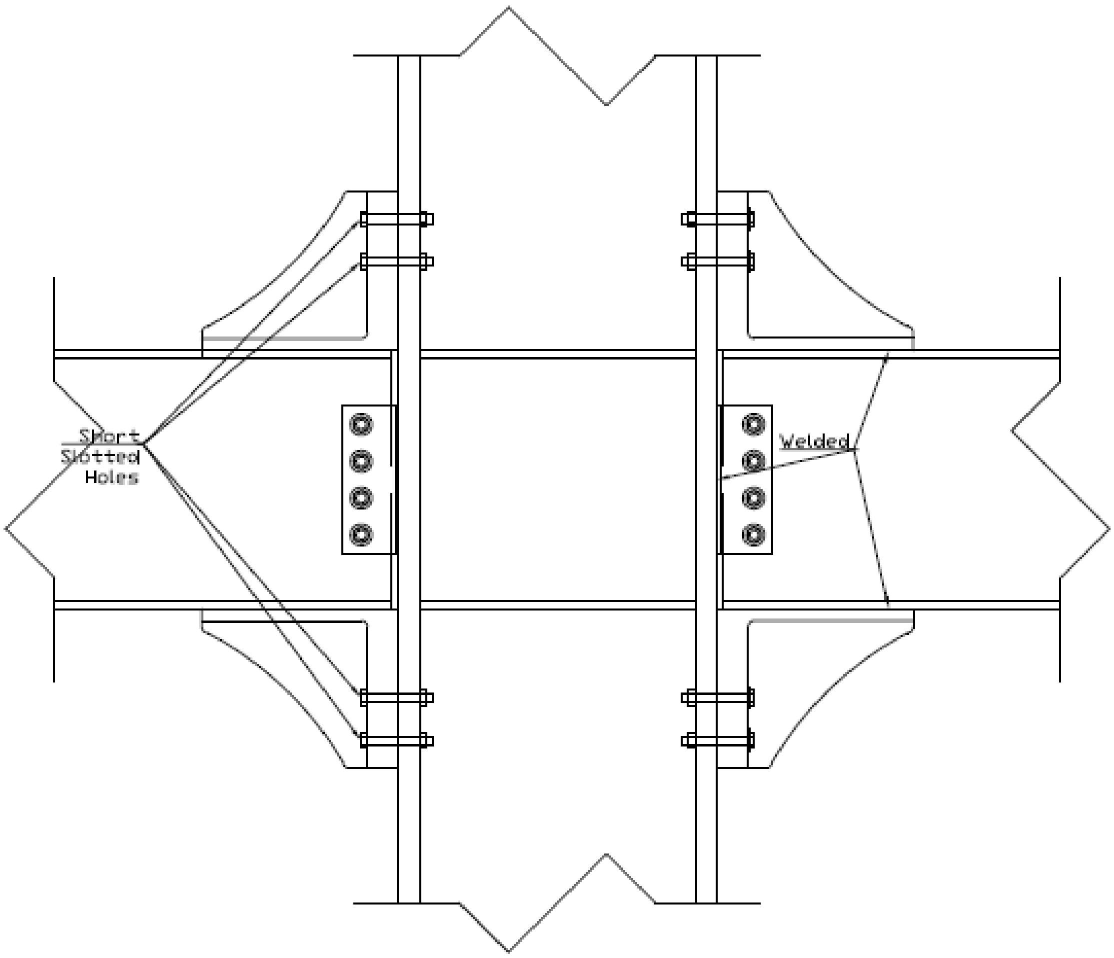

Figure 5-2 KBB Connection Side View

5.2 Beam Limitations

AISC 358 *Prequalified Connections for Special and Intermediate Steel Moment Frames for Seismic* Section 9.3.1 and Commentary state the following beam limitations:

1. Similar to SMF-RBS, beams can be rolled shapes wide-flanged or built-up I-shaped members meeting the requirements of Section 2.3. Of the sizes tested, the lightest is a W16x40 and the heaviest is a W36x210.
2. Maximum beam depth is W33 for rolled shapes. Though the W36x210 section met requirements, the commentary in the Seismic Design Manual 2nd Edition. States that a W36x210 was test but “subsequently experienced an unexpected nonductile failure of the bolts connecting the brackets to the column.”
3. Maximum beam weight is 130 plf. The maximum size that meets the requirements of KBB is the W33x130.
4. Maximum beam flange thickness is 1 inch. The maximum flange thickness was established to match a modest increase above that of the W36x150.
5. Minimum beam flange width is 6 inches for W-series brackets and at least 10 inches for B-series brackets. The minimum width for the beam flange is to accommodate the flange welds for the W-series and tensile rupture of B-series.
6. The clear span-to-depth ratio is limited to 9 or greater for both SMF and IMF systems. Since tests used beam spans between 24 ft. to 30 ft. and the span-to-depth ratios were between 8 and 20, “it was judged reasonable to set the minimum span-to-depth ratio at 9 for both SMF and IMF.”
7. Width-to-thickness ratios for the flanges and web of the beam must conform to the requirements of the AISC 341 *Seismic Provisions for Structural Steel Buildings*. This is to ensure the beam flange and beam web will perform in a ductile manner.
8. To prevent a gradual deterioration of strength due to local flange and web buckling combined with lateral torsional buckling of the beam, lateral bracing of beams must

be provided. For SMF, lateral bracing must be provided at the expected plastic hinge location. This bracing need to meet the requirements of AISC 341 *Seismic Provisions for Structural Steel Buildings*. The attachment of supplemental lateral bracing to the beam must be located at a distance *d* to 1.5*d* from the end of the bracket farthest from the face of the column, where *d* is the depth of the beam. No attachment of lateral bracing can be made in the protected zone - the region extending from the face of the column to a distance of *d* beyond the end of the bracket. A concrete structural slab aids in the stability of the beam which may be stiff enough to eliminate the need for supplemental bracing.

5.3 Column Limitations

AISC 358 *Prequalified Connections for Special and Intermediate Steel Moment Frames for Seismic* Section 9.3.2 and Commentary state the following column limitations.

1. Similar to SMF-RBS, columns can be rolled shapes wide-flanged or built-up I-shaped members meeting the requirements of Section 2.3.
2. Similar to SMF-RBS, the beam must connect to the flange of the column. Due to the lack of test data on the performance KBB attached to the web (weak axis) of the column, KBB are to be attached to flange of the column.
3. Column flange width must be a minimum of 12 inches due to the size of bracket needed for connections.
4. W36 is the maximum column size, width, when a concrete structural slab is provided. Without the concrete structural slab, W14 is the maximum column size. Deeper

columns, W36, behave similar to shallower columns, W14, when a concrete structural slab is present.

5. Column weight is not limited.
6. Column flange thickness has no additional requirements.
7. Columns need to be seismically compact, width-to-thickness ratios for the flanges and web of columns must meet the requirements of the AISC 341 *Seismic Provisions for Structural Steel Buildings*. This is to ensure the beam flange and beam web will perform in a ductile manner.
8. Similar to SMF-RBS, lateral bracing of columns shall conform to the requirements of the AISC 341 *Seismic Provisions for Structural Steel Buildings.*

5.4 Bracket Limitations

AISC 358 *Prequalified Connections for Special and Intermediate Steel Moment Frames for Seismic* Section 9.3.3 and Commentary state the following bracket limitations.

1. Bracket castings must be made of cast steel grade meeting ASTM A958 Grade SC8620 class 80/50 in addition to meeting the quality control and manufacturer document requirements in Appendix A of AISC 358. The manufacture of the brackets "is based on recommendations from the Steel Founders' Society of America (SFSA).
2. Bracket configuration and proportions must meet the requirements Section 9.8 Connection Detailing. The configuration and proportion of the brackets resist prescribed limit states: column flange local buckling, bolt prying action, combined

bending and axial loading, shear, and for B-series, bolt bearing deformation and block shear rupture.

3. To allow for tolerances during construction, vertical short-slotted holes are provided in the bracket for the column bolts and standard holes are provided for the beams.
4. Material thickness, edge distance, and end distance are allowed a tolerance of ± 1/16 inch. The location of a hole is allowed a tolerance of ± 1/16 inch. Bracket overall dimensions have a tolerance of ± 1/8 inch.

5.5 Column-to-Beam Relationship Limitations

AISC 358 *Prequalified Connections for Special and Intermediate Steel Moment Frames for Seismic* Section 9.4 and Commentary state the following column-to-beam limitations.

1. Similar to SMF-RBS, panel zones must meet the requirements in the AISC 341 *Seismic Provisions for Structural Steel Buildings.*
2. Similar to SMF-RBS, column-beam moment ratios shall conform to the requirements of the AISC *Seismic Provisions for Structural Steel Buildings.* Testing has indicated that the reduction of column axial and moment strength due to the column bolt holes is minimal; therefore, need not be considered when checking column-beam moment ratios.

5.6 Bracket-to-Column Flange Limitations

AISC 358 *Prequalified Connections for Special and Intermediate Steel Moment Frames for Seismic* Section 9.5 and Commentary state the following bracket-to-column limitations for wide flange columns connected to wide flange beams:

1. Column flange fasteners must be pretensioned ASTM A490, A354 Grade BD bolts, or A354 Grade BD threaded rods, and must meet the installation requirements of AISC 341 and RCSC Specification, and the quality control and quality assurance in accordance with AISC 341. When possible, column bolts are tightened prior to the bolts in the web shear tab which is similar to testing.
2. Column flange bolt holes are drilled or subpunched and reamed and 1/8 inch larger than the nominal bolt diameter. Punched holes are not permitted.
3. The use of finger shim on either or both sides at the top and/or bottom of the bracket connection is permitted, subject to the limitations of the Research Council on Structural Connections (RCSC) Specification. Finger shims did not affect the performance of the connection during testing.

5.7 Bracket-to-Beam Flange Connection Limitations

AISC 358 *Prequalified Connections for Special and Intermediate Steel Moment Frames for Seismic* Section 9.6 and Commentary state the following bracket-to-beam limitations for wide flange columns connected to wide flange beams:

1. When welding the bracket to the beam flange, fillet welds must be used which conform to the requirements for demand critical welds in the AISC 341 and AWS D1.8, and to the requirements of AWS D1.1. The weld procedure specification (WPS) for the fillet weld joining the bracket to the beam flange must be qualified with the casting material. Cast bracket are not a prequalified material causing the WPS for the fillet weld joining the bracket and beam is required to be qualified by test with specific cast material. In

order to prevent weld failures, welds must not be started or stopped within 2 inches of the bracket tip and must be continuous around the tip.

2. When bolting the bracket to the beam flange, fasteners must be pretensioned ASTM A490 bolts with threads excluded from the shear plane and must meet the installation requirements of AISC 341 and RCSC Specification, and the quality control and quality assurance in accordance with AISC 341.
3. Beam flange bolt holes are 1-5/32 inches and drilled using the bracket as a template. Doing this ensures that bolt holes are aligned and threads of bolts are not damage.
4. When bolted to the beam flange, a 1/8 inch-thick brass, half-hard tempered ASTM B19 or B36 sheet, washer plate with an approximate width and length matching that of the bracket contact surface area is placed between the beam flange and the bracket. According AISC 358, tests indicated when the plate washer was not brass flange net section rupture through outermost bolt holes occurred. The brass plate provides a smooth slip mechanism at the bracket-to-beam interface acting as special friction-based seismic energy dissipater.
5. When bolted to the beam flange, 1 inch-thick by 4 inch-wide ASTM A572 Grade 50 plate washer is used on the opposite side of the connected beam flange. Local flange buckling near the outermost bolt holes is prevented by the restraining force of the clamp plate. During testing without the plate, the increased strain caused necking and fracture through the flange net area and with the clamp plate, yielding and fracture occurred outside the connected region.

5.8 Beam Web-to-Column Connection Limitations

AISC 358 *Prequalified Connections for Special and Intermediate Steel Moment Frames for Seismic* Section 9.7 and Commentary state the following beam web-to-column limitations for wide flange columns connected to wide flange beams:

1. The required shear strength of the beam web connection is based on the probable maximum moment, M_{pr}, at the location of the plastic hinge plus the beam shear force resulting from the load combination of 1.2D+L+0.2S.
2. The single-plate shear connection is connected to the column flange using a two-sided fillet weld, two-sided PJP groove weld, or CJP groove weld. High-strength bolts were used in all of the bolted bracket connection tests.

Chapter 6 - Parametric Study Results

As described in Section 1.1, a comparison of a three-bay, SMF-RBS and SMF-KBB for a 4-story building was performed. This chapter is devoted to the discussion of the results acquired from designing the SMF for the SDC B, C and D. The results from pinned and fixed foundation assumptions and the two types of column-to-beam connections, RBS and KBB, are included. A brief discussion on how the data presented in the tables was determined and the changes made is presented. The original members for this set of trials were determined by the use of structural analysis with the applied gravity loads, then these members were increased for the resistance of lateral loads. RISA 3D was used to refine the member sizes and to determine the member forces and interstory drift. In the RISA model, the beams are labeled Roof Beam, 4^{th} Beam, 3^{rd} Beam, and 2^{nd} Beam. The columns are split into four groups: the columns above the splice are designated U, for upper; the columns below the splice are designated with L, for lower; the columns located on the outside of the three-bay system have a designation of O, for outer; and the columns on the inside of the three-bay frame have a designation of I, for inner. Results from the iterations performed are shown in Appendix B.

The initial member sizes typically need to be increased in size to meet the elastic combined loading checks and must be reiterated before the seismic design checks can be made. They must perform in the desired manner elastically before they can be check for the desired performance inelastically. After the members meet strength requirements, the frames need to meet inelastic behavior requirements – stability and interstory drift. While checking the frames for stability and interstory drift, it proved efficient to find members that met interstory drift, beam, column, and connection limitations simultaneously instead of making changes individually. This method reduce the number iterations in the RISA 3D model and the creation of the data tables for the results from RISA 3D. It was also observed that the change in the member forces while making these "mini" iterations was 10% or less than previous determined values. The possibility of this change in the member forces was taken into account during member selection.

After the first recorded trial, the system failed interstory drift and stability checks. The interstory drift and stability checks are largely dependent on gravity loads, the calculated drift, and the Z_x sectional property of the beam (stiffness of the frame). The gravity loads do not change, and the calculated drift will change when the beams and columns change. To meet the interstory drift and stability checks, the focus is to find a beam with Z_x sectional property that would produce the desired results.

As designing the SMF is an iterative process and finding the most economical design can be time consuming, there came a point in the analysis process where it was decided to keep the columns the same and only change the beam sizes. Changing one aspect of the frame will yield a completely different performance. Keeping the columns unchanged (unless required by the seismic design checks) is a way to limit the variance in the performance of the SMF. The final results after this point are presented in this chapter, and the iterations after this decision are provided in Appendix B.

6.1 Pinned RBS SDC B

The initial beam members used are a W18x40 for the Roof, 4th, and 3rd Beam and a W21x40 for the 2nd Beam. Meeting interstory drift and stability requirements led to the use of W24x76, from W18x40 for the Roof Beam, 4th Beam, and 3rd Beam and a W21x62 for the 2nd Beam, for the roof, 4th, 3rd, and 2nd floor beams. After running RISA 3D to acquire the new member forces and drift and recording the new data, the RBS connection checks required doubler plates be added to the column web of UO and UI columns. To eliminate the need for doubler plates, the size of UO and UI columns were increased in size from W30x116 to W30x132. The final results for the pinned SMF RBS for SDC B are presented in Table 6-1.

RBS Connection: Seismic category B Trial #3										
Member	Member Size	Joint Deflection		Axial Load		Shear Load		Moment Load		
Roof Beam	W24x76	1.678	in	15.681	k	14.671	k	115.28	kft	
4th Beam	W24x76	1.455	in	5.591	k	28.347	k	210.47	kft	
3rd Beam	W24x76	1.115	in	5.158	k	31.757	k	262.14	kft	
2nd Beam	W24x76	0.664	in	9.447	k	35.09	k	308.66	kft	
UO Column	W30x132	-	in	95.01	k	35.419	k	416.18	kft	
UI Column	W30x132	-	in	64.601	k	56.254	k	520.85	kft	
LO Column	W30x211	-	in	251.04	k	54.79	k	767.06	kft	
LI Column	W30x211	-	in	152.26	k	76.26	k	973.67	kft	

Table 6-1 Pinned RBS Connection SDC B Trail #3

6.2 Pinned KBB SDC B

The initial beam members used are a W18x40 for the Roof, 4th, and 3rd Beam and a W21x62 for the 2nd Beam. The initial column sizes are W24x207 for UO and UI columns and W24x250 for LO and LI columns. Similar to the SMF-RBC SDC B, meeting interstory drift and stability requirements led to the use of W24x76 members for the Roof, 4th, and 3rd Beam and W24x84 member for the 2nd floor. Upon running RISA 3D and double checking the seismic design checks for the member and the connection, no further iterations were needed to be performed. UO and UI columns are the same and experience no change from a W24x207. LO and LO columns are the same and experience no change from a W24x250. The final results for the pinned SMF KBB for SDC B are presented in Table 6-2.

Kaiser Connection: Seismic Category B Trial #2										
Member	Member Size	Joint Deflection		Axial Load		Shear Load		Moment Load		
Roof Beam	W24x76	1.626	in	15.951	k	14.755	k	116.92	kft	
4th Beam	W24x76	1.408	in	5.225	k	28.141	k	207.9	kft	
3rd Beam	W24x76	1.089	in	5.422	k	31.034	k	251.32	kft	
2nd Beam	W24x84	0.662	in	9.49	k	35.991	k	320.7	kft	
UO Column	W24x207	-	in	94.93	k	36.346	k	416.07	kft	
UI Column	W24x207	-	in	64.421	k	54.866	k	516.71	kft	
LO Column	W24x250	-	in	251.13	k	54.422	k	761.91	kft	
LI Column	W24x250	-	in	152.74	k	76.476	k	974.95	kft	

Table 6-2 Pinned KBB Connection SDC B Trail #2

6.3 Fixed RBS SDC B

The base connection was changed from a pinned connection (results given in Section 6.1) to a fixed connection to reduce the interstory drift from the base to the first elevated level (2nd floor). The initial beam members used are a W18x40 for the Roof, 4th, and 3rd Beam and a W21x62 for the 2nd Beam. The initial column sizes are W30x108 for UO and UI columns and W30x148 for LO and LI columns. Meeting inelastic stability requirements, interstory drift and stability, led to the use of W24x62 for the Roof Beam and the 4th Beam, W24x55 for the 3rd Beam, and aW21x62 for the 2nd Beam. UO and UI columns are the same and experience no change from a W30x108. LO and LO columns are the same and experience no change from a W30x148. The final results for the pinned SMF KBB for SDC B are presented in Table 6-3.

RBS Connection: Seismic Category B Trial #2									
Member	Member Size	Joint Deflection		Axial Load		Shear Load		Moment Load	
Roof Beam	W24x76	1.218	in	15.488	k	14.208	k	108.8	kft
4th Beam	W21x68	0.958	in	3.859	k	27.227	k	194.07	kft
3rd Beam	W21x62	0.603	in	2.537	k	27.819	k	203.96	kft
2nd Beam	W18x40	0.231	in	5.395	k	27.079	k	190.63	kft
UO Column	W24x192	-	in	90.437	k	39.414	k	329.97	kft
UI Column	W24x192	-	in	64.414	k	52.282	k	401.32	kft
LO Column	W24x229	-	in	210.94	k	59.057	k	877.05	kft
LI Column	W24x229	-	in	150.65	k	64.623	k	899.77	kft

Table 6-3 Fixed RBS Connection SDC B Trail #2

6.4 Fixed KBB SDC B

Similar to the SMF-RBS, the base connection was changed from a pinned connection (results given in Section 6.2) to a fixed connection to reduce the interstory drift from the base to the first elevated level (2nd floor). Meeting interstory drift and stability requirements led to the use of W24x76 for the Roof Beam from W18x40, W21x68 for the 4th Beam from W18x40, W21x62 for the 3rd Beam from W18x40, and the 2nd Beam remains the same at a W18x40. UO and UI are the same and experience upon on going through the seismic design checks the column size W24x192 fails the minimum flange width to prevent prying action. Therefore, the column size was increased to a W24x207. LO and LO are the same and experience no change from a W24x229. The final results for the fixed SMF KBB for SDC B are presented in Table 6-4.

Kaiser Connection: Seismic Category B Trial #3										
Member	Member Size	Joint Deflection		Axial Load		Shear Load		Moment Load		
Roof Beam	W24x76	1.213	in	16.123	k	15.284	k	124.48	kft	
4th Beam	W21x68	0.968	in	4.161	k	26.887	k	190.1	kft	
3rd Beam	W21x62	0.623	in	1.974	k	15.458	k	202.7	kft	
2nd Beam	W18x40	0.24	in	4.774	k	24.288	k	150.27	kft	
UO Column	W24x192	-	in	93.115	k	39.508	k	390.95	kft	
UI Column	W24x192	-	in	64.426	k	52.282	k	454.81	kft	
LO Column	W24x229	-	in	205.56	k	62.053	k	1014.8	kft	
LI Column	W24x229	-	in	150.16	k	62.263	k	1017.5	kft	

Table 6-4 Fixed KBB Connection SDC B Trail #3

6.5 Pinned RBS SDC C

Changing from SDC B to SDC C but keeping the same number of frames in the building increases the amount of seismic force (shear) the building needs to resists during the maximum considered earthquake; therefore, the member sizes will increase to meet strength and stiffness requirements. The initial beam members used are a W18x40 for the Roof Beam, W21x55 for the 4th Beam, W21x62 for the 3rd Beam, and W30x99 for the 2nd Beam. The initial column sizes are

W36x170 for UO and UI columns and W36x194 for LO and LI columns. The member sizes of the frame need to be increase to the use of W24x84 for the Roof Beam, W27x84 for the 4th Beam, W30x99 for the 3rd Beam and W36x150 for the 2nd Beam. UO and UI columns are the same and experience no change from a W36x170. LO and LO columns are the same and need doubler plates, but upon inspection it proved uneconomical as increasing the member size exceeds the 50 lb. to 100 lb as it is the recommended range given in the Seismic Design Manual 2nd Edition Example 4.3.4. LO and LI were not changed from a W36x194. The final results for the pinned SMF RBS for SDC C are presented in Table 6-5.

RBS Connection: Seismic Category C Trial #2										
Member	Member Size	Joint Deflection		Axial Load		Shear Load		Moment Load	
Roof Beam	W24x84	1.764	in	25.341	k	18.399	k	168.01	kft
4th Beam	W27x84	1.447	in	10.052	k	33.807	k	288.28	kft
3rd Beam	W30x99	1.065	in	13.649	k	40.362	k	384.54	kft
2nd Beam	W36x150	0.656	in	14.922	k	62.97	k	726.74	kft
UO Column	W36x170	-	in	122.33	k	76.456	k	568.84	kft
UI Column	W36x170	-	in	65.58	k	118.57	k	800.74	kft
LO Column	W36x194	-	in	384.61	k	113.08	k	1583.1	kft
LI Column	W36x194	-	in	167.74	k	169.94	k	2199.8	kft

Table 6-5 Pinned RBS Connection SDC C Trail #2

6.6 Pinned KBB SDC C

With the increased shear in SDC C and to meet interstory drift and stability, elastic combined loading performance, and flexural strength requirements led to an increase in member size. The initial beam members used are a W14x26 for the Roof, W21x44 for the 4th Beam, W21x55 3rd Beam, and a W21x50 for the 2nd Beam. The initial column sizes are W30x292 for UO and UI columns and W30x292 for LO and LI columns. The member sizes of the frame need to be increase to the use of W24x76 for the Roof Beam, W27x94 for the 4th Beam, W30x108 for the 3rd Beam and W33x130 for the 2nd Beam. UO and UI are the same and experience no change from a W30x292. LO and LO are the same and failed minimum flange thickness to prevent prying action. The size of the columns where increased to W30x326 from W30x292. The final results for the pinned SMF RBS for SDC C are presented in Table 6-6.

Kaiser Connection: Seismic Category C Trial #3										
Member	Member Size	Joint Deflection		Axial Load		Shear Load		Moment Load		
Roof Beam	W24x76	1.758	in	25.493	k	18.062	k	164.43	kft
4th Beam	W27x94	1.444	in	11.67	k	35.313	k	311.01	kft
3rd Beam	W30x108	1.077	in	11.46	k	32.103	k	421.88	kft
2nd Beam	W33x130	0.65	in	14.728	k	58.31	k	640.13	kft
UO Column	W30x292	-	in	126.13	k	71.991	k	630.79	kft
UI Column	W30x292	-	in	65.604	k	123.16	k	906.66	kft
LO Column	W30x326	-	in	383.2	k	113.61	k	1590.5	kft
LI Column	W30x326	-	in	161.92	k	170.31	k	2198.1	kft

Table 6-6 Pinned KBB Connection SDC C Trail #3

6.7 Fixed RBS SDC C

The base connection was changed from a pinned connection (results given in Section 6.5) to a fixed connection to reduce the interstory drift from the base to the first elevated level (2nd floor). The initial beam members used are a W18x40 for the Roof, W21x50 for the 4th Beam, W21x55 3rd Beam, and a W24x62 for the 2nd Beam. The initial column sizes are W30x141 for UO and UI columns and W33x221 for LO and LI columns. Meeting interstory drift and stability and elastic performance requirements led to the use of W24x84 for the Roof Beam, W24x84 for the 4th Beam, W24x68 for the 3rd Beam and W24x68 for the 2nd Beam. UO and UI are the same and experience no change from a W33x141. LO and LO are the same and were not changed from a W33x221. The final results for the fixed SMF RBS for SDC C are presented in Table 6-7.

RBS Connection: Seismic Category C Trial #2					
Member	Member Size	Joint Deflection	Axial Load	Shear Load	Moment Load
Roof Beam	W24x76	1.752 in	26.081 k	19.411 k	181.61 kft
4th Beam	W27x94	1.369 in	8.391 k	34.703 k	300.85 kft
3rd Beam	W30x108	0.848 in	4.977 k	34.467 k	299.58 kft
2nd Beam	W33x130	0.32 in	7.042 k	32.517 k	268.66 kft
UO Column	W30x292	- in	127.74 k	79.476 k	684.66 kft
UI Column	W30x292	- in	67.454 k	115.87 k	903.4 kft
LO Column	W30x292	- in	284.08 k	127.54 k	2165.8 kft
LI Column	W30x292	- in	155.49 k	143.4 k	2227.9 kft

Table 6-7 Fixed RBS Connection SDC C Trail #2

6.8 Fixed KBB SDC C

The base connection was changed from a pinned connection (results given in Section 6.6) to a fixed connection to reduce the interstory drift from the base to the first elevated level (2nd floor). The Roof Beam, 4th Beam, and 3rd Beam, and 2nd Beam also fail the elastic combined loading check. Meeting interstory drift and stability and elastic performance requirements led to the use of W24x84 for the Roof Beam from W18x40, W24x84 for the 4th Beam from W21x55, W24x76 for the 3rd Beam from W21x50, and W24x76 for the 2nd Beam from W21x50. UO and UI are the same and experience no change from a W24x250. LO and LO are the same and were not changed from a W24x279. The final results for the fixed SMF KBB for SDC C are presented in Table 6-8.

Kaiser Connection: Seismic Category C Trial #2					
Member	Member Size	Joint Deflection	Axial Load	Shear Load	Moment Load
Roof Beam	W24x84	1.791 in	26.321 k	19.696 k	186.41 kft
4th Beam	W24x84	1.407 in	8.69 k	34.782 k	302.78 kft
3rd Beam	W24x76	0.894 in	5.525 k	36.184 k	324.27 kft
2nd Beam	W24x76	0.348 in	7.934 k	34.697 k	299.63 kft
UO Column	W24x250	- in	129.11 k	77.991 k	710.94 kft
UI Column	W24x250	- in	67.157 k	117.35 k	939.13 kft
LO Column	W24x279	- in	211.51 k	125.69 k	1879.1 kft
LI Column	W24x279	- in	156.29 k	145.15 k	1960.3 kft

Table 6-8 Fixed KBB Connection SDC C Trail #2

6.9 Pinned RBS SDC D

Changing from SDC C to SDC D but keeping the same number of frames in the building increases the amount of seismic force (shear) the building needs to resists during the maximum considered earthquake; therefore, the member sizes will increase to meet strength and stiffness requirements. The initial beam members used are a W18x55 for the Roof, W24x68 for the 4th Beam, W30x99 3rd Beam, and a W30x116 for the 2nd Beam. The initial column sizes are W36x194 for UO and UI columns and W36x302 for LO and LI columns. Meeting interstory drift and stability and elastic performance requirements led to the use of W30x99 for the Roof Beam, W30x108 for the 4th Beam, W36x135 for the 3rd Beam and W36x210 for the 2nd Beam. UO and UI are the same and experience no change from a W36x194. LO and LO are the same and were not changed from a W36x302. The final results for the pinned SMF RBS for SDC D are presented in Table 6-9.

RBS Connection: Seismic Category D Trial #2										
Member	Member Size	Joint Deflection		Axial Load		Shear Load		Moment Load	
Roof Beam	W30x99	1.844	in	36.462	k	23.889	k	239.15	kft
4th Beam	W30x108	1.518	in	17.882	k	41.887	k	395.46	kft
3rd Beam	W33x130	1.114	in	21.762	k	58.466	k	646.24	kft
2nd Beam	W36x182	0.688	in	21.375	k	87.765	k	1100.5	kft
UO Column	W36x361	-	in	160.09	k	119.45	k	799.15	kft
UI Column	W36x361	-	in	71.622	k	199.71	k	1193.3	kft
LO Column	W36x361	-	in	546.93	k	185.63	k	2598.8	kft
LI Column	W36x361	-	in	171.37	k	280.87	k	3646.5	kft

Table 6-9 Pinned RBS Connection SDC D Trail #2

6.10 Pinned KBB SDC D

With the increased shear in SDC D, the Roof Beam, 4th Beam, and 3rd Beam, and 2nd Beam fail the elastic combined loading check and 4th Beam and 2nd Beam fails to meet the width-thickness ratio for flanges limitation. Meeting interstory drift and stability, width-thickness ratio for beam flanges, and elastic performance requirements led to the use of W30x108 for the Roof Beam from W18x40, W30x108 for the 4th Beam from W21x55, W33x130 for the 3rd Beam from W24x76, and the beam size required meet above failures exceeds the beam weight and size limitations for the 2nd Beam. The initial size for the 2nd Beam is a W30x99, and the size inputted into RISA to determine drift and member forces is W36x182. This is to have a member that works for the majority of the seismic design checks, except the connection check. UO and UI are the same and experience no change from a W36x361. LO and LO are the same and were not changed from a W36x361. The final results for the pinned SMF KBB for SDC D are presented in Table 6-10.

Kaiser Connection: Seismic Category D Trial #2										
Member	Member Size	Joint Deflection		Axial Load		Shear Load		Moment Load		
Roof Beam	W30x108	1.865	in	38.781	k	26.904	k	286.86	kft	
4th Beam	W30x108	1.539	in	16.818	k	42.661	k	409.84	kft	
3rd Beam	W33x130	1.143	in	20.339	k	46.078	k	609.94	kft	
2nd Beam	W36x182	0.688	in	19.698	k	84.984	k	1054.9	kft	
UO Column	W36x361	-	in	172.48	k	117.14	k	974.53	kft	
UI Column	W36x361	-	in	70.367	k	202.28	k	1497.1	kft	
LO Column	W36x361	-	in	546.57	k	184.68	k	2585.5	kft	
LI Column	W36x361	-	in	178.5	k	278.82	k	3664.9	kft	

Table 6-10 Pinned KBB Connection SDC D Trail #2

6.11 Fixed RBS SDC D

The base connection was changed from a pinned connection (results given in Section 6.9) to a fixed connection to reduce the interstory drift from the base to the first elevated level (2nd floor). The Roof Beam and 4th Beam also failed the elastic combined loading check. The 2nd Beam initially met story drift and stability check, but was increased to aid in the drift and stability of the rest of the structure. Meeting interstory drift and stability and elastic performance requirements led to the use of W30x99 for the Roof Beam from W21x41, W30x99 for the 4th Beam from W21x62, W30x99 for the 3rd Beam from W27x84, and W30x99 for the 2nd Beam from W27x84. UO and UI column are the same and experience no change from a W36x182. LO and LO are the same and were not changed from a W36x256. The final results for the fixed SMF RBS for SDC D are presented in Table 6-11.

RBS Connection: Seismic Category D Trial #2					
Member	Member Size	Joint Deflection	Axial Load	Shear Load	Moment Load
Roof Beam	W30x99	1.744 in	37.93 k	25.485 k	263.91 kft
4th Beam	W30x99	1.365 in	14.988 k	43.675 k	419.19 kft
3rd Beam	W30x99	0.857 in	9.718 k	48.489 k	496.49 kft
2nd Beam	W30x99	0.335 in	11.35 k	45.269 k	445.01 kft
UO Column	W36x182	- in	170.21 k	124.19 k	1013.8 kft
UI Column	W36x182	- in	73.256 k	195.25 k	1412.8 kft
LO Column	W36x256	- in	302.37 k	204.34 k	3070.8 kft
LI Column	W36x256	- in	168.88 k	241.93 k	3220.3 kft

Table 6-11 Fixed RBS Connection SDC D Trail #2

6.12 Fixed KBB SDC D

The base connection was changed from a pinned connection (results given in Section 6.10) to a fixed connection to reduce the interstory drift from the base to the first elevated level (2nd floor) but with the increase seismic force from SDC C to SDC D, the Roof Beam, 4th Beam, and 3rd Beam, and 2nd Beam also fail the elastic combined loading check. Meeting interstory drift and stability and elastic performance requirements led to the use of W30x108 for the Roof Beam from W18x40, W30x108 for the 4th Beam from W21x62, W30x108 for the 3rd Beam from W21x68, and W24x76 for the 2nd Beam from W21x68. UO and UI are the same and experience no change from a W27x307. LO and LO are the same and were not changed from a W27x307. The final results for the fixed SMF KBB for SDC C are presented in Table 6-12.

Kaiser Connection: Seismic Category D Trial #2										
Member	Member Size	Joint Deflection		Axial Load		Shear Load		Moment Load		
Roof Beam	W30x108	1.899	in	37.058	k	23.105	k	264.63	kft	
4th Beam	W30x108	1.541	in	16.027	k	41.009	k	425.62	kft	
3rd Beam	W30x108	1.034	in	6.739	k	48.087	k	536.27	kft	
2nd Beam	W24x76	0.428	in	12.288	k	38.401	k	344.73	kft	
UO Column	W27x307	-	in	178.36	k	118.51	k	1170.1	kft	
UI Column	W27x307	-	in	73.559	k	200.89	k	1614.1	kft	
LO Column	W27x307	-	in	403.37	k	211.47	k	3115.5	kft	
LI Column	W27x307	-	in	169.69	k	238.05	k	3223.1	kft	

Table 6-12 Fixed KBB Connection SDC D Trail #2

Chapter 7 - Comparison Summary

This chapter is devoted to discussing the comparison of the parametric study, results presented in Chapter 6. The data analyzed in this chapter is from the final iterations performed for determining the members of the SMF systems. The data can be revisited in the previous chapter. Likewise, graphs showing the change in member forces and drift during the iteration process for all SDC have and for fixed and pinned foundation connections are in Appendices. Also, the charts comparing RBS pinned vs. fixed foundation connection, KBB pinned vs. fixed foundation connection, pinned RBS vs. KBB, and fixed RBS vs. KBB can be found in the Appendices C-F. Since this parametric study is very broad in scope, SDC D comparison results are displayed in charts in this chapter with a brief discussion of the relationship. The charts for the other two SDC's are not present in this chapter, but are located in the Appendices. For elevations with all the member sizes for pinned RBS, pinned KBB, fixed RBS, and fixed KBB, refer to Appendix C-F.

7.1 RBS Member Forces Comparison: Pinned vs. Fixed Supports

In Figure 7-1, the axial load experienced is highest for the Roof Beam for both pinned and fixed connections with the fixed foundation connection (FPC) being slightly higher than the pinned foundation connection (PFC). The 4th Beam experiences a drop in axial load for both foundation connections from the Roof Beam with the FFC 4th Beam experiencing less axial load than the PFC 4th Beam. The 3rd Beam PFC experiences a slight increase in axial load, from the 4th Beam, while the FFC 3rd Beam continues to decrease in axial load. The 2nd Beam for both PFC and FFC experience a drop in axial load from the 3rd Beam with FFC beam have a lower axial load than the PFC beam. The beams for the fixed connection is smaller than the pinned connection, which means the beams in the pinned connection are stiffer and can take more axial load than the fixed connections. The Roof Beam experiences a 4% increase in axial load, the 4th Beam experiences a 16% decrease in axial load, the 3rd Beam a 55% decrease axial load, and the 2nd Beam experiences a 47% decrease in axial load. The seismic shear is the axial load of the beams.

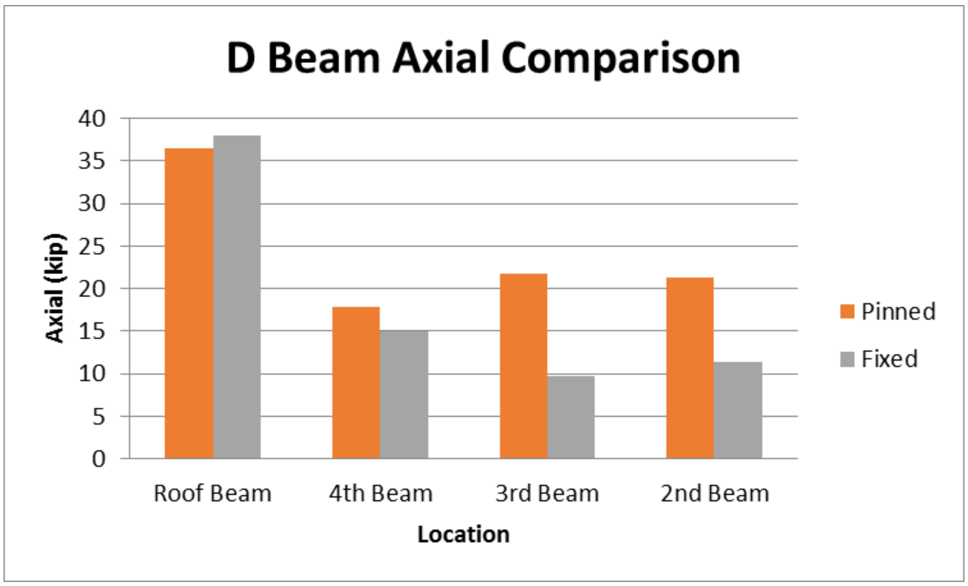

Figure 7-1 RBS SDC D Beam Axial Comparison for Frames with Pinned and Fixed Supports.

In Figure 7-2, the shear load experienced is lowest for the Roof Beam for both pinned and fixed connections with the fixed foundation connection, FFC, being slightly higher than the pinned foundation connection, PFC. The 4th Beam experiences an increase in shear load for both foundation connection types compared to the Roof Beam shear with the FFC 4th Beam experiencing more shear load than the PFC 4th Beam. The 3rd Beam experiences an increase in shear load for both foundation connections, from the 4th Beam, while the FFC beam becomes less than PFC beam. The 2nd Beam for PFC continues to increase in shear load while the FFC beam experiences a drop in shear load from the 3rd Beam with FFC beam having a lower shear load than the PFC beam. The Roof Beam experiences a 6.7% increase in shear load, the 4th Beam experiences a 4.3% increase in shear load, the 3rd Beam a 17% decrease shear load, and the 2nd Beam experiences a 48% decrease in shear load. A reduction in beam weight reduces the shear in the beam where a reduction is notices. Otherwise, similar shear is experienced in the beams. Beam weight for FFC is lower than for PFC.

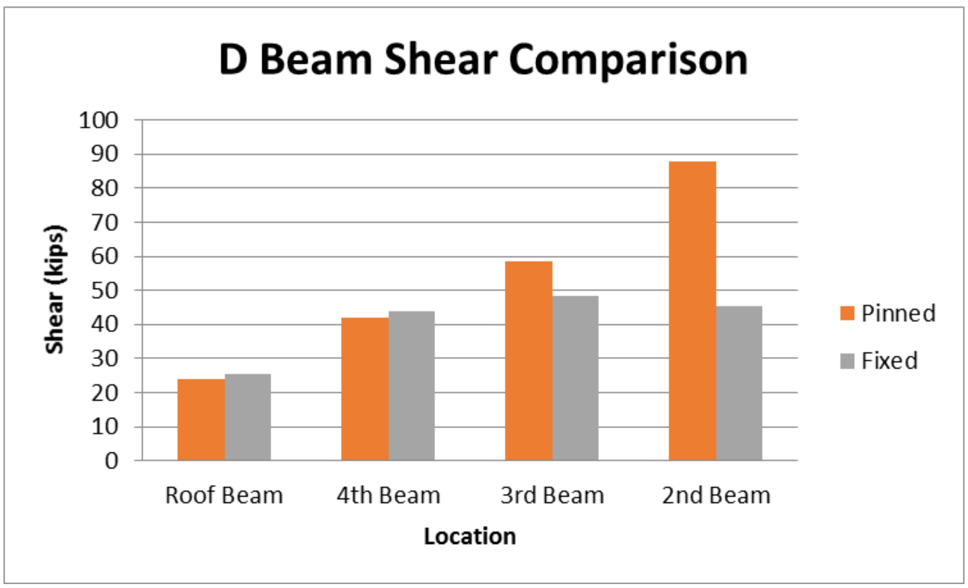

Figure 7-2 RBS SDC D Beam Shear Comparison of Frames with Pinned and Fixed Supports.

In Figure 7-3, the moment load experienced is lowest for the Roof Beam for both PFC and FFC frames with the PFC being slightly higher than the FFC. The 4th Beam experiences an increase in moment load for both foundation connections from the Roof Beam with the PFC 4th Beam experiencing less moment load than the FFC 4th Beam. The 3rd Beam experiences an increase in moment load for both foundation connections, from the 4th Beam, while the FFC beam experiences less moment than PFC beam. The 2nd Beam for PFC continues to increase in moment load while the FFC beam experiences a drop in moment load from the 3rd Beam with FFC beam having a lower moment load than the PFC beam. The Roof Beam experiences a 10.4% increase in moment load, the 4th Beam experiences a 6% increase in moment load, the 3rd Beam a 23.2% decrease moment load, and the 2nd Beam experiences a 59.6% decrease in moment load. The 2nd Beam moment is lower due to the moment being transferred to the foundation for the fixed connections, whereas members have to resist all of the moment for the pinned connection.

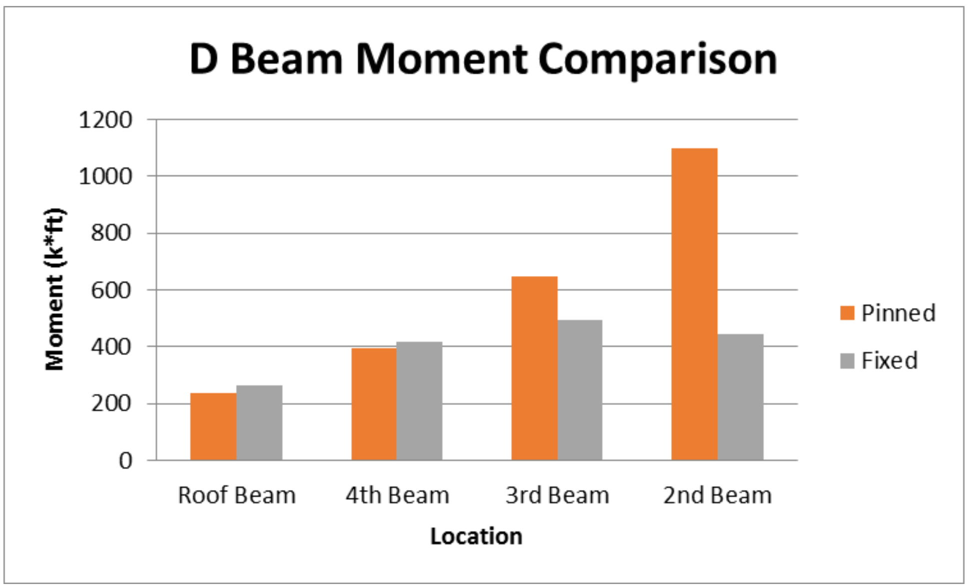

Figure 7-3 RBS SDC D Beam Moment Comparison for Frames with Pinned and Fixed Supports.

In Figure 7-4, UO Columns and UI Columns experience similar axial loads while UI Columns axial load is less than UO Column axial load. FFC UI sand UO Columns experience slightly higher axial load than PFC UI and UO Columns. FFC Column axial load for LO and LI are lower than the PFC LO and LI Columns. Both UO and UI Columns experience less axial load than LO and LI Columns primarily due to the fact that they bear less of the building weight than the LO and LI Columns. UO and LO Columns experience higher axial load than UI and LI columns due to the seismic force and the proximity to its counterpart. Since UO and LO Columns are farther apart the UO and LO Columns can experience a higher axial load in member whereas the column on the opposite side of the frame experiences less. Since seismic loads are cyclic, both sides are expected to experience the highest magnitude of axial load. The UO column experiences a 6.4% increase in axial load, the UI column experiences a 2.3% increase in axial load, the LO column 44.9% decrease axial load, and the LI column experiences a 9.5% decrease in axial load. The column transfer the weight of the building axially to the foundation. The axial load experienced by the column is the result of the shear that the beam experiences.

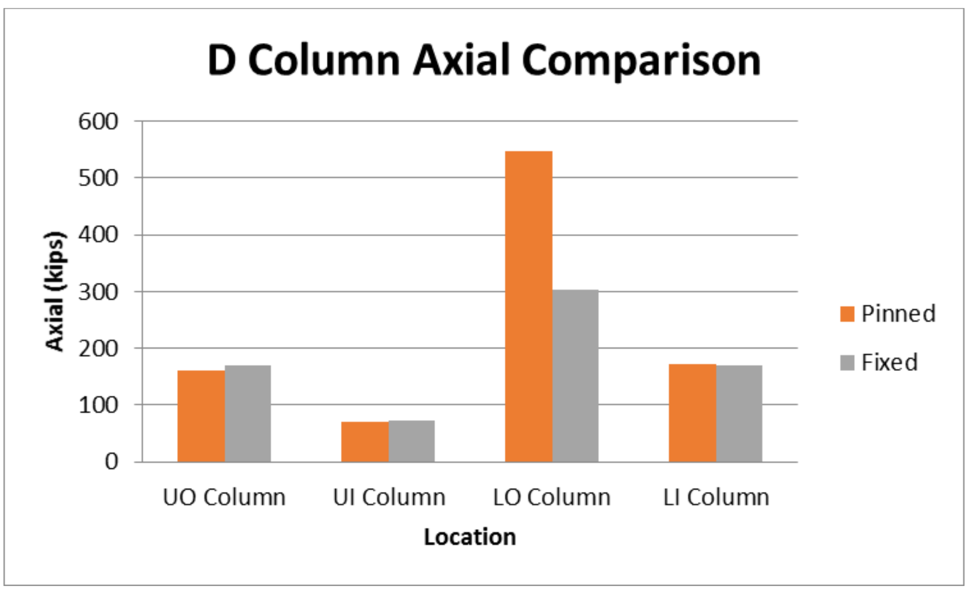

Figure 7-4 RBS SDC D Column Axial Comparison of Frames with Pinned and Fixed Supports.

In Figure7-5, both UI and UO Columns experience similar shear force with respect to their foundation connections with FPC UO Column experiencing a larger shear force than PFC, and the FFC UI Column experiencing less shear than PFC UI Column. UI Columns have a larger shear than the UO Columns. UI Columns and LO Columns see approximately the same shear. The same pattern can be observed with the comparison LO and LI Columns. The LO Column shear is less than the LI Column shear. The FFC LO Columns experience larger shear than PFC Columns, and PFC LI Columns experiences larger shear than FFC LI Columns. The UO column experiences a 4% increase in shear load, the UI column experiences a 2.2% decrease in shear load, the LO column 10% increase shear load, and the LI column experiences a 13.9% decrease in shear load. The shear that the column experiences is the result of the seismic design forces.

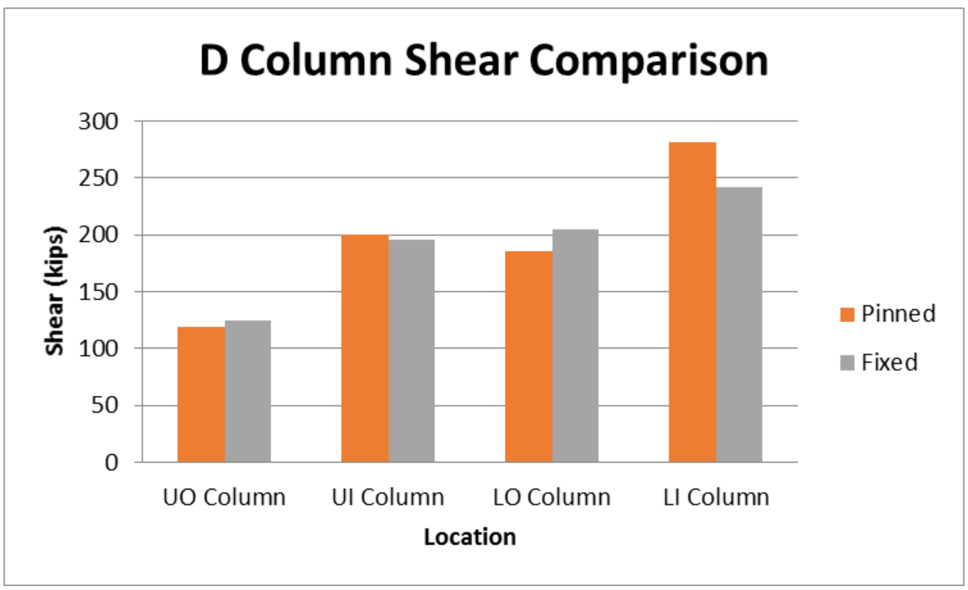

Figure 7-5 RBS SDC D Column Shear Comparison of Frames with Pinned and Fixed Supports.

In Figure 7-6, FPC Columns experience lower moment than the PFC Columns for all 4 types of Columns. UO Columns experience less moment than UI columns, and LO Columns experience less moment LI Columns. The UO column experiences a 26.9% increase in moment load, the UI column experiences a 18.9% increase in moment load, the LO column 18.2% increase shear load, and the LI column experiences a 11.7% decrease in shear load.

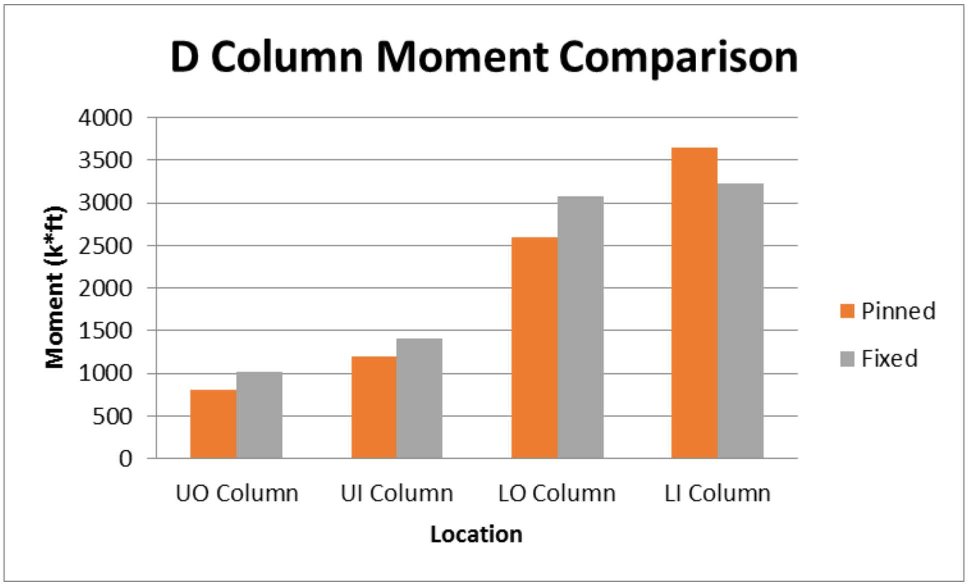

Figure 7-6 RBS SDC D Column Moment Comparison of Frames with Pinned and Fixed Supports.

7.2 KBB Member Forces Comparison: Pinned vs. Fixed Supports

In Figure 7-7, the axial load experienced is highest for the Roof Beam for both pinned and fixed connections with the PFC being slightly higher than the FFC. The 4th Beam experiences a drop in axial load for both foundation connections types from the Roof Beam with the FFC 4th Beam experiencing less axial load than the PFC 4th Beam. The 3rd Beam PFC experiences a slight increase in axial load, from the 4th Beam, while the FFC 3rd Beam continues to decrease in axial load. The 2nd Beam for PFC experiences a drop in axial load, and the 2nd Beam FFC experiences an increase in axial load from the 3rd Beam with FFC beam have a lower axial load than the PFC beam. The Roof Beam experiences a 4.4% increase in axial load, the 4th Beam experiences a 4.7% increase in axial load, the 3rd Beam a 26% decrease axial load, and the

2nd Beam experiences a 1.8% decrease in axial load. The seismic shear is the axial load of the beams.

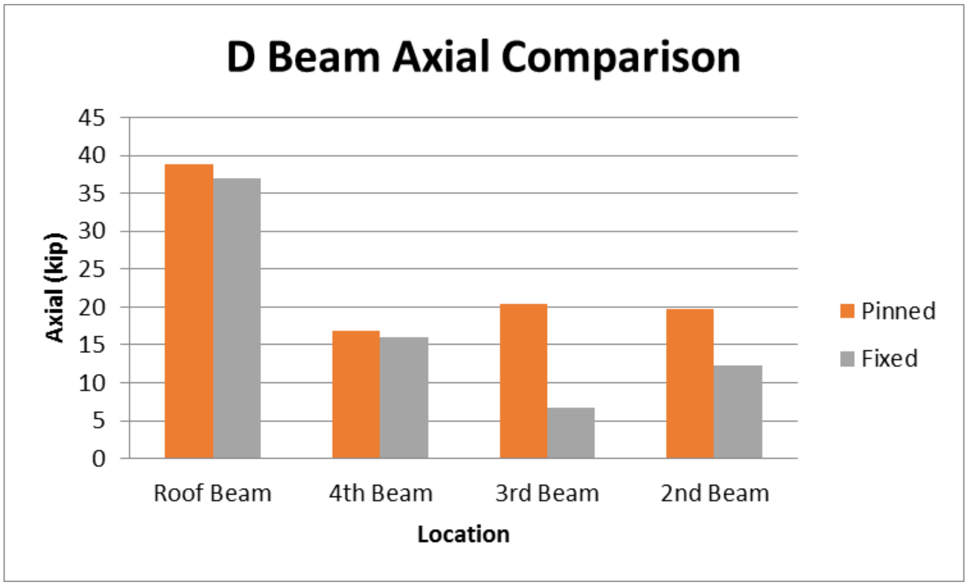

Figure 7-7 KBB SDC D Beam Axial Comparison of Frames with Pinned and Fixed Supports.

In Figure 7-8, the shear load experienced is lowest for the Roof Beam for both pinned and fixed connections with the FPC Roof Beam being slightly lower than the PFC. The 4th Beam experiences an increase in shear load for both foundation connections from the Roof Beam with the FFC 4th Beam experiencing less shear load than the PFC 4th Beam. The 3rd Beam experiences an increase in shear load for both foundation connections, from the 4th Beam, while the FFC beam continues to be less than PFC beam. The 2nd Beam for PFC continues to increase in shear load while the FFC beam experiences a drop in shear load from the 3rd Beam with FFC beam having a lower shear load than the PFC beam. The Roof Beam experiences a 14.1% decrease in shear load, the 4th Beam experiences a 3.9% decrease in shear load, the 3rd Beam a 14.3% decrease shear load, and the 2nd Beam experiences a 54.8% decrease in shear load. A reduction in beam weight reduces the shear in the beam where a reduction is notices. Otherwise, similar shear is experienced in the beams. Beam weight for FFC is lower than for PFC.

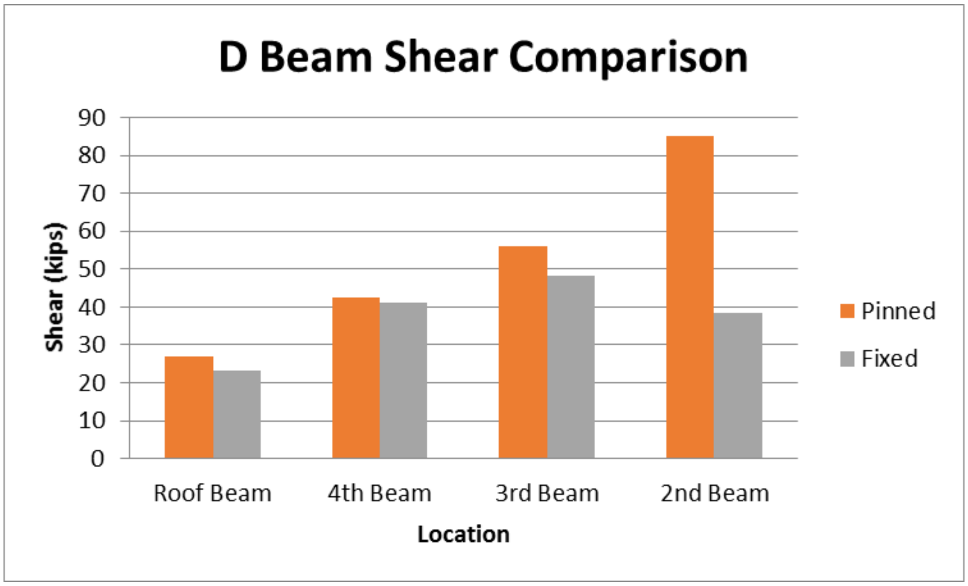

Figure 7-8 KBB SDC D Beam Shear Comparison of Frames with Pinned and Fixed Supports.

In Figure 7-9, the moment load experienced is lowest for the Roof Beam for both pinned and fixed connections with the FPC being slightly lower than the PFC. The 4th Beam experiences an increase in moment load for both foundation connections from the Roof Beam with the FFC 4th Beam experiencing a slightly higher moment load than the PFC 4th Beam. The 3rd Beam experiences an increase in moment load for both foundation connections, from the 4th Beam, while the FFC beam is now less than PFC beam. The 2nd Beam for PFC continues to increase in moment load while the FFC beam experiences a drop in moment load from the 3rd Beam with FFC beam having a lower moment load than the PFC beam. The Roof Beam experiences a 7.8% decrease in moment load, the 4th Beam experiences a 3.9% increase in moment load, the 3rd Beam a 12.8% decrease moment load, and the 2nd Beam experiences a

67.3% decrease in moment load. The 2^{nd} Beam moment is lower due to the moment being transferred to the foundation for the fixed connections, whereas members have to resist all of the moment for the pinned connection.

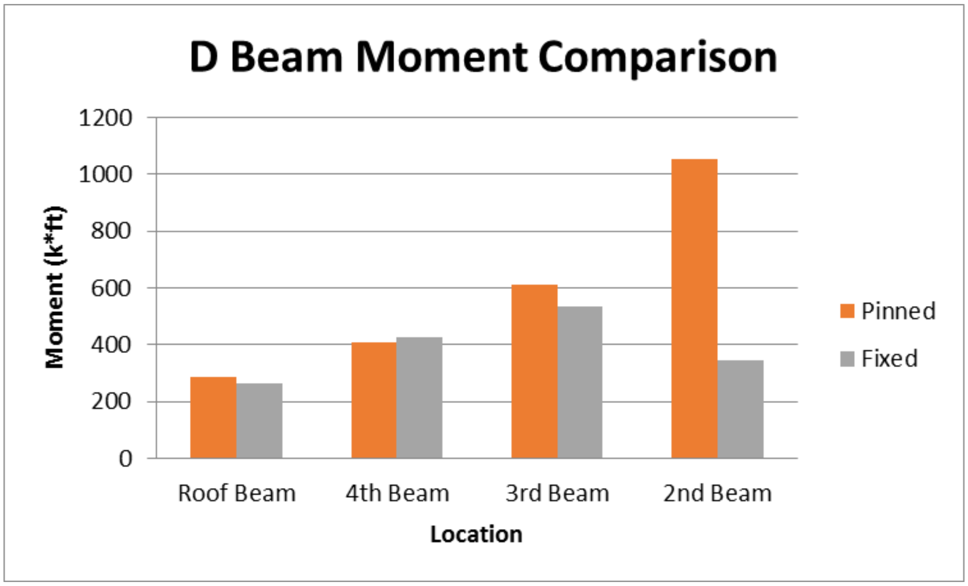

Figure 7-9 KBB SDC D Beam Moment Comparison of Frames with Pinned and Fixed Supports.

In Figure 7-10, UO Columns and UI Columns experience similar axial loads while UI Columns axial load is less than UO Column axial load. PFC UI and UO Columns experience slightly lower axial load. FFC LO Columns is lower than the PFC LO, and FFC LI Columns are higher than the PFC LI Columns. Both UO and UI Columns experience less axial load than LO and LI Columns primarily due to the fact that they bear less of the building weight than the LO and LI Columns. UO and LO Columns experience higher axial load than UI and LI columns due to the seismic force and the proximity to its counterpart. Since UO and LO Columns are farther apart the UO and LO Columns can experience a higher axial load in member whereas the column on the opposite side of the frame experiences less. Since seismic loads are cyclic, both sides are expected to experience the highest magnitude of axial load. The UO column experiences a 3.4% increase in axial load, the UI column experiences a 4.5% increase in axial load, the LO column 26.2% decrease axial load, and the LI column experiences a 1.8% increase in axial load. The columns transfer the weight of the building axially to the foundation. The axial load experienced by the column is the result of the shear that the beam experiences.

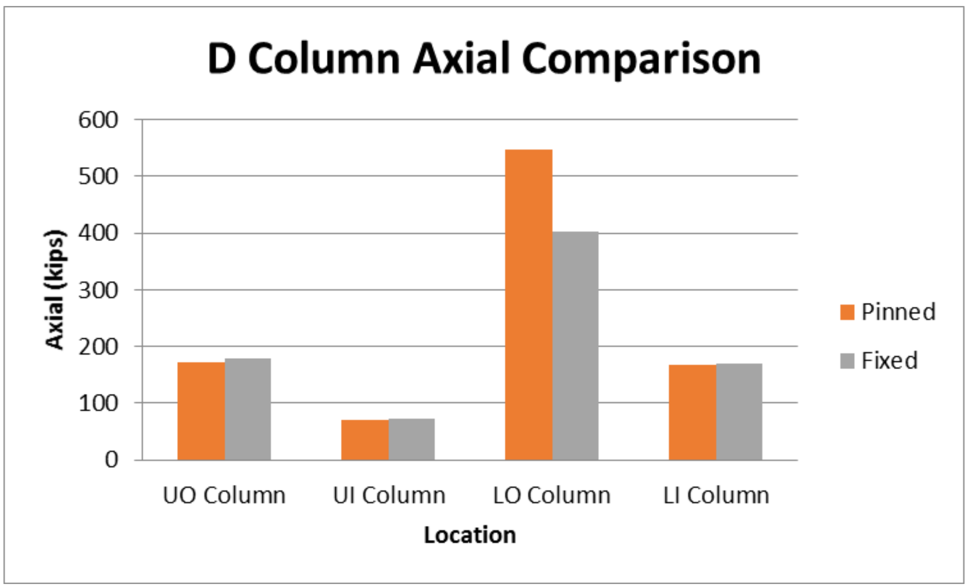

Figure 7-10 KBB SDC D Column Axial Comparison of Frames with Pinned and Fixed Supports.

In Figure7-11, both UI and UO Columns experience similar shear force with respect to their foundation connections with FPC UO Column being seeing a larger shear than PFC, and the FFC UI Column experiencing less shear load than PFC UI Column. UI Columns have a larger shear than the UO Columns. UI Columns and LO Columns see approximately the same shear. The same pattern can be observed with the comparison LO and LI Columns. The LO Column shear is less than the LI Column shear. The FFC LO Columns experience larger shear than PFC Columns, and PFC LI Columns experiences larger shear than FFC LI Columns. The UO column experiences a 1.2% increase in shear load, the UI column experiences a 0.69% decrease in shear load, the LO column 14.5% increase shear load, and the LI column experiences a 14.6% decrease in shear load. The shear that the columns experience is the result of the seismic design forces.

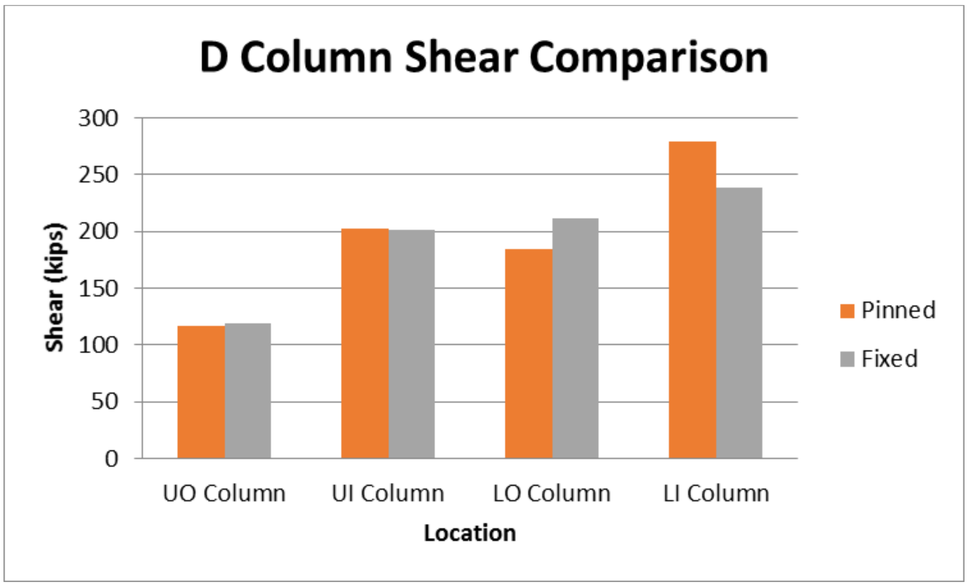

Figure 7-11 KBB SDC D Column Shear Comparison of Frames with Pinned and Fixed Supports.

In Figure 7-12, FPC Columns experience higher moment than the PFC Columns for UO, UI, and LO Columns. The FFC LI Columns experience more moment than the PFC LI Column. UO Columns experience less moment than UI columns, and LO Columns experience less moment LI Columns. The UO column experiences a 20.1% increase in moment load, the UI column experiences a 7.8% increase in moment load, the LO column 20.5% increase shear load, and the LI column experiences a 12.1% decrease in shear load.

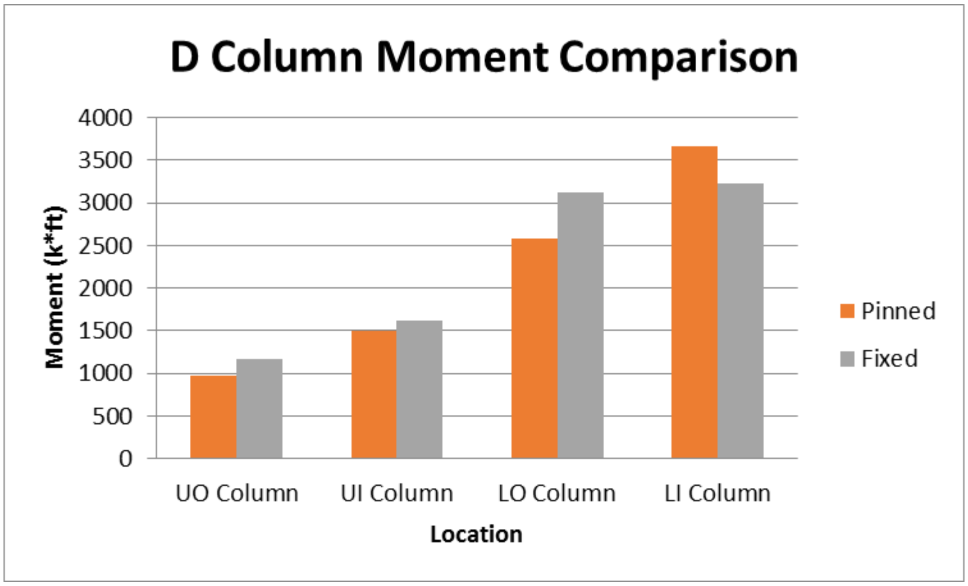

Figure 7-12 KBB SDC D Column Moment Comparison of Frames with Pinned and Fixed Supports.

7.3 PFC Member Forces Comparison: RBS vs. KBB

In Figure 7-13, the axial load experienced is highest for the Roof Beam for both KBB and RBS with the KBB being slightly higher than the RBS. The 4th Beam experiences a drop in axial load for both RBS and KBB connections from the Roof Beam with the RBS 4th Beam experiencing more axial load than the KBB 4th Beam. The 3rd Beam RBS and KBB connections experience a slight increase in axial load, from the 4th Beam, while the RBS 3rd Beam continues to have a higher axial load than KBB beam. The 2nd Beam for KBB and RBS remain approximately the same as the 3rd Beam axial load with KBB beam experiencing less axial load than RBS beam. The Roof Beam experiences a 6.4% increase in axial load, the 4th Beam experiences a 6% decrease in axial load, the 3rd Beam a 6.5% decrease axial load, and the 2nd Beam experiences a 7.9% decrease in axial load. The seismic shear is the axial load of the beams.

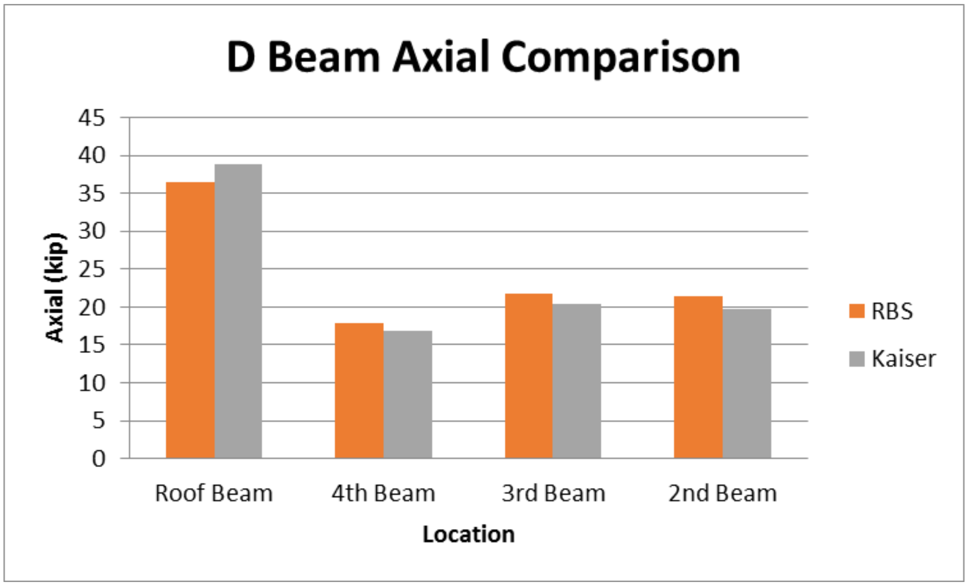

Figure 7-13 PFC SDC D Beam Axial Comparison RBS vs KKB

In Figure 7-14, the shear load experienced is lowest for the Roof Beam for both RBS and KBB connections with the RBS Roof Beam being slightly lower than the KBB Roof Beam. The 4th Beam experiences an increase in shear load for both RBS and KBB connections from the Roof Beam with the RBS 4th Beam experiencing less shear load than the KBB 4th Beam. The 3rd Beam experiences an increase in shear load for both foundation connections, from the 4th Beam, while the RBS beam continues to be less than KBB beam. The 2nd Beam for continues to increase in shear load for both RBS and KBB beam connections with respect to the 3rd Beam with KBB beam having a lower shear load than the RBS beam. The Roof Beam experiences a 12.6% increase in shear load, the 4th Beam experiences a 1.9% increase in shear load, the 3rd Beam a 4.8% decrease shear load, and the 2nd Beam experiences a 3.2% decrease in shear load.

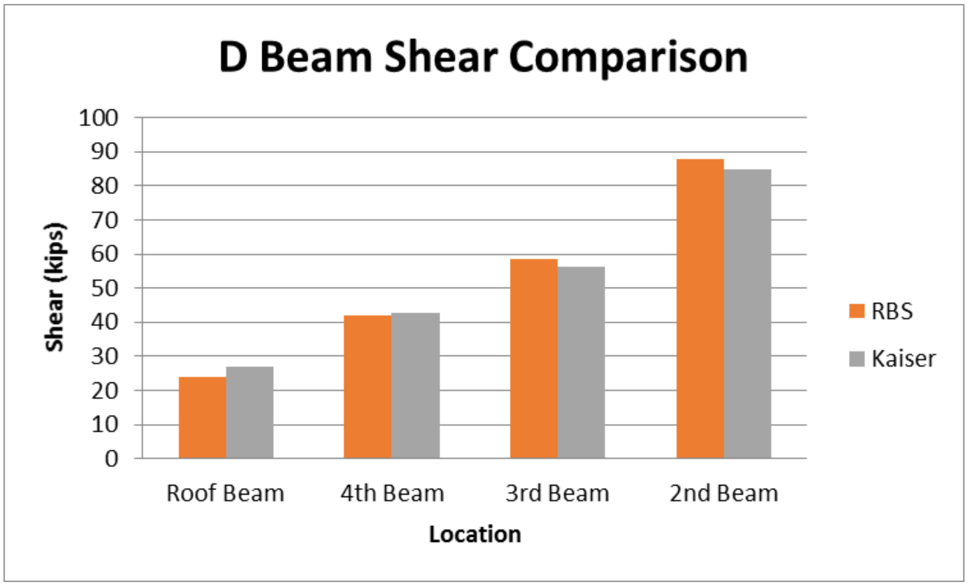

Figure 7-14 PFC SDC D Beam Shear Comparison RBS vs KKB

In Figure 7-15, the moment load experienced is lowest for the Roof Beam for both RBS and KBB connections with the RBS being slightly lower than the KBB. The 4th Beam experiences an increase in moment load for both RBS and KBB connections from the Roof Beam with the KBB 4th Beam experiencing a slightly higher moment load than the RBS 4th Beam. The 3rd Beam experiences an increased in moment load for both RBS and KBB connections, from the 4th Beam, while the KBB beam is now less than RBS beam. The 2nd Beam moment load continues to increase for both KBB and RBS beams with respect to the 3rd Beam. RBS is record as having the higher moment load. The Roof Beam experiences a 20% increase in moment load, the 4th Beam experiences a 3.6% increase in moment load, the 3rd Beam a 5.6% decrease moment load, and the 2nd Beam experiences a 4.2% decrease in moment load.

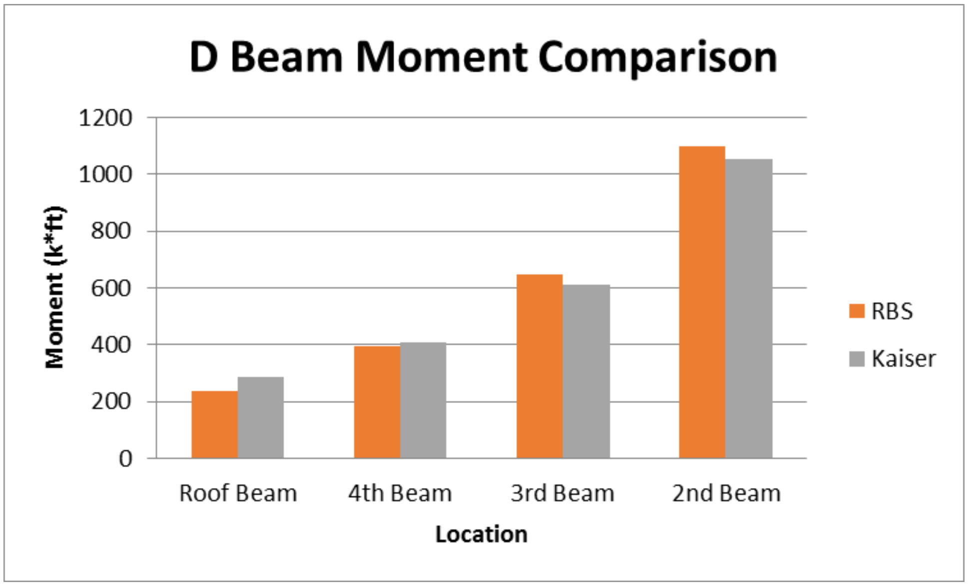

Figure 7-15 PFC SDC D Beam Moment Comparison RBS vs KKB

In Figure 7-16, UO Columns and UI Columns experience similar axial loads while UI Columns axial load is less than UO Column axial load. RBS UO Column axial load is less than KBB UO Column. UI Columns for both RBS and KBB connections have similar loads. KBB LO Columns is lower than the RBS LO Columns, and RBS LI Columns are higher than the KBB LI Columns. Both UO and UI Columns experience less axial load than LO and LI Columns primarily due to the fact that they bear less of the building weight than the LO and LI Columns. UO and LO Columns experience higher axial load than UI and LI columns due to the seismic force and the proximity to its counterpart. Since UO and LO Columns are farther apart the UO and LO Columns can experience a higher axial load in member whereas the column on the opposite side of the frame experiences less. Since seismic loads are cyclic, both sides are expected to experience the highest magnitude of axial load. The UO column experiences a 7.7% increase in axial load, the UI column experiences a 1.8% increase in axial load, the LO column 0.36% decrease axial load, and the LI column experiences a 10.7% decrease in axial load.

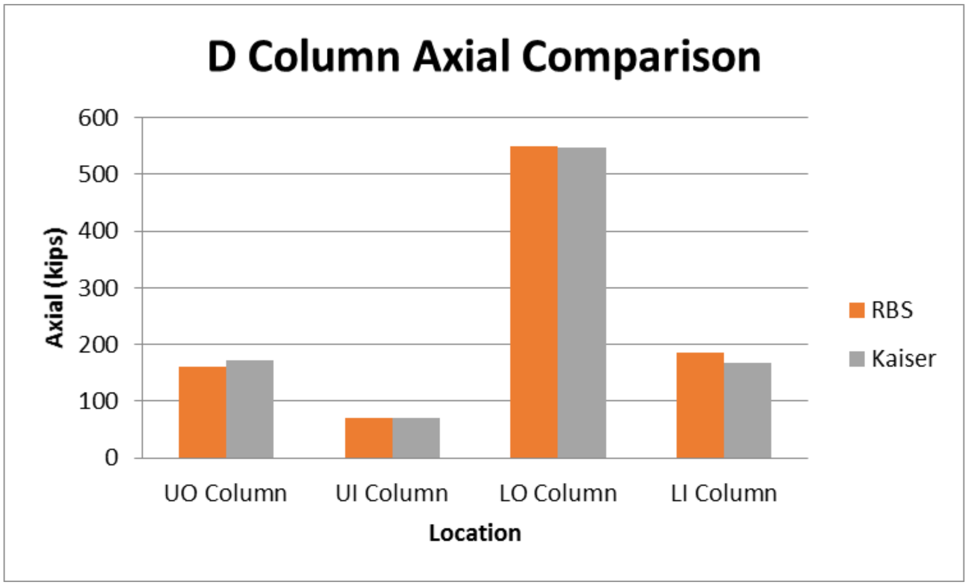

Figure 7-16 PFC SDC D Column Axial Comparison RBS vs KKB

In Figure7-17, all the column types experience similar shear force with respect to their beam-to-column connections. RBS UO Column being seeing a larger shear than KBB UO Column, and the RBS UI Column experiencing less shear load than KBB UI Column. UI Columns have a larger shear than the UO Columns. The LO Column shear is less than the LI Column shear. The RBS LO Columns experience larger shear than KBB Columns, and RBS LI Columns experiences larger shear than KBB LI Columns. The UO column experiences a 12.6% increase in moment load, the UI column experiences a 1.9% decrease in moment load, the LO column 4.1% increase shear load, and the LI column experiences a 12.1% decrease in shear load.

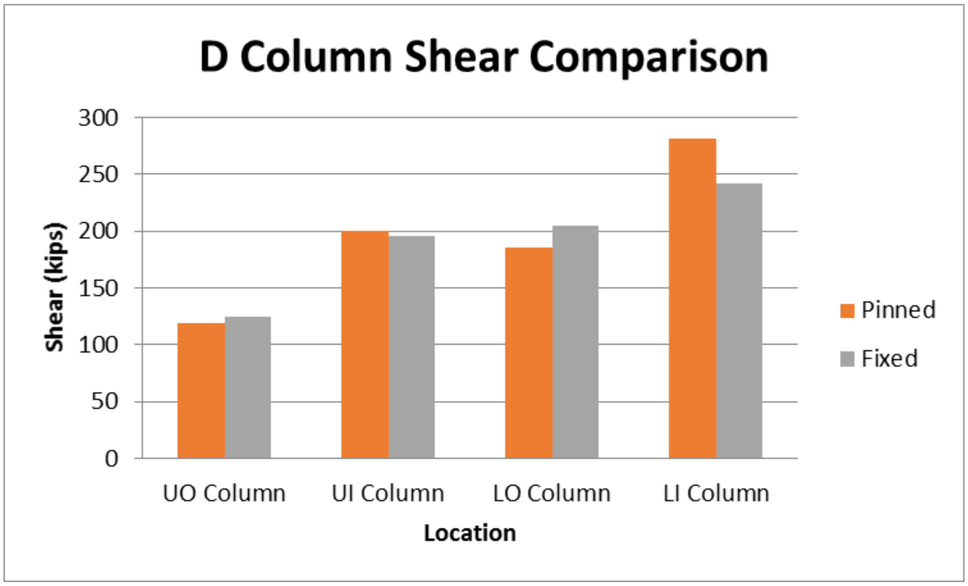

Figure 7-17 PFC SDC D Column Shear Comparison RBS vs KKB

In Figure 7-18, KBB Columns experience higher moment than the RBS Columns for UO, UI, and LI Columns. The RBS LO Columns experiences a moment more than the KBB LO Column. UO Columns experience less moment load than UI columns, and the LO Columns experience less moment load LI Columns. The UO column experiences a 22% increase in moment load, the UI column experiences a 25.5% increase in moment load, the LO column 0.51% decrease shear load, and the LI column experiences a 0.5% increase in shear load.

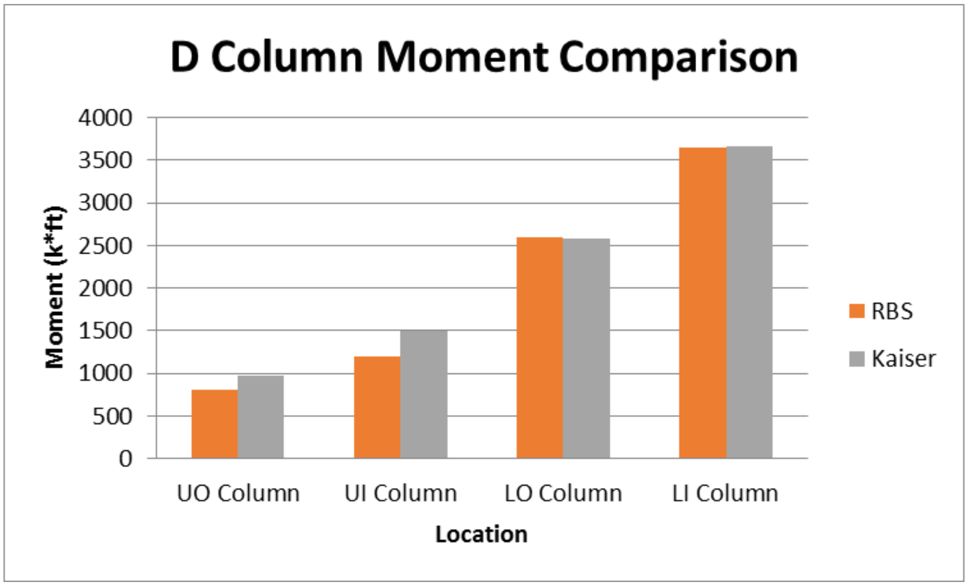

Figure 7-18 PFC SDC D Column Moment Comparison RBS vs KKB

7.4 FFC Member Forces Comparison: RBS vs. KBB

In Figure 7-19, the axial load experienced is highest for the Roof Beam for both KBB and RBS with the RBS being slightly higher than the KBB. The 4th Beam experiences a drop in axial load for both RBS and KBB connections from the Roof Beam. The KBB 4th Beam experiencing more axial load than the RBS 4th Beam. The 3rd Beam RBS and KBB continue to decrease in axial load, from the 4th Beam, while the RBS 3rd Beam has a higher axial load than KBB beam. The 2nd Beam for KBB and RBS experience an increase in axial load with respect to the 3rd Beam axial load with RBS beam experiencing less axial load than KBB beam. The Roof Beam experiences a 2.3% decrease in axial load, the 4th Beam experiences a 6.9% increase in axial load, the 3rd Beam a 30.7% decrease axial load, and the 2nd Beam experiences an 8.3% increase in axial load. The seismic shear is the axial load of the beams.

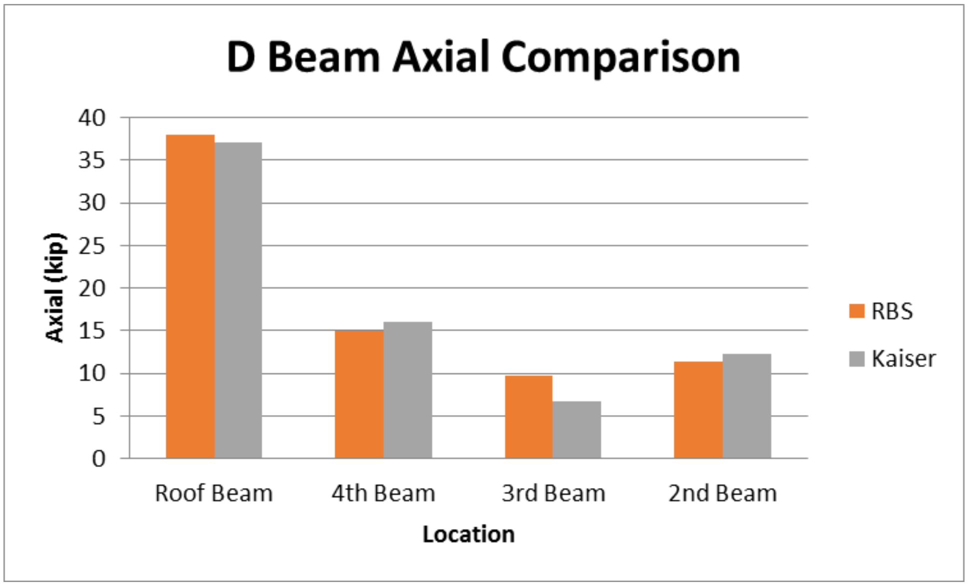

Figure 7-19 FFC SDC D Beam Axial Comparison RBS vs KKB

In Figure 7-20, the shear load experienced is lowest for the Roof Beam for both RBS and KBB connections with the KBB Roof Beam being slightly lower than the RBS Roof Beam. The 4th Beam experiences an increase in shear load for both RBS and KBB connections from the Roof Beam with the RBS 4th Beam experiencing more shear load than the KBB 4th Beam. The 3rd Beam experiences an increase in shear load for both RBS and KBB connections, from the 4th Beam, while the RBS beam continues to be more than KBB beam. The 2nd Beam exhibits a decrease in shear, respect to the 3rd Beam, and RBS beam continues to be greater than the KBB beam. The Roof Beam experiences a 9.3% decrease in shear load, the 4th Beam experiences a 6.1% decrease in shear load, the 3rd Beam a 0.83% decrease shear load, and the 2nd Beam experiences a 15.2% decrease in shear load.

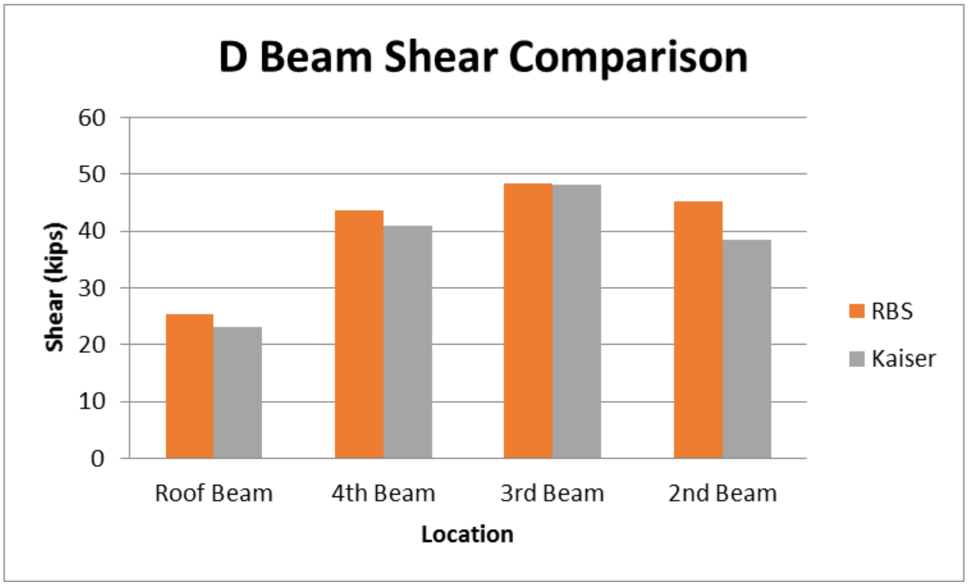

Figure 7-20 FFC SDC D Beam Shear Comparison RBS vs KKB

In Figure 7-21, the moment load experienced is lowest for the Roof Beam for both RBS and KBB connections with the RBS being slightly lower than the KBB. The 4th Beam experiences an increase in moment load for both RBS and KBB beams from the Roof Beam with the KBB 4th Beam experiencing a slightly higher moment load than the RBS 4th Beam. The 3rd Beam experiences an increase in moment load for both RBS and KBB connections, from the 4th Beam, while the KBB beam continues to higher than RBS beam. The 2nd Beam moment load decreases for both KBB and RBS beams with respect to the 3rd Beam. RBS is recorded as having the higher moment load. The Roof Beam experiences a 0.27% increase in moment load, the 4th Beam experiences a 1.5% increase in moment load, the 3rd Beam an 8% increase moment load, and the 2nd Beam experiences a 22.5% decrease in moment load.

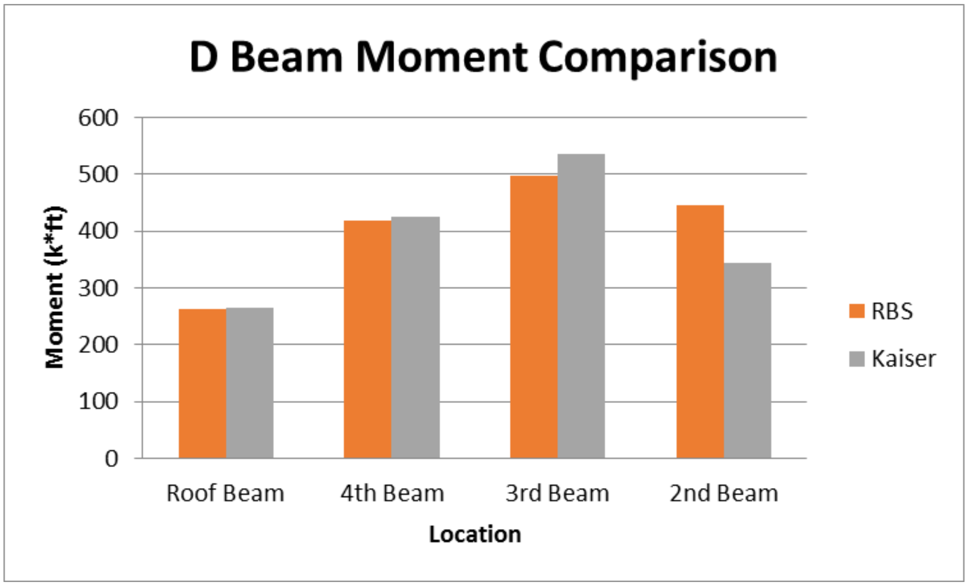

Figure 7-21 FFC SDC D Beam Moment Comparison RBS vs KKB

In Figure 7-22, UO Columns and UI Columns experience similar axial loads while UI Columns axial load is less than UO Column axial load. RBS UO Column axial load is less than KBB UO Column. UI Columns for both RBS and KBB connections have similar loads. KBB LO Columns is higher than the RBS LO Columns, and RBS LI Columns are lower than the KBB LI Columns. Both UO and UI Columns experience less axial load than LO and LI Columns primarily due to the fact that they bear less of the building weight than the LO and LI Columns. UO and LO Columns experience higher axial load than UI and LI columns due to the seismic force and the proximity to its counterpart. Since UO and LO Columns are farther apart the UO and LO Columns can experience a higher axial load in member whereas the column on the opposite side of the frame experiences less. Since seismic loads are cyclic, both sides are expected to experience the highest magnitude of axial load. The UO column experiences a 4.7% increase in axial load, the UI column experiences a 0.41% increase in axial load, the LO column 33.4% increase axial load, and the LI column experiences a 0.48% increase in axial load.

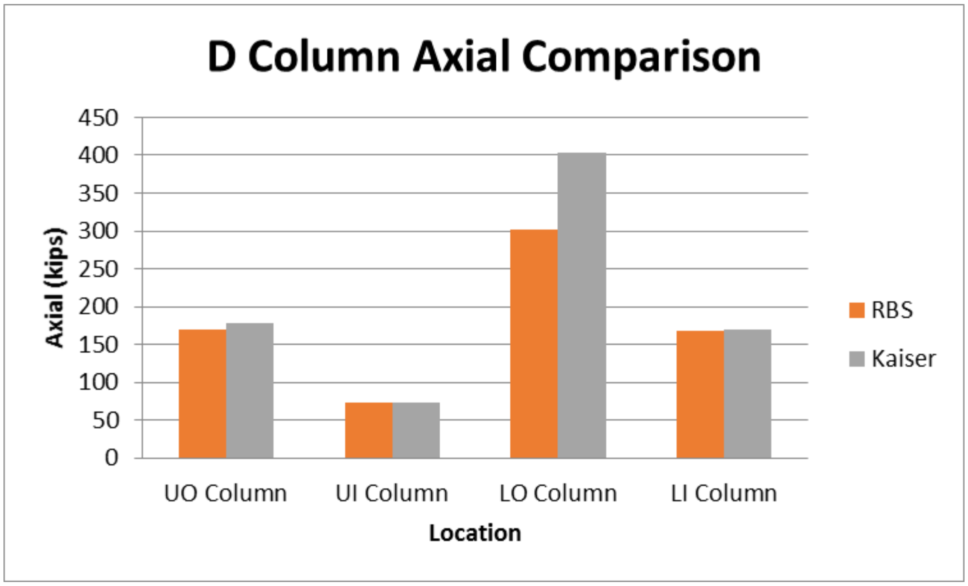

Figure 7-22 FFC SDC D Column Axial Comparison RBS vs KKB

In Figure7-23, all the column types experience similar shear force with respect to their beam-to-column connections with exception to LI columns. RBS UO Column being seeing a slightly larger shear than KBB UO Column, and the RBS UI Column experiencing less shear load than KBB UI Column. UI Columns have a larger shear than the UO Columns. The LO Column shear is less than the LI Column shear. The RBS LO Columns experience smaller shear than KBB Columns, and RBS LI Columns experiences smaller shear than KBB LI Columns. The UO column experiences a 4.6% decrease in moment load, the UI column experiences a 2.9% increase in moment load, the LO column 3.5% increase shear load, and the LI column experiences a 1.6% decrease in shear load.

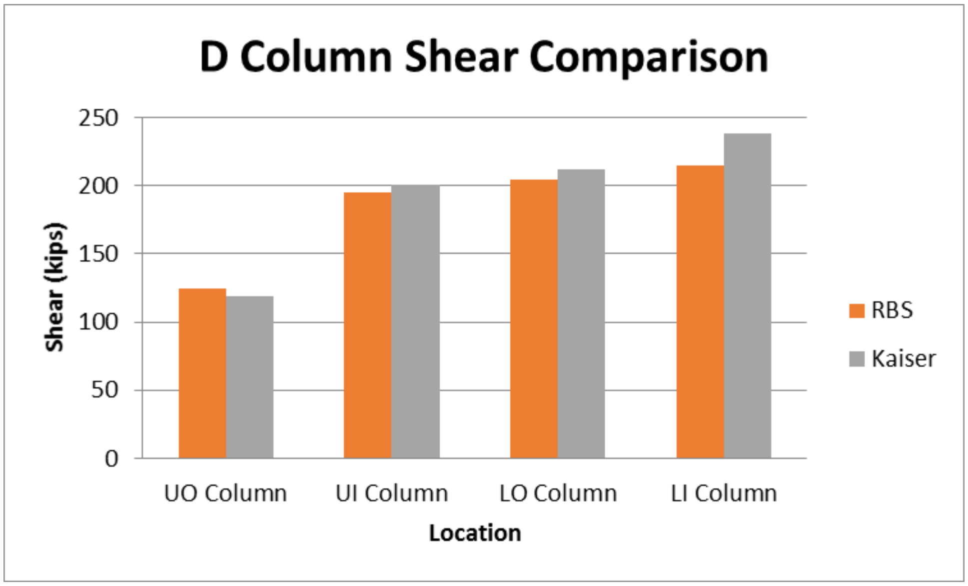

Figure 7-23 FFC SDC D Column Shear Comparison RBS vs KKB

In Figure 7-24, KBB Columns experience higher moment than the RBS Columns for UO, UI, and L0 Columns. The RBS LO Columns experiences a less moment load than the KBB LO Column. UO Columns experience less moment load than UI columns, and LO Columns experience less moment load LI Columns. LI Columns experience approximately same moment with respect to RBS and KBB connections. The UO column experiences a 15.4% increase in moment load, the UI column experiences a 14.3% increase in moment load, the LO column 1.5% decrease shear load, and the LI column experiences a 0.09% increase in shear load.

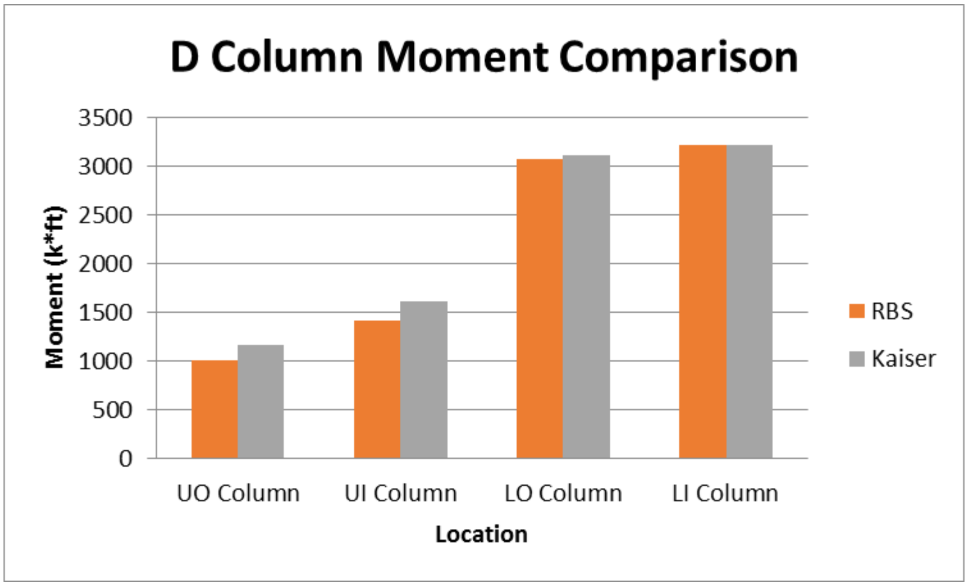

Figure 7-24 FFC SDC D Column Moment Comparison RBS vs KKB

7.5 Drift Comparison

In Figure 7-25, it is clear that the type of foundation connection can affect the story drift. With the use of RBS connections the story drift for PFC at each floor is higher than the story drift for FFC. The Roof Beam experiences a 5.4% decrease in drift, the 4th Beam experiences a 10.1% decrease in drift, the 3rd Beam a 23.1% decrease drift, and the 2nd Beam experiences a 51.3% decrease in drift.

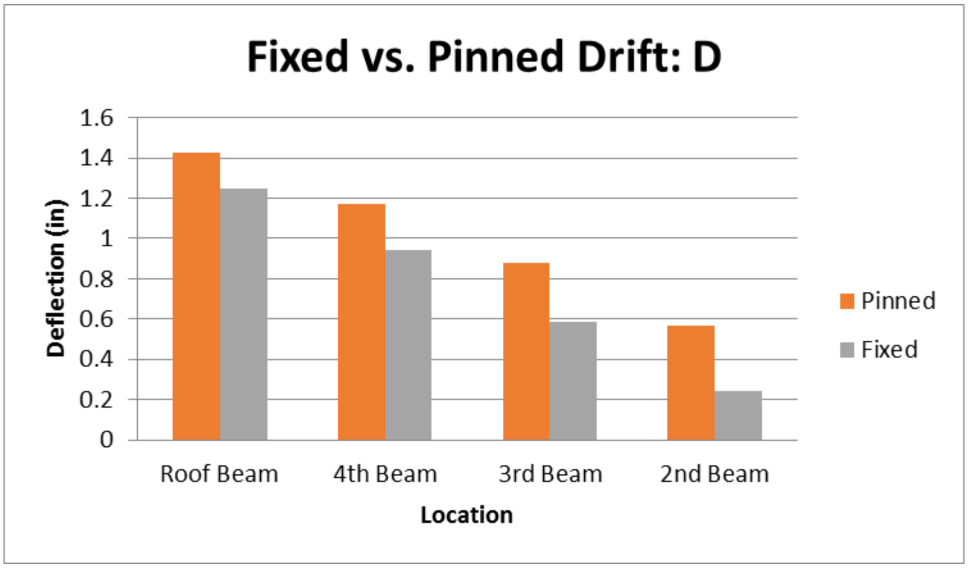

Figure 7-25 RBS SDC D Drift Comparison

In Figure 7-26, the difference in the type of foundation used is not as apparent as the RBS connection. The two systems, despite one connection type being more flexible than the other, are preforming in a similar manner. The difference in story drift between the two foundation types becomes more noticeable the closer the floor is to the ground; as depicted by 3rd and 2nd floor levels. For the roof and 4th levels, they are approximately the same. The Roof Beam experiences a 1.8% increase in drift, the 4th Beam experiences a 0.13% increase in drift, the 3rd Beam a 9.5% decrease drift, and the 2nd Beam experiences a 37.8% decrease in drift.

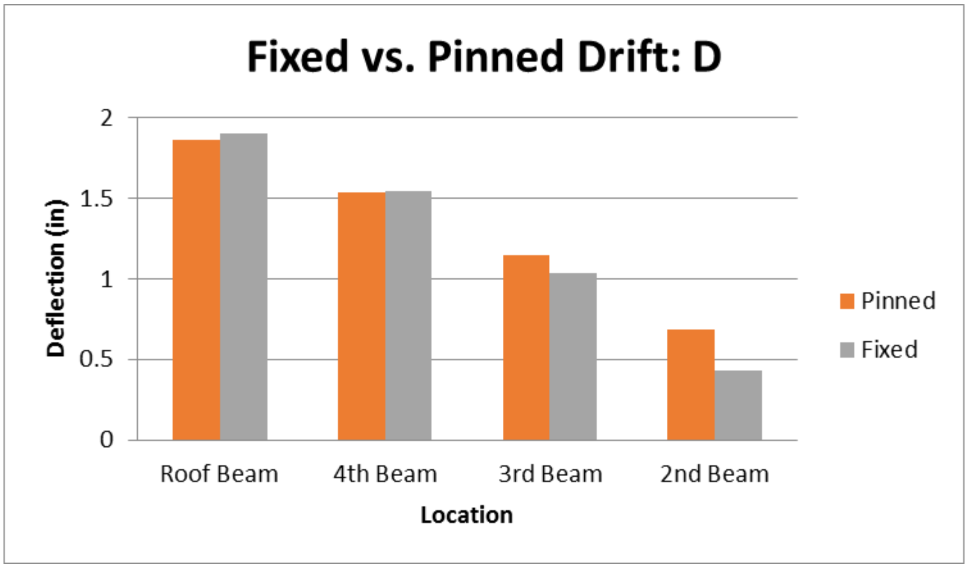

Figure 7-26 KBB SDC D Drift Comparison

In Figure 7-27, are approximately the same with the KBB having a tendency of being slightly higher than RBS. The Roof Beam experiences a 1.1% increase in drift, the 4th Beam experiences a 1.4% increase in drift, the 3rd Beam a 2.6% increase drift, and the 2nd Beam experiences no change in drift.

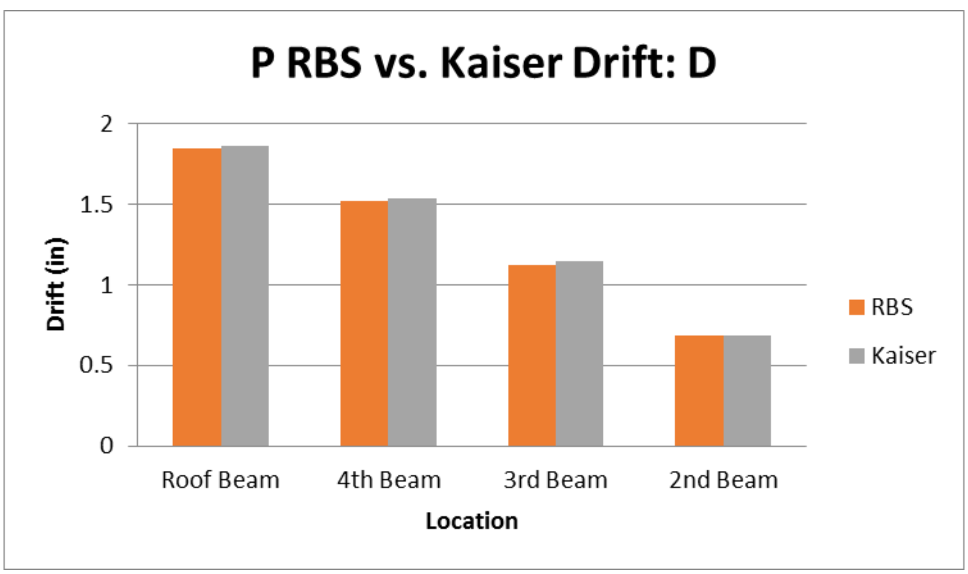

Figure 7-27 PFC SDC D Drift Comparison

In Figure 7-28, for FFC, KBB story drift is constantly higher than RBS. The Roof Beam experiences an 8.9% increase in drift, the 4th Beam experiences a 12.9% increase in drift, the 3rd Beam a 20.7% increase drift, and the 2nd Beam experiences a 27.8% increase in drift.

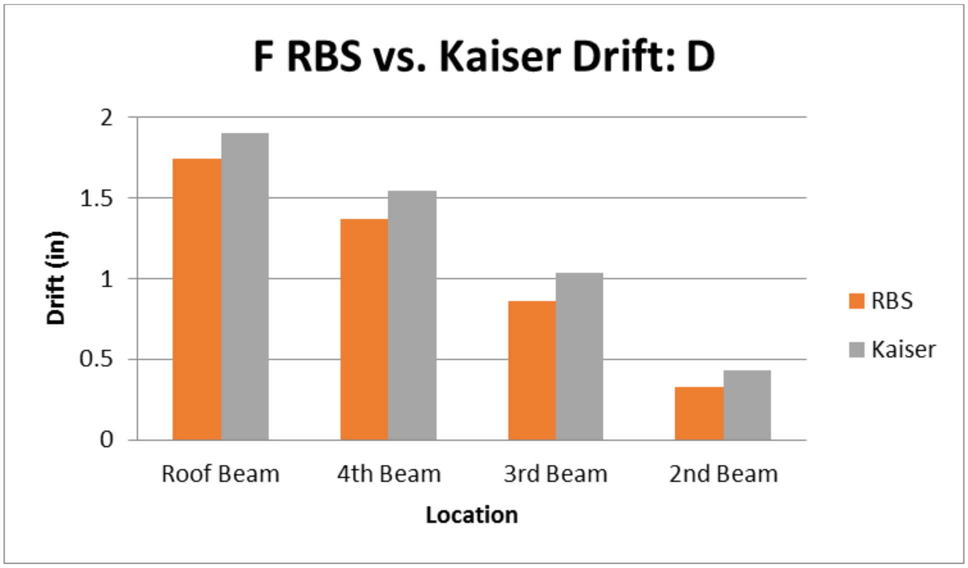

Figure 7-28 FFC SDC D Drift Comparison

Chapter 8 - Conclusion

This parametric study is to illustrate the differences and similarities between the use of KBB and RBS for pinned and fixed foundations. The member sizes were selected because they are able to resist the loads and meet the seismic design checks. It is highly probable that continuity plates are may be need in the connection. For KBB continuity plates are required for a column larger than a W14, and it can be difficult to eliminate the need for continuity plates for RBS connection columns when the seismic forces get large without dramatically increasing the size of the column. Thus eliminating any cost savings to additional material in the column and transportation of the column. For KBB, a major concern is prying action. Since the bracket is bolted to the column flange. A bolted connection gives than a welded connection, meaning it is going to translate and rotate more independently than a welded connection. In LFRS design, the beam-column connection cannot fail and prying of the bolted connection can under cyclic loading. The column flange must be thick enough to resist prying action, and often the column size needs to be increased to accommodate for prying action.

8.1 Member Size Conclusion

Table 8-1 summarizes members used in the final results of SDC B of this parametric study. RBS beams, whether for pinned or fixed connections show a similar member size in both weight and size, whereas KBB show, pinned, to be around the same member size and for fixed a gradual transition in member size from 2nd Beam with the lowest member to the Roof beam being the highest member. Member sizes are smaller for fixed foundation connection than for a pinned connection, but the difference is not large. Columns sizes are different between upper and lower sections for both RBS and KBB.

Seismic Design Category B					
Pinned			Fixed		
Member	RBS Member Size	KBB Member Size	Member	RBS Member Size	KBB Member Size
Roof Beam	W24x76	W24x76	Roof Beam	W24x62	W24x76
4th Beam	W24x76	W24x76	4th Beam	W24x62	W24x68
3rd Beam	W24x76	W24x76	3rd Beam	W24x55	W21x62
2nd Beam	W24x76	W24x84	2nd Beam	W21x62	W18x40
UO Column	W30x132	W24x207	UO Column	W30x108	W24x192
UI Column	W30x132	W24x207	UI Column	W30x108	W24x192
LO Column	W30x211	W24x250	LO Column	W30x148	W24x229
LI Column	W30x211	W24x250	LI Column	W30x148	W24x229

Table 8-1 SDC B Member Size Summary

Table 8-2 summarizes members used in the final results of SDC C of this parametric study. Both RBS beams and KBB whether for pinned or fixed connections show a similar member size in both weight and size. Member sizes are smaller for fixed foundation connection than for a pinned connection, but the difference between the two types of foundation connections is becoming more apparent. Columns sizes are different between upper and lower sections for both RBS and KBB.

Seismic Design Category C					
Pinned			Fixed		
Member	RBS Member Size	KBB Member Size	Member	RBS Member Size	KBB Member Size
Roof Beam	W24x84	W24x84	Roof Beam	W24x84	W24x84
4th Beam	W27x84	W24x84	4th Beam	W24x84	W24x84
3rd Beam	W30x99	W24x68	3rd Beam	W24x68	W24x76
2nd Beam	W36x150	W24x68	2nd Beam	W24x68	W24x76
UO Column	W36x170	W33x141	UO Column	W33x141	W24x250
UI Column	W36x170	W33x141	UI Column	W33x141	W24x250
LO Column	W36x194	W33x221	LO Column	W33x221	W24x279[h]
LI Column	W36x194	W33x221	LI Column	W33x221	W24x279[h]

Table 8-2 SDC C Member Size Summary

Table 8-3 summarizes members used in the final results of SDC D of this parametric study. The cell that is yellow is to signify that member does not fulfill the limitations set forth by the Seismic Design Manual 2nd Edition. The 2nd Beam for KBB exceeds the size and weight limit for the use of KBB. RBS beams, whether for pinned or fixed connections show a gradually increase in member size in both weight and size, whereas KBB tend to be around the same member size. For pinned KBB, to prevent prying action of bolts from the column flanges, the column flange thickness had to be increased, and they are all the same size. This increase in member size required the use of heavy sections whose additional requirements are beyond the scope of this study. Columns for RBS don't require heavy sections and have two different column sizes.

Seismic Design Category D					
Pinned			Fixed		
Member	RBS Member Size	KBB Member Size	Member	RBS Member Size	KBB Member Size
Roof Beam	W27x84	W30x108	Roof Beam	W30x99	W30x108
4th Beam	W33x130	W30x108	4th Beam	W30x116	W30x108
3rd Beam	W36x194	W33x130	3rd Beam	W36x150	W30x108
2nd Beam	W36x282	W36x182	2nd Beam	W36x150	W24x76
UO Column	W36x194	W36x361	UO Column	W36x182	W27x307
UI Column	W36x194	W36x361	UI Column	W36x182	W27x307
LO Column	W36x302	W36x361	LO Column	W36x256	W27x307
LI Column	W36x302	W36x361	LI Column	W36x256	W27x307

Table 8-3 SDC D Member Size Summary

8.2 Drift and Stability Conclusion

In order to meet stability requirements of the ASIC 341 *Seismic Provisions for Structural Steel Buildings Seismic Design*, the member sizes were increased to meet stiffness requirements. Therefore, the SMF RBS and SMF KBB with FFC or PRC were designed to meet the same interstory drift amount - these four systems performed similarly. Smaller and lighter weight columns and beams were able to meet the drift requirements of the SMF with FFC compared to the SMF with PFC. Some of the MF systems are more flexible than others, which explain the slight differences in drift between the systems. Tables 8-4 and 5 show that story drift for SDC B and C for KBB and RBS, fixed and pinned, similar story drift. These four systems performed similarly. Table 8-6 shows that for SDC D drift performance begins to be dissimilar.

Seismic Design Category B													
Pinned					Fixed				
Member	RBS Drift		KBB Drift		Member	RBS Drift		KBB Drift	
Roof Beam	1.678	in	1.626	in	Roof Beam	1.218	in	1.213	in
4th Beam	1.455	in	1.408	in	4th Beam	0.958	in	0.968	in
3rd Beam	1.115	in	1.089	in	3rd Beam	0.782	in	0.623	in
2nd Beam	0.664	in	0.662	in	2nd Beam	0.274	in	0.24	in
UO Column	-	in	-	in	UO Column	-	in	-	in
UI Column	-	in	-	in	UI Column	-	in	-	in
LO Column	-	in	-	in	LO Column	-	in	-	in
LI Column	-	in	-	in	LI Column	-	in	-	in

Table 8-4 SDC B Drift Summary

Seismic Design Category C									
Pinned					Fixed				
Member	RBS Drift		KBB Drift		Member	RBS Drift		KBB Drift	
Roof Beam	1.764	in	1.752	in	Roof Beam	1.752	in	1.791	in
4th Beam	1.447	in	1.369	in	4th Beam	1.369	in	1.407	in
3rd Beam	1.065	in	0.848	in	3rd Beam	0.848	in	0.894	in
2nd Beam	0.656	in	0.32	in	2nd Beam	0.32	in	0.348	in
UO Column	-	in	-	in	UO Column	-	in	-	in
UI Column	-	in	-	in	UI Column	-	in	-	in
LO Column	-	in	-	in	LO Column	-	in	-	in
LI Column	-	in	-	in	LI Column	-	in	-	in

Table 8-5 SDC C Drift Summary

Seismic Design Category D									
Pinned					Fixed				
Member	RBS Drift		KBB Drift		Member	RBS Drift		KBB Drift	
Roof Beam	1.427	in	1.865	in	Roof Beam	1.247	in	1.899	in
4th Beam	1.174	in	1.539	in	4th Beam	0.943	in	1.541	in
3rd Beam	0.882	in	1.143	in	3rd Beam	0.588	in	1.034	in
2nd Beam	0.565	in	0.688	in	2nd Beam	0.246	in	0.428	in
UO Column	-	in	-	in	UO Column	-	in	-	in
UI Column	-	in	-	in	UI Column	-	in	-	in
LO Column	-	in	-	in	LO Column	-	in	-	in
LI Column	-	in	-	in	LI Column	-	in	-	in

Table 8-6 SDC D Drift Summary

8.3 Member Axial Forces Conclusion

Table 8-7, 8-8, and 8-9 summarizes the member internal axial load for SDC B, SDC C, and SDC D, respectively, of this study. Upon looking at the tables, in general, the Roof Beam for all SDCs experiences the highest axial load, with the 3rd Beam experiencing the lowest axial load except for SDC D with PFC where the lowest axial load occurs in the 4th Beam with the axial load being larger in 3rd and 2nd Beams. . The 4th and 2nd Beam results are between the values that the Roof and 3rd Beam. For SDC B, the axial load between KBB and RBS can generally be assumed to equivalent with one being a little higher or lower than the other for both beams and columns. Comparing SMF RBS and SMF KBB frames for SDC C, mixed results are observed. For PFC condition, the Roof Beams have similar axial loads, but the axial load in the SMF KBB become significantly less than that of the SMF RBS beams. For FFC condition, the axial load between KBB and RBS can generally be assumed to equivalent with one being a little higher or lower than the other. Similarly, comparing SMF RBS and SMF KBB frames for SDC D mixed results are observed. For the FFC condition, larger variances occur for the 4th, 3rd, UO Column, and LO Column. For the PFC condition, the axial load between SMF KBB and SMF

RBS is approximately equivalent with one being a little higher or lower than the other with an exception to LI Columns.

Seismic Design Category B					
Pinned			Fixed		
Member	RBS Axial Force	KBB Axial Force	Member	RBS Axial Force	KBB Axial Force
Roof Beam	16 k	16 k	Roof Beam	15 k	16 k
4th Beam	6 k	5 k	4th Beam	4 k	4 k
3rd Beam	5 k	5 k	3rd Beam	3 k	2 k
2nd Beam	9 k	10 k	2nd Beam	5 k	5 k
UO Column	95 k	95 k	UO Column	90 k	93 k
UI Column	65 k	64 k	UI Column	64 k	64 k
LO Column	251 k	251 k	LO Column	211 k	206 k
LI Column	152 k	153 k	LI Column	151 k	150 k

Table 8-7 SDC B Axial Force Summary

Seismic Design Category C					
Pinned			Fixed		
Member	RBS Axial Force	KBB Axial Force	Member	RBS Axial Force	KBB Axial Force
Roof Beam	25 k	26 k	Roof Beam	26 k	26 k
4th Beam	10 k	8 k	4th Beam	8 k	9 k
3rd Beam	14 k	5 k	3rd Beam	5 k	6 k
2nd Beam	15 k	7 k	2nd Beam	7 k	8 k
UO Column	122 k	128 k	UO Column	128 k	129 k
UI Column	66 k	67 k	UI Column	67 k	67 k
LO Column	385 k	284 k	LO Column	284 k	212 k
LI Column	168 k	155 k	LI Column	155 k	156 k

Table 8-8 SDC C Axial Force Summary

Seismic Design Category D					
Pinned			Fixed		
Member	RBS Axial Force	KBB Axial Force	Member	RBS Axial Force	KBB Axial Force
Roof Beam	36 k	39 k	Roof Beam	38 k	37 k
4th Beam	18 k	17 k	4th Beam	15 k	16 k
3rd Beam	22 k	20 k	3rd Beam	10 k	7 k
2nd Beam	21 k	20 k	2nd Beam	11 k	12 k
UO Column	160 k	172 k	UO Column	170 k	178 k
UI Column	72 k	70 k	UI Column	73 k	74 k
LO Column	549 k	547 k	LO Column	302 k	403 k
LI Column	187 k	167 k	LI Column	169 k	170 k

Table 8-9 SDC D Axial Force Summary

8.4 Member Shear Forces Conclusion

Tables 8-10, 8-11, and 8-12 summarize the member shear forces for SDC B, SCD C, and SDC D, respectively, from this study. Upon reviewing the results, for PFC condition, the Roof Beam experiences the lowest internal shear force, with a gradual increase in shear to the 2nd Beam, with exception for FFC at the 2nd Beam. For PFC and FFC conditions, similar results are observed. For PFC condition, the lowest shear occurs at the Roof Beam, but for KBB beams, the shear force stays approximately the same for the other members. For SMF RBS and SMF KBB columns, the shear forces starts low and increases in shear force. For the both PFC and FFC columns, the shear forces for the columns are approximately the same.

Seismic Design Category B					
Pinned			Fixed		
Member	RBS	KBB	Member	RBS	KBB
Roof Beam	15 k	15 k	Roof Beam	14 k	15 k
4th Beam	28 k	28 k	4th Beam	27 k	27 k
3rd Beam	32 k	31 k	3rd Beam	28 k	15 k
2nd Beam	35 k	36 k	2nd Beam	27 k	24 k
UO Column	35 k	36 k	UO Column	39 k	40 k
UI Column	56 k	55 k	UI Column	52 k	52 k
LO Column	55 k	54 k	LO Column	59 k	62 k
LI Column	76 k	76 k	LI Column	65 k	62 k

Table 8-10 SDC B Shear Summary

Seismic Design Category C					
Pinned			Fixed		
Member	RBS	KBB	Member	RBS	KBB
Roof Beam	18 k	19 k	Roof Beam	19 k	20 k
4th Beam	34 k	35 k	4th Beam	35 k	35 k
3rd Beam	40 k	34 k	3rd Beam	34 k	36 k
2nd Beam	63 k	33 k	2nd Beam	33 k	35 k
UO Column	76 k	79 k	UO Column	79 k	78 k
UI Column	119 k	116 k	UI Column	116 k	117 k
LO Column	113 k	128 k	LO Column	128 k	126 k
LI Column	170 k	143 k	LI Column	143 k	145 k

Table 8-11 SDC C Shear Summary

Seismic Design Category D					
Pinned			Fixed		
Member	RBS	KBB	Member	RBS	KBB
Roof Beam	24 k	27 k	Roof Beam	25 k	23 k
4th Beam	42 k	43 k	4th Beam	44 k	41 k
3rd Beam	58 k	56 k	3rd Beam	48 k	48 k
2nd Beam	88 k	85 k	2nd Beam	45 k	38 k
UO Column	119 k	117 k	UO Column	124 k	119 k
UI Column	200 k	202 k	UI Column	195 k	201 k
LO Column	186 k	185 k	LO Column	204 k	211 k
LI Column	281 k	279 k	LI Column	242 k	238 k

Table 8-12 SDC D Shear Force Summary

8.5 Member Moment Forces Conclusion

Table 8-13 summarizes the moment load for SDC B of the parametric study. Upon looking at the table, for both PFC, the Roof Beam will experience the lowest moment load, with a gradual increase in moment to the 2nd Beam. For FFC beams, the moment increases like PFC, but drops at the 2nd beam with the drop being larger in KBB. For PFC columns, RBS and KBB, experience a gradual increase in moment load. For FFC columns, moment in RBS columns are significantly less than the KBB, but share the increasing moment load in the table.

Seismic Design Category B					
Pinned			Fixed		
Member	RBS Moment	KBB Moment	Member	RBS Moment	KBB Moment
Roof Beam	115 kft	117 kft	Roof Beam	109 kft	124 kft
4th Beam	210 kft	208 kft	4th Beam	194 kft	190 kft
3rd Beam	262 kft	251 kft	3rd Beam	204 kft	203 kft
2nd Beam	309 kft	321 kft	2nd Beam	191 kft	150 kft
UO Column	416 kft	416 kft	UO Column	330 kft	391 kft
UI Column	521 kft	517 kft	UI Column	401 kft	455 kft
LO Column	767 kft	762 kft	LO Column	877 kft	1015 kft
LI Column	974 kft	975 kft	LI Column	900 kft	1018 kft

Table 8-13 SDC B Moment Force Summary

Table 8-14 summarizes the moment load for SDC C of the parametric study. Upon looking at the table, for both PFC and KFF, mixed results can be observed. The PFC RBS Roof Beam experiences the lowest moment load, with a gradual increase in moment to the 2nd Beam. The PFC KBB Roof Beam experiences the lowest moment load, with an increase in moment load on the 4th beam and decrease in moment through the 2nd Beam. The FFC KBB Roof Beam experiences the lowest moment load, with a gradual increase in moment to the 3nd Beam, and then drops in moment on the 2nd Beam. The PFC RBS Roof Beam experiences the lowest moment load, with an increase in moment load on the 4th beam and decrease in moment through the 2nd Beam. For both PFC and FFC columns, experience a gradual increase in moment load. For PFC RBS columns have a lower moment demand than PFC KBB columns. For FFC KBB columns have a lower moment demand than FFC RBS columns

Seismic Design Category C									
Pinned					Fixed				
Member	RBS Moment		KBB Moment		Member	RBS Moment		KBB Moment	
Roof Beam	168	kft	182	kft	Roof Beam	182	kft	186	kft
4th Beam	288	kft	301	kft	4th Beam	301	kft	303	kft
3rd Beam	385	kft	300	kft	3rd Beam	300	kft	324	kft
2nd Beam	727	kft	268	kft	2nd Beam	268	kft	300	kft
UO Column	569	kft	685	kft	UO Column	685	kft	711	kft
UI Column	801	kft	903	kft	UI Column	903	kft	939	kft
LO Column	1583	kft	2166	kft	LO Column	2166	kft	1879	kft
LI Column	2200	kft	2228	kft	LI Column	2228	kft	1960	kft

Table 8-14 SDC C Moment Force Summary

Table 8-15 summarizes the moment load for SDC C of the parametric study. Upon looking at the table, for both PFC and KFF, RBS beams has higher moment demand the KBB beams. The PFC RBS Roof Beam experiences the lowest moment load, with a gradual increase in moment to the 2nd Beam. For both PFC and FFC, KBB Roof Beam experiences the lowest moment load at the Roof Beam, with an increase in moment load through the 3rd beam and decrease in moment through the 2nd Beam. The FFC RBS Roof Beam experiences the lowest moment load, with an increase in moment load on the 3rd beam and decrease in moment on the 2nd Beam. For both PFC and FFC columns, experience a gradual increase in moment load. For PFC RBS columns have a lower moment demand than PFC KBB columns. For FFC KBB columns have a lower moment demand than FFC RBS columns

Seismic Design Category D					
Pinned			Fixed		
Member	RBS Moment	KBB Moment	Member	RBS Moment	KBB Moment
Roof Beam	239 kft	287 kft	Roof Beam	264 kft	265 kft
4th Beam	395 kft	410 kft	4th Beam	419 kft	426 kft
3rd Beam	646 kft	610 kft	3rd Beam	496 kft	536 kft
2nd Beam	1101 kft	1055 kft	2nd Beam	445 kft	345 kft
UO Column	799 kft	975 kft	UO Column	1014 kft	1170 kft
UI Column	1193 kft	1497 kft	UI Column	1413 kft	1614 kft
LO Column	2599 kft	2585 kft	LO Column	3071 kft	3116 kft
LI Column	3646 kft	3665 kft	LI Column	3220 kft	3223 kft

Table 8-15 SDC D Moment Summary

8.6 General Conclusion

It was found that SMF RBS and SMF KBB systems behave similarly in resisting extreme seismic events. SMF RBS gives the designer a larger range of beam sizes for use in the moment frame while SMF KBB is more limited in beam choices. For this study, SMF RBS required deeper column sizes for drift reasons than SMF KBB, but weigh less than the SMF KBB columns. The SMF KBB column sizes were controlled by prying action at the beam/column connection. The LFRS that has a FFC experiences lower moment forces than the PFC and similar shear and axial forces. In a FFC, the foundation must resist some of the moment generated by the seismic force which will increase the size of the footing. The largest member forces generated can be found in SDC D, with SDC C in the middle, and SDC B being the lowest. This is because the seismic forces for the same LFRS system are different for each SDC. With that being said, larger members attract more forces and draw forces away from other members. This can work to the designer's advantage as well be as source of frustration. In general, the story drift compliance depends on the stiffness of LFRS beams and the calculated story drift. The most economical member for resisting the applied loads does not always meet the limitations imposed of the system design process. This study was conducted to explore a different connection type (SMF KBB) and compare it to one that is familiar (SMF RBS). Both systems have their benefits; additional studies are recommended for site specific locations due to construction preferences and economics.

References

Adan, S. M., & Gibb, W. (2009). Experimental evaluation of kaiser bolted bracket steel moment-resisting connections. Engineering journal, 46(3), 181.

AISC 341 (2010). AISC 341-10. *Seismic provisions for structural steel buildings. Chicago (IL): American Institute of Steel Construction*.

AISC 358 (2010). AISC 358–10 prequalified connections for special and intermediate steel moment frames for seismic applications. *American Institute of Steel Construction Inc., Chicago*.

American Society of Civil Engineers. Minimum design loads for buildings and other structures. Vol. 7. American Society of Civil Engineers, 2010.

Atila Zekioglu, S. E., Mozaffarian, H., Le Chang, S. E., Uang, C. M., & Noel, S. (1997). Designing after Northridge. Modern Steel Construction.

Carter, C. J. (1999). AISC Design Guide 13 wide-flange column stiffening at moment connections: Wind and seismic applications. American Institute of Steel Construction, Chicago.

Chambers, J. J., Almudhafar, S., & Stenger, F. (2003). Effect of reduced beam section frame elements on stiffness of moment frames. Journal of Structural Engineering, 129(3), 383-393.

Chen, S. J., & Chao, Y. C. (2001). Effect of composite action on seismic performance of steel moment connections with reduced beam sections. Journal of Constructional Steel Research, 57(4), 417-434.

Chen, S. J., Yeh, C. H., & Chu, J. M. (1996). Ductile steel beam-to-column connections for seismic resistance. Journal of Structural Engineering, 122(11), 1292-1299.

CorDova, P. P. (2011). Proprietary or Public Domain?. Modern Steel Construction.

Engelhardt, M. D. (1999a). Design of reduced beam section moment connections. In Proceedings, North American Steel Construction Conference, Toronto Canada, 1999 (Vol. 1).

Engelhardt, M. D. (1999b). Experimental Investigation of dogbone monent connections. Engineering Journal, 35(4), 128-139.

Engelhardt, M. D., Fry, G., Jones, S., Venti, M., & Holliday, S. (2000). Behavior and design of radius cut reduced beam section connections. Rep. No. SAC/BD-00, 17.

Engelhardt, M. D., Winneberger, T., Zekany, A. J., & Potyraj, T. J. (1996). The dogbone connection: Part II. Modern Steel Construction, 36(8), 46-55.

Engelhardt, M. D., Winneberger, T., Zekany, A.J. and Potyraj, T.J. (1998). Experimental Investigation of dogbone monent connections. Engineering Journal, 35(4), 128-139.

Engelhardt, M.D., Winneberger, T., Zekany, A.J. and Potyraj, T.J. (1997). “Experimental Investigation of Dogbone Moment Connections,” Proceedings; 1997 National Steel Construction Conference, American Institute of Steel Construction, Chicago.

FEMA (2000), “Recommended Seismic Design Criteria for New Steel Moment-Frame Buildings,” Report No. FEMA-350, Federal Emergency Management Agency, Washington, D.C.

Grigorian, C.E., Yang, T.S. and Popov, E.P. (1992), “Slotted Bolted Connection Energy Dissipators.” EERC Report No. 92/10, Earthquake Engineering Research Center, University of California, Berkeley, CA.

Gross, J. L. (2001, May). AISC Design Guide No. 12 Modification of Existing Welded Steel Moment Frame Connections for Seismic Resistance. In North American Steel Constrction Conference; 2001.

Grubbs, K. V. (1997). The effect of the dogbone connection on the elastic stiffness of steel moment frames (Doctoral dissertation, University of Texas at Austin).

Hamburger, R. O., Krawinkler, H., Malley, J. O., & Adan Scott, M. (2009). Seismic design of steel special moment frames. NEHRP Seismic Design Technical Brief, (2).

Iwankiw, N. R., & Carter, C. J. (1996). The dogbone: A new idea to chew on. Modern Steel Construction, 36(1), 18-23.

Jones, S. L., Fry, G. T., & Engelhardt, M. D. (2002). Experimental evaluation of cyclically loaded reduced beam section moment connections. Journal of Structural Engineering, 128(4), 441-451.

Kasai, K., & Bleiman, D. (1996, January). Bolted brackets for repair of damaged steel moment frame connections. In Proceedings of the 7th US–Japan Workshop on the Improvement of Structural Design and Construction Practices: Lessons Learned from Northridge and Kobe, Kobe, Japan. Applied Technology Council, Redwood City, CA, USA.

Kulak, G. L., Fisher, J. W., & Struik, J. H. (2001). Guide to Design Criteria for Bolted and Riveted Joints Second Edition.

Lee, C. H., & Kim, J. H. (2004). Seismic Design of Reduced Beam Section (RBS) Steel Moment Connections with Bolted Web Attachment. Journal of the Earthquake Engineering Society of Korea, 8(3), 87-96.

Lee, C. H., Kim, J. H., Jeon, S. W., & Kim, J. H. (2004). Influence of panel zone strength and beam web connection method on seismic performance of reduced beam section steel moment connections. In Proceedings of the CTBUH 2004 Seoul Conference—Tall Buildings for Historical Cities.

Masuda, H., Tamaka, A., Hirabayashi, K., & Genda, I. (1998). Experimental Study on the Effect of Partial Loss of Sectional Area on the Static Characteristics of H-Beams. Journal of Structural and Construction Engineering, 157-164.

Moore, K. S., Malley, J. O., & Engelhardt, M. D. (1999). Design of reduced beam section (RBS) moment frame connections. Steel Committee of California.

Newell, J. D., & Uang, C. M. (2006). Cyclic Testing of Steel Moment Connections for the CALTRANS District 4 Office Building Seismic Rehabilitation. Department of Structural Engineering, University of California, San Diego.

Okahashi, Y. (2008). Reduced Beam Section Connection without Continuity Plates (Doctoral dissertation, Department of Civil and Environmental Engineering, University of Utah).

Osteraas, J., and H. Krawinkler. "The Mexico earthquake of September 19, 1985—Behavior of steel buildings." Earthquake spectra 5.1 (1989): 51-88.

Plumier, A. (1990). New idea for safe structures in seismic zones. In IABSE Symposium. Mixed structures including new materials-Brussels (pp. 431-436).

Plumier, A. (1997). The dogbone: back to the future. ENGINEERING JOURNAL-AMERICAN INSTITUTE OF STEEL CONSTRUCTION, 34, 61-67.

Popov, E. P., Yang, T. S., & Chang, S. P. (1998). Design of steel MRF connections before and after 1994 Northridge earthquake. Engineering Structures, 20(12), 1030-1038.

Reis, E., & Bonowitz, D. (2000). State of the Art Report on Past Performance of Steel Moment-Frame Buildings in Earthquakes. SAC Rep. No. FEMA 355e, Federal Emergency Management Agency, Washington, DC.

Ricles, J. M., Zhang, X., Lu, L. W., & Fisher, J. (2004). Development of seismic guidelines for deep-column steel moment connections. Rep. No. 04, 13.

Ricles, J. M., Zhang, X., Lu, L. W., & Fisher, J. (2004). Development of seismic guidelines for deep-column steel moment connections. Rep. No. 04, 13.

Seek, M. W., & Murray, T. M. (2008). Seismic strength of moment end-plate connections with attached concrete slab. Proceedings, Connections VI, American Institute of Steel Construction, Chicago, IL, June, 23-25.

Seismology Committee. Structural Engineers Association of California-SEAOC (1999). Recommended lateral force requirements and commentary.

Shen, J., Astaneh-Asl, A., & McCallen, D. B. (2002). Use of deep columns in special steel moment frames. Steel Tips.

Shen, J., Kitjasateanphun, T., & Srivanich, W. (2000). Seismic performance of steel moment frames with reduced beam sections. Engineering Structures, 22(8), 968-983.

Suita, K., Tamura, T., Morita, S., Nakashima, M., & Engelhardt, M. D. (1999). Plastic Rotation Capacity of Steel Beam-to-Column Connections Using a Reduced Beam Section and No Weld Access Hole Design—Full Scale Tests for Improved Steel Beamto-Column Subassemblies—Part 1. Structural Journal, 177-184.

Tide, R.H.R (2010), “Bolt Shear Design Considerations,” Engineering Journal, American Institute of Steel Construction, Vol. 47 No. 1, pp. 47-63.

Tremblay, R., Tchebotarev, N., & Filiatrault, A. (1997). Seismic performance of RBS connections for steel moment resisting frames: Influence of loading rate and floor slab. Proceedings, Stessa’97.

Tsai, K. C., Chen, W. Z., & Lin, K. C. (1999, May). Steel Reduced Beam Section to Weak Panel Zone Moment Connections. In Proceedings: Workshop on Design Technologies of Earthquake-Resistant Moment-Resisting Connections in Steel Buildings (pp. 17-18).

Uang, C. M., & Fan, C. C. (1999). Cyclic instability of steel moment connections with reduced beam sections. Department of Structural Engineering, University of California, San Diego.

Uang, C. M., Gilton, C., & Chi, B. (2000). Cyclic response of RBS moment connections: Weak-axis configuration and deep column effects. Rep. No. SAC/BD-00, 23.

Uang, C.M. and Richards, P. (2002), “Cyclic Testing of Steel Moment Connections for East Tower of Hoag Memorial Hospital Presbyterian,” Third Progress Report, University of California, San Diego, CA.

Yu, Q.S. Gilton, C. and Uang, C.M. (2000) “Cyclic Response of RBS Moment Connections: Loading Sequence and Lateral Bracing Effects,” Report No. SAC/BD-00/22, SAC Joint Venture, Sacramento, CA, 2000.

Zekioglu, A., Mozaffarian, H., & Uang, C. M. (1997). Moment frame connection development and testing for the city of hope national medical center. In Building to Last (pp. 100-104). ASCE.

Appendix A - Design Example

Seismic Force

Step Description	Computation												Reference
	S_S =	1.5	TL =	16									ASCE 7-10
	S_l =	0.5	I_e =	1									Fig. 22.1
	S. Cl.	D	h =	51.5									Fig. 22.2
	F_a =	1											
	F_v =	1.5											
Site Class													ASCE 7-10
	$S_{MS} = F_a*S_S$				$S_{MI} = F_v*S_l$								Table 11.4-1
		F_a	S_S			F_v	S_l						Table 11.4-2
	S_{MS} =	1	1.5		S_{MI} =	1.5	0.5						Eqn 11.4-1
	S_{MS} =	1.5			S_{MI} =	0.75							Eqn 11.4-2
Spectral													ASCE 7-10
Response	$S_{DS} = 2/3*S_{MS}$				$S_{DI} = 2/3*S_{MI}$								Eqn 11.4-3
		Coeff	S_{MS}			Coeff	S_{MI}						Eqn 11.4-4
	S_{DS} =	0.667	1.5		S_{DI} =	0.667	0.75						
	S_{DS} =	1			S_{DI} =	0.5							
Response													ASCE 7-10
Modification	Structure with no irregularities and not exceeding 160												Table 12.2-1
Coefficient	ft in structural height: Lateral Force Method Permitted												Table 12.6-1
		Special Moment Frames											Sect. 12.2.5.6
		R =	8	Ω =	3	C_d =	5.5						Sect. 12.2.5.5
Seismic	$T_a = C_t*h_n^x$												ASCE 7-10
Response		C_t	h_n	x		T ≤ TL	8	-	16	s			Sect. 12.8.2
	T_a =	0.028	51.5	0.8									Sect. 12.8.2.1
	T_a =	0.656											Eqn 12.8-1
													Table 12.8-2
	$C_s = S_{DI}/(T*R/I_e)$					≤	$C_s = S_{DS}/(R/I_e)$						Eqn 12.8-3
		S_{DI}	T	R	I_e			S_{DS}	R	I_e			Eqn 12.8-5
	C_s =	0.5	0.656	8	1		C_s =	1	8	1			Eqn 12.8-6
	C_s =	0.095					C_s =	0.125					
	$C_s = S_{DS}/(R/I_e)$				≥	$C_s = .044*S_{DS}*I_e$				≥	0.01		
		S_{Ds}	R	I_e			Coeff.	S_{DS}	I_e				
	C_s =	1	8	1		C_s =	0.044	1	1				
	C_s =	0.125				C_s =	0.044						
	$C_s = S_{DS}/(R/I_e)$				≥	$C_s = .5*S_l/(R/I_e)$							
		S_{Ds}	R	I_e			Coeff.	S_l	R	I_e			
	C_s =	1	8	1		C_s =	0.5	0.5	8	1			
	C_s =	0.125				C_s =	0.031						
Seismic Weight	Roof Weight					3rd & 4th Weight							
	$W_r = W_b*L_b*DL$					$W_{3,4} = W_b*L_b*DL$							
		W_b	L_b	D_L			W_b	L_b	D_L				
	W_r =	75	150	70		$W_{3,4}$ =	75	150	85				
	W_r =	787.5	k			$W_{3,4}$ =	956.3	k					ASCE 7-10
													Eqn 12.8-1
	2nd Weight					Curtain Wall Weight							
	$W_2 = W_b*L_b*DL$					$W_{ct} = W_{ct}*H*P$							
		W_b	L_b	D_L			W_{ct}	H	P				
	W_2 =	75	150	85		W_{ct} =	15	51.5	450				
	W_2 =	956.3	k			W_{ct} =	347.6						
	W_t =	4004											

Step Description	Computation							Reference
Seismic Shear	$V = C_s * W_t$							
		C_s	W_t					
	V =	0.095	4004					
	V =	381.73	kips					
k Exponent								ASCE 7-10
	T < .5, k = 1; .5 < T < 2.5, Interpolate btw 1 & 2; T > 2.5, k =2							Section 12.8.3
		T_a	Coeff. P_l	Coeff. P_h	Coeff. k_l	Coeff. k_h		
	k =	0.656	0.5	2.5	1	2		
	k =	1.078						
Vertical &	Level	h_x (ft)	w_x (k)	$w_x*h_x^k$	C_{vx}	F_x	V_x (k)	ASCE 7-10
Horizontal	Roof	51.5	4004	280169.56	0.40	154.21	154.21	Sect. 12.8.3
Distribution	4th Flr	39	4004	207628.88	0.30	114.28	268.49	Eqn 12.8-11
	3rd Flr	26.5	4004	136904.33	0.20	75.35	343.85	Eqn 12.8-12
	2nd Flr	14	4004	68825.11	0.10	37.88	381.73	Eqn 12.8-13
	Ground					381.73	k	Sect. 12.8.4

Accidental Torsional SDC D Roof Beam

Step Description	Computation										Reference
Seismic Class D	T =	75	ft		R_c =	1	k/in	A_{mic} =	125	ft2	
	L =	150	ft		R_d =	1	k/in	V_r =	154.2	k	
	R_a =	1	k/in		A_{tot} =	11250	ft2				
	R_b =	1	k/in		A_{st} =	250	ft2				
Eccentricity and Rigidity Properties	$x_R = \Sigma A_i*x_i/A_{net}$										ASCE 7-10 Sect 12.8.4.1
		A_{tot}	A_{st}	A_{mic}	x_1	x_2	x_3	x_4			
	x_R =	11250	250	125	75	5	145	65			
	x_R =	76.14	ft								
	$y_R = \Sigma A_i*y_i/A_{net}$										
		A_{tot}	A_{st}	A_{mic}	y_1	y_2	y_3	y_4	y_5		
	y_R =	11250	250	125	37.5	62.5	12.5	31.25	43.75		
	y_R =	37.42	ft								
	$e_x = L/2 - x_R$				$e_y = T/2 - y_R$						
		L	x_R			T	y_R				
	e_x =	150	76.14		e_y =	75	37.42				
	e_x =	-1.137	ft		e_y =	0.075	ft				
	$J = R_a*x_R$^2 $+ R_b*(L - x_R)$^2 $+ R_c*y_R$^2 $+ R_d*(T - y_R)$										
		R_a	R_b	R_c	R_d	L	x_R	T	y_R		
	J =	1	1	1	1	150	76.14	75	37.42		
	J =	14065	k*ft2/in								
Direct Shear	$V_D = (R_a*V_r)/(R_a + R_b)$					$V_D = (R_b*V_r)/(R_a + R_b)$					
		R_a	R_b	V_r			R_a	R_b	V_r		
	V_D =	1	1	154.21		V_D =	1	1	154.21		
	V_D =	77.11	k			V_D =	77.11	k			
	$V_D = (R_c*V_r)/(R_c + R_d)$					$V_D = (R_d*V_r)/(R_c + R_d)$					
		R_c	R_d	V_r			R_c	R_d	V_r		
	V_D =	1	1	154.21		V_D =	1	1	154.21		
	V_D =	77.11	k			V_D =	77.11	k			
Plan Irregularity	$e_{acc,x} = 0.05*L$				$e_{acc,y} = 0.05*T$						ASCE 7-10 Sect 12.8.4.2
		L				T					
	$e_{acc,x}$ =	150			$e_{acc,y}$ =	75					
	$e_{acc,x}$ =	7.5	ft		$e_{acc,y}$ =	3.75	ft				
	$V'_{T,a} = (V_r*(e - e_{acc})*x_R*R_a)/J$										
		V_r	e	$e_{acc,x}$	x_R	R_a	J				
	$V'_{T,a}$ =	154.21	-1.137	7.5	76.14	1	14065				
	$V'_{T,a}$ =	-7.21	k								
	$V'_{T,b} = (V_r*(e + e_{acc})*x_R*R_c)/J$										
		V_r	e	$e_{acc,x}$	x_R	R_b	J				
	$V'_{T,b}$ =	154.21	-1.137	7.5	76.14	1	14065				
	$V'_{T,b}$ =	5.311	k								
	$V'_{T,c} = (V_r*(e - e_{acc})*y_R*R_c)/J$										
		V_r	e	$e_{acc,y}$	y_R	R_c	J				
	$V'_{T,c}$ =	154.21	0.075	3.75	37.42	1	14065				
	$V'_{T,c}$ =	-1.508	k								

Step Description	Computation							Reference
	$V'_{T,d} = (V_r*(e + e_{acc})*y_R*R_d)/J$							
		V_r	e	$e_{acc,y}$	y_R	R_d	J	
	$V'_{T,d}$ =	154.21	0.075	3.75	37.42	1	14065	
	$V'_{T,d}$ =	1.57	k					
Initial Total Shear	$V'_a = V_{D,a} - V'_{T,a}$			$V'_a = V_{D,a} + V'_{T,a}$				
		$V_{D,a}$	$V'_{T,A}$		$V_{D,a}$	$V'_{T,A}$		
	V'_a =	77.11	-7.21	V'_a =	77.11	-7.21		
	V'_a =	84.32	k	V'_a =	69.89	k		
	$V'_a = -V_{D,a} - V'_{T,a}$			$V'_a = -V_{D,a} + V'_{T,a}$				
		$V_{D,a}$	$V'_{T,A}$		$V_{D,a}$	$V'_{T,A}$		
	V'_a =	77.11	-7.21	V'_a =	77.11	-7.21		
	V'_a =	-69.89		V'_a =	-84.32	k		
	V'_a =	84.32	k					
	$V'_b = V_{D,b} - V'_{T,b}$			$V'_b = V_{D,b} + V'_{T,b}$				
		$V_{D,b}$	$V'_{T,b}$		$V_{D,b}$	$V'_{T,b}$		
	V'_b =	77.11	5.311	V'_b =	77.11	5.311		
	V'_b =	71.79	k	V'_b =	82.42	k		
	$V'_b = -V_{D,b} - V'_{T,b}$			$V'_b = -V_{D,b} - V'_{T,b}$				
		$V_{D,b}$	$V'_{T,b}$		$V_{D,b}$	$V'_{T,b}$		
	V'_b =	77.11	5.311	V'_b =	77.11	5.311		
	V'_b =	-82.42	k	V'_b =	-71.79	k		
	V'_b =	82.42	k					
	$V'_c = V_{D,c} - V'_{T,c}$			$V'_c = V_{D,c} + V'_{T,c}$				
		$V_{D,c}$	$V'_{T,c}$		$V_{D,c}$	$V'_{T,c}$		
	V'_c =	77.11	-1.508	V'_c =	77.11	-1.508		
	V'_c =	78.61	k	V'_c =	75.6	k		
	$V'_c = -V_{D,c} - V'_{T,c}$			$V'_c = -V_{D,c} - V'_{T,c}$				
		$V_{D,c}$	$V'_{T,c}$		$V_{D,c}$	$V'_{T,c}$		
	V'_c =	77.11	-1.508	V'_c =	77.11	-1.508		
	V'_c =	-75.6	k	V'_c =	-78.61	k		
	V'_c =	78.61	k					
	$V'_d = V_{D,d} - V'_{T,d}$			$V'_d = V_{D,d} + V'_{T,d}$				
		$V_{D,d}$	$V'_{T,d}$		$V_{D,d}$	$V'_{T,d}$		
	V'_d =	77.11	1.57	V'_d =	77.11	1.57		
	V'_d =	75.54	k	V'_d =	78.67	k		
	$V'_d = -V_{D,d} - V'_{T,d}$			$V'_d = -V_{D,d} - V'_{T,d}$				
		$V_{D,d}$	$V'_{T,d}$		$V_{D,d}$	$V'_{T,d}$		
	V'_d =	77.11	1.57	V'_d =	77.11	1.57		
	V'_d =	-78.67	k	V'_d =	-75.54	k		
	V'_d =	78.67	k					

Step Description	Computation								Reference
Resulting Displacements	$\delta_a = V'_a/R_a$				$\delta_b = V'_b/R_b$				
		V'_a	R_a			V'_b	R_b		
	$\delta_a =$	84.32	1		$\delta_b =$	82.42	1		
	$\delta_a =$	84.32	in		$\delta_b =$	82.42	in		
	$\delta_c = V'_c/R_c$				$\delta_d = V'_d/R_d$				
		V'_c	R_c			V'_d	R_d		
	$\delta_c =$	78.61	1		$\delta_d =$	78.67	1		
	$\delta_c =$	78.61	in		$\delta_d =$	78.67	in		
	$\delta_{avg,ab} = (\delta_a + \delta_b)/2$				$\delta_{avg,cd} = (\delta_c + \delta_d)/2$				
		δ_a	δ_b			δ_c	δ_d		
	$\delta_{avg,ab} =$	84.32	82.42		$\delta_{avg,cd} =$	78.61	78.67		
	$\delta_{avg,ab} =$	83.37	in		$\delta_{avg,cd} =$	78.64	in		
	$\delta_{max,ab} =$	84.32	in		$\delta_{max,cd} =$	78.67	in		
	$\delta_{max,ab}/\delta_{avg,ab}$				$\delta_{max,cd}/\delta_{avg,cd}$				
		$\delta_{max,ab}$	$\delta_{avg,ab}$			$\delta_{max,cd}$	$\delta_{avg,cd}$		
	=	84.32	83.37		=	78.67	78.64		
	=	1.011	< 1.4		=	1	< 1.4		
	$A_x = (\delta_{max,ab}/(1.2*\delta_{avg,ab}))$^2					$A_y = (\delta_{max,cd}/(1.2*\delta_{avg,cd}))$^2			
		$\delta_{max,ab}$	$\delta_{avg,ab}$				$\delta_{max,ab}$	$\delta_{avg,ab}$	
	$A_x =$	84.32	83.37			$A_y =$	78.67	78.64	
	$A_x =$	0.71	< 3			$A_y =$	0.695	< 3	
Torsional Shear	$V_{T,a} = (V_r*(e - A_x*e_{acc})*x_R*R_a)/J$								
		V_r	e	A_x	$e_{acc,x}$	x_R	R_a	J	
	$V_{T,a} =$	154.21	-1.137	0.71	7.5	76.14	1	14065	
	$V_{T,a} =$	-5.397	k						
	$V_{T,b} = (V_r*(e + A_x*e_{acc})*x_R*R_c)/J$								
		V_r	e	A_x	$e_{acc,x}$	x_R	R_b	J	
	$V_{T,b} =$	154.21	-1.137	0.71	7.5	76.14	1	14065	
	$V_{T,b} =$	3.498	k						
	$V_{T,c} = (V_r*(e - A_x*e_{acc})*y_R*R_d)/J$								
		V_r	e	A_y	$e_{acc,y}$	y_R	R_c	J	
	$V_{T,c} =$	154.21	0.075	0.695	3.75	37.42	1	14065	
	$V_{T,c} =$	-1.038	k						
	$V_{T,d} = (V_r*(e + A_x*e_{acc})*y_R*R_d)/J$								
		V_r	e	A_y	$e_{acc,y}$	y_R	R_d	J	
	$V_{T,d} =$	154.21	0.075	0.695	3.75	37.42	1	14065	
	$V_{T,d} =$	1.1	k						
Total Shear	$V_a = V_{D,a} + V_{T,a}$				$V_b = V_{D,b} + V_{T,b}$				
		$V_{D,a}$	$V_{T,a}$			$V_{D,a}$	$V_{T,a}$		
	$V_a =$	77.11	5.397		$V_b =$	77.11	3.498		
	$V_a =$	82.5	k		$V_b =$	80.6	k		
	$V_c = V_{D,c} + V_{T,c}$				$V_d = V_{D,d} + V_{T,d}$				
		$V_{D,c}$	$V_{T,c}$			$V_{D,a}$	$V_{T,a}$		
	$V_c =$	77.11	1.038		$V_d =$	77.11	1.1		
	$V_c =$	78.14	k		$V_d =$	78.21	k		

Fixed Story Drift and Stability Check

Step Description	Computation											Reference
	Roof D	70	psf		N2	0.335	in			Section	Z_x	
	Floor D	85	psf		N3	0.857	in		Column	36x182	718	
	C. Wall	15	psf		N5	1.365	in		Roof B	30x99	312	
	Roof L	20	psf		N6	1.744	in		4th B	30x99	312	
	Floor L	80	psf		A =	11250	ft^2		3rd B	30x99	312	
					C_d =	5.5			2nd B	30x99	312	
					β =	1						
					I_e =	1						
Allowable Story Drift	**2nd**					**3rd**						ASCE 7-10 Table 12.12-1
	$\Delta_2 = .025*h_{sx}$					$\Delta_3 = .025*h_{sx}$						
		Coeff	hsx				Coeff	h_{sx}				
	Δ_2 =	0.025	168			Δ_3 =	0.025	150				
	Δ_2 =	4.2	in			Δ_3 =	3.75	in				
	4th					**Roof**						
	$\Delta_4 = .025*h_{sx}$					$\Delta_r = .025*h_{sx}$						
		Coeff	hsx				Coeff	h_{sx}				
	Δ_4 =	0.025	150			Δ_r =	0.025	150				
	Δ_4 =	3.75	in			Δ_r =	3.75	in				
Story Drift	**Base to 2nd**					**2nd to 3rd**						ASCE 7-10 Section 12.8.6
	$\delta_{xe} = \delta_2 - \delta_1$					$\delta_{xe} = \delta_3 - \delta_2$						
		δ_2	δ_1				δ_3	δ_2				
	δ_{xe} =	0.335	0			δ_{xe} =	0.857	0.335				
	δ_{xe} =	0.335	in			δ_{xe} =	0.522	in				
	$\delta_{xe,rbs} = 1.1*\delta_{xe}$					$\delta_{xe,rbs} = 1.1*\delta_{xe}$						
		Coeff	δ_{xe}				Coeff	δ_{xe}				
	$\delta_{xe,rbs}$ =	1.1	0.335			$\delta_{xe,rbs}$ =	1.1	0.522				
	$\delta_{xe,rbs}$ =	0.369	in			$\delta_{xe,rbs}$ =	0.574	in				
	$\Delta_x = C_d*\delta_{xe}/I_e$					$\Delta_x = C_d*\delta_{xe}/I_e$						
		C_d	δ_{xe}	I_e			C_d	δ_{xe}	I_e			
	Δ_x =	5.5	0.369	1		Δ_x =	5.5	0.574	1			
	Δ_x =	2.027	in			Δ_x =	3.158	in				
	$\Delta_x < \Delta_2$		TRUE			$\Delta_x < \Delta_3$		TRUE				
	3rd to 4th					**4th to Roof**						
	$\delta_{xe} = \delta_4 - \delta_3$					$\delta_{xe} = \delta_r - \delta_4$						
		δ_4	δ_3				δ_r	δ_4				
	δ_{xe} =	1.365	0.857			δ_{xe} =	1.744	1.365				
	δ_{xe} =	0.508	in			δ_{xe} =	0.379	in				
	$\delta_{xe,rbs} = 1.1*\delta_{xe}$					$\delta_{xe,rbs} = 1.1*\delta_{xe}$						
		Coeff	δ_{xe}				Coeff	δ_{xe}				
	$\delta_{xe,rbs}$ =	1.1	0.508			$\delta_{xe,rbs}$ =	1.1	0.379				
	$\delta_{xe,rbs}$ =	0.559	in			$\delta_{xe,rbs}$ =	0.417	in				
	$\Delta_x = C_d*\delta_{xe}/I_e$					$\Delta_x = C_d*\delta_{xe}/I_e$						
		C_d	δ_{xe}	I_e			C_d	δ_{xe}	I_e			
	Δ_x =	5.5	0.559	1		Δ_x =	5.5	0.417	1			
	Δ_x =	3.073	in			Δ_x =	2.293	in				
	$\Delta_x < \Delta_4$		TRUE			$\Delta_x < \Delta_r$		TRUE				

Step Description	Computation												Reference
Dead & Live Load	**DL Roof**							**Roof LL**					
	DL = DL_r*A+MD*Peri*H							$LL_r = LL_r$*A					
		DL	A	C. Wall	Peri.	H			LL_r	A			
	DL =	70	11250	15	225	6.25		LL_r =	20	11250			
	DL =	808.6	k					LL_r =	225	k			
	DL 4th							**LL 4th**					
	DL = DL_4*A+MD*Peri*H+SD*A							LL = LL*A					
		DL	A	C. Wall	Peri.	H			LL	A			
	DL =	85	11250	15	225	12.5		LL_r =	80	11250			
	DL =	998.4	k					LL_r =	900	k			
	DL 3th							**LL 3th**					
	DL = DL_3*A+MD*Peri*H							LL = LL*A					
		DL	A	C. Wall	Peri.	H			LL	A			
	=	85	11250	15	225	12.5		=	80	11250			
	=	998.4	k					=	900	k			
	DL 2th							**LL 2th**					
	DL = DL_2*A+MD*Peri*H+SD*A							LL = LL*A					
		DL	A	C. Wall	Peri.	H			LL	A			
	DL =	85	11250	15	225	13.25		=	80	11250			
	DL =	1001	k					=	900	k			
	$P_{DL} = DL_r+DL_4+DL_3+DL_2$						P_{LL} = .25*(SL+LL_4+LL_3+LL_2)						
		Roof DL	4th DL	3rd DL	2nd DL			LL_r	LL_4	LL_3	LL_2		
	P_{DL} =	808.6	998.4	998.4	1001		P_{LL} =	225	900	900	900		
	P_{DL} =	3806	k				P_{LL} =	731.3	k				
	$P_x = P_{DL}+P_{LL}$												
		P_{DL}	P_{LL}										
	P_x =	3806	731.3										
	P_x =	4538	k										
Plastic Moment	**Roof B**						**4th B**						
	M_p= 1.1*R_y*F_y*Z_x						M_p= 1.1*R_y*F_y*Z_x						
		Coeff	R_y	F_y	Z_x			Coeff	R_y	F_y	Z_x		
	M_p =	1.1	1.1	50	312		M_p =	1.1	1.1	50	312		
	M_p =	1573	kft				M_p =	1573	kft				
	3rd B						**2nd B**						
	M_p= 1.1*R_y*F_y*Z_x						M_p= 1.1*R_y*F_y*Z_x						
		Coeff	R_y	F_y	Z_x			Coeff	R_y	F_y	Z_x		
	M_p =	1.1	1.1	50	312		M_p =	1.1	1.1	50	312		
	M_p =	1573	kft				M_p =	1573	kft				
Seismic Shear	**Roof Beam**						**3rd Beam**						
	V_{yi} = 2*Σ*M_p/H						V_{yi} = 2*Σ*M_p/H						
		Coeff	#Frame	#Beam	M_p	H		Coeff	#Frame	#Beam	M_p	H	
	V =	2	3	1	1573	51.5	V =	2	3	1	1573	26.5	
	V =	183.3	k				V =	356.2	k				
	4th Beam						**2nd Beam**						
	V_{yi} = 2*Σ*M_p/H						V_{yi} = 2*Σ*M_p/H						
		Coeff	#Frame	#Beam	M_p	H		Coeff	#Frame	#Beam	M_p	H	
	V =	2	3	1	1573	39	V =	2	3	1	1573	14	
	V =	242					V =	674.1	k				

Step Description	Computation												Reference
Stability	**Roof Beam**								2nd Order Adjustment				ASCE 7-10
Coefficient	$\theta = (P_x*\Delta*I_e)/(V_x*h_{sx}*C_d)$								$\theta/(1+\theta)$				Eqn. 12.8-16
		P_x	Δ	I_e	V_x	h_{sx}	C_d			θ			Eqn. 12.8-17
	θ =	4538	2.293	1	183.3	150	5.5		=	0.069			
	θ =	0.069							=	0.064			
	$\theta_{max} = .5/(\beta*C_d)$												
		Coeff	β	C_d									
	θ_{max} =	0.5	1	5.5									
	θ_{max} =	0.091				$\theta < \theta_{max}$		TRUE					
	4th Beam								2nd Order Adjustment				
	$\theta = (P_x*\Delta*I_e)/(V_x*h_{sx}*C_d)$								$\theta/(1+\theta)$				
		P_x	Δ	I_e	V_x	h_{sx}	C_d			θ			
	θ =	4538	3.073	1	242	150	5.5		=	0.07			
	θ =	0.07							=	0.065			
	$\theta_{max} = .5/(\beta*C_d)$												
		Coeff	β	C_d									
	θ_{max} =	0.5	1	5.5									
	θ_{max} =	0.091				$\theta < \theta_{max}$		TRUE					
	3rd Beam								2nd Order Adjustment				
	$\theta = (P_x*\Delta*I_e)/(V_x*h_{sx}*C_d)$								$\theta/(1+\theta)$				
		P_x	Δ	I_e	V_x	h_{sx}	C_d			θ			
	θ =	4538	3.158	1	356.2	150	5.5		=	0.049			
	θ =	0.049							=	0.047			
	$\theta_{max} = .5/(\beta*C_d)$												
		Coeff	β	C_d									
	θ_{max} =	0.5	1	5.5									
	θ_{max} =	0.091				$\theta < \theta_{max}$		TRUE					
	2nd Beam								2nd Order Adjustment				
	$\theta = (P_x*\Delta*I_e)/(V_x*h_{sx}*C_d)$								$\theta/(1+\theta)$				
		P_x	Δ	I_e	V_x	h_{sx}	C_d			θ			
	θ =	4538	2.027	1	674.1	168	5.5		=	0.015			
	θ =	0.015							=	0.015			
	$\theta_{max} = .5/(\beta*C_d)$												
		Coeff	β	C_d									
	θ_{max} =	0.5	1	5.5									
	θ_{max} =	0.091				$\theta < \theta_{max}$		TRUE					

Fixed Roof Beam Seismic Design Check

Step Description	Computation: RB p1												Reference
	F_y =	50	ksi		F_u =	65	ksi		M_{ur} =	277.16	kft		
	E =	29000	ksi		R_y =	1.1			P_{ur} =	38.961	k		
	$\phi_{b,c}$ =	0.9			t_w =	0.52	in		V_{ur} =	26.337	k		
	Section	t_f	$(s-d_c)/h_b$	b_f	d	A	Z_x	r_x	r_y	S_x	h/t_w	h_0	
	30x99	0.67	10.303	10.5	29.7	29	312	11.7	2.1	269	51.9	29	
RBS Dimensions	$.5*b_f$ =	5.25	≤	a =	7.75	≤	$.75*b_f$ =	7.875					AISC 2nd Ed.
	$.65*d$ =	19.305	≤	b =	25	≤	$.85*d$ =	25.245					Eq. 5.8-1
	$.1*b_f$ =	1.05	≤	c =	2.5	≤	$.25*b_f$ =	2.625					Eq. 5.8-2
													Eq. 5.8-3
Check Beam Element Slenderness	$R = (4*c^2 + b^2)/(8*c)$				$b_{f,rbs} = 2*(R - c) + b_f - 2*\sqrt{R^2 - (b/3)^2}$								AISC 341 2010
		c	b			R	c	b_f	b				Section D1.1
	R =	2.5	25		$b_{f,rbs}$ =	32.5	2.5	10.5	25				Table D1.1
	R =	32.5	in		$b_{f,rbs}$ =	7.6731	in						AISC 14th ED.
													Section B4.1
	$\lambda_f = b_{f,rbs}/(2*t_f)$			≤	$\lambda_{hd} = .3*\sqrt{E/F_y}$								Section B4.2
		$b_{f,rbs}$	t_f			E	F_y						
	λ_f =	7.6731	0.67		λ_{hd} =	29000	50						
	λ_f =	5.7262		≤	λ_{hd} =	7.225		TRUE					
	$C_a = P_u/(\phi_b*F_y*A_g)$												
		P_u	ϕ_b	F_y	A_g								
	C_a =	38.961	0.9	50	29								
	C_a =	0.0299											
	If $C_a \leq 0.125$, then $\lambda_{hd} = 2.45*\sqrt{E/F_y}*(1-.93*C_a)$												
	If $C_a > 0.125$, then $\lambda_{hd} = 0.77*\sqrt{E/F_y}*(2.93 - C_a) \geq 1.49*\sqrt{E/F_y}$												
		E	Fy	C_a									
	λ_{hd} =	29000	50	0.0299									
	λ_{hd} =	57.366	>	$\lambda_w = h/t_w$ =		51.9	≥	$1.49*\sqrt{E/F_y}$ =		35.884	TRUE		
Lateral Bracing Requirements	$L_b = 0.086*r_y*E/F_y$												AISC 341 2010
		r_y	E	F_y									Sect. E.4.b
	L_b =	2.1	29000	50									Sect. D.1.2b
	L_b =	8	ft										AISC 14th Ed.
													Table 3-2
	L_p =	7.42	<	L_b =	8	<	L_r =	21.3					
Available Flexural Strength	$C_{b,ext} = 12.5*M/(2.5*M + 3*.875*M + 4*.75*M + 3*.625*M)$												AISC 14th ED.
		M_1	M_2	M_a	M_b	M_c							Eq. F2-2
	$C_{b,ext}$ =	12.5	2.5	2.625	3	1.875							Eq. F2-1
	$C_{b,ext}$ =	1.25											
	$C_{b,int} = 12.5*.5*M/(2.5*.5*M + 3*.375*M + 4*.25*M + 3*.125*M)$												
		M_1	M_2	M_a	M_b	M_c							
	$C_{b,int}$ =	6.25	1.25	1.125	1	0.375							
	$C_{b,int}$ =	1.6667											
	$M_p = Z_x*F_y$												
		Z_x	F_y										
	M_p =	312	50										
	M_p =	1300	kft										
	$M_n = C_b*(M_p-(M_p-.7*S_x*F_y*((L_b-L_p)/(L_r-L_p)))) \leq M_p$												
		C_b	M_p	S_x	F_y	L_b	L_p	L_r					
	M_n =	1.25	1300	269	50	8	7.42	21.3					
	M_n =	40.981	kft	≤	M_p =	1300							

Step Description	Computation: RB p2												Reference
Reduced Section Modulus	$Z_{rbs} = Z_x - 2*c*t_f*(d-t_f)$												
		Z_x	c	t_f	d								
	Z_{rbs} =	312	2.5	0.67	29.7								
	Z_{rbs} =	214.75	in3										
Available & Required Flexural Strength	$\phi_b M_{n,rbs} = \phi_b*F_y*Z_{rbs}$												
		ϕ_b	F_y	Z_{rbs}									
	$\phi_b M_{n,rbs}$ =	0.9	50	214.75									
	$\phi_b M_{n,rbs}$ =	805.31	kft	≥	M_u =	277.16	kft	TRUE					
	$\phi M_n = \phi_b*M_p = \phi_b*F_y*Z_x$												
		ϕ_b	F_y	Z_x									
	ϕM_n =	0.9	50	312									
	ϕM_n =	1170	kft	≥	M_u =	277.16	kft	TRUE					
Available Shear Strength	If $h/t_w \le 2.24*\sqrt{E/F_y}$, then $C_v = 1$												AISC 14th Ed.
	h/t_w		E	F_y									Sect. G2
	51.9	≤	29000	50									
		≤	53.946										
	If $h/t_w > 2.24*\sqrt{E/F_y}$, then C_v is determined as followed:												
	For webs w/out transverse stiffners k_v =					5							
		When $h/t_w \le 1.10*\sqrt{k_v*E/F_y}$, then $C_v = 1$											
		When $1.10*\sqrt{k_v*E/F_y} < h/t_w \le 1.37*\sqrt{k_v*E/F_y}$, then $C_v = 1.1*\sqrt{k_v*E/F_y}/(h/t_w)$											
		When $h/t_w > 1.37*\sqrt{k_v*E/F_y}$, then $C_v = 1.51*k_v*E/((h/t_w)^2*F_y)$											
			C_v =	1									
	$\phi V_n = \phi*0.6*F_y*A_w*C_v$												
		ϕ_v	F_y	t_w	d	C_v							
	ϕV_n =	1	50	0.52	29.7	1							
	ϕV_n =	463.32	k	>	V_u =	26.337	k	TRUE					
Reduce Beam Section Shear	$S_h = a+b/2$				$L_h = L-2*(d_c/2)-2*S_h$								AISC 358
		a	b			L	d_c	S_h					Eqn. C5.8-1
	S_h =	7.75	25		L_h =	336	30	20.25					Eqn. C5.8-2
	S_h =	20.25	in		L_h =	265.5	in						Eqn. C5.8-6
													Eqn. C5.8-7
	$V_{rbs} = 2*M_p/L_h+V_u$					$V_{rbs}' = 2*M_p/L_h-V_u$							Eqn. C5.8-8
		M_p	L_h	V_u			M_p	L_h	V_u				Eqn. C5.8-9
	V_{rbs} =	1300	22.125	33.517		V_{rbs}' =	1300	22.125	33.517				
	V_{rbs} =	151.03	k			V_{rbs}' =	83.997	k					
Required Strength of Bracing	$M_r = M_u = R_y*F_y*Z_x$					$P_u = .06*R_y*F_y*Z_x/h_0$							AISC 341
		R_y	F_y	Z_x			R_y	F_y	Z_x	h_0			Eqn. D1-4a
	M_r =	1.1	50	312		P_u =	1.1	50	312	29			Eqn. D1-4b
	M_r =	1430	kft			P_u =	591.72	k					Eqn. D1-5a
													Eqn. D1-5b
	$L = \sqrt{a^2+b^2}$												Eqn. D1-6a
		a	b										Eqn. D1-6b
	L =	288	21.5										
	L =	24.067	in										
	$\beta_{br} = (10*M_r*C_d)/(\phi*L_b*h_0)$							$\theta = \tan^{-1}(d/l)$					
		M_r	C_d	ϕ	L_b	h_0			d	L			
	β_{br} =	1430	1	0.75	96	29		θ =	12.1	150			
	β_{br} =	6.8487	k/in					θ =	12.37	rad			

Step Description	Computation: RB p3												Reference
	Use L5x5x5/16												
	$K = A_g*E*cos^2(\theta)/L$												
		A_g	E	θ	L								
	K =	3.03	29000	12.37	288								
	K =	293.47	k/in	>	β_{br} =	6.8487	k/in	TRUE					

Fixed LO Column Seismic Design Check

Step Description	Computation												Reference
Column LO p1	M_u =	3071	kft	F_y =	50	ksi	ρ =	1.3		$\phi_{c,b}$ =	0.9		
W36x256	P_u =	302.4	k	E =	29000	ksi	β =	1		α =	1		
	V_u =	204.3	k	L_b =	14	ft	S_{ds} =	1		K_x =	1		
	A =	11250	ft^2	I_e =	1		C_d =	5.5		K_y =	1		
	Column Geomtric Properties												
	Sect.	d	A	Z_x	h/t_w	t_w	r_x	b_f	t_f	I_x	r_y	h_0	
		37.4	75.3	1040	33.8	0.96	14.9	12.2	1.73	16800	2.65	35.7	
	36x256	J	S_x	T									
		35.7	895	32.13									
Check Column	**Flange:**												AISC 341
Element	$\lambda_f = b_f/(2{*}t_f)$					$\lambda_{hd} = .3{*}\sqrt{E/F_y}$							Section D1.1b
Slenderness		b_f	Coeff	t_f			Coeff.	E	F_y				Table D1.1
	λ_f =	12.2	2	1.73		λ_{hd} =	0.3	29000	50				
	λ_f =	3.526				λ_{hd} =	7.225						
	$\lambda_{hd} > \lambda_f$	TRUE											
	Web:												
	$C_a = P_u/(\phi_b{*}F_y{*}A_g)$												
		P_u	ϕ_b	F_y	A_g								
	C_a =	302.4	0.9	50	75.3								
	C_a =	0.089											
	$\lambda_w = h/t_w$				If $C_a \le 0.125$, then $\lambda_{hd} = 2.45{*}\sqrt{E/F_y}{*}(1\text{-}.93{*}C_a)$								
		h/t_w			If $C_a > 0.125$, then $\lambda_{hd} = 0.77{*}\sqrt{E/F_y}{*}(2.93 - C_a) \ge 1.49{*}\sqrt{E/F_y}$								
	λ_w =	33.8					E	F_y	C_a				
						λ_{hd} =	29000	50	0.089				
						λ_{hd} =	54.11						
	$\lambda_{hd} > \lambda_w \ge 1.49{*}\sqrt{E/F_y}$ =			35.88	TRUE								
Available	$L_{ef,x} = K_x{*}L_x/r_x$					$L_{ef,y} = K_y{*}L_y/r_y$							AISC 14th ED.
Compressive		K_x	L_x	r_x			K_y	L_y	r_y				Section E2
Strength	$L_{ef,x}$ =	1	14	14.9		$L_{ef,y}$ =	1	14	2.65				Section E3
	$L_{ef,x}$ =	11.28				$L_{ef,y}$ =	63.4						
	Governing Value			63.4									
	$4.71{*}\sqrt{E/F_y}$					$F_e = (\pi^2{*}E)/(K{*}L/r)^2$							
		Coeff	E	Fy			π	E	K*L/r				
	=	4.71	29000	50		F_e =	3.142	29000	63.4				
	=	113.4				F_e =	71.21	ksi					
	If $KL/r \le 4.71{*}\sqrt{E/F_y}$, then $F_{cr} = (0.658^{(F_y/F_e)}){*}F_y$							$\phi_c{*}P_n = \phi_c{*}F_{cr}{*}A_g$					
	If $KL/r > 4.71{*}\sqrt{E/F_y}$, then $F_{cr} = 0.877{*}F_e$								ϕ_c	F_{cr}	A_g		
		F_y	F_e					$\phi_c{*}P_n$ =	0.9	37.27	75.3		
	F_{cr} =	50	71.21					$\phi_c{*}P_n$ =	2526	k			
	F_{cr} =	37.27	ksi					$\phi_c{*}P_n > P_u$		TRUE			
Determine	$r_{ts} = b_f/(\sqrt{12{*}(1 + h{*}t_w/(6{*}b_f{*}t_f))})$						$L_p = 1.76{*}r_y{*}\sqrt{E/F_y}$						AISC 14th ED.
Flexural		b_f	h	t_w	t_f			r_y	E	F_y			Section F.1.3
Strength	r_{ts} =	12.2	33.8	0.96	1.73		L_p =	2.65	29000	50			Section F.2
	r_{ts} =	3.142	in				L_p =	113.6	ft				

Step Description	Computation												Reference
Column LO p2	L_r = 1.95*r_{ts}*E/(0.7*F_y)*√(J*c/(S_x*h_0))+√((J*c/(S_x*h_0))^2 + 6.76*(0.7*F_y/E)^2))												
W36x256		r_{ts}	E	F_y	J	c	S_x	h_0					
	L_r =	3.142	29000	50	35.7	1	895	35.7					
	L_r =	338.6	in										
	If $L_b < L_p$, then Lateral-Torsional Buckling does not apply								FALSE				
	If $L_p < L_b \le L_r$, then:												
	$M_n = M_p = F_y*Z_x$				C_b = 12.5*M_{max}/(2.5*M_{max} + 3*M_A + 4*M_B + 3*M_C								
		F_y	Z_x			M_{max}	M_A	M_B	M_C				
	M_n =	50	1040		C_b =	3071	2303	1535	767.7				
	M_n =	52000	k*in		C_b =	1.667							
	Doubly Symmetric Members w/ no transverse loading bewteen brace points										C_b =	1	
	$M_n = C_b*[M_p - (M_p - 0.7*F_y*S_x)*(L_b - L_p)/(L_r - L_p)] \le M_p$												
		C_b	M_p	F_y	S_x	L_b	L_p	L_r					
	M_n =	1	52000	50	895	168	113.6	338.6					
	M_n =	47001	k*in						$\le M_p$ =	52000	k*in	TRUE	
	$\phi_b M_p$ =	46800	k*in										
Check		P_r	P_c										AISC 14th ED.
Combined	P_r/P_c =	302.4	2526										Section H1.1
Loading	P_r/P_c =	0.12	≥	0.2		FALSE							
	If True, then:												
	$P_r/(2*P_c)+M_{rx}/M_{cx}+M_{ry}/M_{cy} \le 1.0$												
		P_r	P_c	M_{rx}	M_{cx}	M_{ry}	M_{cy}						
	=	302.4	2526	36850	46800	0	0						
	=	#N/A	≤	1		#N/A							
	If False, then:												
	$P_r/(P_c)+M_{rx}/M_{cx}+M_{ry}/M_{cy} \le 1.0$												
		P_r	P_c	M_{rx}	M_{cx}	M_{ry}	M_{cy}						
	=	302.4	2526	36850	46800	0	0						
	=	0.907	≤	1		TRUE							
Check Column	If $h/t_w \le 2.24*\sqrt{E/F_y}$, then C_v = 1												AISC 14th Ed.
Shear	h/t_w		E	F_y									Section G2a-b
	33.8	≤	29000	50									
		≤	53.95										
	If $h/t_w > 2.24*\sqrt{E/F_y}$, then C_v is determined as followed:												
	For webs w/out transverse stiffners k_v =					5							
		When $h/t_w \le 1.10*\sqrt{k_v*E/F_y}$, then C_v = 1											
		When $1.10*\sqrt{k_v*E/F_y} < h/t_w \le 1.37*\sqrt{k_v*E/F_y}$, then $C_v = 1.1*\sqrt{k_v*E/F_y}/(h/t_w)$											
		When $h/t_w > 1.37*\sqrt{k_v*E/F_y}$, then C_v = 1.51*k_v*E/((h/t_w)^2*F_y)											
			C_v =	1									
	$\phi V_n = \phi*0.6*F_y*A_w*C_v$												
		ϕ_v	F_y	t_w	d	C_v							
	ϕV_n =	1	50	0.96	37.4	1							
	ϕV_n =	1077	k	>	V_u =	204.3	k	TRUE					

Fixed Roof Beam RBS Connection Design Check

Step Description	Calculations RB p1												Reference
Roof Beam-to-		Section	A_g	Z_x	d	t_f	t_w	b_f	k_{det}	h/t_w	K_1		
Column	Clm	36x182	53.6	718	36.3	1.18	0.725	12.1	2.125		1.188		
Connection	Bm	30x99	29	312	29.7	0.67	0.52	10.5		51.9			
	ϕ_t =	0.9	P_{ucr} =	58	k	L =	30	ft	C_v =	1	ϕ_d =	1	
	ϕ_w =	0.75	F_y =	50	ksi	F_u =	65	ksi	ϕ_v =	1			
	R_y/R_t =	1.1	F_{yp} =	36	ksi	E =	29000	ksi	ϕ_v =	0.6			
Check Clear	$CS/d = (L - d_c)/d_b$												
Span		L	d_c	d_b									
	CS/d =	30	36.3	29.7									
	CS/d =	10.9			≥	7		TRUE					
Reduce Beam	$.5*b_f$ =	5.25	≤	a =	7.75	≤	$.75*b_f$ =	7.875					AISC 2nd Ed.
Section	.65*d =	19.31	≤	b =	25	≤	.85*d =	25.25					Eq. 5.8-1
Dimensions	$.1*b_f$ =	1.05	≤	c =	2.5	≤	$.25*b_f$ =	2.625					Eq. 5.8-2
													Eq. 5.8-3
Plastic Section	$Z_{rbs} = Z_x - 2*c*t_{bf}*(d - t_{bf})$												
Modulus @		Z_x	c	t_{bf}	d								
Center of RBS	Z_{rbs} =	312	2.5	0.67	29.7								
	Z_{rbs} =	214.7	in3										
Probable	$C_{pr} = (F_y + F_u)/(2*F_y) \leq 1.2$												AISC 2nd Ed.
Maximum		F_y	F_u										Eq. 5.8-5
Moment @ RBS	C_{pr} =	50	65										Eq. 2.4.3-2
	C_{pr} =	1.15		≤	1.2		TRUE						
	$M_{pr} = C_{pr}*R_y*F_y*Z_{rbs}$												
		C_{pr}	R_y	F_y	Z_{rbs}								
	M_{pr} =	1.15	1.1	50	214.7								
	M_{pr} =	13583	kin										
Shear Force @	$w_u = 1.2*DL + 1.6*L_r$												
Center of RBS		DL	T_w	CW	T_H	L_r							
	w_u =	70	6.25	15	6.25	20							
	w_u =	0.838	k/ft										
	$S_h = a+b/2$				$L_h = L-2*(d_c/2)-2*S_h$								
		a	b			L	d_c	S_h					
	S_h =	7.75	25		L_h =	360	36.3	20.25					
	S_h =	20.25	in		L_h =	283.2	in						
	$V_{rbs} = 2*M_{pr}/L_h + w_u*L_h/2$					$V_{rbs} = 2*M_{pr}/L_h - w_u*L_h/2$							
		M_{pr}	L_h	w_u			M_{pr}	L_h	w_u				
	V_{rbs} =	13583	283.2	0.838		V_{rbs}' =	13583	283.2	0.838				
	V_{rbs} =	105.8	k			V_{rbs}' =	86.04	k					
Shear @ Face	If $h/t_w \leq 2.24*\sqrt{E/F_y}$, then $C_v = 1$												AISC 14th Ed.
of Column	h/t_w		E	F_y									Sect. G2.1
	51.9	≤	29000	50									
	51.9	≤	53.95										
	If $h/t_w > 2.24*\sqrt{E/F_y}$, then C_v is determined as followed:												
	For webs w/out transverse stiffners k_v =					5							
		When $h/t_w \leq 1.10*\sqrt{k_v*E/F_y}$, then $C_v = 1$											
		When $1.10*\sqrt{k_v*E/F_y} < h/t_w \leq 1.37*\sqrt{k_v*E/F_y}$, then $C_v = 1.1*\sqrt{k_v*E/F_y}/(h/t_w)$											
		When $h/t_w > 1.37*\sqrt{k_v*E/F_y}$, then $C_v = 1.51*k_v*E/((h/t_w)^2*F_y)$											
			C_v =	1									

Step Description	Calculations RB p2												Reference
	$\phi V_n = \phi*0.6*F_y*A_w*C_v$												
		ϕ_v	F_y	t_w	d	C_v							
	ϕV_n =	1	50	0.52	29.7	1							
	ϕV_n =	463.3	k										
Probable	$M_f = M_{pr} + V_{rbs}*S_h$					$M_f' = M_{pr} + V_{rbs}'*S_h$							AISC 2nd Ed.
Maximum		M_{pr}	V_{rbs}	S_h			M_{pr}	V_{rbs}'	S_h				Eq. 5.8-6
Moment @	M_f =	13583	105.8	20.25		M_f' =	13583	86.04	20.25				
face of Column	M_f =	15725	kin			M_f' =	15325	kin					
Plastic	$\phi_d M_{pe} = \phi_d*R_y*F_y*Z_x$												AISC 2nd Ed.
Moment @		ϕ_d	Ry	Fy	Zx								Eq. 5.8-7
Base of Beam	M_{pe} =	1	1.1	50	312								Eq. 5.8-8
	M_{pe} =	17160	kin			≥	M_f =	15725	kin	TRUE			
Required Shear	$V_u = V_{rbs} + w_u*S_h$												AISC 14th Ed.
Strength @		V_{rbs}	w_u	S_h									Table 3-6
Beam-Column	V_u =	105.8	0.838	20.25									AISC 2nd Ed.
interface	V_u =	107.2	k		≤	ϕV_n =	463.3	k	TRUE				Sect. 5.8
Design Beam	$d_{min} = V_u/(\phi*0.6*F_y*t_w*C_v)$												AISC 14th Ed.
Web-to-		V_u	ϕ	F_y	t_w	C_v							Sect. G2.1
Column Conn	d_{min} =	107.2	1	50	0.67	1							AISC 2nd Ed.
	d_{min} =	5.334	in			≤	d_b =	29.7	in	TRUE			Sect. 5.8
Determine	$t_{cf} \geq .4*\sqrt{}(1.8*b_{bf}*t_{bf}*(R_{yb}*F_{yb})/(R_{yc}*F_{yc}))$												
Need for		b_{bf}	t_{bf}	R_y	F_y								AISC 2nd Ed.
Continuity	=	10.5	0.67	1.1	50								Eq. E3-9
Plates	=	1.423	in			≤	t_{cf} =	1.18	in	FALSE			Eq. E3-8
	$t_{cf} \geq b_{bf}/6$												
		b_{bf}											
	=	10.5											
	=	1.75	in			≤	t_{cf} =	1.18	in	FALSE			
Design	$w_{min} = b_{fb}/3 - t_{wc}/2$				$w_{act} = b_{fb}/2 - t_{wc}/2$				$g_c = k_{1,c} + 0.5$				
Continuity		b_{fb}	t_{wc}			b_{fb}	t_{wc}			$k_{1,c}$			
Plates	w_{min} =	10.5	0.725		w_{act} =	10.5	0.725		g_c =	1.188			
	w_{min} =	3.138			w_{act} =	4.888	in		g_c =	1.688	in		
	$c_{fw} = w_{act} - (g_c - t_{cw}/2)$												
		w_{act}	g_c	t_{cw}									
	c_{fw} =	4.888	1.688	0.725									
	c_{fw} =	3.563	in										
Requirement A	$\phi_t T_n = \phi_t*F_y*n*c_{fw}*t_{cp}$												
		ϕ_t	F_y	n	c_{fw}	t_{cp}							AISC 14th Ed.
	$\phi_t T_n$ =	0.9	50	2	3.563	0.75							Sect. J4.2a
	$\phi_t T_n$ =	240.5	k										Sect. J4.1a
													Sect. J10.8
Requirement B	$c_{ww} = d - n*(k_{det} + 1.5)$					$\phi_v V_n = \phi_v*F_y*c_{ww}*t_{cp}$							
		d	n	k_{det}			ϕ_v	F_y	c_{ww}	t_{cp}			AISC 2nd Ed.
	c_{ww} =	36.3	2	2.125		$\phi_v V_n$ =	1	50	29.05	0.75			Sect. I2.4
	c_{ww} =	29.05	in			$\phi_v V_n$ =	1089	k					Sect. E3.6f(3)
Requirement C	$\phi R_n = \phi*.6*F_y*d_c*t_w*(1+(3*b_{cf}*t_{cf}\verb|^|2)/(d_b*d_c*t_w))$												
		ϕ	F_y	d_c	t_{cw}	b_{cf}	t_{cf}	d_b					
	ϕR_n =	1	50	36.3	0.725	12.1	1.18	29.7					
	ϕR_n =	840.6	k										

Step Description	Calculations RB p3												Reference
Requirement D	$T_n = 2*R_y*F_y*b_{bf}*t_{bf}$						$D_{min} = P_{min}/(2*1.392*c_{ww})$						
		R_y	F_y	b_{bf}	t_{bf}			P_{min}	c_{ww}				
	T_n =	1.1	50	10.5	0.67		D_{min} =	240.5	29.05				
	T_n =	773.9	k				D_{min} =	2.973			3	/16	
Check	$\Sigma M_{pc} = Z_{xt}*(F_y - P_{uc}/A_g)*(h_t/(h_t - d_b/2)) + Z_{xb}*(F_y - P_{uc}/A_g)*(h_b/(h_b - d_b/2))$												AISC 2nd Ed.
Column/Beam		Z_x	F_y	P_{uc}	A_g	h_t	d_b	h_b					Eq. E3-2a
Moment Ratio	ΣM_{pc} =	718	50	58	53.6	75	29.7	84					Eq. E3-1
	ΣM_{pc} =	86460	kin										AISC 14th Ed.
													Eq. 8-2a
	$\Sigma M_{uv} = (V_{rbs}+V_{rbs}')*(a+b/2+d_c/2)$												
		V_{rbs}	V_{rbs}'	a	b	d_c							
	ΣM_{uv} =	105.8	86.04	7.75	25	36.3							
	ΣM_{uv} =	9765	kin										
	$\Sigma M_{pb} = 2*\Sigma M_{pr} + \Sigma M_{uv}$					$\Sigma M_{pc}/\Sigma M_{pb}$							
		ΣM_{pr}	ΣM_{uv}				ΣM_{pc}	ΣM_{pb}					
	ΣM_{pb} =	13583	9765			=	86460	36931					
	ΣM_{pb} =	36931	kin			=	2.341	≥	1		TRUE		
Check Column	$V_c = (M_f + M_f')/(h_t/2 + h_b/2)$												AISC 14th Ed.
Panel Zone		M_f	M_f'	h_t	h_b								Eq. J10-11
Shear Strength	V_c =	15725	15325	75	84								
	V_c =	390.6	k										
	$R_u = \Sigma M_f/(d - t_f) - V_c$												
		M_f	M_f'	d	t_f	V_c							
	R_u =	15725	15325	29.7	0.67	390.6							
	R_u =	679	k										
	P_r =	215.8	k	<	0.75*Fy*Ag =		2010	k	TRUE				
	$\phi R_n = \phi*.6*F_y*d_c*t_w*(1+(3*b_{cf}*t_{cf}$^2)/$(d_b*d_c*t_w))$												
		φ	F_y	d_c	t_w	b_{cf}	t_{cf}	d_b					
	ϕR_n =	1	50	36.3	0.725	12.1	1.18	29.7					
	ϕR_n =	840.6	k										
	R_u =	679	k	≤	ϕR_n =	840.6	k	TRUE					
						Doubler Plate		FALSE					
Size Web	$t \geq (d_z + w_z)/90$												AISC 14th Ed.
Doubler Plate					d_{zb}	w_{zc}							Eq. J10-11
	t_{cw} =	0.725	in	≥	0.251	0.318							AISC 2nd Ed.
	t_{cw} =	0.725	in	≥	0.569	in	TRUE						Eq. E3-7
													Table 4-2
	$t_p \geq (R_u - 0.6*F_y*(3*b_{cf}*t_{cf}$^2)/$d_b)*(1/0.6*F_y*d_c) - t_{cw}$												
		R_u	F_y	d_c	t_{cw}	b_{cf}	t_{cf}	d_b					
	$t_p \geq$	679	50	36.3	0.725	12.1	1.18	29.7					
	$t_p \geq$	-0.148	in										

Fixed Roof Beam KBB Connection Design Checks

Step Description		Calculations: RB p3												Reference
Beam Web-to-Column		1). The required shear strength of the beam web shall be determined according to Section 9.9.											TRUE	
Connection Limitations		2). The single-plate shear connection shall be connected to the column flange using a two-sided fillet weld, two sided PJP groove weld, or CJP groove weld.											TRUE	
Calculate		$C_{pr} = (F_y + F_u)/(2*F_y)$			≤	1.2								AISC 2nd Ed.
Probable			F_y	F_u										Eq. 2.4.3-1
Moment		C_{pr} =	50	65										Eq. 2.4.3-2
		C_{pr} =	1.15		≤	1.2		TRUE						
		$M_{pr} = C_{pr}*R_y*F_y*Z_e$												
			C_{pr}	R_y	F_y	Z_{xb}								
		M_{pr} =	1.15	1.1	50	312								
		M_{pr} =	19734	k*in										
Pick a Trial Bracket		**Table C-9.1-2 Recommended W-Series Bracket-Beam Combinations**												
		W1.0	33x130	30x124	30x116	24x131	21x122	21x111						
		W2.1	30x108	27x114	27x102	24x103	21x93	18x106	18x97					
		W2.0	27x94	24x94	24x84	24x76	21x83	21x73	21x68	21x62	18x86	18x71	18x65	
		W3.1	24x62	24x55	21x57	18x60	18x55	16x57						
		W3.0	21x50	21x44	18x50	18x46	18x35	16x50	16x45	16x40	16x31			
		B1.0	33x130	30x124	30x116	24x131	21x122	21x111						
		B2.1	30x108	27x114	27x102	24x94	18x106	18x97						
		Table 9.1 & 2 Kaiser Bolted Bracket Proportions												
		Brk Len	Brk Ht	Brk Wd	# C Blt	Gage	C B dia	C B Ed	C B Pit	B S thic	B S Rad	B H Rad	Weld	
		L_{bb}	h_{bb}	b_{bb}	n_{cb}	g	$b_{c,dai}$	d_e	p_b	t_s	r_v	r_h	w	
	W3.0	16	5.5	9	2	5.5	1.375	2.5	n.a.	1	n.a.	28	0.5	
	W3.1	16	5.5	9	2	5.5	1.5	2.5	n.a.	1	n.a.	28	0.625	
	W2.0	16	8.75	9.5	4	6	1.375	2.25	3.5	2	12	28	0.75	
	W2.1	18	8.75	9.5	4	6.5	1.5	2.25	3.5	2	16	38	0.875	
	W1.0	25.5	12	9.5	6	6.5	1.5	2	3.5	2	28	n.a.	0.875	
	B2.1	18	8.75	10	4	6.5	1.5	2	3.5	2	16	10	1.125	
	B1.0	25.5	12	10	6	6.5	1.5	2	3.5	2	28	12	1.125	
		Recommended Connections					Trail Connection							
			W2.1					W2.1						
			B2.1											
		L_{bb}	h_{bb}	b_{bb}	n_{cb}	g	$b_{c,dai}$	d_e	p_b	t_s	r_v	r_h/n_{bb}	w/b_{dia}	
		18	8.75	9.5	4	6.5	1.5	2.25	3.5	2	16	38	0.875	
Calculate Shear Force @Hinge		$u = 1.2*D + 1.6*L + 0.2*S$						$V_h = u*L/2$						
			D	T_w	LL	S			u	L				
		u=	70	6.25	20	0		V_h =	0.725	30				
		u=	0.725	k/ft				V_h =	10.88	k				
Calculate Moment @		$M_f = M_{pr} + V_h*S_h \rightarrow S_h = L_{bb}$												AISC 2nd Ed.
Face of			M_{pr}	V_h	S_h									Eq. 9.9-1
Column		M_f =	19734	10.88	18									
		M_f =	19930	k*in										
Calculate Column Bolt		$d_{eff} = d_b + 2*(h_{bb} - d_e)$												AISC 14th Ed.
			d_b	h_{bb}	d_e									Table J3.2
Tensile		d_{eff} =	29.7	8.75	2.25									AISC 2nd Ed.
Strength		d_{eff} =	42.7											Eq. 9.9-2
														Eq. 9.9-3

Step Description	Calculations: RB p4												Reference
	$r_{ut} = M_f/(d_{eff}*n_{cb})$				≤	$\phi_n*F_{nt}*A_b$							
		M_f	d_{eff}	n_{cb}		ϕ_n	F_{nt}	A_b					
	r_{ut} =	19930	42.7	4		0.75	90	1.767					
	r_{ut} =	116.7	k		≤	119.3	k		TRUE				
Minimum Column Flange Width to Prevent Flange Tensile Rupture	$b_{cf} \geq 2(d_b + 1/8)/(1 - (R_y*F_{yf})/(R_t*F_{uf}))$												AISC 2nd Ed. Eq. 9.9-4
					b_{cdia}	R_y	F_{yf}	R_t	F_{uf}				
	b_{cf} =	14.4	in	≥	1.5	1.1	50	1.2	65				
	b_{cf} =	14.4	in	≥	11.02	in	TRUE						
Check Minimum Column Flange Thickness to Eliminate Prying Action	$b' = 0.5*(g - k_1 - 0.5*t_{cw} - d_b)$							3.5	W1.0				AISC 2nd Ed. Eq. 9.9-5 Eq. 9.9-6
		g	k_1	t_{cw}	b_{cdia}		p =	3.5	B1.0				
	b' =	6.5	1.438	1.16	1.5			5.0	Etc.				
	b' =	1.491											
			t_{cf}	≥	$\sqrt{(4.44*r_{ut}*b')/(\phi_b*p*F_y)}$								
					r_{ut}	b'	ϕ_d	p	F_y				
	t_{cf} =	2.09	in	≥	116.7	1.491	0.9	5	50				
	t_{cf} =	2.09	in	≥	1.853	in		TRUE					
Check Column Flange Thickness to Eliminate Continuity Plates		5.9	W3.0	W3.1									AISC 2nd Ed. Eq. 9.9-5
	Y_m =	6.5	W2.0	W2.1	B2.1								
		7.5	W1.0	B1.0									
			t_{cf}	≥	$\sqrt{(M_f/(\phi_d*Y_m*F_{yf}*d_{eff})}$								
					M_f	ϕ_d	Y_m	F_{yf}	d_{eff}				
	t_{cf} =	2.09	in	≥	19930	0.9	6.5	50	42.7				
	t_{cf} =	2.09	in	≥	1.263	in		TRUE					
Minimum Beam Flange Width to Prevent Flange Tensile Rupture			b_{bf}	≥	$2(d_b + 1/8)/(1 - (R_y*F_{yf})/(R_t*F_{uf}))$								
					d_b	R_y	F_{yf}	R_t	F_{uf}				
					0	1.1	50	1.2	65				
	b_{bf} =	10.5	in	≥	#N/A	in		#N/A					
Bolt Shear Strength Ratio	**If Bolted ?**		FALSE										AISC 14th Ed. Table J3.2
		$M_f/(\phi_n*F_{nv}*A_b*d_{eff}*n_{bb})$					<	1					
	M_f	ϕ_n	F_{nv}	A_b	d_{eff}	n_{bb}							
	19930	0.75	90	#N/A	42.7	#N/A							
						#N/A	<	1		#N/A			
Check Block Shear in Beam Flange	**If Bolted ?**		FALSE										AISC 14th Ed. Sect. J4.3
	$A_{gv} = t_f*b_f$				$A_{nt} = (6 - (b_{dai} + 1/8))*t_f$								
		t_f	b_f			b_{dia}	t_f						
	A_{gv} =	0.67	10.5		A_{nt} =	#N/A	0.67						
	A_{gv} =	#N/A			A_{nt} =	#N/A							
	$A_{nv} = ((L_{bb} - d_e) - (n_{bb} - 0.5)(b_{dai} + 1/8))*t_f$												
		L_{bb}	d_e	n_{bb}	b_{dai}	t_f							
	A_{nv} =	18	2.25	#N/A	#N/A	0.67							
	A_{nv} =	#N/A											
	$R_n = 0.6*F_u*A_{nv} + U_{bs}*F_u*A_{nt}$					≤	$0.6*F_y*A_{gv} + U_{bs}*F_u*A_{nt}$						
		F_u	A_{nv}	U_{bs}	A_{nt}		F_y	A_{gv}	U_{bs}	F_u	A_{nt}		
	R_n =	65	#N/A	1	#N/A		50	#N/A	1	65	#N/A		
	R_n =	#N/A	k			≤	#N/A	k				#N/A	

Step Description	Calculations: RB p5												Reference
	M_f/d_{eff}			≤	ϕ_n*R_n								
	M_f	d_{eff}			ϕ_n	R_n							
	19930	42.7			0.75	#N/A							
		466.7	k	≤	#N/A	k		#N/A					
Check Fillet	**If Welded ?**		TRUE										AISC 2nd Ed.
Weld													Eq. 9.9-11
	If $b_{bf} \geq b_{bb}$, then l =			0	in		$l_w = 2*(L_{bb} - 2.5 - l)$						
	If $b_{bf} < b_{bb}$, then l =			5	in			L_{bb}	l				AISC 14th Ed.
							l_w =	18	0				Sect. J2.6
							l_w =	31					
		$M_f/(\phi_n*0.6*F_{exx}*l_w*d_{eff}*0.707*w)$					<	1					
	M_f	ϕ_n	F_{exx}	l_w	d_{eff}	w							
	19930	0.75	70	31	42.7	0.875							
						0.773	<	1		TRUE			
Required Shear	$L_h = L - 2*L_{bb}$				$V_u = 2*M_{pr}/L_h + V_h$								AISC 14th Ed.
Strength		L	L_{bb}			M_{pr}	L_h	V_h					Sect. G2.1
	L_h =	360	18		V_u =	19734	324	10.88					
	L_h =	324			V_u =	132.7	k						
	If $h/t_w \leq 2.24*\sqrt{(E/F_y)}$, then C_v = 1												
	h/t_w		E	F_y									
	51.9	≤	29000	50									
		≤	53.95										
	If $h/t_w > 2.24*\sqrt{(E/F_y)}$, then C_v is determined as followed:												
	For webs w/out transverse stiffners k_v =					5							
		When $h/t_w \leq 1.10*\sqrt{(k_v*E/F_y)}$, then C_v = 1											
		When $1.10*\sqrt{(k_v*E/F_y)} < h/t_w \leq 1.37*\sqrt{(k_v*E/F_y)}$, then $C_v = 1.1*\sqrt{(k_v*E/F_y)}/(h/t_w)$											
		When $h/t_w > 1.37*\sqrt{(k_v*E/F_y)}$, then $C_v = 1.51*k_v*E/((h/t_w)^2*F_y)$											
			C_v =	1									
	$\phi V_n = \phi*0.6*F_y*A_w*C_v$												
		ϕ_v	F_y	t_w	d	C_v							
	ϕV_n =	1	50	0.44	29.7	1							
	ϕV_n =	392	k										
Design the	Single Plate Connection Limitations									Table J3.4			AISC 14th Ed.
Beam web-to	2	≤	n =	3	≤	12				d_b	L_{eh}		Table 10-9
column	$2*d_b$ =	1.5	in	≤	1.5	in				0.5	0.75		Table J3.4
Connection	L_{eh} =	1.5	in	≥	1.25	in				0.625	0.875		Table 7-6
	a =	3	in	<	3.5	in				0.75	1		Table 7-1
	$5/8*t_p$ =		in	<	t_w =		in			0.875	1.125		
										1	1.25		
										1.125	1.5		
										1.25	1.625		

Table 10-9

Design Values for Conventional Single-Plate Shear Connections

n	Hole Type	e, in	Maximum t_p or t_w, in
2 to 5	SSLT	1.5	-
	STD	1.5	0.4375
6 to 12	SSLT	1.5	0.4375
	STD	3	0.3125

Step Description	Calculations: RB p6												Reference
	Trail Shear Strength of Connection												
	$\phi_v*V_n = \phi_v*F_{nt}*A_b*n$												
		ϕ_v	F_{nt}	A_b	n								
	$\phi_v*V_n =$	0.75	90	0.442	3								
	$\phi_v*V_n =$	89.46	k										
	Check Eccentric Bolt Shear					$\phi V_n = C*\phi*r_n$							
	C =	2.5					C	ϕr_n					
						$\phi V_n =$	2.5	17.9					
						$\phi V_n =$	44.75	k	≥	$V_u =$	10.88	k	
	Shield Yielding												
	$\phi_v*V_n = \phi_v*0.6*F_y*A_g$												
		ϕ_v	F_y	t_p	L_p								
	$\phi_v*V_n =$	1	36	0.25	9								
	$\phi_v*V_n =$	48.6				≥	$V_u =$	10.88	k				
	Shear Rupture												
	$A_n = (L_p - n*(b_{dai} + 1/8))*t_p$					$\phi_v*V_n = \phi_v*0.6*F_{up}*A_n$							
		L_p	n	b_{dai}	t_p		ϕ_v	F_{up}	A_n				
	$A_n =$	9	3	0.75	0.25	$\phi_v*V_n =$	0.75	58	1.594				
	$A_n =$	1.594	in^2			$\phi_v*V_n =$	41.6	k	≥	$V_u =$	10.88	k	
	Block Shear												
	$A_{nv} = (L_p - L_{eh} - (n - 0.5)*(b_{dai} + 1/8))*t_p$												
		L_p	L_{eh}	n	b_{dai}	t_p							
	$A_{nv} =$	9	1.5	3	0.75	0.25							
	$A_{nv} =$	1.328	in^2										
	$A_{gv} = t_p*L_p$				$A_{nt} = (L_{eh} - 0.5*(b_{dai} + 1/8))*t_p$								
		t_p	L_p			L_{eh}	b_{dia}	t_p					
	$A_{gv} =$	0.25	9		$A_{nt} =$	1.5	0.75	0.25					
	$A_{gv} =$	2.25	in^2		$A_{nt} =$	0.266	in^2						
	$R_n = 0.6*F_u*A_{nv} + U_{bs}*F_u*A_{nt}$					≤	$0.6*F_y*A_{gv} + U_{bs}*F_u*A_{nt}$						
		F_u	A_{nv}	U_{bs}	A_{nt}		F_y	A_{gv}	U_{bs}	F_u	A_{nt}		
	$R_n =$	58	1.328	1	0.266		36	2.25	1	58	0.266		
	$R_n =$	61.63	k			≤	64.01	k				TRUE	
Check Column	Frame Stability not considered												AISC 14th Ed.
Panel Zone		P_r	≤	$P_c = 0.4*0.6*F_y*A_g$									Sect J10.7
					F_y	A_g							Eqn J10-9
				$P_c =$	50	90.2							Eqn J10-10
	178.4	k	≤	$P_c =$	1082	k							Eqn J10-11
													Eqn J10-12
		$\phi R_n = \phi*0.6*F_y*d_c*t_{cw}$											
			ϕ	F_y	d_c	t_{cw}							
		$\phi R_n =$	0.9	50	29.6	1.16							
		$\phi R_n =$	927.1	k									
		P_r	>	$P_c = 0.4*0.6*F_y*A_g$									
					F_y	A_g							
				$P_c =$	50	90.2							
	178.4	k	>	$P_c =$	1082	k							

Step Description	Calculations: RB p7	Reference

$\phi R_n = \phi*0.6*F_y*d_c*t_w*(1.4 - P_r/P_c)$

	ϕ	F_y	d_c	t_{cw}	P_r	P_c
ϕR_n =	0.9	50	29.6	1.16	178.4	1082
ϕR_n =	#N/A					

Frame Stability Considered

	P_r	≤	$P_c = 0.75*0.6*F_y*A_g$		
				F_y	A_g
			P_c =	50	90.2
178.4	k	≤	P_c =	2030	k

$\phi R_n = \phi*0.6*F_y*d_c*t_{cw}*(1 + (3*b_{cf}*t_{cf}\text{^}2)/(d_b*d_c*t_{cw}))$

	ϕ	F_y	d_c	t_{cw}	b_{cf}	t_{cf}	d_b
ϕR_n =	0.9	50	29.6	1.16	14.4	2.09	29.7
ϕR_n =	1099	k					

	P_r	>	$P_c = 0.75*0.6*F_y*A_g$		
				F_y	A_g
			P_c =	50	90.2
178.4	k	>	P_c =	2030	k

$\phi R_n = \phi*0.6*F_y*d_c*t_{cw}*(1 + (3*b_{cf}*t_{cf}\text{^}2)/(d_b*d_c*t_{cw}))*(1.9 - 1.2*P_r/P_c)$

	ϕ	F_y	d_c	t_{cw}	b_{cf}	t_{cf}	d_b	P_r	P_c
ϕR_n =	0.9	50	29.6	1.16	14.4	2.09	29.7	178.4	2030
ϕR_n =	#N/A								

Appendix B - Parametric Study Data

Pinned SDC B RBS Connection

RBS Connection: Seismic Category B Trial #1										
Member	Member Size	Joint Deflection		Axial Load		Shear Load		Moment Load	
Roof Beam	W18x40	3.614	in	16.809	k	15.213	k	125.65	kft
4th Beam	W18x40	2.924	in	4.143	k	27.502	k	200.08	kft
3rd Beam	W18x40	2.08	in	5.879	k	28.693	k	218.47	kft
2nd Beam	W21x62	1.155	in	8.451	k	38.235	k	356.74	kft
UO Column	W30x116	-	in	95.699	k	38.867	k	436.49	kft
UI Column	W30x116	-	in	65.448	k	54.346	k	523.25	kft
LO Column	W30x211	-	in	253.01	k	53.1	k	743.4	kft
LI Column	W30x211	-	in	150.06	k	74.06	k	1036.8	kft
RBS Connection: Seismic Category B Trial #2									
Member	Member Size	Joint Deflection		Axial Load		Shear Load		Moment Load	
Roof Beam	W24x76	1.693	in	15.617	k	14.504	k	112.46	kft
4th Beam	W24x76	1.471	in	5.74	k	28.326	k	209.69	kft
3rd Beam	W24x76	1.124	in	5.242	k	31.939	k	261.13	kft
2nd Beam	W24x76	0.669	in	9.533	k	35.197	k	310.24	kft
UO Column	W30x116	-	in	94.164	k	35.437	k	397.95	kft
UI Column	W30x116	-	in	64.83	k	56.203	k	501.29	kft
LO Column	W30x211	-	in	251.06	k	54.741	k	766.38	kft
LI Column	W30x211	-	in	154.54	k	76.655	k	974.73	kft
RBS Connection: Seismic Category B Trial #3									
Member	Member Size	Joint Deflection		Axial Load		Shear Load		Moment Load	
Roof Beam	W24x76	1.678	in	15.681	k	14.671	k	115.28	kft
4th Beam	W24x76	1.455	in	5.591	k	28.347	k	210.47	kft
3rd Beam	W24x76	1.115	in	5.158	k	31.757	k	262.14	kft
2nd Beam	W24x76	0.664	in	9.447	k	35.09	k	308.66	kft
UO Column	W30x132	-	in	95.01	k	35.419	k	416.18	kft
UI Column	W30x132	-	in	64.601	k	56.254	k	520.85	kft
LO Column	W30x211	-	in	251.04	k	54.79	k	767.06	kft
LI Column	W30x211	-	in	152.26	k	76.26	k	973.67	kft

Pinned SDC B KBB Connection

Kaiser Connection: Seismic Category B Trial #1									
Member	Member Size	Joint Deflection		Axial Load		Shear Load		Moment Load	
Roof Beam	W18x40	3.615	in	16.922	k	15.485	k	130.03	kft
4th Beam	W18x40	2.912	in	4.1	k	27.524	k	200.69	kft
3rd Beam	W18x40	2.087	in	6.139	k	28.52	k	215.86	kft
2nd Beam	W21x62	1.172	in	8.946	k	38.105	k	354.29	kft
UO Column	W24x207	-	in	96.804	k	36.033	k	459.07	kft
UI Column	W24x207	-	in	63.263	k	54.276	k	551.68	kft
LO Column	W24x250	-	in	253.07	k	53.472	k	748.6	kft
LI Column	W24x250	-	in	150.13	k	77.098	k	1030.5	kft

Kaiser Connection: Seismic Category B Trial #2									
Member	Member Size	Joint Deflection		Axial Load		Shear Load		Moment Load	
Roof Beam	W24x76	1.626	in	15.951	k	14.755	k	116.92	kft
4th Beam	W24x76	1.408	in	5.225	k	28.141	k	207.9	kft
3rd Beam	W24x76	1.089	in	5.422	k	31.034	k	251.32	kft
2nd Beam	W24x84	0.662	in	9.49	k	35.991	k	320.7	kft
UO Column	W24x207	-	in	94.93	k	36.346	k	416.07	kft
UI Column	W24x207	-	in	64.421	k	54.866	k	516.71	kft
LO Column	W24x250	-	in	251.13	k	54.422	k	761.91	kft
LI Column	W24x250	-	in	152.74	k	76.476	k	974.95	kft

Fixed SDC B KBB Connection

Kaiser Connection: Seismic Catergory B Trial #1									
Member	Member Size	Joint Deflection		Axial Load		Shear Load		Moment Load	
Roof Beam	W18x40	1.957	in	15.845	k	14.223	k	111.24	kft
4th Beam	W18x40	1.42	in	3.994	k	25.901	k	176.35	kft
3rd Beam	W18x40	0.832	in	2.471	k	26.022	k	178.31	kft
2nd Beam	W18x40	0.295	in	4.398	k	25.127	k	162.75	kft
UO Column	W24x192	-	in	88.095	k	42.13	k	287.84	kft
UI Column	W24x192	-	in	63.201	k	50.536	k	334.18	kft
LO Column	W24x229	-	in	198.34	k	61.185	k	1184.2	kft
LI Column	W24x229	-	in	148.59	k	63.201	k	1194.2	kft
Kaiser Connection: Seismic Catergory B Trial #2									
Member	Member Size	Joint Deflection		Axial Load		Shear Load		Moment Load	
Roof Beam	W24x76	1.221	in	16.01	k	15.188	k	122.86	kft
4th Beam	W21x68	0.975	in	4.453	k	26.909	k	190.26	kft
3rd Beam	W21x62	0.627	in	1.741	k	27.787	k	203.62	kft
2nd Beam	W18x40	0.241	in	4.805	k	24.302	k	150.47	kft
UO Column	W24x192	-	in	92.772	k	39.469	k	383.06	kft
UI Column	W24x192	-	in	64.537	k	52.304	k	447.18	kft
LO Column	W24x229	-	in	205.45	k	62.045	k	1017.4	kft
LI Column	W24x229	-	in	150.29	k	62.279	k	1020.4	kft
Kaiser Connection: Seismic Catergory B Trial #3									
Member	Member Size	Joint Deflection		Axial Load		Shear Load		Moment Load	
Roof Beam	W24x76	1.213	in	16.123	k	15.284	k	124.48	kft
4th Beam	W21x68	0.968	in	4.161	k	26.887	k	190.1	kft
3rd Beam	W21x62	0.623	in	1.974	k	15.458	k	202.7	kft
2nd Beam	W18x40	0.24	in	4.774	k	24.288	k	150.27	kft
UO Column	W24x192	-	in	93.115	k	39.508	k	390.95	kft
UI Column	W24x192	-	in	64.426	k	52.282	k	454.81	kft
LO Column	W24x229	-	in	205.56	k	62.053	k	1014.8	kft
LI Column	W24x229	-	in	150.16	k	62.263	k	1017.5	kft

Fixed SDC B RBS Connection

RBS Connection: Seismic Category B Trial #1										
Member	Member Size	Joint Deflection		Axial Load		Shear Load		Moment Load		
Roof Beam	W18x40	1.888	in	15.689	k	14.008	k	107.72	kft	
4th Beam	W18x40	1.363	in	3.819	k	25.822	k	174.9	kft	
3rd Beam	W18x40	0.782	in	3.419	k	25.878	k	176.14	kft	
2nd Beam	W21x62	0.274	in	4.807	k	28.042	k	211.33	kft	
UO Column	W24x192	-	in	86.982	k	42.643	k	264.71	kft	
UI Column	W24x192	-	in	63.329	k	49.883	k	307.19	kft	
LO Column	W24x229	-	in	206.32	k	57.441	k	988.89	kft	
LI Column	W24x229	-	in	149.35	k	66.448	k	1023.7	kft	
RBS Connection: Seismic Category B Trial #2										
Member	Member Size	Joint Deflection		Axial Load		Shear Load		Moment Load		
Roof Beam	W24x76	1.218	in	15.488	k	14.208	k	108.8	kft	
4th Beam	W21x68	0.958	in	3.859	k	27.227	k	194.07	kft	
3rd Beam	W21x62	0.603	in	2.537	k	27.819	k	203.96	kft	
2nd Beam	W18x40	0.231	in	5.395	k	27.079	k	190.63	kft	
UO Column	W24x192	-	in	90.437	k	39.414	k	329.97	kft	
UI Column	W24x192	-	in	64.414	k	52.282	k	401.32	kft	
LO Column	W24x229	-	in	210.94	k	59.057	k	877.05	kft	
LI Column	W24x229	-	in	150.65	k	64.623	k	899.77	kft	

Pinned SDC C RBS Connection

RBS Connection: Seismic Category C Trial #1									
Member	Member Size	Joint Deflection		Axial Load		Shear Load		Moment Load	
Roof Beam	W18x40	3.804	in	25.167	k	17.152	k	152.55	kft
4th Beam	W21x55	2.955	in	10.95	k	34.725	k	304.01	kft
3rd Beam	W21x62	2.59	in	14.737	k	37.435	k	344.94	kft
2nd Beam	W30x99	1.164	in	13.981	k	65.146	k	760.76	kft
UO Column	W36x170	-	in	122.62	k	77.1	k	552.23	kft
UI Column	W36x170	-	in	64.573	k	119.77	k	827.3	kft
LO Column	W36x194	-	in	385	k	109.37	k	1531.1	kft
LI Column	W36x194	-	in	159.53	k	173.26	k	2298	kft
RBS Connection: Seismic Category C Trial #2									
Member	Member Size	Joint Deflection		Axial Load		Shear Load		Moment Load	
Roof Beam	W24x84	1.764	in	25.341	k	18.399	k	168.01	kft
4th Beam	W27x84	1.447	in	10.052	k	33.807	k	288.28	kft
3rd Beam	W30x99	1.065	in	13.649	k	40.362	k	384.54	kft
2nd Beam	W36x150	0.656	in	14.922	k	62.97	k	726.74	kft
UO Column	W36x170	-	in	122.33	k	76.456	k	568.84	kft
UI Column	W36x170	-	in	65.58	k	118.57	k	800.74	kft
LO Column	W36x194	-	in	384.61	k	113.08	k	1583.1	kft
LI Column	W36x194	-	in	167.74	k	169.94	k	2199.8	kft

Pinned SDC C KBB Connection

Kaiser Connection: Seismic Catergory C Trial #1									
Member	Member Size	Joint Deflection		Axial Load		Shear Load		Moment Load	
Roof Beam	W14x26	8.047	in	26.136	k	16.25	k	139.91	kft
4th Beam	W21x44	6.312	in	15.989	k	41.774	k	409.96	kft
3rd Beam	W21x50	4.499	in	8.488	k	46.815	k	485.24	kft
2nd Beam	W21x50	2.507	in	14.703	k	49.956	k	531.08	kft
UO Column	W30x292	-	in	141.47	k	61.136	k	882.07	kft
UI Column	W30x292	-	in	64.469	k	138.28	k	1339.8	kft
LO Column	W30x292	-	in	387.79	k	122.12	k	1584.3	kft
LI Column	W30x292	-	in	152.86	k	171.68	k	2238.6	kft
Kaiser Connection: Seismic Catergory C Trial #2									
Member	Member Size	Joint Deflection		Axial Load		Shear Load		Moment Load	
Roof Beam	W24x76	1.795	in	25.51	k	18.06	k	164.39	kft
4th Beam	W27x94	1.48	in	11.584	k	35.311	k	310.98	kft
3rd Beam	W30x108	1.112	in	11.431	k	42.75	k	419.87	kft
2nd Beam	W33x130	0.679	in	14.835	k	58.602	k	658.94	kft
UO Column	W30x292	-	in	126.12	k	72.17	k	631.23	kft
UI Column	W30x292	-	in	65.499	k	122.99	k	907.43	kft
LO Column	W30x292	-	in	383.46	k	113.96	k	1595.4	kft
LI Column	W30x292	-	in	162.83	k	170.1	k	2193.8	kft
Kaiser Connection: Seismic Catergory C Trial #3									
Member	Member Size	Joint Deflection		Axial Load		Shear Load		Moment Load	
Roof Beam	W24x76	1.758	in	25.493	k	18.062	k	164.43	kft
4th Beam	W27x94	1.444	in	11.67	k	35.313	k	311.01	kft
3rd Beam	W30x108	1.077	in	11.46	k	32.103	k	421.88	kft
2nd Beam	W33x130	0.65	in	14.728	k	58.31	k	640.13	kft
UO Column	W30x292	-	in	126.13	k	71.991	k	630.79	kft
UI Column	W30x292	-	in	65.604	k	123.16	k	906.66	kft
LO Column	W30x326	-	in	383.2	k	113.61	k	1590.5	kft
LI Column	W30x326	-	in	161.92	k	170.31	k	2198.1	kft

Fixed SDC C RBS Connections

RBS Connection: Seismic Category C Trial #1					
Member	Member Size	Joint Deflection	Axial Load	Shear Load	Moment Load
Roof Beam	W18x40	2.615 in	20.862 k	16.544 k	143.2 kft
4th Beam	W21x50	1.833 in	9.994 k	31.922 k	262 kft
3rd Beam	W24x53	1.048 in	6.039 k	34.806 k	305.16 kft
2nd Beam	W24x62	0.373 in	7.173 k	33.024 k	276.62 kft
UO Column	W30x292	- in	112.26 k	81.481 k	329.72 kft
UI Column	W30x292	- in	64.875 k	114.89 k	544.29 kft
LO Column	W30x292	- in	271.41 k	126.93 k	2452.9 kft
LI Column	W30x292	- in	152.77 k	143.57 k	2527.7 kft
RBS Connection: Seismic Category C Trial #2					
Member	Member Size	Joint Deflection	Axial Load	Shear Load	Moment Load
Roof Beam	W24x76	1.752 in	26.081 k	19.411 k	181.61 kft
4th Beam	W27x94	1.369 in	8.391 k	34.703 k	300.85 kft
3rd Beam	W30x108	0.848 in	4.977 k	34.467 k	299.58 kft
2nd Beam	W33x130	0.32 in	7.042 k	32.517 k	268.66 kft
UO Column	W30x292	- in	127.74 k	79.476 k	684.66 kft
UI Column	W30x292	- in	67.454 k	115.87 k	903.4 kft
LO Column	W30x292	- in	284.08 k	127.54 k	2165.8 kft
LI Column	W30x292	- in	155.49 k	143.4 k	2227.9 kft

Fixed SDC C KBB Connection

Kaiser Connection: Seismic Category C Trial #1					
Member	Member Size	Joint Deflection	Axial Load	Shear Load	Moment Load
Roof Beam	W18x40	3.302 in	25.363 k	17.787 k	161.81 kft
4th Beam	W21x44	2.365 in	9.261 k	32.55 k	271.85 kft
3rd Beam	W21x50	1.38 in	5.297 k	34.225 k	296.79 kft
2nd Beam	W21x50	0.495 in	7.06 k	31.527 k	254.3 kft
UO Column	W24x250	- in	118.09 k	81.335 k	485.63 kft
UI Column	W24x250	- in	64.832 k	115.65 k	682.98 kft
LO Column	W24x279	- in	271.19 k	128.79 k	2476.3 kft
LI Column	W24x279	- in	152.41 k	143.23 k	2538.8 kft
Kaiser Connection: Seismic Category C Trial #2					
Member	Member Size	Joint Deflection	Axial Load	Shear Load	Moment Load
Roof Beam	W24x84	1.791 in	26.321 k	19.696 k	186.41 kft
4th Beam	W24x84	1.407 in	8.69 k	34.782 k	302.78 kft
3rd Beam	W24x76	0.894 in	5.525 k	36.184 k	324.27 kft
2nd Beam	W24x76	0.348 in	7.934 k	34.697 k	299.63 kft
UO Column	W24x250	- in	129.11 k	77.991 k	710.94 kft
UI Column	W24x250	- in	67.157 k	117.35 k	939.13 kft
LO Column	W24x279	- in	211.51 k	125.69 k	1879.1 kft
LI Column	W24x279	- in	156.29 k	145.15 k	1960.3 kft

Pinned SDC D RBS Connections

RBS Connection: Seismic Catergory D Trial #1									
Member	Member Size	Joint Deflection		Axial Load		Shear Load		Moment Load	
Roof Beam	W18x55	3.84	in	35.938	k	20.732	k	195.77	kft
4th Beam	W24x68	3.002	in	22.059	k	42.639	k	410.46	kft
3rd Beam	W30x99	2.153	in	21.732	k	65.261	k	751.33	kft
2nd Beam	W30x116	1.25	in	22.941	k	81.399	k	995.96	kft
UO Column	W36x194	-	in	154.8	k	111.19	k	658.21	kft
UI Column	W36x194	-	in	68.908	k	209.61	k	1107.6	kft
LO Column	W36x302	-	in	546.93	k	186.29	k	2608.1	kft
LI Column	W36x302	-	in	171.37	k	289.97	k	3695.6	kft
RBS Connection: Seismic Catergory D Trial #2									
Member	Member Size	Joint Deflection		Axial Load		Shear Load		Moment Load	
Roof Beam	W30x99	1.844	in	36.462	k	23.889	k	239.15	kft
4th Beam	W30x108	1.518	in	17.882	k	41.887	k	395.46	kft
3rd Beam	W33x130	1.114	in	21.762	k	58.466	k	646.24	kft
2nd Beam	W36x182	0.688	in	21.375	k	87.765	k	1100.5	kft
UO Column	W36x361	-	in	160.09	k	119.45	k	799.15	kft
UI Column	W36x361	-	in	71.622	k	199.71	k	1193.3	kft
LO Column	W36x361	-	in	546.93	k	185.63	k	2598.8	kft
LI Column	W36x361	-	in	171.37	k	280.87	k	3646.5	kft

Pinned SDC D KBB Connection

Kaiser Connection: Seismic Catergory D Trial #1									
Member	Member Size	Joint Deflection		Axial Load		Shear Load		Moment Load	
Roof Beam	W18x40	5.345	in	35.656	k	21.509	k	210.1	kft
4th Beam	W21x55	4.099	in	20.078	k	30.728	k	401.5	kft
3rd Beam	W24x76	2.841	in	21.861	k	57.528	k	634.5	kft
2nd Beam	W30x99	1.572	in	17.985	k	88.56	k	1104.4	kft
UO Column	W36x361	-	in	156	k	114.25	k	677.38	kft
UI Column	W36x361	-	in	68.135	k	208.03	k	1148.4	kft
LO Column	W36x361	-	in	547.39	k	179.45	k	2512.3	kft
LI Column	W36x361	-	in	166.69	k	273.3	k	3826.1	kft
Kaiser Connection: Seismic Catergory D Trial #2									
Member	Member Size	Joint Deflection		Axial Load		Shear Load		Moment Load	
Roof Beam	W30x108	1.865	in	38.781	k	26.904	k	286.86	kft
4th Beam	W30x108	1.539	in	16.818	k	42.661	k	409.84	kft
3rd Beam	W33x130	1.143	in	20.339	k	46.078	k	609.94	kft
2nd Beam	W36x182	0.688	in	19.698	k	84.984	k	1054.9	kft
UO Column	W36x361	-	in	172.48	k	117.14	k	974.53	kft
UI Column	W36x361	-	in	70.367	k	202.28	k	1497.1	kft
LO Column	W36x361	-	in	546.57	k	184.68	k	2585.5	kft
LI Column	W36x361	-	in	178.5	k	278.82	k	3664.9	kft

Fixed SDC D RBS Connection

RBS Connection: Seismic Category D Trial #1										
Member	Member Size	Joint Deflection		Axial Load		Shear Load		Moment Load		
Roof Beam	W21x44	2.856	in	34.814	k	20.76	k	197.7	kft	
4th Beam	W21x62	1.977	in	18.209	k	38.059	k	342.72	kft	
3rd Beam	W27x84	1.127	in	11.426	k	50.921	k	534.88	kft	
2nd Beam	W27x84	0.412	in	12.191	k	44.346	k	432.61	kft	
UO Column	W24x250	-	in	1441.3	k	126.59	k	658.32	kft	
UI Column	W24x250	-	in	68.935	k	194.27	k	914.63	kft	
LO Column	W24x279	-	in	379.96	k	204.69	k	3605.2	kft	
LI Column	W24x279	-	in	163.82	k	242.17	k	3759.7	kft	
RBS Connection: Seismic Category D Trial #2										
Member	Member Size	Joint Deflection		Axial Load		Shear Load		Moment Load		
Roof Beam	W30x99	1.744	in	37.93	k	25.485	k	263.91	kft	
4th Beam	W30x99	1.365	in	14.988	k	43.675	k	419.19	kft	
3rd Beam	W30x99	0.857	in	9.718	k	48.489	k	496.49	kft	
2nd Beam	W30x99	0.335	in	11.35	k	45.269	k	445.01	kft	
UO Column	W36x182	-	in	170.21	k	124.19	k	1013.8	kft	
UI Column	W36x182	-	in	73.256	k	195.25	k	1412.8	kft	
LO Column	W36x256	-	in	302.37	k	204.34	k	3070.8	kft	
LI Column	W36x256	-	in	168.88	k	241.93	k	3220.3	kft	

Fixed SDC D KBB Connection

Kaiser Connection: Seismic Category D Trial #1										
Member	Member Size	Joint Deflection		Axial Load		Shear Load		Moment Load		
Roof Beam	W18x40	3.783	in	35.603	k	20.21	k	190.27	kft	
4th Beam	W21x62	2.677	in	18.697	k	42.261	k	405.41	kft	
3rd Beam	W21x68	1.57	in	8.003	k	48.102	k	492.67	kft	
2nd Beam	W21x68	0.572	in	11.476	k	39.286	k	358.7	kft	
UO Column	W27x307	-	in	152.47	k	123.77	k	617.98	kft	
UI Column	W27x307	-	in	68.948	k	198.05	k	1039.7	kft	
LO Column	W27x307	-	in	367.97	k	210.31	k	3907.2	kft	
LI Column	W27x307	-	in	162.34	k	237.45	k	4025.6	kft	
Kaiser Connection: Seismic Category D Trial #2										
Member	Member Size	Joint Deflection		Axial Load		Shear Load		Moment Load		
Roof Beam	W30x108	1.899	in	37.058	k	23.105	k	264.63	kft	
4th Beam	W30x108	1.541	in	16.027	k	41.009	k	425.62	kft	
3rd Beam	W30x108	1.034	in	6.739	k	48.087	k	536.27	kft	
2nd Beam	W24x76	0.428	in	12.288	k	38.401	k	344.73	kft	
UO Column	W27x307	-	in	178.36	k	118.51	k	1170.1	kft	
UI Column	W27x307	-	in	73.559	k	200.89	k	1614.1	kft	
LO Column	W27x307	-	in	403.37	k	211.47	k	3115.5	kft	
LI Column	W27x307	-	in	169.69	k	238.05	k	3223.1	kft	

Appendix C - RBS: Pinned vs. Fixed Comparison

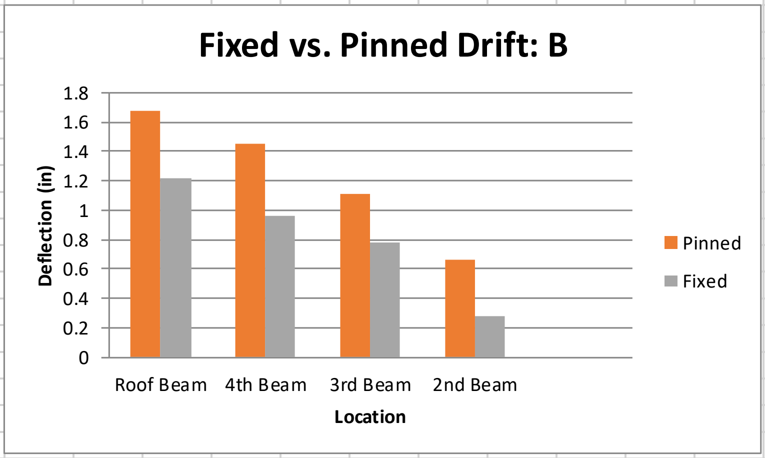

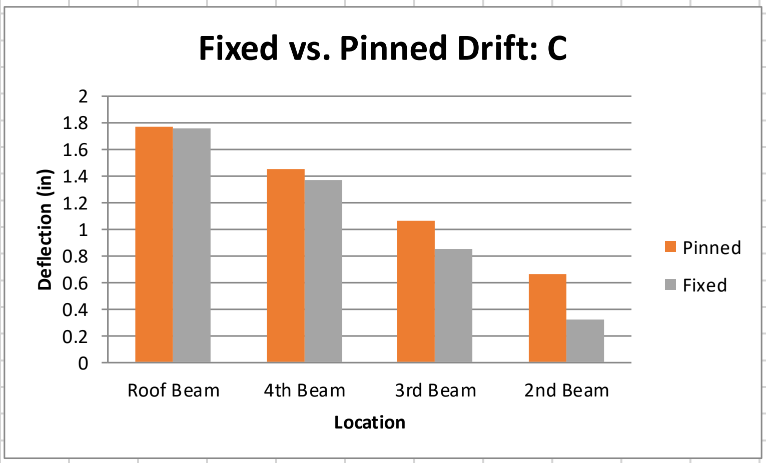

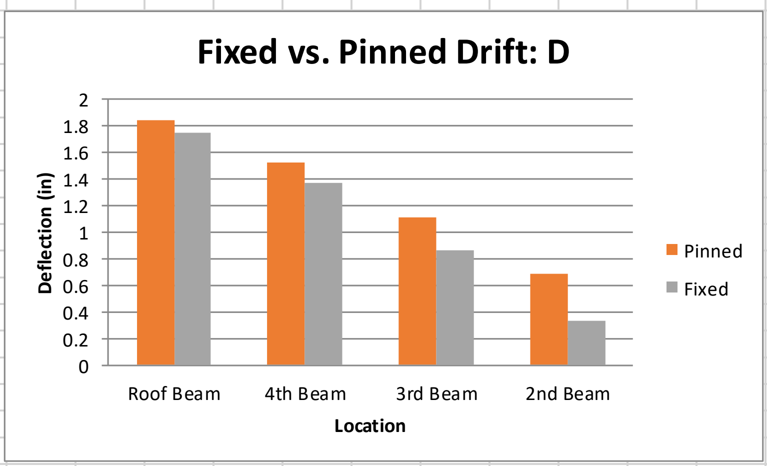

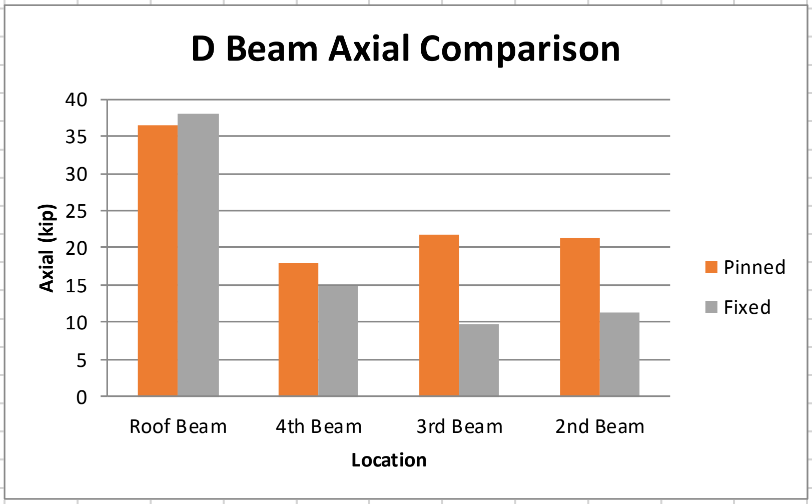

D Beam Axial Comparison
Axial (kip)
40
35
30
25
20
15
10
5
0
Roof Beam
4th Beam
3rd Beam
2nd Beam
Location
Pinned
Fixed

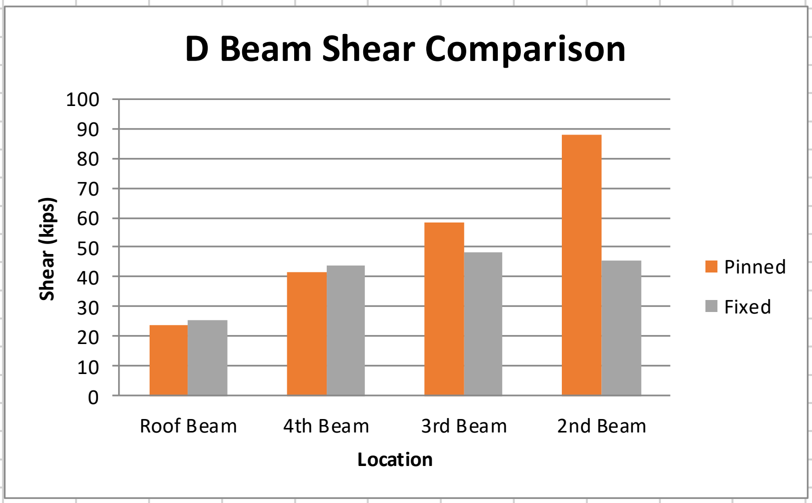

D Beam Shear Comparison
Shear (kips)
100
90
80
70
60
50
40
30
20
10
0
Roof Beam
4th Beam
3rd Beam
2nd Beam
Location
Pinned
Fixed

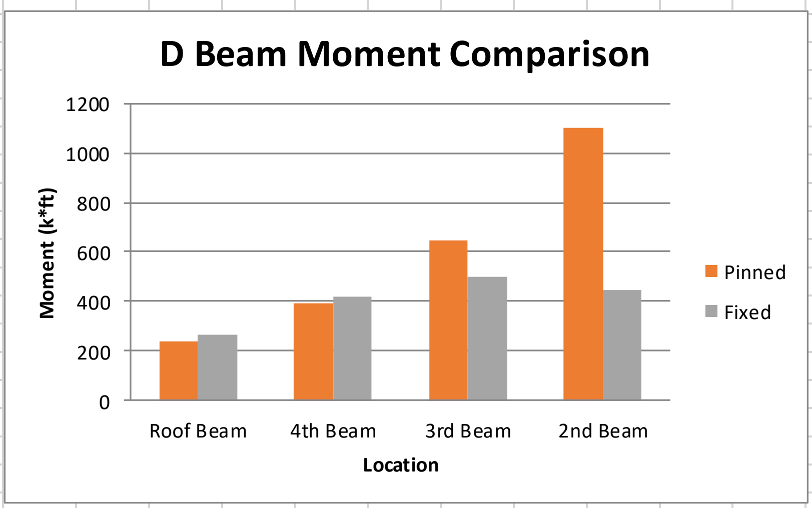

D Beam Moment Comparison
Moment (k*ft)
1200
1000
800
600
400
200
0
Roof Beam
4th Beam
3rd Beam
2nd Beam
Location
Pinned
Fixed

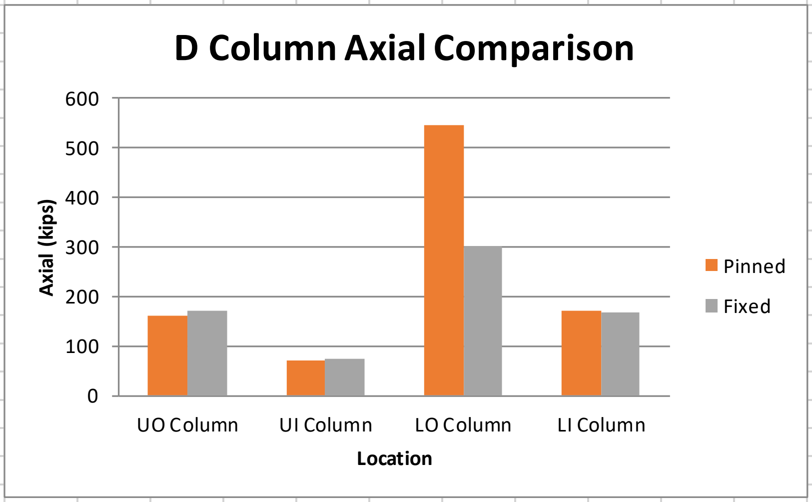
D Column Axial Comparison
Axial (kips)
600
500
400
300
200
100
0
UO Column
UI Column
LO Column
LI Column
Location
Pinned
Fixed

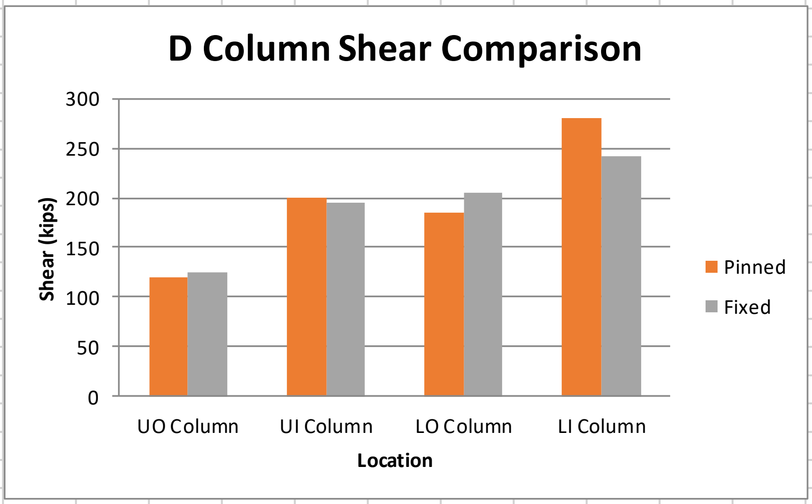
D Column Shear Comparison
Shear (kips)
300
250
200
150
100
50
0
UO Column
UI Column
LO Column
LI Column
Location
Pinned
Fixed

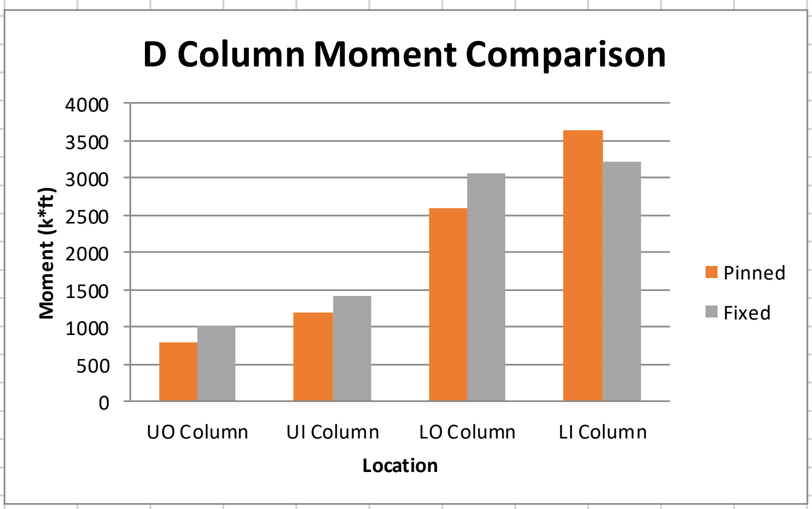
D Column Moment Comparison
Moment (k*ft)
4000
3500
3000
2500
2000
1500
1000
500
0
UO Column
UI Column
LO Column
LI Column
Location
Pinned
Fixed

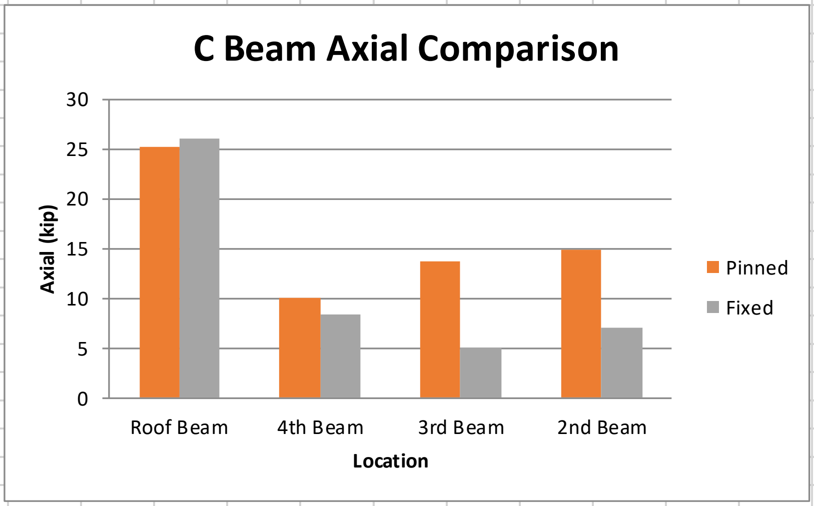
C Beam Axial Comparison
Axial (kip)
30
25
20
15
10
5
0
Roof Beam
4th Beam
3rd Beam
2nd Beam
Location
Pinned
Fixed

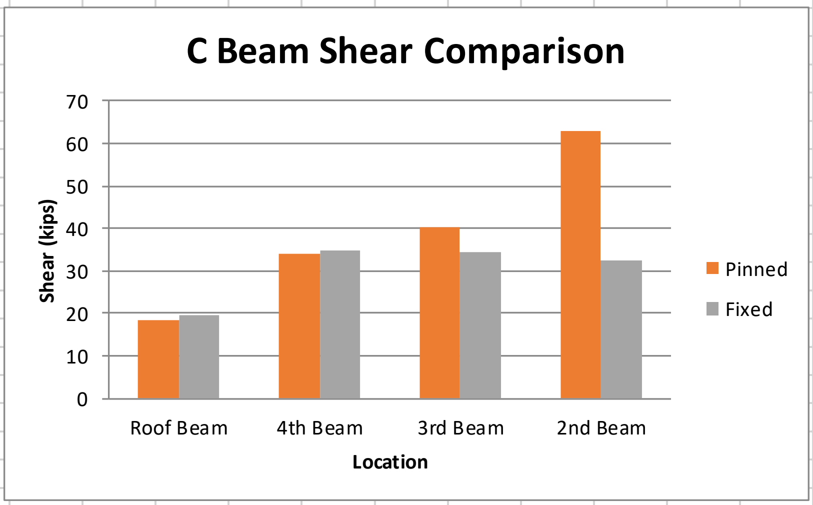
C Beam Shear Comparison
Shear (kips)
70
60
50
40
30
20
10
0
Roof Beam
4th Beam
3rd Beam
2nd Beam
Location
Pinned
Fixed

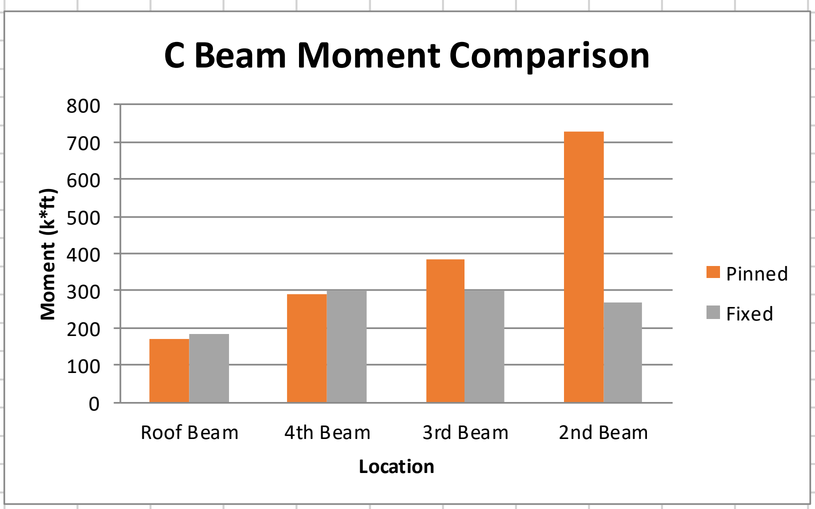
C Beam Moment Comparison
Moment (k*ft)
800
700
600
500
400
300
200
100
0
Roof Beam
4th Beam
3rd Beam
2nd Beam
Location
Pinned
Fixed

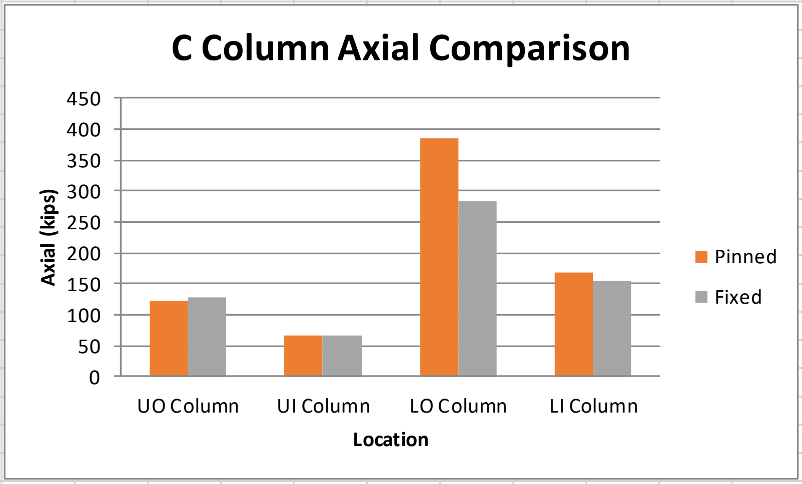

C Column Axial Comparison
Axial (kips)
450
400
350
300
250
200
150
100
50
0
UO Column
UI Column
LO Column
LI Column
Location
Pinned
Fixed

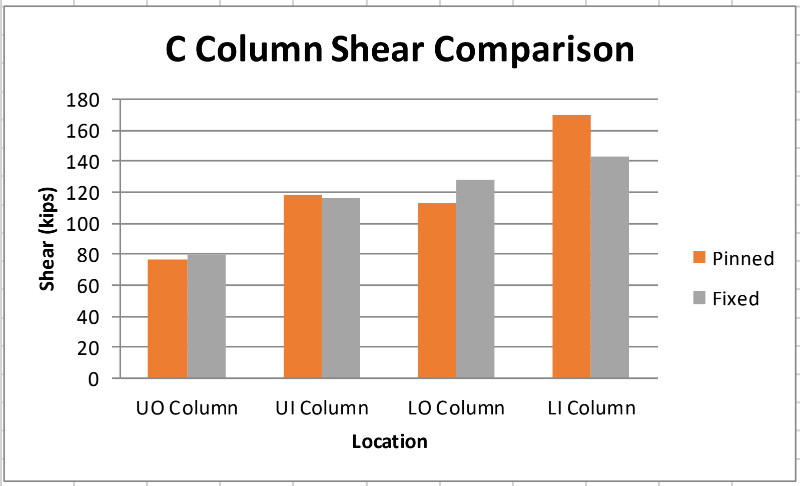

C Column Shear Comparison
Shear (kips)
180
160
140
120
100
80
60
40
20
0
UO Column
UI Column
LO Column
LI Column
Location
Pinned
Fixed

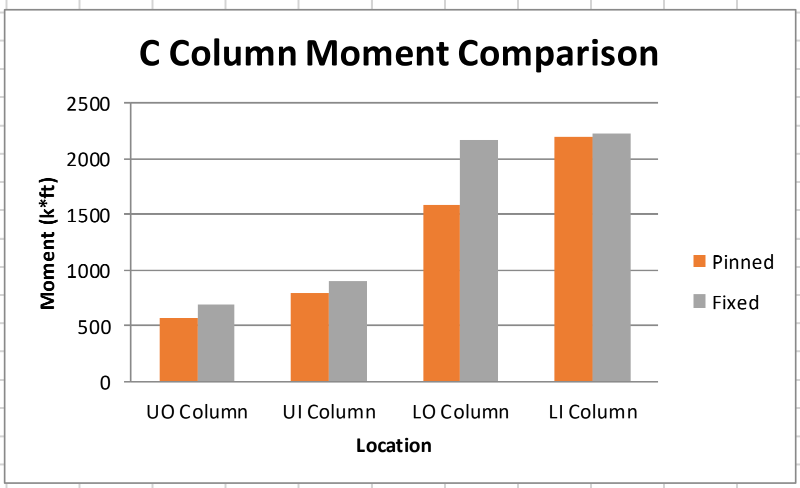

C Column Moment Comparison
Moment (k*ft)
2500
2000
1500
1000
500
0
UO Column
UI Column
LO Column
LI Column
Location
Pinned
Fixed

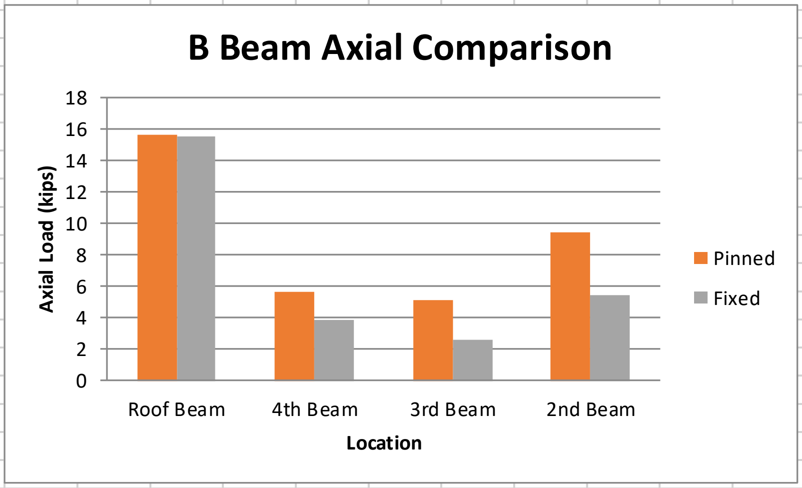
B Beam Axial Comparison
Axial Load (kips)
18
16
14
12
10
8
6
4
2
0
Roof Beam
4th Beam
3rd Beam
2nd Beam
Location
Pinned
Fixed

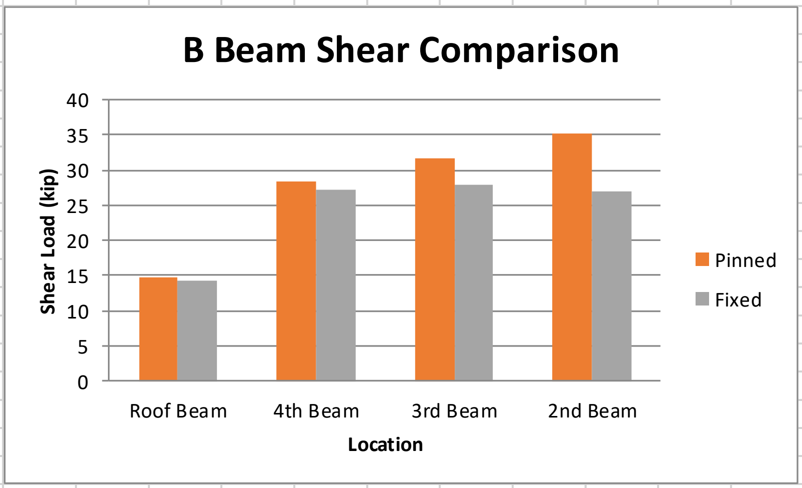
B Beam Shear Comparison
Shear Load (kip)
40
35
30
25
20
15
10
5
0
Roof Beam
4th Beam
3rd Beam
2nd Beam
Location
Pinned
Fixed

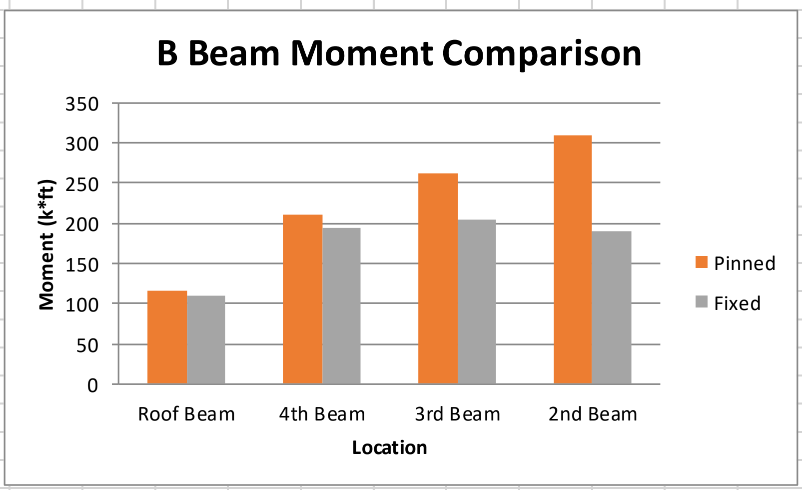
B Beam Moment Comparison
Moment (k*ft)
350
300
250
200
150
100
50
0
Roof Beam
4th Beam
3rd Beam
2nd Beam
Location
Pinned
Fixed

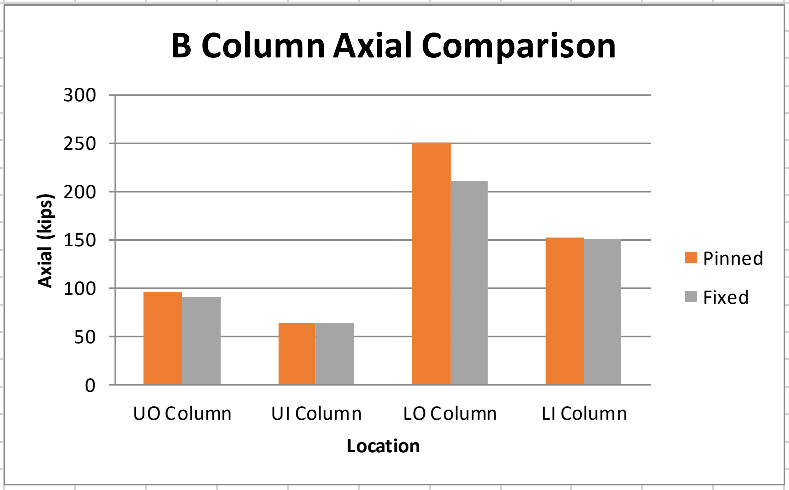
B Column Axial Comparison
Axial (kips)
300
250
200
150
100
50
0
UO Column
UI Column
LO Column
LI Column
Location
Pinned
Fixed

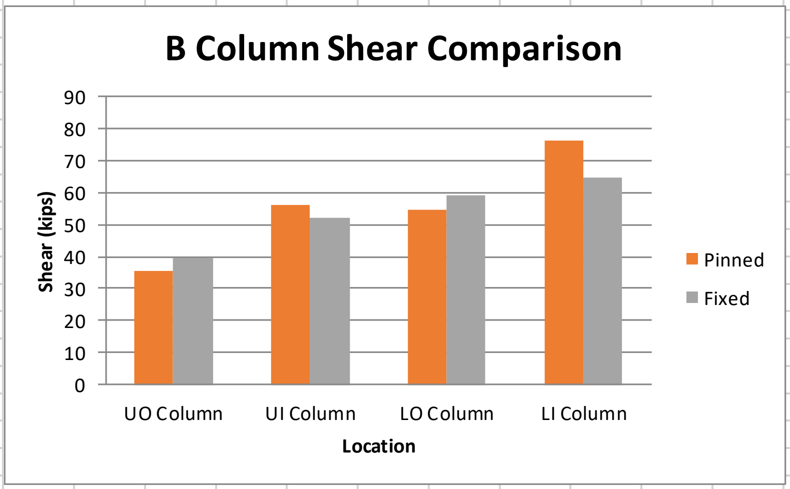
B Column Shear Comparison
Shear (kips)
90
80
70
60
50
40
30
20
10
0
UO Column
UI Column
LO Column
LI Column
Location
Pinned
Fixed

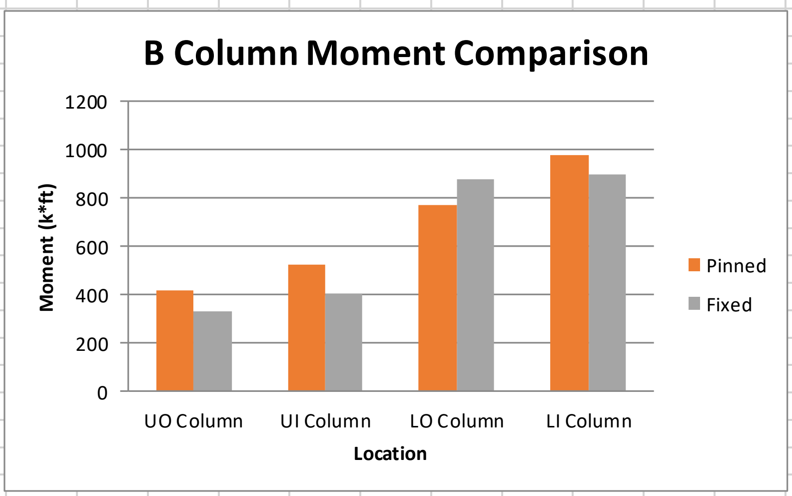
B Column Moment Comparison
Moment (k*ft)
1200
1000
800
600
400
200
0
UO Column
UI Column
LO Column
LI Column
Location
Pinned
Fixed

Appendix D - KBB: Pinned vs. Fixed Comparison

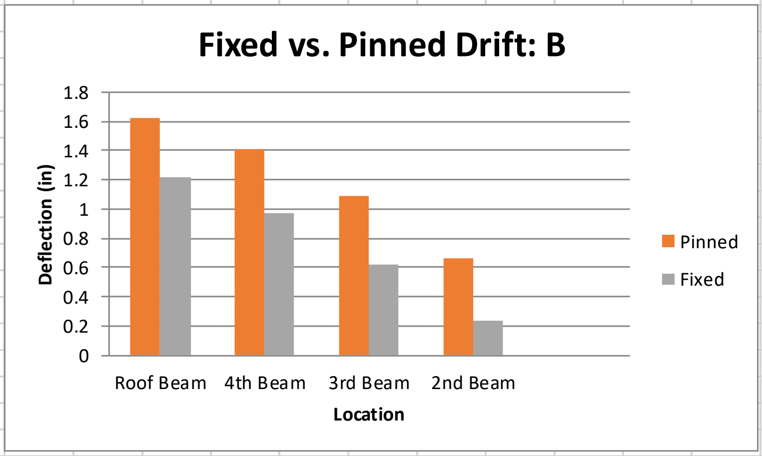

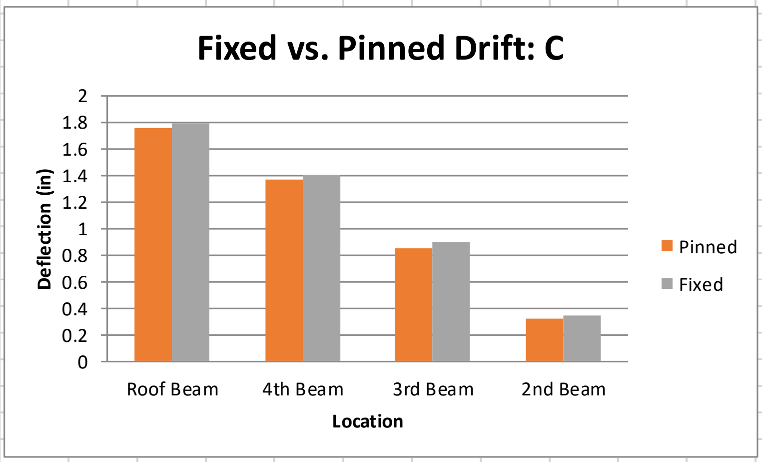

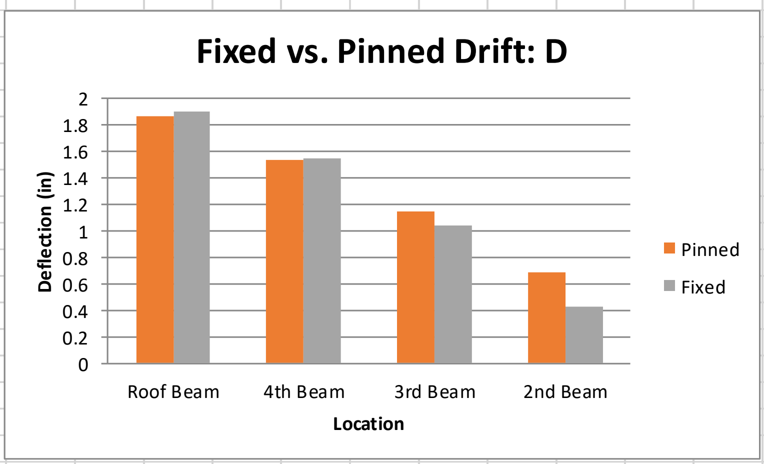

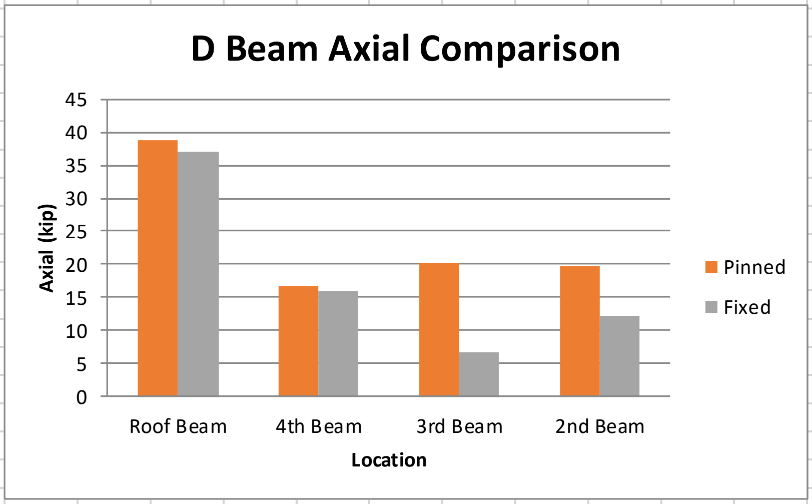
D Beam Axial Comparison
Axial (kip)
45
40
35
30
25
20
15
10
5
0
Roof Beam
4th Beam
3rd Beam
2nd Beam
Location
Pinned
Fixed

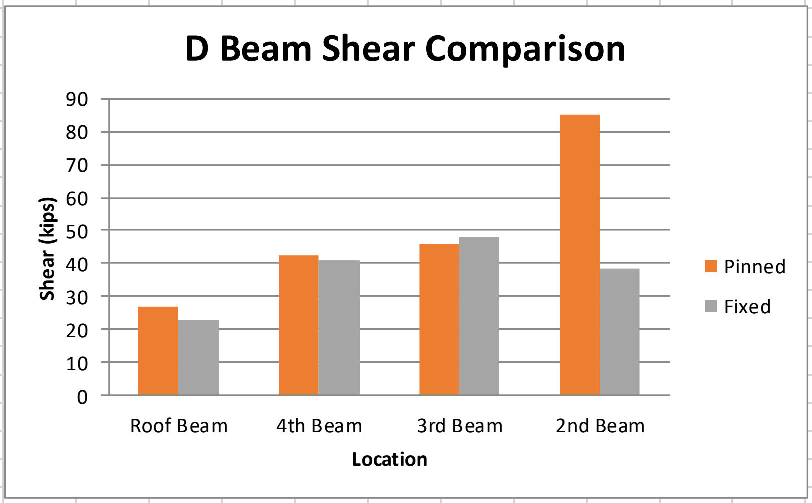
D Beam Shear Comparison
Shear (kips)
90
80
70
60
50
40
30
20
10
0
Roof Beam
4th Beam
3rd Beam
2nd Beam
Location
Pinned
Fixed

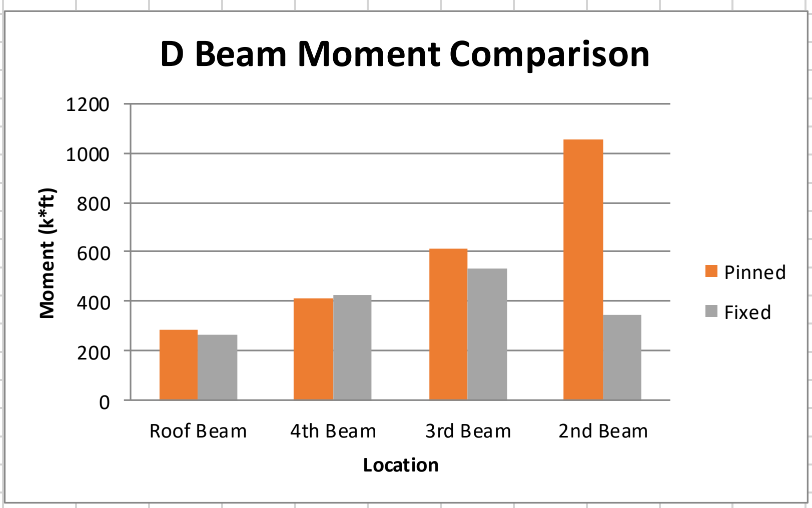
D Beam Moment Comparison
Moment (k*ft)
1200
1000
800
600
400
200
0
Roof Beam
4th Beam
3rd Beam
2nd Beam
Location
Pinned
Fixed

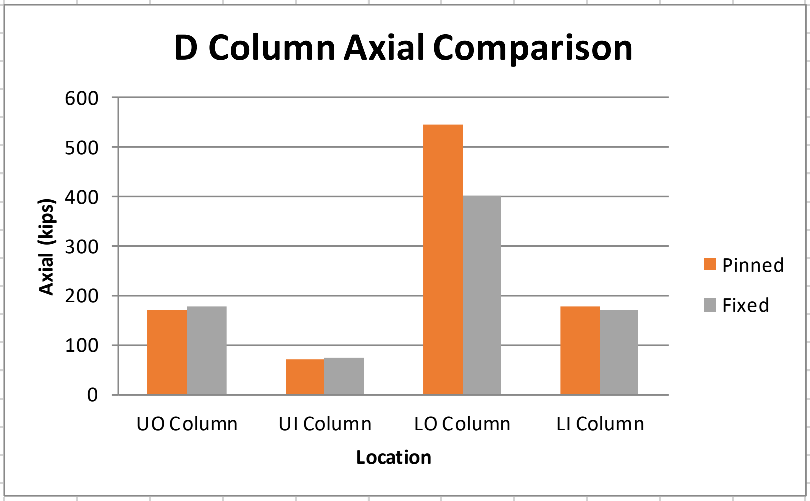
D Column Axial Comparison
600
500
400
300
200
100
0
Axial (kips)
UO Column
UI Column
LO Column
LI Column
Location
Pinned
Fixed

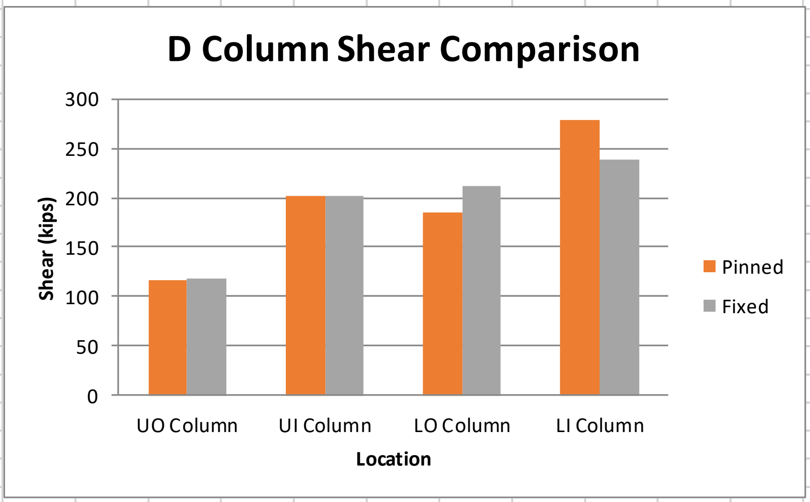
D Column Shear Comparison
300
250
200
150
100
50
0
Shear (kips)
UO Column
UI Column
LO Column
LI Column
Location
Pinned
Fixed

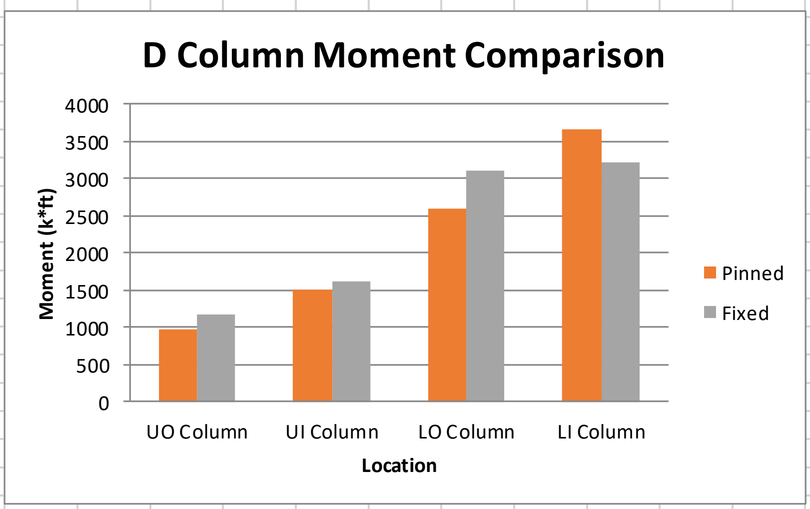
D Column Moment Comparison
4000
3500
3000
2500
2000
1500
1000
500
0
Moment (k*ft)
UO Column
UI Column
LO Column
LI Column
Location
Pinned
Fixed

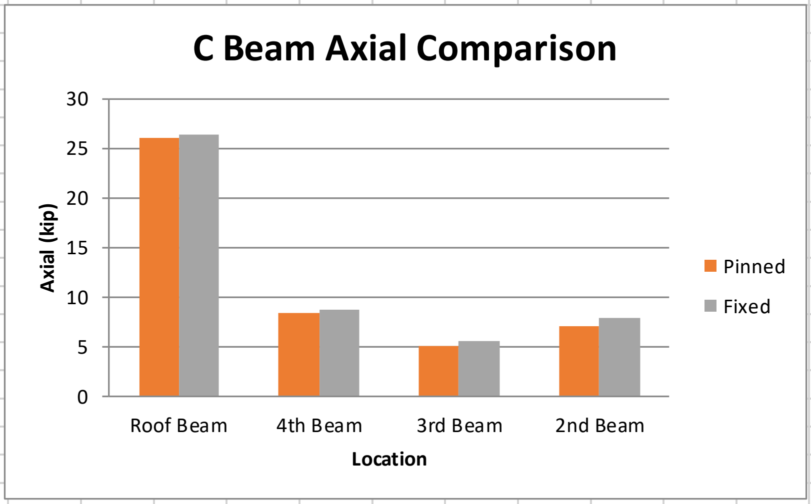
C Beam Axial Comparison
30
25
20
15
10
5
0
Axial (kip)
Roof Beam
4th Beam
3rd Beam
2nd Beam
Location
Pinned
Fixed

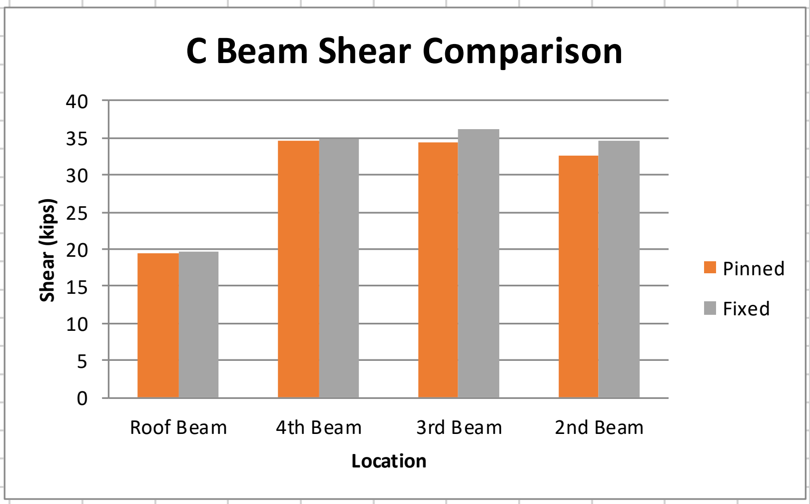
C Beam Shear Comparison
40
35
30
25
20
15
10
5
0
Shear (kips)
Roof Beam
4th Beam
3rd Beam
2nd Beam
Location
Pinned
Fixed

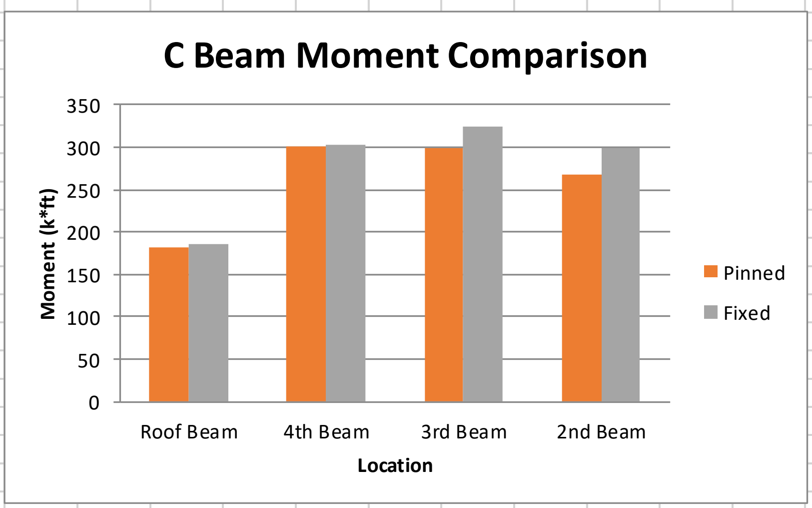
C Beam Moment Comparison
350
300
250
200
150
100
50
0
Moment (k*ft)
Roof Beam
4th Beam
3rd Beam
2nd Beam
Location
Pinned
Fixed

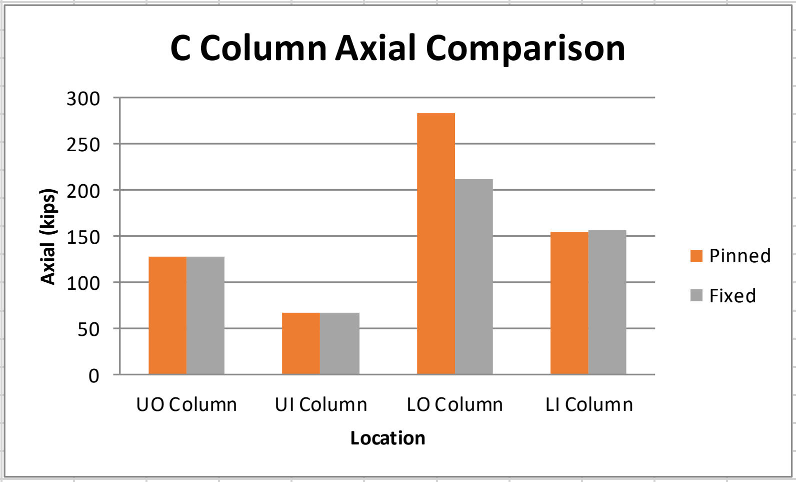
C Column Axial Comparison
Axial (kips)
300
250
200
150
100
50
0
UO Column
UI Column
LO Column
LI Column
Location
Pinned
Fixed

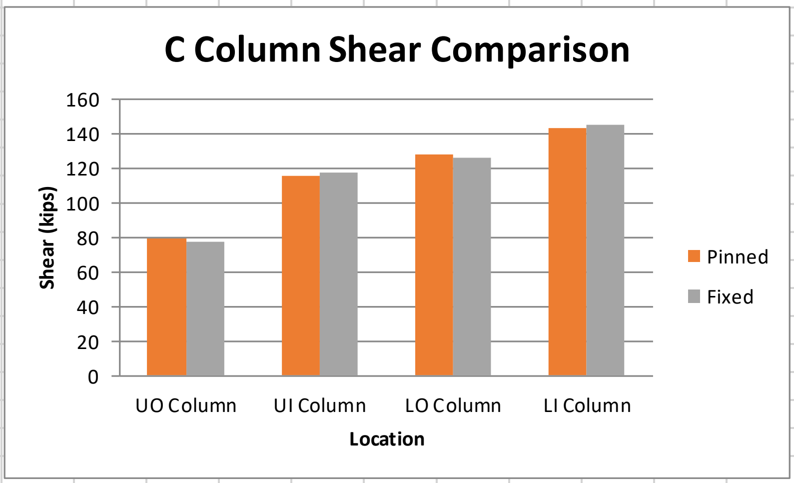
C Column Shear Comparison
Shear (kips)
160
140
120
100
80
60
40
20
0
UO Column
UI Column
LO Column
LI Column
Location
Pinned
Fixed

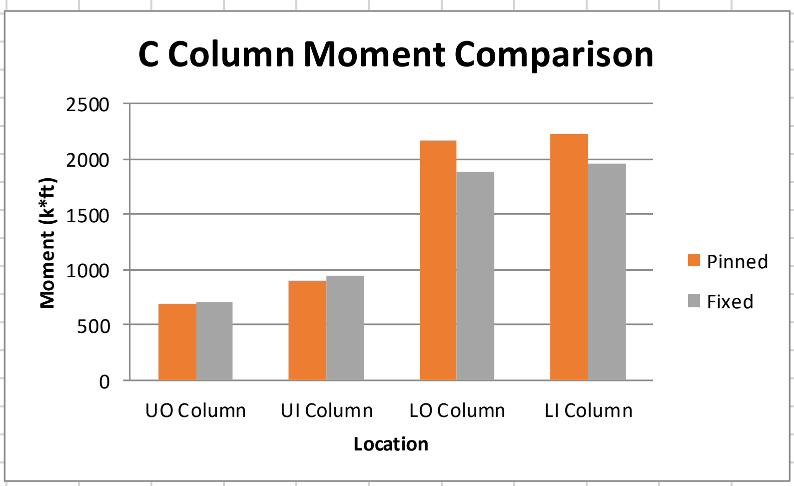
C Column Moment Comparison
Moment (k*ft)
2500
2000
1500
1000
500
0
UO Column
UI Column
LO Column
LI Column
Location
Pinned
Fixed

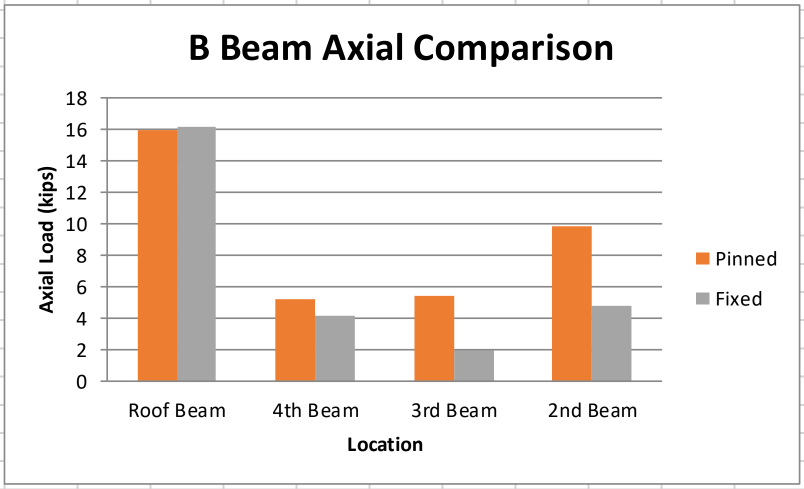

B Beam Axial Comparison
18
16
14
12
10
8
6
4
2
0
Axial Load (kips)
Roof Beam
4th Beam
3rd Beam
2nd Beam
Location
Pinned
Fixed

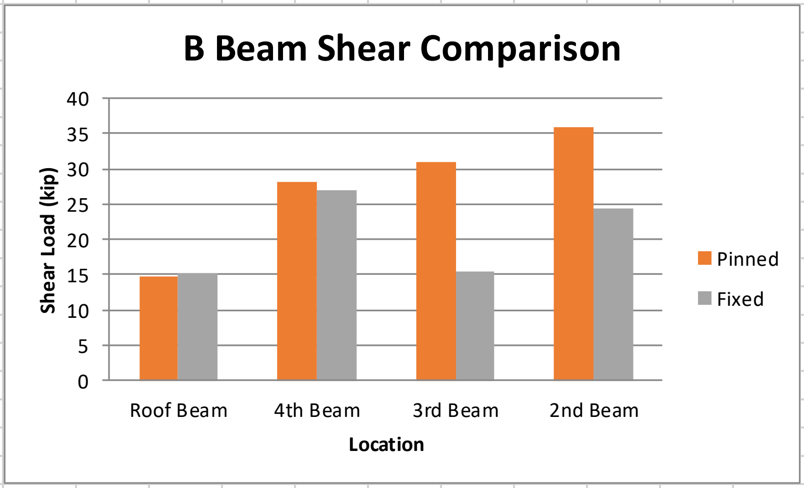

B Beam Shear Comparison
40
35
30
25
20
15
10
5
0
Shear Load (kip)
Roof Beam
4th Beam
3rd Beam
2nd Beam
Location
Pinned
Fixed

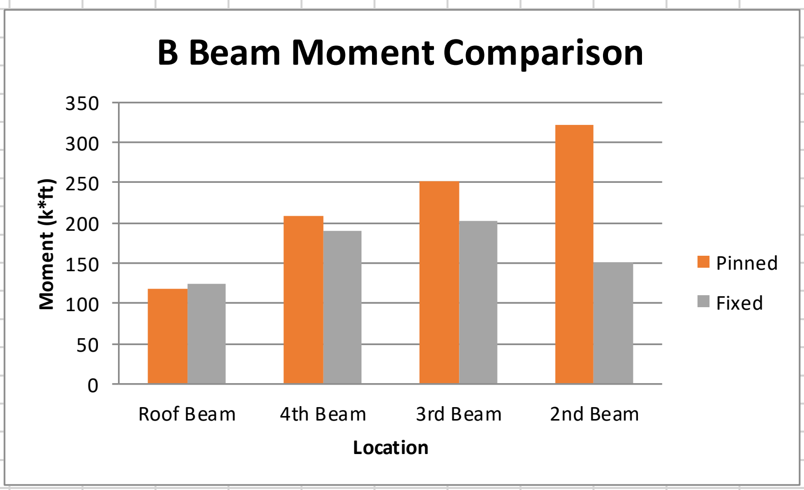

B Beam Moment Comparison
350
300
250
200
150
100
50
0
Moment (k*ft)
Roof Beam
4th Beam
3rd Beam
2nd Beam
Location
Pinned
Fixed

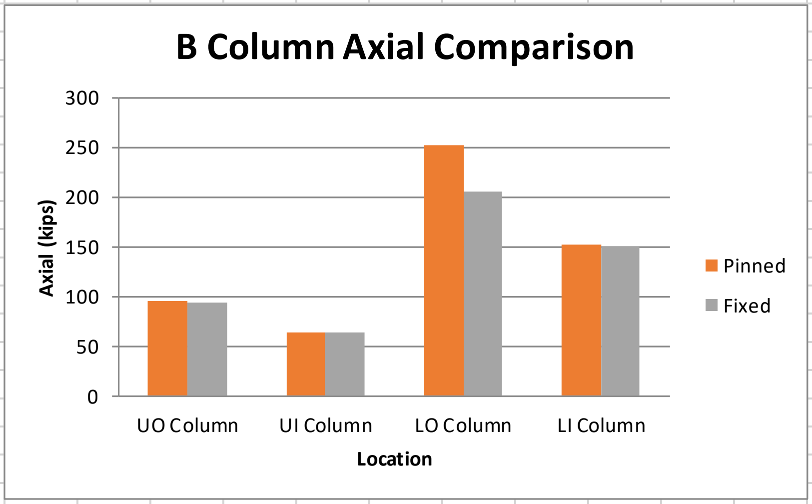
B Column Axial Comparison
300
250
200
150
100
50
0
Axial (kips)
UO Column
UI Column
LO Column
LI Column
Location
Pinned
Fixed

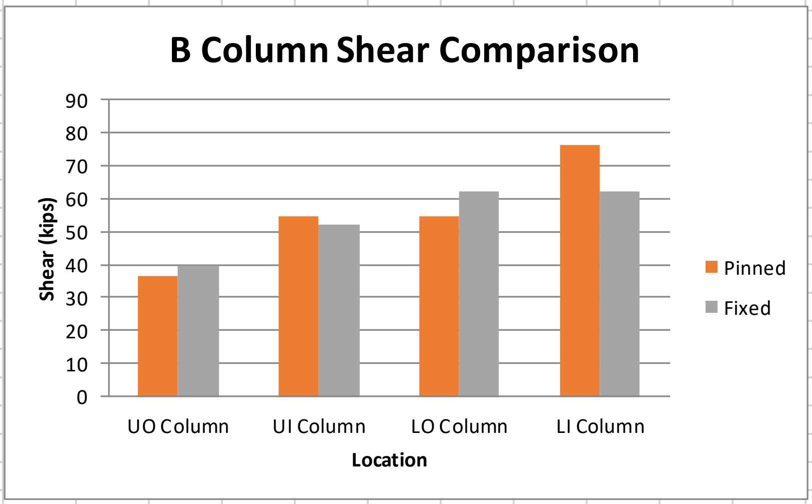
B Column Shear Comparison
90
80
70
60
50
40
30
20
10
0
Shear (kips)
UO Column
UI Column
LO Column
LI Column
Location
Pinned
Fixed

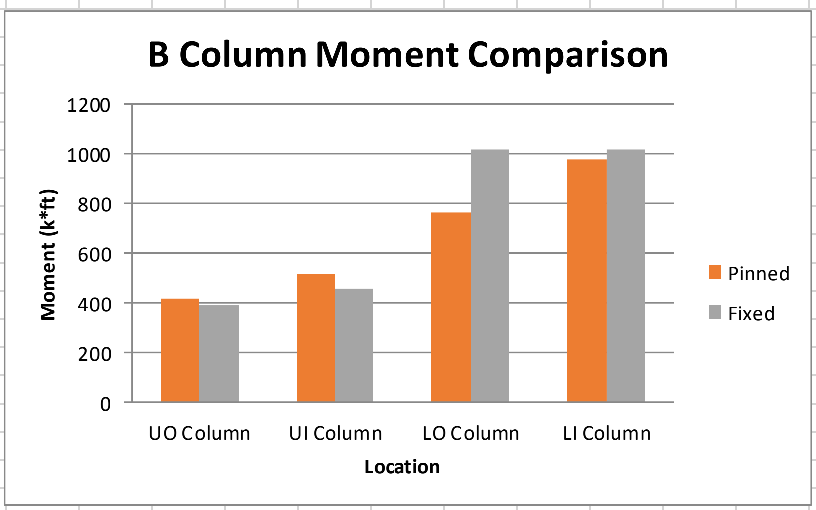
B Column Moment Comparison
1200
1000
800
600
400
200
0
Moment (k*ft)
UO Column
UI Column
LO Column
LI Column
Location
Pinned
Fixed

Appendix E - Pinned: RBS vs. KBB Comparison

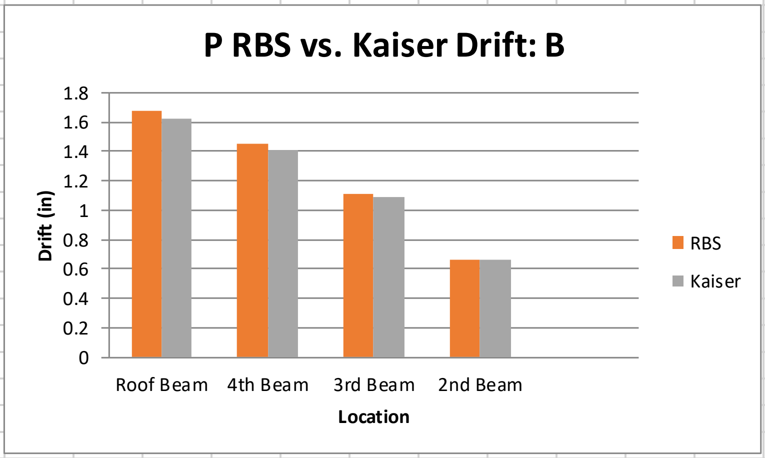

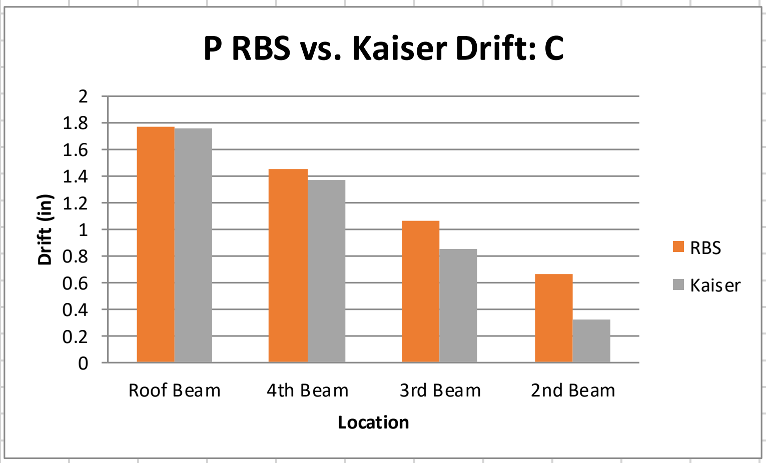

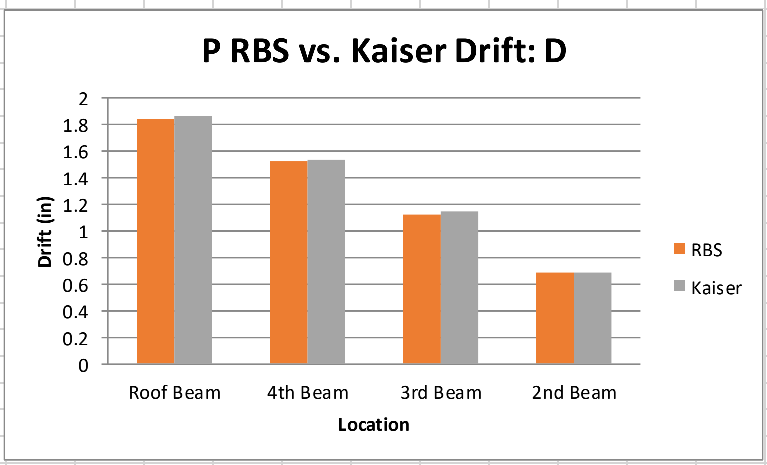

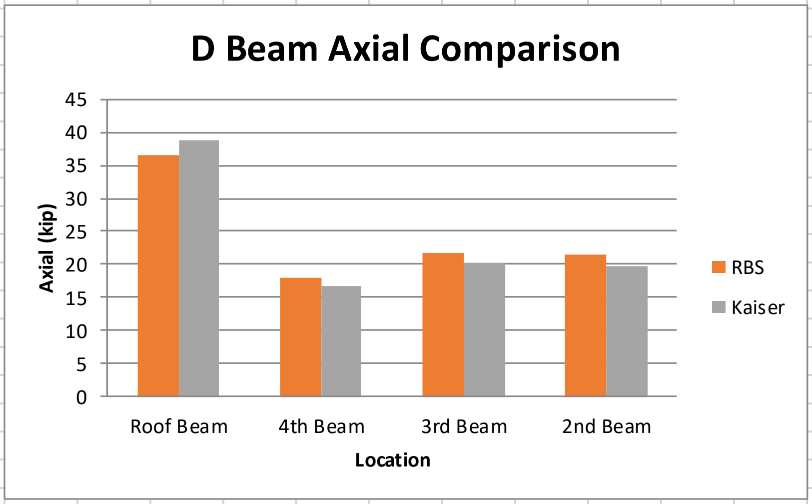
D Beam Axial Comparison
Axial (kip)
45
40
35
30
25
20
15
10
5
0
Roof Beam
4th Beam
3rd Beam
2nd Beam
Location
RBS
Kaiser

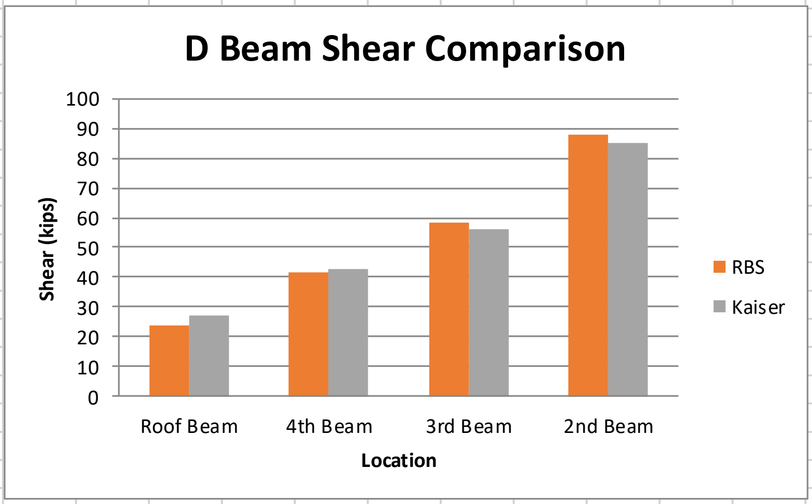
D Beam Shear Comparison
Shear (kips)
100
90
80
70
60
50
40
30
20
10
0
Roof Beam
4th Beam
3rd Beam
2nd Beam
Location
RBS
Kaiser

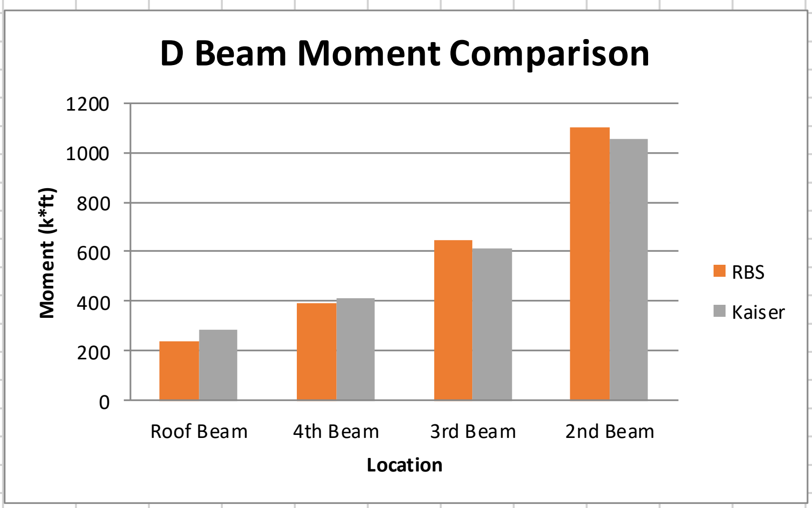
D Beam Moment Comparison
Moment (k*ft)
1200
1000
800
600
400
200
0
Roof Beam
4th Beam
3rd Beam
2nd Beam
Location
RBS
Kaiser

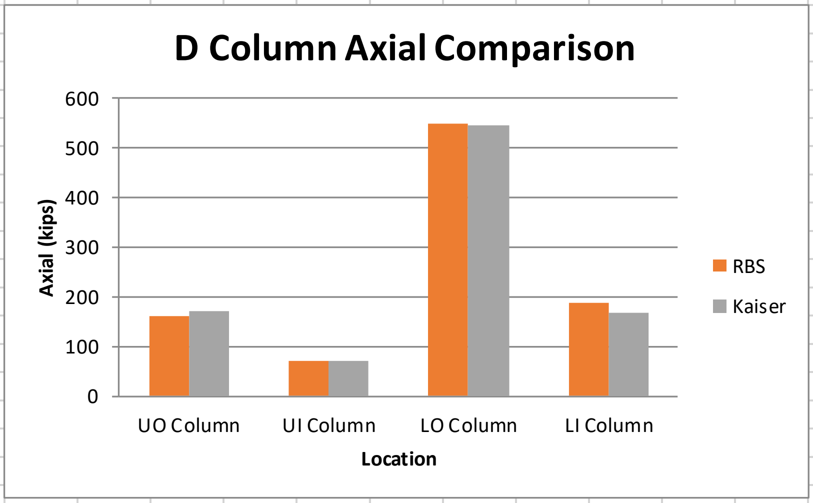
D Column Axial Comparison
600
500
400
300
200
100
0
Axial (kips)
UO Column
UI Column
LO Column
LI Column
Location
RBS
Kaiser

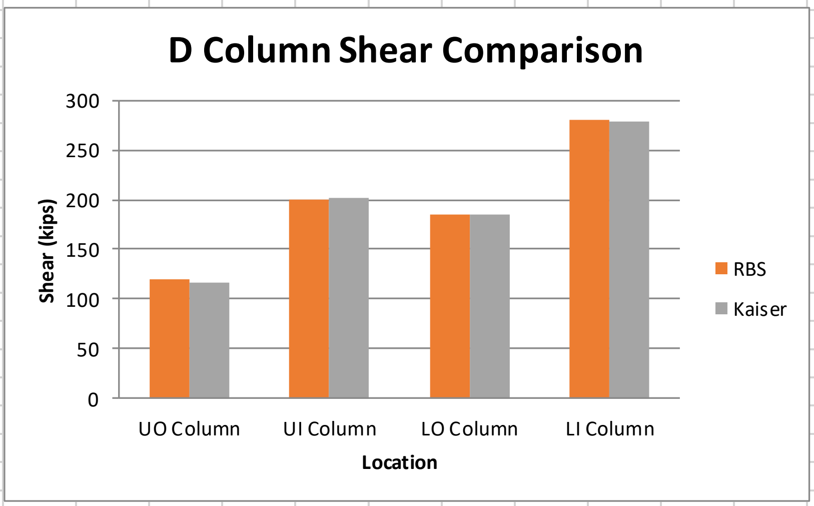
D Column Shear Comparison
300
250
200
150
100
50
0
Shear (kips)
UO Column
UI Column
LO Column
LI Column
Location
RBS
Kaiser

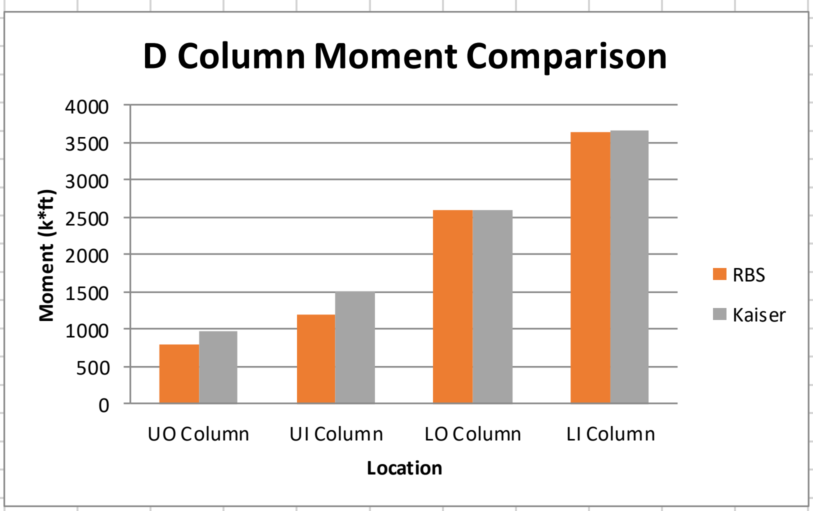
D Column Moment Comparison
4000
3500
3000
2500
2000
1500
1000
500
0
Moment (k*ft)
UO Column
UI Column
LO Column
LI Column
Location
RBS
Kaiser

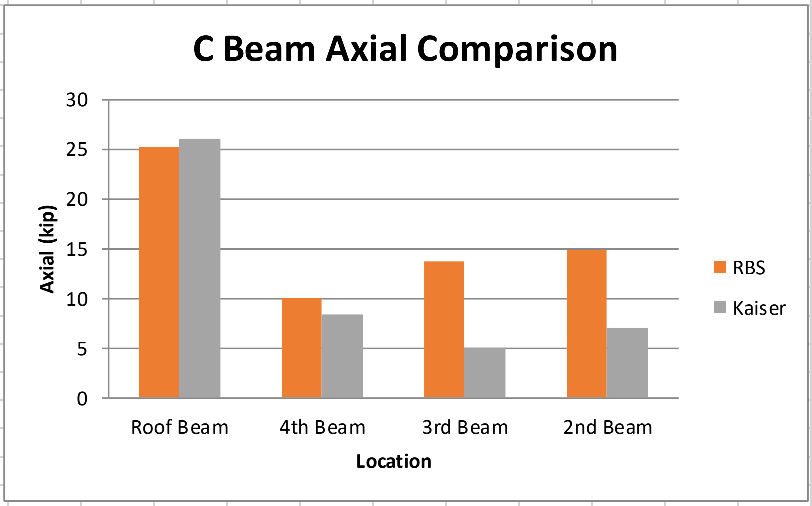
C Beam Axial Comparison
Axial (kip)
30
25
20
15
10
5
0
Roof Beam
4th Beam
3rd Beam
2nd Beam
Location
RBS
Kaiser

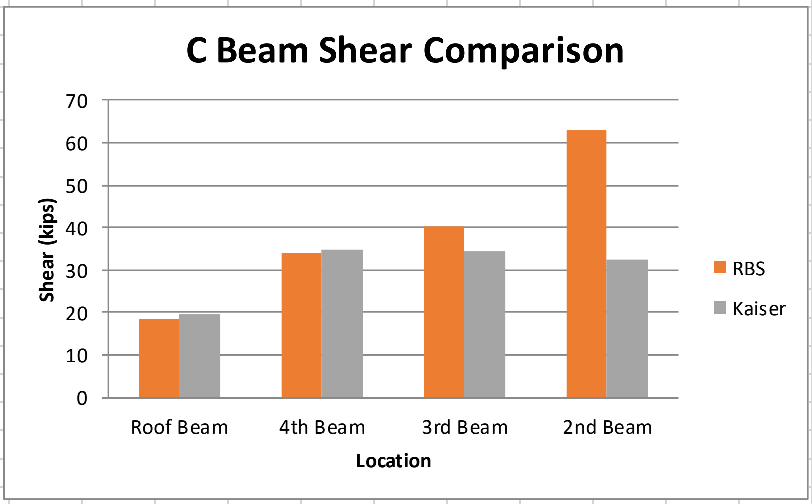
C Beam Shear Comparison
Shear (kips)
70
60
50
40
30
20
10
0
Roof Beam
4th Beam
3rd Beam
2nd Beam
Location
RBS
Kaiser

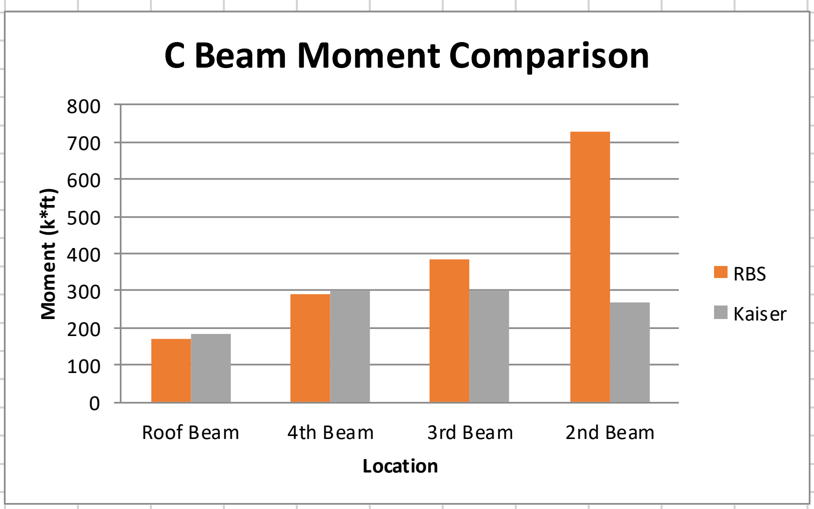
C Beam Moment Comparison
Moment (k*ft)
800
700
600
500
400
300
200
100
0
Roof Beam
4th Beam
3rd Beam
2nd Beam
Location
RBS
Kaiser

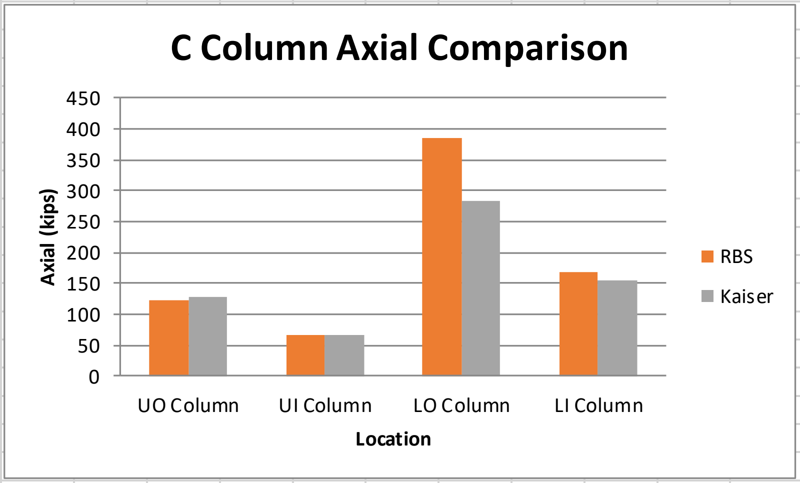
C Column Axial Comparison
Axial (kips)
450
400
350
300
250
200
150
100
50
0
UO Column
UI Column
LO Column
LI Column
Location
RBS
Kaiser

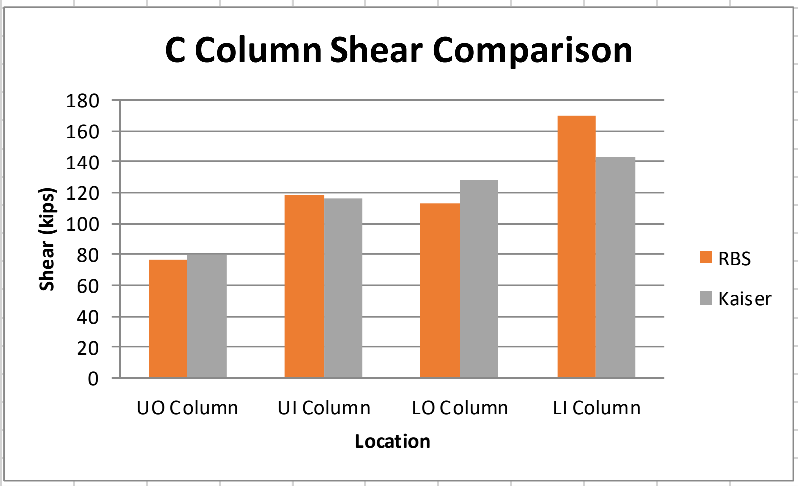
C Column Shear Comparison
Shear (kips)
180
160
140
120
100
80
60
40
20
0
UO Column
UI Column
LO Column
LI Column
Location
RBS
Kaiser

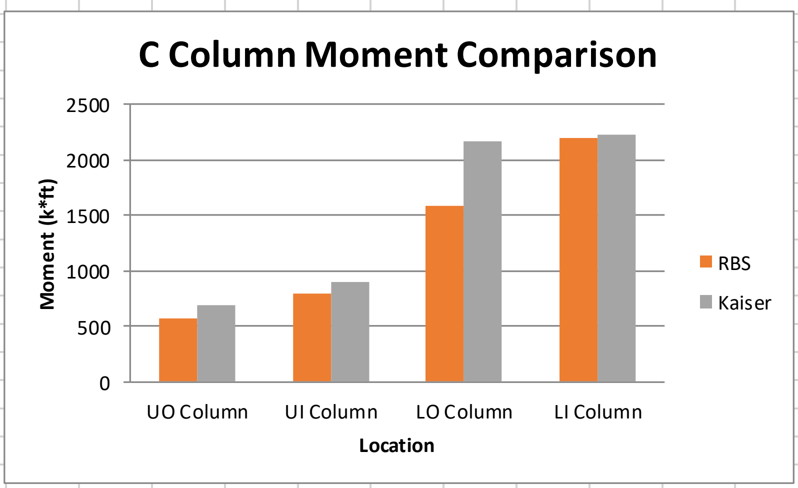
C Column Moment Comparison
Moment (k*ft)
2500
2000
1500
1000
500
0
UO Column
UI Column
LO Column
LI Column
Location
RBS
Kaiser

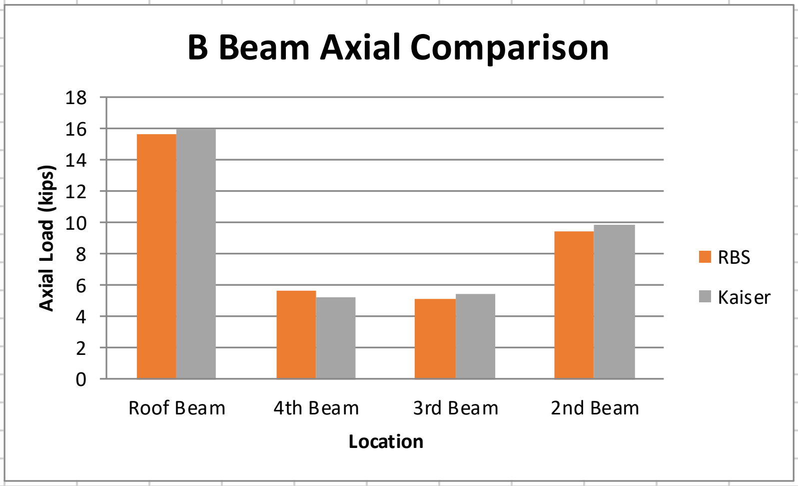
B Beam Axial Comparison
Axial Load (kips)
18
16
14
12
10
8
6
4
2
0
Roof Beam
4th Beam
3rd Beam
2nd Beam
Location
RBS
Kaiser

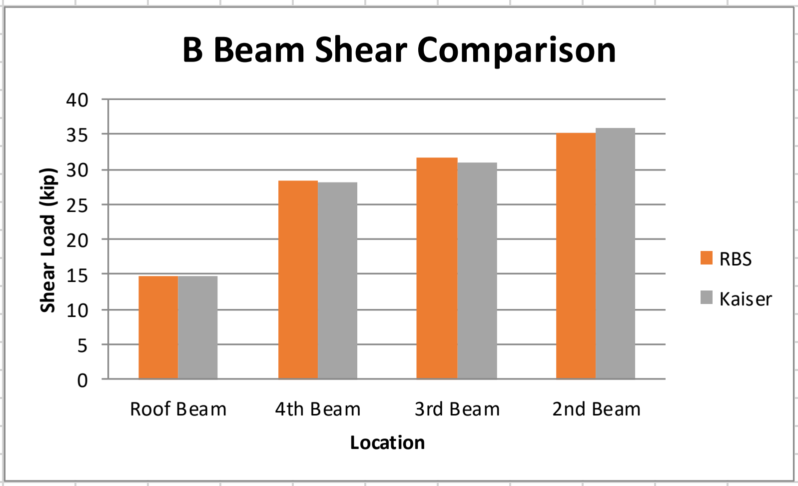
B Beam Shear Comparison
Shear Load (kip)
40
35
30
25
20
15
10
5
0
Roof Beam
4th Beam
3rd Beam
2nd Beam
Location
RBS
Kaiser

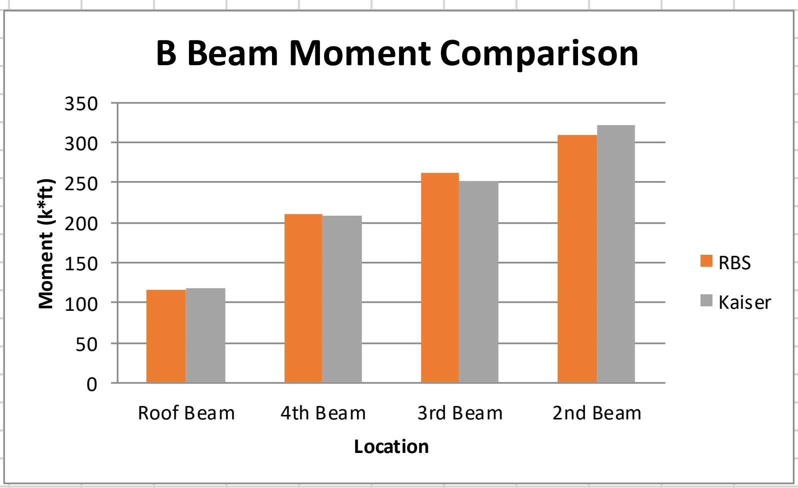
B Beam Moment Comparison
Moment (k*ft)
350
300
250
200
150
100
50
0
Roof Beam
4th Beam
3rd Beam
2nd Beam
Location
RBS
Kaiser

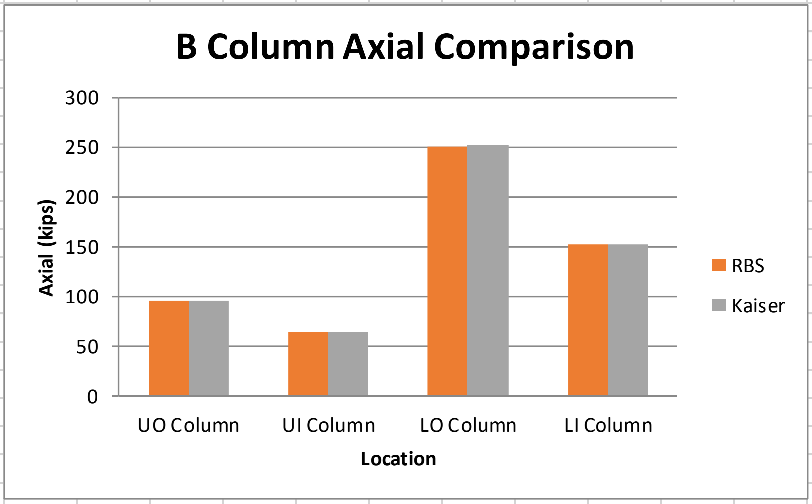
B Column Axial Comparison
Axial (kips)
300
250
200
150
100
50
0
UO Column
UI Column
LO Column
LI Column
Location
RBS
Kaiser

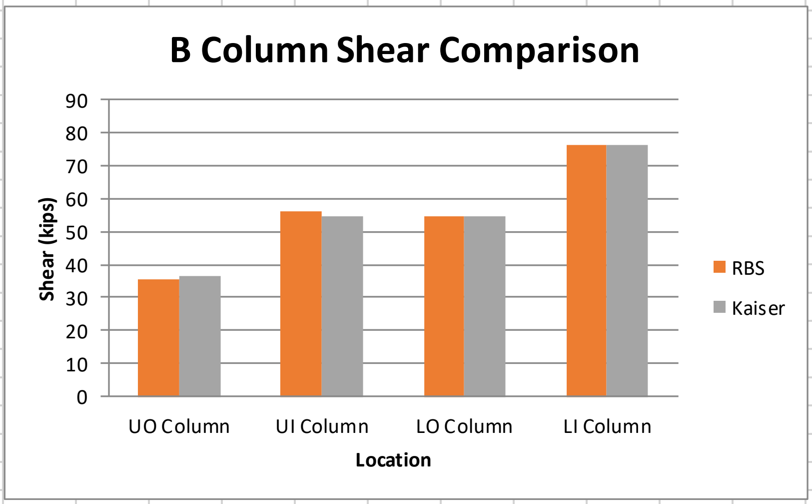
B Column Shear Comparison
Shear (kips)
90
80
70
60
50
40
30
20
10
0
UO Column
UI Column
LO Column
LI Column
Location
RBS
Kaiser

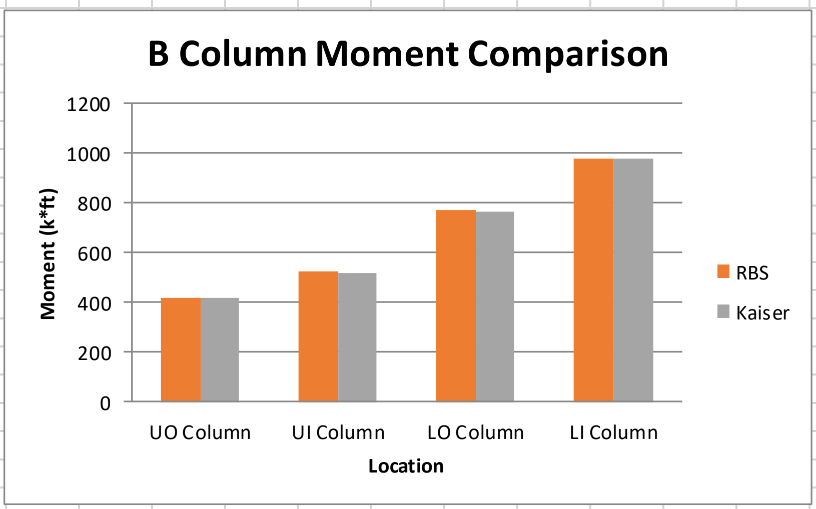
B Column Moment Comparison
Moment (k*ft)
1200
1000
800
600
400
200
0
UO Column
UI Column
LO Column
LI Column
Location
RBS
Kaiser

Appendix F - Fixed: RBS vs. KBB Comparison

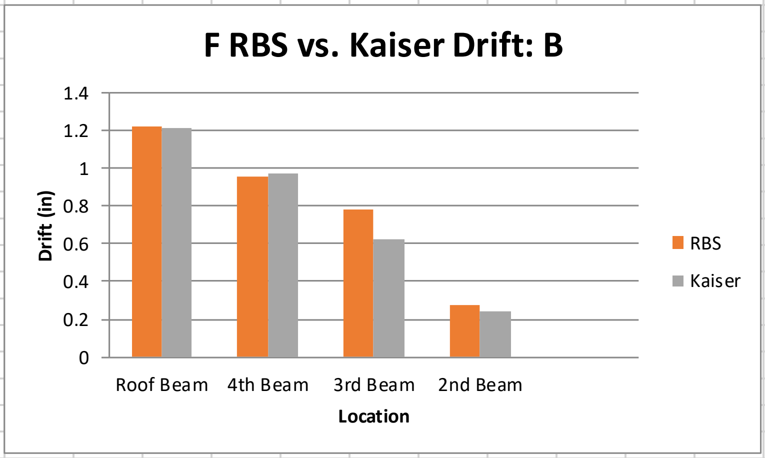

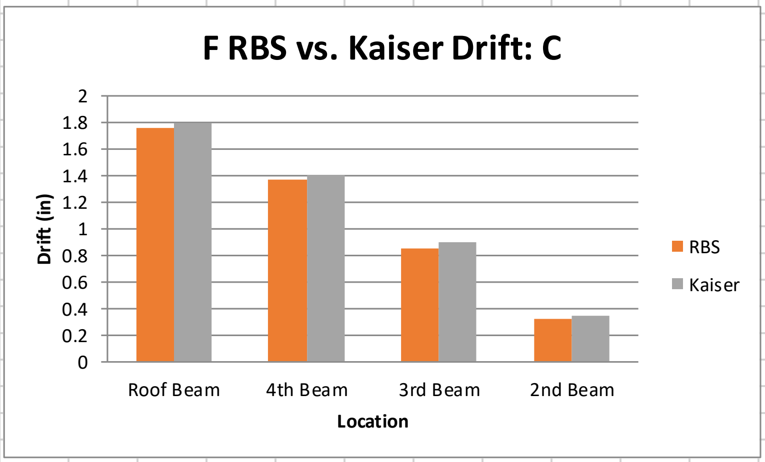

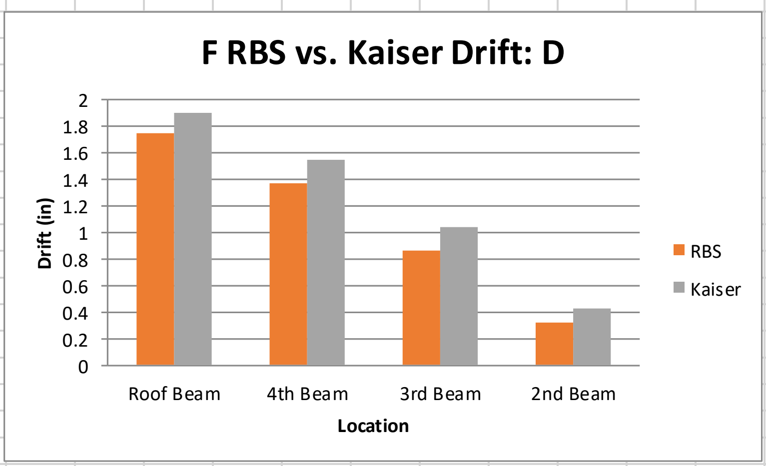

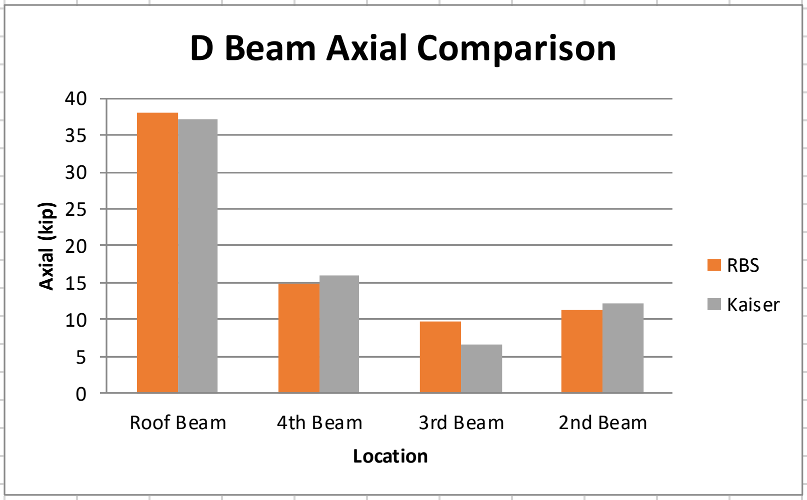
D Beam Axial Comparison
Axial (kip)
40
35
30
25
20
15
10
5
0
Roof Beam
4th Beam
3rd Beam
2nd Beam
Location
RBS
Kaiser

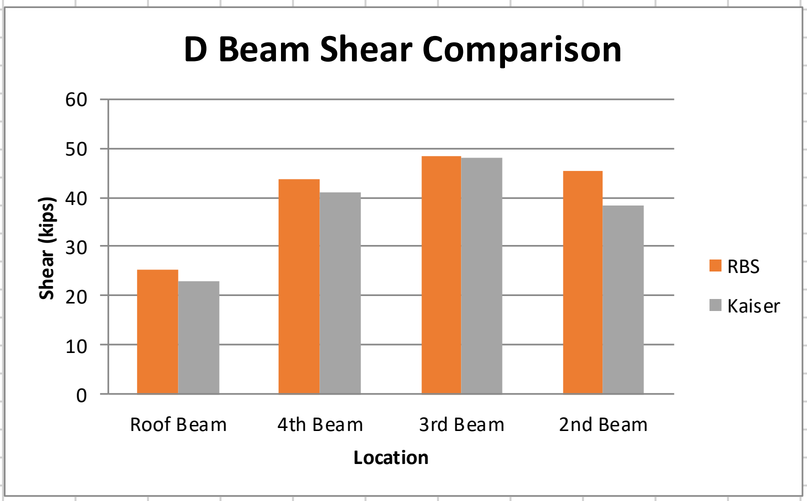
D Beam Shear Comparison
Shear (kips)
60
50
40
30
20
10
0
Roof Beam
4th Beam
3rd Beam
2nd Beam
Location
RBS
Kaiser

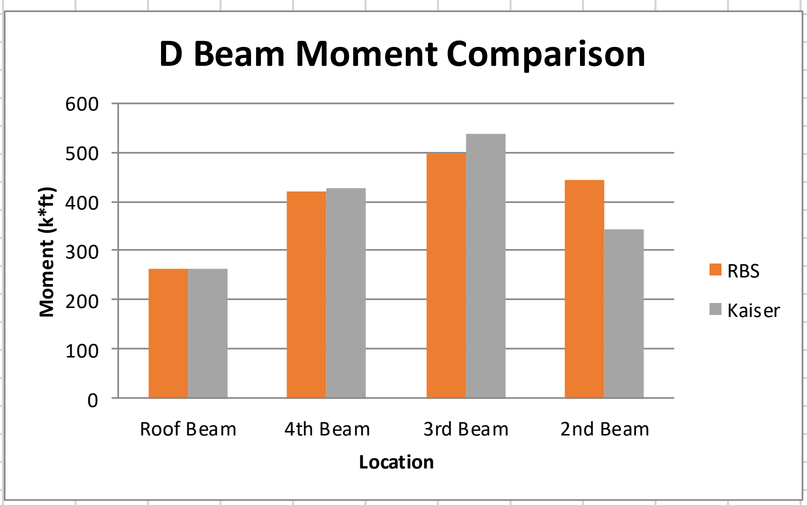
D Beam Moment Comparison
Moment (k*ft)
600
500
400
300
200
100
0
Roof Beam
4th Beam
3rd Beam
2nd Beam
Location
RBS
Kaiser

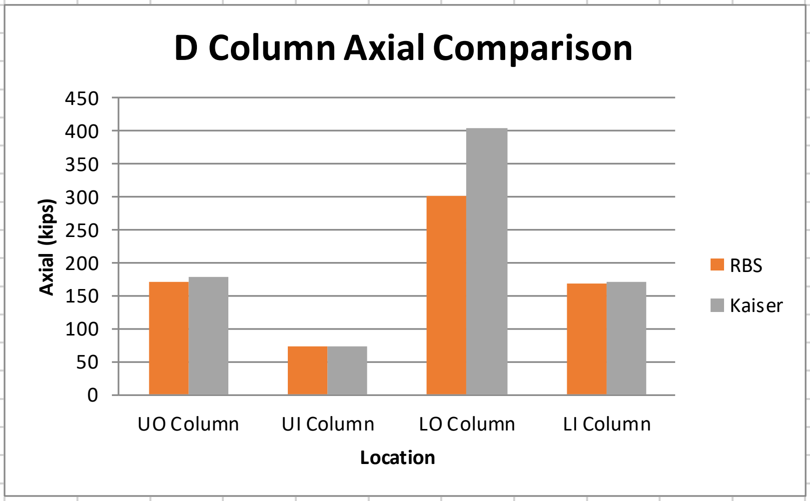
D Column Axial Comparison
450
400
350
300
250
200
150
100
50
0
Axial (kips)
UO Column
UI Column
LO Column
LI Column
Location
RBS
Kaiser

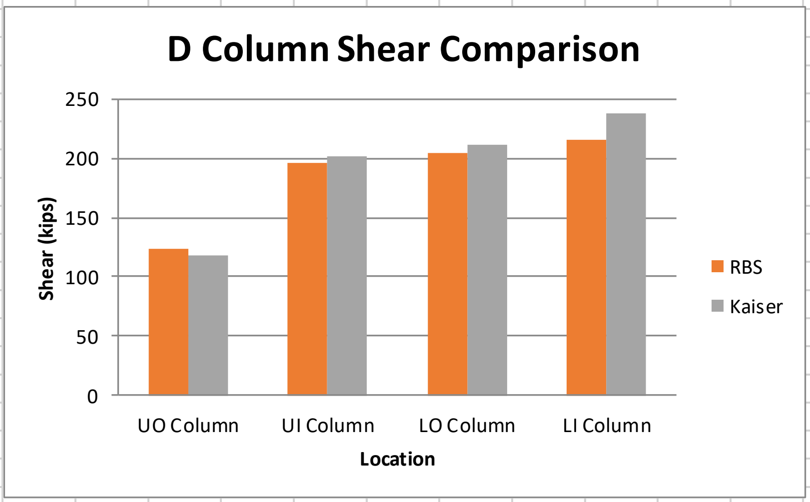
D Column Shear Comparison
250
200
150
100
50
0
Shear (kips)
UO Column
UI Column
LO Column
LI Column
Location
RBS
Kaiser

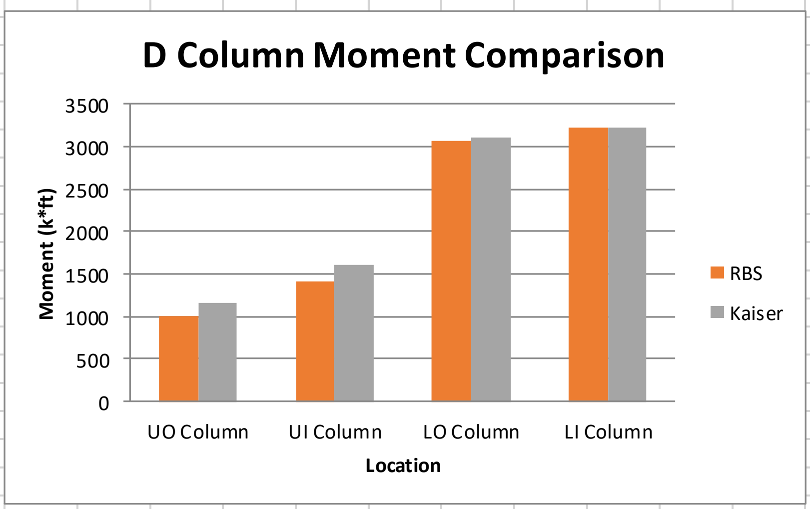
D Column Moment Comparison
3500
3000
2500
2000
1500
1000
500
0
Moment (k*ft)
UO Column
UI Column
LO Column
LI Column
Location
RBS
Kaiser

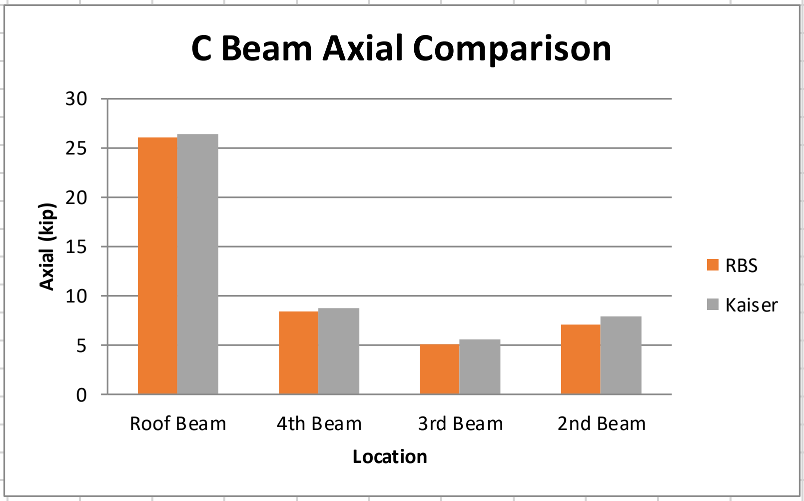
C Beam Axial Comparison
30
25
20
15
10
5
0
Axial (kip)
Roof Beam
4th Beam
3rd Beam
2nd Beam
Location
RBS
Kaiser

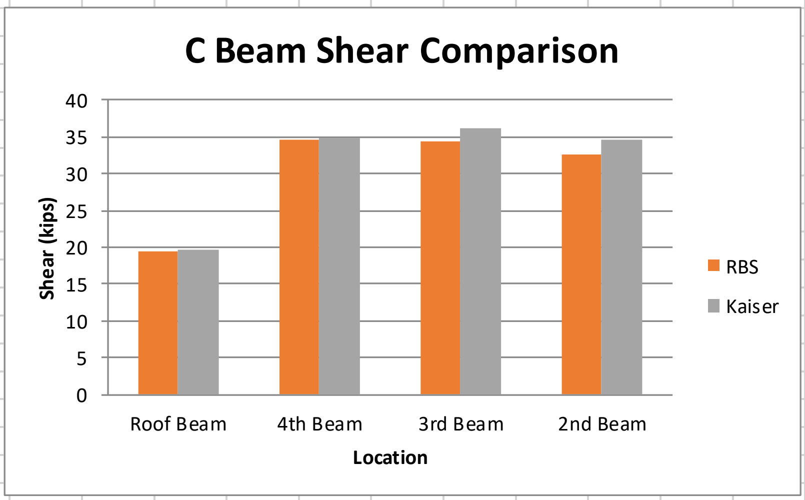
C Beam Shear Comparison
40
35
30
25
20
15
10
5
0
Shear (kips)
Roof Beam
4th Beam
3rd Beam
2nd Beam
Location
RBS
Kaiser

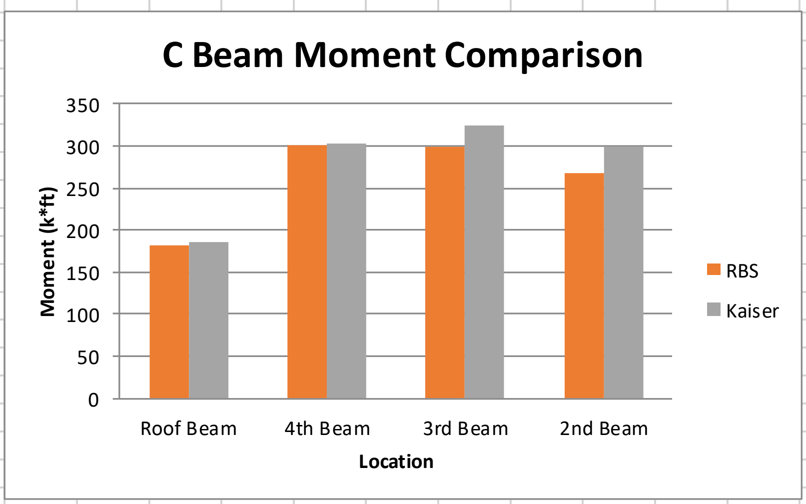
C Beam Moment Comparison
350
300
250
200
150
100
50
0
Moment (k*ft)
Roof Beam
4th Beam
3rd Beam
2nd Beam
Location
RBS
Kaiser

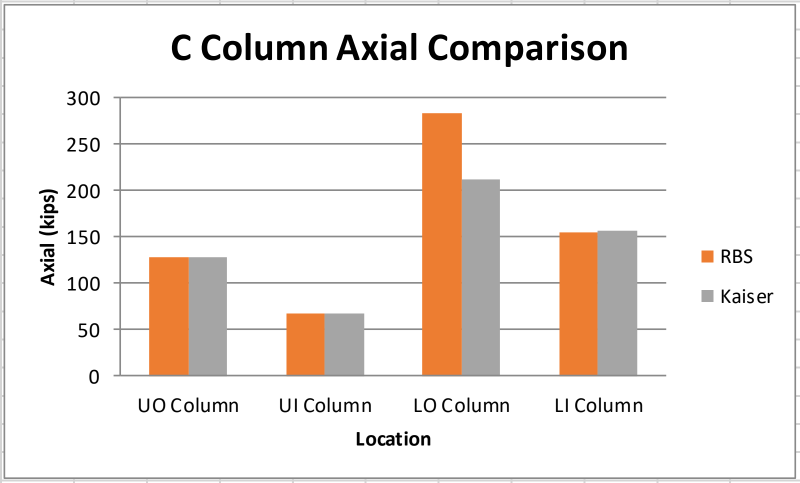
C Column Axial Comparison
Axial (kips)
300
250
200
150
100
50
0
UO Column
UI Column
LO Column
LI Column
Location
RBS
Kaiser

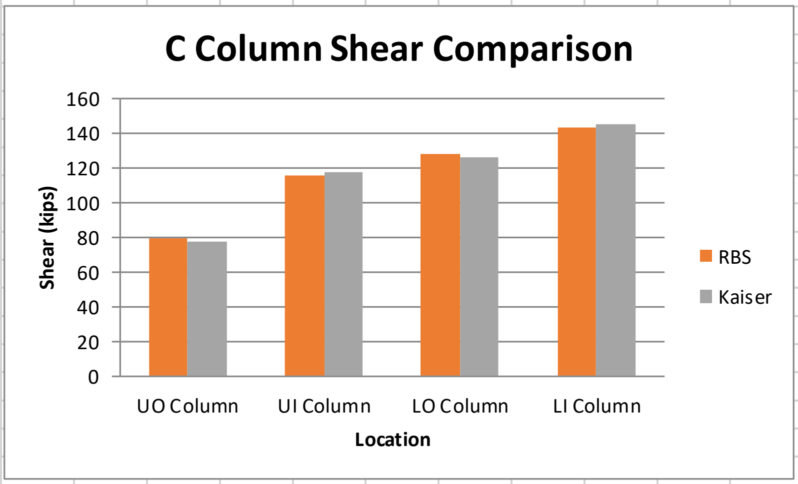
C Column Shear Comparison
Shear (kips)
160
140
120
100
80
60
40
20
0
UO Column
UI Column
LO Column
LI Column
Location
RBS
Kaiser

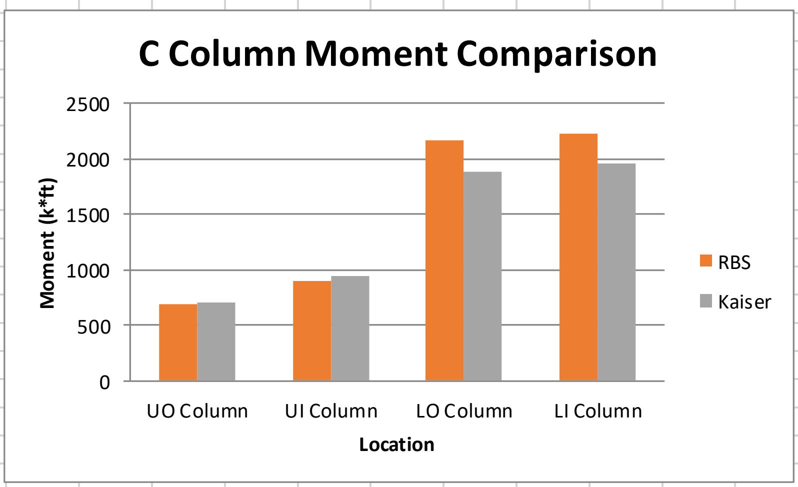
C Column Moment Comparison
Moment (k*ft)
2500
2000
1500
1000
500
0
UO Column
UI Column
LO Column
LI Column
Location
RBS
Kaiser

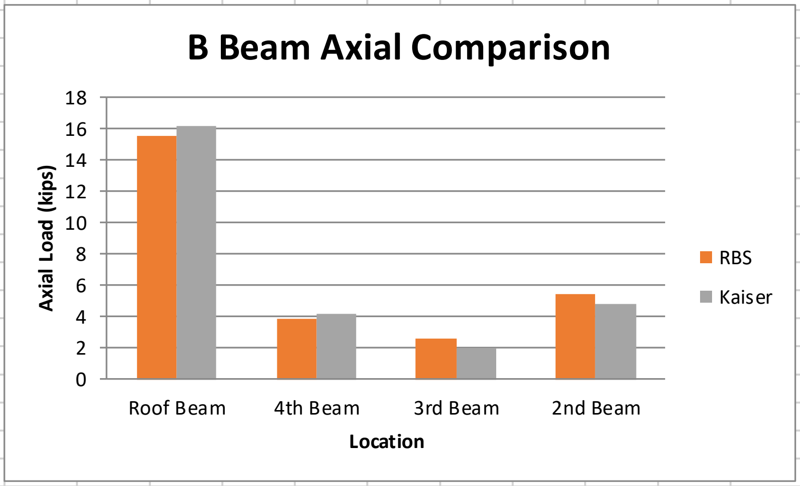
B Beam Axial Comparison
Axial Load (kips)
18
16
14
12
10
8
6
4
2
0
Roof Beam
4th Beam
3rd Beam
2nd Beam
Location
RBS
Kaiser

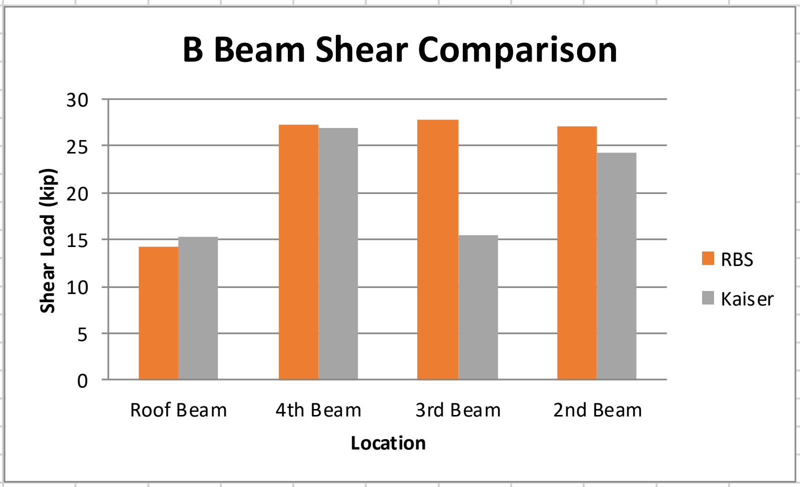
B Beam Shear Comparison
Shear Load (kip)
30
25
20
15
10
5
0
Roof Beam
4th Beam
3rd Beam
2nd Beam
Location
RBS
Kaiser

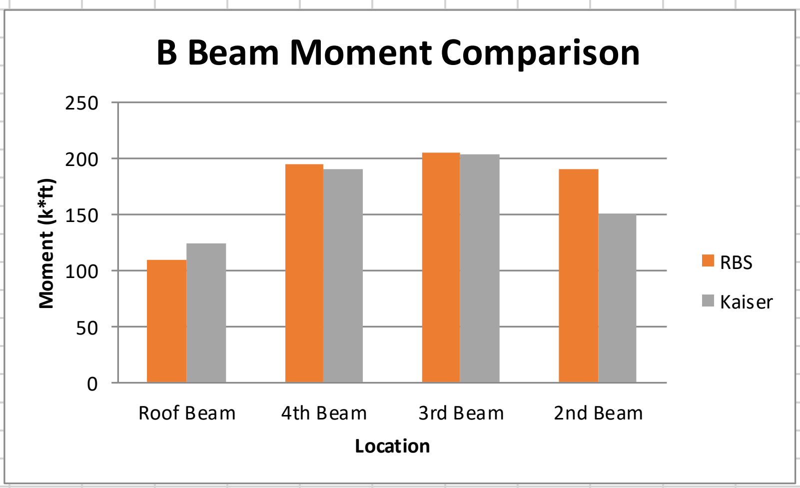
B Beam Moment Comparison
Moment (k*ft)
250
200
150
100
50
0
Roof Beam
4th Beam
3rd Beam
2nd Beam
Location
RBS
Kaiser

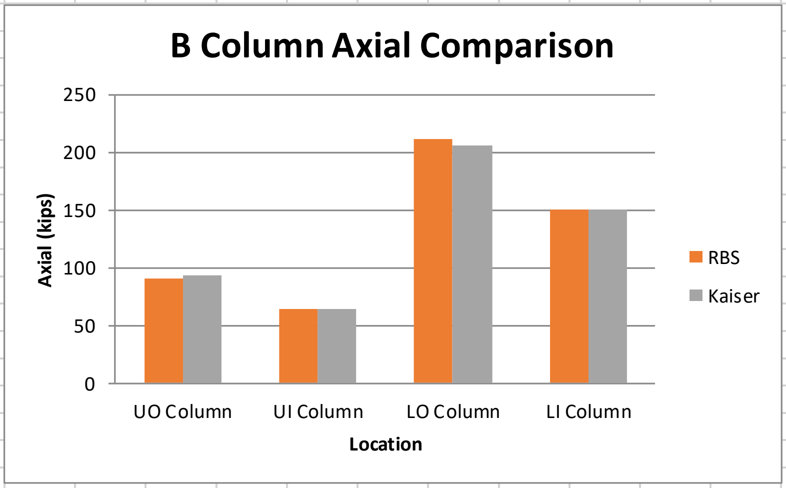
B Column Axial Comparison
250
200
150
100
50
0
Axial (kips)
UO Column
UI Column
LO Column
LI Column
Location
RBS
Kaiser

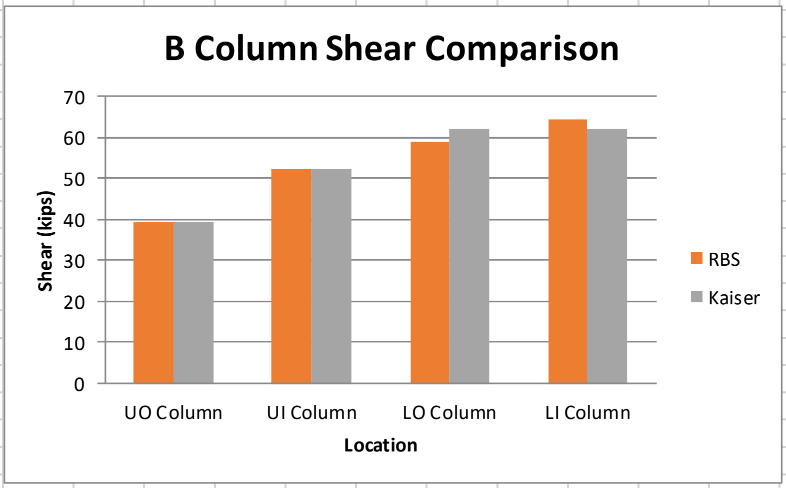
B Column Shear Comparison
70
60
50
40
30
20
10
0
Shear (kips)
UO Column
UI Column
LO Column
LI Column
Location
RBS
Kaiser

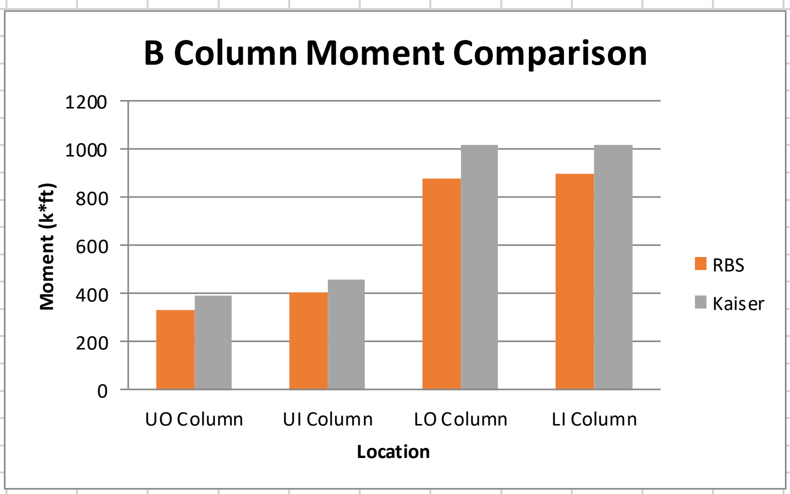
B Column Moment Comparison
1200
1000
800
600
400
200
0
Moment (k*ft)
UO Column
UI Column
LO Column
LI Column
Location
RBS
Kaiser